ROLE OF SPHINSOSINE-1-PHOSPHATE RECEPTOR 1 IN VASCULAR SMOOTH MUSCLE CELLS IN EXPERIMENTAL ATHEROSCLEROSIS

THE ROLE OF THE SPHINGOSINE-1-PHOSPHATE RECEPTOR 1 IN ARTERIAL SMOOTH MUSCLE CELLS IN ATHEROSCLEROSIS DEVELOPMENT

By NARMADAA THYAGARAJAN, B. Tech, M.Sc

A Thesis Submitted to the School of Graduate Studies in Partial Fulfillment of the Requirement for the Degree Doctor of Philosophy.

McMaster University

McMaster University DOCTOR OF PHILOSOPHY (2024) Hamilton, Ontario
(Biochemistry and Biomedical Sciences)

TITLE:	THE ROLE OF SPHINGOSINE-1-PHOSPHATE RECEPTOR 1 IN ARTERIAL SMOOTH MUSCLE CELLS IN ATHEROSCLEROSIS DEVELOPMENT
AUTHOR:	Narmadaa Thyagarajan, B. Tech, MSc
SUPERVISOR:	Dr. Bernardo Trigatti
NUMBER OF PAGES:	XIV, 243

Abstract

Sphingosine-1-phosphate receptor type 1 (S1PR1), one of the five S1PRs that signals in response to bioactive lysosphingolipid S1P, regulates several fundamental processes in distinct cell types and is implicated in atherosclerosis. Using the cre-lox recombination system, previous studies identified that knocking out S1PR1 in myeloid and endothelial cells promotes plaque development in atherogenic mouse models. In the process of generating *S1pr1*$^{lox/lox}$*; ApoE*$^{KO/KO}$ control mice, we unexpectedly noticed that *S1pr1*$^{lox/lox}$ mutation alone, in the absence of cre recombinase, reduces high-fat (HF) diet-induced atherosclerosis in *S1pr1*$^{lox/lox}$*; ApoE*$^{KO/KO}$ mice compared to *S1pr1*$^{WT/WT}$*; ApoE*$^{KO/KO}$ mice. Although *S1pr1*$^{lox/lox}$ allele partially suppressed *S1pr1* levels in macrophages and vascular smooth muscle cells (VSMC), the presence of this mutation in a non-BM derived cell type was responsible for this reduced atherosclerosis in *S1pr1*$^{lox/lox}$*; ApoE*$^{KO/KO}$ mice. We speculated that it could be VSMCs due to their abundance in the vascular wall and their role in foam cell formation.

In this thesis, we directly tested the effects of inactivating S1PR1 in smooth muscle cells (*Tagln-cre*^{TG}*; S1pr1*$^{lox/lox}$*; ApoE*$^{KO/KO}$ mice) on atherosclerosis. Our results demonstrated that deleting S1PR1 in smooth muscle cells drastically reduces atherosclerosis in apoE-deficient mice. The aortic SMCs isolated from these mice also exhibited reduced cell proliferation and lipid droplet formation in response to S1PR1 agonist SEW2871 compared to S1PR1-WT VSMCs.

Furthermore, we also tested the effects of directly inhibiting S1PR1 with S1PR1 selective antagonist Ex26 at a dosage of 0.1 mg/kg/hr in *S1pr1*$^{WT/WT}$; *ApoE*$^{KO/KO}$ mice and *Tagln-cre*^{TG}; *S1pr1*$^{lox/lox}$; *ApoE*$^{KO/KO}$ mice. The prolonged exposure to Ex26 substantially reduced atherosclerotic plaque development in apoE KO mice on an HFD compared to DMSO-treated apoE KO mice. However, this protection was completely lost in mice that lack the *S1pr1* gene in VSMCs. Overall, our results suggest that knocking out S1PR1 in VSMCs results in atheroprotection that surpasses the effects of inactivating S1PR1 in macrophages and endothelial cells which are known to promote atherosclerosis.

Acknowledgements

First and foremost, I would like to express my sincere gratitude to my supervisor Dr. Bernardo Trigatti (Dino) for providing his valuable guidance and support throughout my PhD journey. Dino has always been generous in sharing his knowledge and wisdom with me. In these 6.5 years I spent in the lab, Dino tolerated all my ignorance and never failed to teach me with patience and care. I hope to use the knowledge I gained from him wisely in my future endeavors. I would also like to extend my sincere thanks to my committee members Dr. Geoff Werstuck and Dr. Patricia Liaw for providing me with their valuable support and constructive feedback throughout this journey.

Next, I would like to express my heartfelt thanks to all full-time current (Alex Qian, Jeongah Yoo, Ting Xiong, Summayah Sookechand, and Inbar Akiva Habaz) and past lab members (Christine Bassila, Yak Deng, Wei Wang, George Kluk, Sam Lee, Louise Lee, and Emmanuel Sakarya). Thank you to each one of you for making the lab feel like home. We all shared so many fond memories and I hope to meet you all sometime in the future. I also would like to extend my thanks to previous and present undergraduate students Yuan Qiu, Mila Pastrak, Jennifer Nouanesengsy, and Ayesha Umair. You all made valuable contributions to this project and Kudos to you all!

Finally, I am very grateful for all the love and support I received from my family members and close friends. Mom (Sundari Thyagarajan), you've always

been a strong moral pillar for me. Whenever I faced problems, I always wanted to run away. However, you always motivated me to stand and face it with courage. You always pray for my strength and happiness. I am extremely grateful for everything you did for me as both a father and mother, and I would love to dedicate this thesis to you. Finally, I would like to express my heartfelt thanks to my husband (Vignaesh alias Vicky). The support you have provided for me for the past two years is tremendous and I am very grateful for it. I am so glad we decided to patch up the relationship and mend the differences. You all were very patient with me, listened to all my naggings, loved me with my flaws, and stood with me through thick and thin. Thank you everyone for your love and kindness.

- Narmadaa-

Table of Contents

List of Figures and Tables

List of Abbreviations

ABCA1	ATP Binding Cassette Subfamily A Member 1
ABCG1	ATP Binding Cassette Subfamily G Member 1
AIM	apoptosis inhibitor of macrophages
Apo E	apolipoprotein E
BCL2	B-cell lymphoma 2
BM	bone marrow
BMT	bone marrow transplantation
CAD	coronary artery disease
CD	cluster of differentiation
DAPI	DNA 4’,6-diamidino-2-phenylindole dihydrochloride
DMEM	Dulbecco’s Modified Eagle Medium
EDTA	Ethylenediaminetetraacetic acid
eNOS	endothelial nitric oxide synthase
ER	endoplasmic reticulum
FBS	fetal bovine serum
HBSS	Hanks Balanced Salt Solution

HDL	high-density lipoprotein
HFD	high-fat diet
ICAM	intracellular adhesion molecule
IFN	interferon
IL	interleukin
KO	knock out
LAL	lysosomal acid lipase
LDL	low-density lipoprotein
LDLR	low-density lipoprotein receptor
LOX1	lectin-type oxidized low-density lipoprotein receptor 1
MCP-1	monocyte chemotactic protein 1
MLKL	multilineage kinase-like domain
MTT	3-(4,5-dimethylthiazol-2-yl)-2,5-diphenyltetrazolium bromide
NCLPDS	newborn calf lipoprotein deficient serum
NF-κB	nuclear factor kappa B
NO	nitric oxide
oxLDL	oxidized low-density lipoprotein

PBS	Phosphate buffer saline
PDGF	platelet derived growth factor
PECAM1	platelet endothelial cell adhesion molecule-1
PPAR	peroxisome proliferator-activated receptor
RT-PCR	real time reverse transcriptase-polymerase chain reaction
S1PR1	sphingosine-1-1phosphate receptor 1
SMA	smooth muscle actin
SMC	smooth muscle cell
SRA	scavenger receptor A
STAT	signal transducer and activation of transcription
Tagln	transgelin
TGF	transforming growth factor
TIM	T-cell immunoglobulin and mucin domain
VCAM	vascular cell adhesion molecule
VE-cadherin	vascular endothelium cadherin
VSMC	vascular smooth muscle cells

Chapter 1: Introduction

1.1 Atherosclerotic Coronary artery disease

Atherosclerotic coronary artery disease (CAD), also known as coronary heart disease, is a heart condition that affects coronary arteries and has been reported as the number one cause of death worldwide and the second leading cause of death in Canada (Kreatsoulas and Anand 2010). In 2015, atherosclerotic CAD alone was estimated to have caused 8.9 million deaths, constituting about 45% of all non-transmittable disease deaths worldwide (Wang et al. 2016). Atherosclerotic CAD is caused due to the buildup of atherosclerotic plaque in the arterial wall, which blocks or stiffens blood vessels over time and restricts oxygen-rich blood supply to the heart. In general, the arterial wall comprises three layers: 1) The tunica externa, the outermost layer, which contains fibroblast, leukocytes, and progenitor cells (Hu et al. 2004; Galkina et al. 2006; Houtkamp et al. 2001; Shi et al. 1996); 2) the tunica media, the middle layer which is comprised of multiple layers of longitudinally oriented vascular smooth muscle cells (VSMCs) (Tellides and Pober 2015; Zorc-Pleskovič et al. 2018); 3) The tunica intima, the inner most layer, consists of a single layer of endothelial cells separating the vessel wall from the lumen of the vessel, and covering a layer of intimal vascular smooth muscle cells, present in human but absent from murine arteries (Nakashima et al. 2007; Nakashima, Wight, and Sueishi 2008). Although the structure and function of all three layers are affected extensively during CAD, atherosclerotic plaque development occurs focally in the intima. Genetic factors, environmental factors,

and lifestyle are the main risk factors for the development of CAD (Girelli et al. 2009; Yusuf et al. 2004).

1.2 Overview of atherosclerosis

Atherosclerosis is a chronic inflammatory condition (**Figure 1.1**) that develops primarily in medium and large-sized arteries, notably in the arterial branch and bifurcation regions due to disturbed laminar flow and low shear stress (Gimbrone Jr and García-Cardeña 2016). The key initiation step in this disease involves accumulation of low-density lipoprotein (LDL) and triglyceride-rich lipoprotein remnants in the intimal layer of the vessel (Björkegren and Lusis 2022; Duran and Pradhan 2021). These lipoproteins in the intima are subject to physical and chemical modifications such as aggregation, oxidation, and proteolytic digestion. Some of these modified lipoproteins, such as oxidized LDL (oxLDL), activate endothelial cells express adhesion molecules and secrete chemokines which results in the recruitment of blood-borne monocytes into the sub-endothelial space and their differentiation into macrophages. These cells as well as smooth muscle cells, can take up modified lipoproteins to become lipid engorged foam cells (Kzhyshkowska, Neyen, and Gordon 2012; Kunjathoor et al. 2002; Allahverdian et al. 2014b). The accumulation of macrophage and smooth muscle cell-derived foam cells in the arterial wall leads to the formation of fatty streaks which often appear as yellow-colored streaks under the microscope (Gerrity 1981). This is an early visible stage in the atherosclerosis development.

A

Human Atherosclerosis

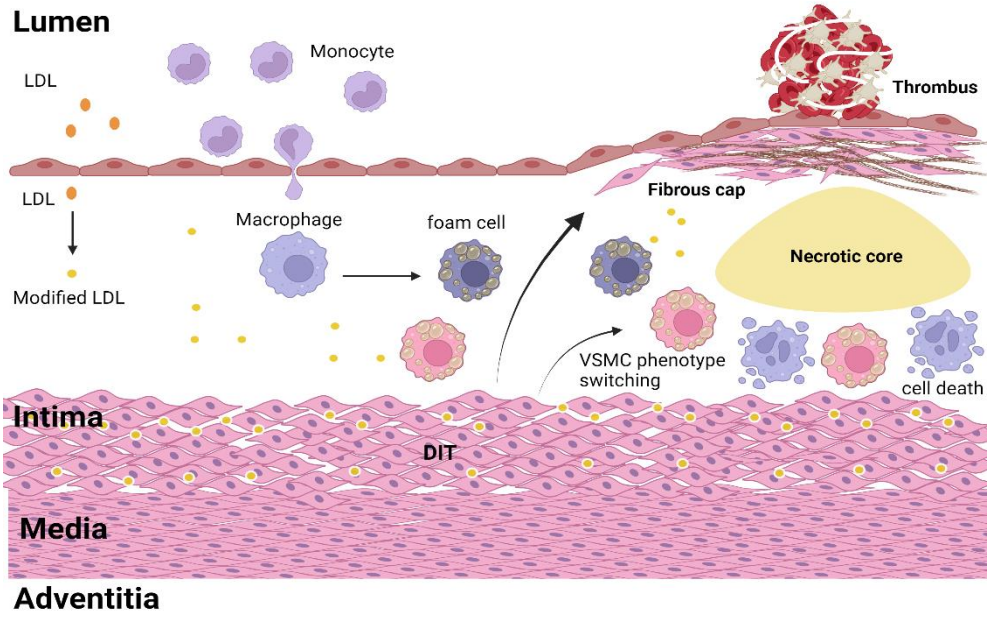

B

Murine Atherosclerosis

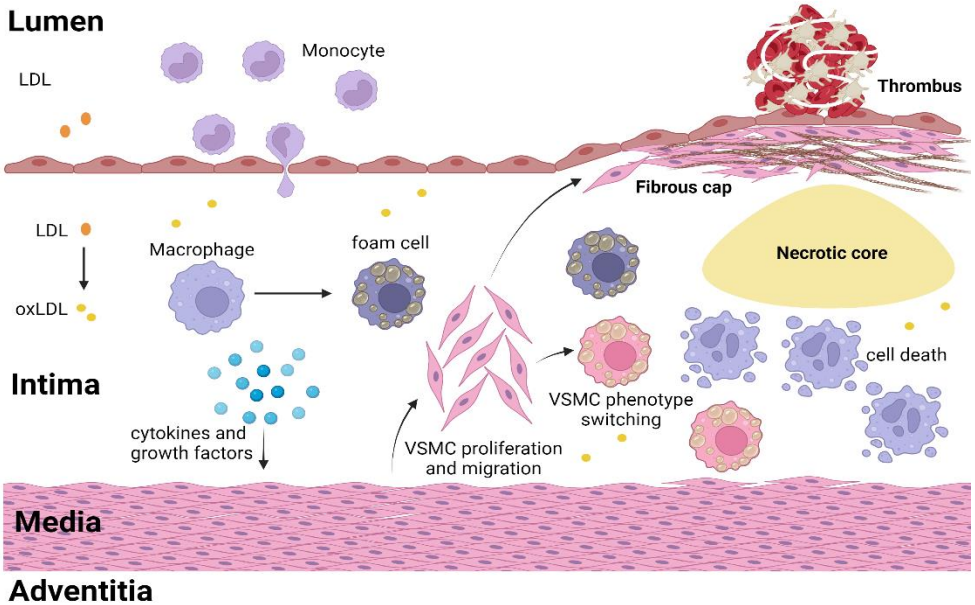

Figure 1.1: Comparison between human and murine atherosclerosis

Atherosclerosis, an inflammatory disease condition, is triggered by the accumulation of low-density lipoprotein (LDL) in the tunica intima. LDL undergoes modification by reactive oxygen species which results in monocyte recruitment and their differentiation into macrophages. These macrophages take up modified lipoproteins, becoming lipid-laden foam cells. In addition to these cells, smooth muscle cells in the thickened intima (referred to as DIT) present in humans **(A)** also take up lipids and become foam cells. They also lose their cell markers and gain the expression of macrophage markers, causing them to transdifferentiate into macrophage-like cells. Although this DIT is not present in mice **(B)**, SMCs that migrate and proliferate from the media to intima in response to cytokines and growth factors also take up modified lipoproteins and become foam cells. These SMCs in the intima also contribute to fibrous cap formation which prevents the plaque from rupturing. In advanced plaques, the foam cells eventually undergo apoptosis and necroptosis. As the necrotic core grows and the fibrous cap thins, the plaque becomes vulnerable to rupture, resulting in acute cardiovascular events such as thrombosis. The image was created using Biorender (BioRender.com).

As the plaque progresses, the vascular endothelium and macrophages in the vessel wall secrete cytokines, chemokines and growth factors which causes proliferation and migration of medial smooth muscle cells (SMCs) into the intimal space (Buschmann et al. 2003; Schober and Zernecke 2007; Björkegren and Lusis 2022). In humans, atherosclerotic plaque formation is preceded by diffuse intimal thickening (DIT) driven by SMC proliferation and migration. The SMCs in the intima take up lipids and then transdifferentiate into macrophage-like cells (SMCs lose their lineage marker genes and acquire macrophage marker genes) as they become foam cells within the atherosclerotic plaques (Feil et al. 2014; Rong et al. 2003). In addition, intimal VSMCs also form fibrous connective tissue, referred to as “fibrous caps”, underneath the endothelial layer which prevents the plaque from rupturing (Newby and Zaltsman 1999). The fibrous cap mainly consists of collagen, elastin, VSMCs, macrophages, and lymphocytes (Björkegren and Lusis 2022). Initially it was thought that only SMCs contribute to the formation of extracellular matrix in the fibrous caps. However, a recent study reported that the majority of cells found in fibrous caps originated from endothelial cells or macrophages that transformed into mesenchymal cells (Newman et al. 2021). Cholesterol accumulation and endoplasmic reticulum (ER) stress causes macrophages and aortic SMCs to undergo programmed cell death (referred to as apoptosis) (Li et al. 2005; Kedi et al. 2009; Feng et al. 2003; Scull and Tabas 2011). In advanced plaques, accumulation of apoptotic bodies and defective clearance of these apoptotic bodies (efferocytosis) promotes the formation of necrotic cores (that

contains cholesterol crystals and cell debris) (Rayner 2017). Over time, secondary necrosis and thinning of fibrous caps together with advanced inflammatory response and vascular calcification results in plaque rupture, which may ultimately result in clinical complications, such as myocardial infarction and stroke (Glass and Witztum 2001; Björkegren and Lusis 2022).

1.2.1 The role of endothelial cells in atherosclerosis

The vascular endothelium is a key mediator of vascular homeostasis and a major regulator of several fundamental processes, including vascular tone, barrier integrity, and inflammatory responses (Davignon and Ganz 2004). Endothelial cells release several vasoconstrictor substances and vasodilator substances to regulate vascular tone (Drexler 1998; Sowers 2002; Kinlay et al. 2001). The major vasoconstrictor substances include endothelin and angiotensin II. In addition to vasoconstrictive properties, angiotensin II also stimulates the generation of ROS and the production of endothelin. The other cell types, such as macrophages and VSMCs, when activated also generate a huge amount of endothelin. Both endothelin and angiotensin II were shown to be involved in atherosclerotic plaque development by inducing VSMC proliferation (Drexler 1998). On the flip side, vasodilatory substances, such as nitric oxide (NO), prostacyclin, bradykinin, and endothelial-derived hyperpolarizing factors counteract the effects of endothelium-derived-vasoconstrictive substances (Drexler 1998; Davignon and Ganz 2004). A major vasodilator NO is produced by endothelial cells from L-arginine through the

enzyme endothelial NO synthase (eNOS). Accumulation of oxLDL in the arterial wall decreases the production and activity of vasodilatory substances, particularly endothelium-derived NO resulting in endothelial dysfunction. The imbalance between vasoconstriction and vasodilation disrupts the vascular endothelium leading to enhanced permeability, leucocyte adhesion/infiltration, proinflammatory cytokine production, and platelet aggregation (Davignon and Ganz 2004).

The barrier function of the endothelium is critical in controlling the exudation of different substances, such as fluids, lipids, ions, and immune cells (Radeva and Waschke 2018). The endothelial cell-cell junctions are structures that play a key role in regulating vascular integrity. Tight junctions are structures that mainly comprise cell adhesion proteins, such as claudins, occludin, and junctional adhesion molecules (Abdullahi, Tripathi, and Ronaldson 2018). These adhesion proteins interact with adjacent cells and induce intracellular signaling through their cytoplasmic and extracellular domains to maintain vascular endothelium integrity and promote selective permeability of the endothelial barrier. Damage to intercellular junctions, particularly tight and adherens junctions, leads to uncontrolled exudation of leukocytes into the arterial wall which may result in the progression of atherosclerosis (Sluiter et al. 2021). In addition, lipoproteins, and other solutes can also be transported across endothelial cells via transcytosis, wherein plasma membrane derived vesicles transfer these substances from lumen to basal side of the endothelium (Frank et al. 2009).

Mechanistic studies in mouse models have revealed that in the arterial wall, both biomechanical (such as disturbed blood flow) and biochemical stimuli (for example, modified LDL, pro-inflammatory cytokines, and endotoxins) cause endothelial cells to undergo activation (Pober and Cotran 1990; Pober and Sessa 2007). This involves the activation of a transcription factor nuclear factor kappa B (NF-κB) resulting in upregulated expression of adhesion molecules, such as vascular cell adhesion molecule 1 (VCAM1), intercellular adhesion molecule 1 (ICAM1), and E-selectins (Collins and Cybulsky 2001). Both VCAM1 and ICAM1 expression are upregulated in endothelial cells at atherosclerotic lesion-prone regions aortas of apolipoprotein E (apoE) KO mice (Nakashima et al. 1998). However, genetically disrupting VCAM-1 alone, but not ICAM1 reduced nascent lesion formation in low-density lipoprotein (LDLR) KO mice when they were fed a cholesterol-rich diet for 8 weeks (Cybulsky et al. 2001). Similarly, deficiency of both P- and E-selectins was also shown to reduce experimental atherosclerosis in mice (Dong et al. 1998). Together, these findings support a critical role of these adhesion molecules expressed on the endothelium in atherosclerotic plaque development. Furthermore, activated endothelial cells also produce chemokines, including monocyte chemoattractant protein-1 (MCP-1), and pro-thrombotic mediators, such as tissue factor and von Willebrand factor (Gimbrone Jr and García-Cardeña 2016). These effector proteins work collectively to regulate the selective recruitment of leukocytes to the lesion-prone regions in the arterial wall and their emigration into the intima resulting in the initiation and progression of

atherosclerosis. While the roles of endothelial cell activation and monocyte recruitment in murine models of atherosclerosis development has been well established, the contributions of these processes to atherosclerosis development in humans is less well-established.

1.2.2 Role of macrophages in atherosclerosis

Macrophages are considered to be a key player in murine atherosclerosis models due to their influence on both plaque progression and regression (Moore, Sheedy, and Fisher 2013). The LDL in the arterial wall undergoes modifications through different mechanisms mediated by a variety of enzymes (such as myeloperoxidase, proteases, lipases, and 12/15-lipoxygenase) and free-radicals (such as superoxide and hydrogen peroxide). These modified lipoproteins (that act as “damage signals”) are recognized by scavenger receptors, a type of pattern recognition receptors found on macrophages. Several scavenger receptors, including a cluster of differentiation (CD) 36, scavenger receptor A (SRA), and lectin-type oxidized low-density lipoprotein receptor 1 (Lox1), have been identified to take up oxLDL and transform macrophages into lipid-laden foam cells (Kzhyshkowska, Neyen, and Gordon 2012; Kunjathoor et al. 2002). Indeed, deleting these scavenger receptors in atherogenic mice not only reduced foam cell formation, but also reduced the expression of inflammatory genes, macrophage cell death, and secondary necrosis (Kuchibhotla et al. 2008; Manning-Tobin et al. 2009). Therefore, suggesting that these scavenger receptors are implicated in several other processes in addition to oxLDL uptake. In addition to modified LDL,

macrophages also uptake native LDL through a receptor-independent endocytic pathway, also referred to as pinocytosis, leading to foam cell formation (Kruth 2011).

The plaque macrophages exhibit profound plasticity which allows them to polarize into distinct phenotypes in response to stimuli in their local microenvironment (Moore, Sheedy, and Fisher 2013; Colin, Chinetti-Gbaguidi, and Staels 2014). Previously, macrophages were broadly classified into two extreme phenotypes: classically activated M1 phenotype and alternatively activated M2 phenotype. M1 macrophage activation occurs in response to T-helper (Th) cell cytokines (such as IFN-γ), toll-like receptor signaling, pathogen-associated molecular complexes, lipopolysaccharides, and lipoproteins. These pro-inflammatory macrophages express NF- κB transcription factor and secrete reactive oxygen and nitrogen species in addition to several pro-inflammatory cytokines (including interleukin (IL)-6, IL-1β and IL-12). On the other hand, M2 macrophage polarization occurs in response to Th-2 cytokines, such as IL-4, IL-13, and IL-33. These macrophages are activated through peroxisome proliferator-activated receptor (PPAR)- γ and signal transducer and activation of transcription (STAT) 6 pathways and secrete anti-inflammatory cytokines, such as IL-10 and transforming growth factor (TGF)-β. Furthermore, the M2 phenotype expresses high levels of arginase-1 in addition to their expression in mannose receptor 1, CD163, and resistin like-β. It was believed that $Ly6C^{hi}$ monocytes tend to differentiate into M1 macrophages, whereas $Ly6C^{low}$ monocytes may give rise to

M2 macrophages. However, the current concepts are that "M1" and "M2" states are artificial phenotypes that are produced in culture, and they do not exist as such in vivo. They are examples of the extremes of macrophage phenotypes, but in vivo, macrophage phenotypes fit along spectrum between these extremes and that different stimuli move macrophages in different directions along this spectrum of phenotypes. In addition to M1 and M2, several other alternative macrophage phenotypes are observed in the atherosclerotic plaques. These subsets include Mox, Mhem, M(Hb), and M4 macrophages. These macrophages are activated by distinct factors. Among these phenotypes, Mhem and M(Hb) are considered atheroprotective while Mox and M4 macrophage phenotypes are pro-atherogenic. Thus, depending on the microenvironment stimulus, macrophages may acquire distinct phenotypes to regulate inflammatory responses within the intima either contributing to the progression or regression of the atherosclerotic plaque.

The balance between cholesterol influx and efflux is critical to maintaining macrophage cholesterol homeostasis. The lack of this balance and enhanced accumulation of cholesterol causes macrophages to become foam cells (Chinetti-Gbaguidi et al. 2011). The efflux of lipids is mainly mediated through lipid transporters, such as ATP-binding cassette transporters ABCA1 and ABCG1, and SR-B1 in macrophage foam cells (Yvan-Charvet, Wang, and Tall 2010). *Abca1* and *Abcg1* expression is regulated by transcription factors called liver X receptors (LXRs). These transcription factors act as a sterol sensor. High levels of cholesterol content within macrophages elevate LXR levels which in turn promotes ABCA1

and ABCG1 expression. ABCA1 transports lipids to ApoA1, a major apolipoprotein component of HDL, and ABCG1 transports cholesterol to mature HDL. In addition to lipid transporters, cholesterol efflux also occurs through passive diffusion or transcellular cholesterol movement from macrophage foam cells (Yvan-Charvet, Wang, and Tall 2010; Westerterp and Tall 2020). Furthermore, macrophages within the atherosclerotic plaques also tend to display reduced emigration. During hypoxia, macrophages were shown to express high levels of a migration inhibitory molecule called netrin 1 (Ramkhelawon et al. 2013). Deletion of netrin 1 in bone-marrow derived cells had previously been shown to increase macrophage migration and reduce atherosclerotic plaque development in LDLR KO mice (Van Gils et al. 2012). Similarly, enhanced accumulation of cholesterol content in the lipid-laden macrophages is also associated with reduced macrophage migration (Nagao et al. 2007; Park et al. 2012; Qin et al. 2006). Nevertheless, increased macrophage lipid efflux and emigration from plaques may help to accomplish atherosclerosis regression.

Enhanced macrophage apoptosis, impaired efferocytosis, and the formation of larger necrotic cores are some of the characteristic features of advanced atherosclerotic plaques (Rayner 2017). Enhanced cholesterol accumulation and ER stress can induce the unfolded protein response in activated macrophages resulting in apoptosis (Moore, Sheedy, and Fisher 2013; Rayner 2017; Feng et al. 2003; Zhou et al. 2005; Li et al. 2005). Apoptotic cell death can be good or bad depending on the stage of atherosclerosis. For instance, deletion of an anti-

apoptotic protein AIM (apoptosis inhibitor of macrophages) was shown to enhance apoptosis in macrophages and reduce plaque formation (Arai et al. 2005). In addition, over-expression of another anti-apoptotic protein B-cell lymphoma (BCL)-2 specifically in macrophages increased plaque size during the initial stages of atherosclerosis, however, reduced lesion size in advanced plaques (Gautier et al. 2009). In general, apoptotic cells are efficiently cleared by a process referred to as efferocytosis. This process is regulated by numerous proteins and lipid mediators, including 1) tyrosine-protein kinase Mer (MerTK) receptor (Li et al. 2006), 2) T-cell immunoglobulin and mucin domain (TIM) protein family (Foks et al. 2016), 3) a chaperone protein calreticulin (Kojima et al. 2019), and 4) resolvin E and D, lipid mediators derived from omega-3 fatty acids. Defects in these proteins (or genes that encode them) or resolvin synthesis impaired efferocytosis and exacerbated plaque development *in-vivo* (Ait-Oufella et al. 2008; Foks et al. 2016; Kojima et al. 2019). Furthermore, the accumulation of apoptotic bodies and defective efferocytosis results in necrotic core formation, a key feature of vulnerable plaques. Programmed cell necrosis is tightly regulated by receptor-interacting protein (RIP) kinase 1 and 3, and multilineage kinase-like domain (MLKL) (Karunakaran et al. 2016; Rayner 2017). Recruitment and activation of these oligomeric necrosome proteins results in pore formation and membrane rupture (Rayner 2017). Indeed, the inhibition of RIP kinase 3 has been shown to significantly reduce necrotic cores and lesion size in the advanced plaques of atherogenic mice (Lin et al. 2013).

Nonetheless, preventing macrophage cell death in advanced stages of plaque formation may be an effective therapeutic strategy against atherosclerosis.

1.2.3 Role of VSMC in atherosclerosis

Although cardiac arteries comprise several cell types, VSMCs are the most abundant cell type observed in the arterial walls of both human and non-human primates. The key function of this cell type is to regulate blood pressure and arterial tone through vascular contraction and relaxation. Arterial SMCs originate from different sources of progenitors from distinct embryonic origins. For instance, VSMC in the descending aorta have been shown to originate mainly from somatic precursors, while cells in the aortic arch, ascending aorta, and carotid arteries are derived from the neural crest (Grootaert and Bennett 2021). Depending on their embryonic origin, these cells had been shown to exhibit different functional consequences in response to PDGF (Madura et al. 1996), NF-κB (Trigueros-Motos et al. 2013), and TGF-β (Topouzis and Majesky 1996; Xie et al. 2013) signaling pathways. Of note, BM-derived myeloid cells, adventitial mesenchymal stem cells, pericytes, and endothelial cells have also been shown to express SMC lineage markers (such as α-SMA and Tagln) in the atherosclerotic lesions suggesting that intimal SMCs may also originate from distinct sources in the vessel wall (Tigges, Komatsu, and Stallcup 2013; Chen et al. 2015; Evrard et al. 2016; Coen, Gabbiani, and Bochaton-Piallat 2011; Caplice et al. 2003; Sata et al. 2002). However, several studies, including lineage tracing studies now convincingly indicate that the VSMCs in the intima mainly originate from local medial (mouse) and/or intimal (human)

SMCs through clonal expansion and give rise to most foam cells in the atherosclerotic plaques (Allahverdian et al. 2014a; Shankman et al. 2015; Feil et al. 2014; Jacobsen et al. 2017).

The VSMCs display profound phenotype plasticity (Gomez and Owens 2012). Under normal circumstances, VSMCs are the only cell type observed in the tunica media layer, and they exhibit a contractile phenotype, and have a low proliferative rate. They express a wide variety of contractile proteins, such as smooth muscle cell alpha-actin 2 (α-SMA), Transgelin (TAGLN, also referred to as SM22α), SM myosin heavy chain (MHC), calponin, and smoothelin (Gabbiani et al. 1981; Mack and Owens 1999; Babij, Kelly, and Periasamy 1991; Miano et al. 1994; Duband et al. 1993; Van der Loop et al. 1996; Kim et al. 1997). During atherosclerosis development, the contractile genes are down-regulated due to the activation of the guanine/cytosine (G/C) repressor element in them which drives the VSMCs to change from contractile to synthetic phenotype causing increased proliferation and extracellular matrix remodeling to enable migration (Regan et al. 2000).

VSMCs are involved in all the stages of atherosclerosis in humans. Diffuse intimal thickening (DIT) is a thickened intima that mainly consists of SMCs and which forms even before the atherosclerosis begins (Nakashima et al. 2007; Nakashima, Wight, and Sueishi 2008). DIT is generally present in lesion-prone arteries where the shear stress is less (Bonert et al. 2003). Unlike humans where SMCs are already present in pre-atherosclerotic intima, mice do not exhibit DIT

(Allahverdian et al. 2018). In mice, the medial SMCs proliferate and migrate into the intima in response to environmental cues. Of note, multiple *in-vitro* studies have shown that bioactive lysosphingolipids (such as sphingosine-1-phosphate), growth factors (such as platelet-derived growth factor (PDGF), fibroblast growth factor, and TGF-β), and cytokines (such as IL-1β) regulate VSMC proliferation and migration *in-vitro* (Kluk et al. 2003; Kluk and Hla 2001; Liu et al. 2019; Khan, Agrotis, and Bobik 2007; Eun et al. 2015). The VSMCs in the intima can play a beneficial role by contributing to fibrous cap formation or a detriment role by transforming into inflammatory-like phenotypes. A fibrous cap is crucial for maintaining plaque stabilization. SMCs promote fibrous cap formation by secreting elastin, collagen, and proteoglycans (Allahverdian et al. 2018). Loss of collagen VIII has been shown to reduce SMC proliferation and migration and decrease fibrillar type I collagen levels which in turn resulted in thinning of fibrous caps in apoE-deficient mice (Lopes et al. 2013). In addition, manipulating the expression of certain proteins that are involved in SMC proliferation and migration led to modification in fibrous cap thickness in atherogenic mice. For instance, blocking PDGFR signaling substantially reduced fibrous cap formation (Sano et al. 2001) while overexpressing insulin growth factor 1 in SMCs enhanced fibrous cap formation in apoE-deficient mice (Shai et al. 2010). These findings suggest that certain stimuli can shift the direction of SMC's phenotype switching, leading to plaque stabilization.

The contribution of VSMC in the early and late stages of atherosclerosis was underappreciated compared to monocyte-derived macrophages until the early 2000s. Similar to macrophages, SMCs also express scavenger receptors (such as CD36, and SRA) through which they can take up modified lipoproteins and become foam cells. Some studies demonstrated that lipid loading can cause aortic SMCs to undergo phenotypic switching into macrophage-like cells in culture (Rong et al. 2003). These transdifferentiated cells tend to lose their differentiation marker genes (such as *Acta2* and *Tagln*), gain macrophage marker genes (such as *Cd68* and *Mac2*), and adopt phagocytic properties of macrophages as well (Rong et al. 2003). Indeed, a large proportion of foam cells has been shown to arise from intimal SMC in both human and mouse atheromas (Allahverdian et al. 2014a; Wang et al. 2019). In addition, these SMCs have also been shown to display relatively low levels of ABCA1 expression, a key protein that regulates cholesterol efflux, in comparison to myeloid-origin cells/ macrophages both in culture and in the atherosclerotic plaques. Furthermore, a recent study by Dubland et al. (Dubland et al. 2021) reported an underlying mechanism through which intimal SMCs may contribute to arterial foam cell formation. Lysosomal acid lipase (LAL) is an enzyme that is encoded by *Lipa* (lipase A) gene. This enzyme catalyzes the hydrolysis of cholesteryl esters to free cholesterol in the lysosome within the cells. In this study, the authors showed that aortic SMCs (both from mice and humans) exhibited markedly lower*Lipa* expression and LAL activity either human or mouse macrophages. Similar *lipa*/LAL expression patterns were also observed in the

intimal SMCs of both human and mouse atherosclerotic plaques *in-vivo* (Dubland et al. 2021). These observations suggest that the low LAL activities may be responsible for the lipid accumulation in intimal SMCs.

Using SMC fate mapping experiments and single cell genomics, recent studies have identified that SMCs could undergo lineage reprogramming into distinct SMC-derived cell types in addition to macrophage-like cell phenotype. For instance, studies by Pan et al. (Pan et al. 2020) revealed that SMCs can transition into an intermediate state, referred to as “SEM” cells (Stem, endothelial cell, and monocyte) in the atherosclerotic plaques of both mouse and humans. These SEM cells are multipotent cells that can differentiate into macrophage-like cells, fibrochondrocyte-like cells, and back towards their original SMC phenotype state. The authors also identified that this SMC to SEM transition is primarily regulated by retinoic acid (RA) signalling pathway; and activating this pathway using all-trans RA (ATRA) hindered SMC to SEM transdifferentiation, reduced atherosclerotic plaques and elevated plaque stability *in-vivo*. A study by Wirka et al. (Wirka et al. 2019) reported that transcription factor 21 (TCF21), the basic helix-loop-helix transcription factor, regulates phenotypic switching from contractile SMCs to fibroblast-like cells (referred to as fibromyocyte), and associated with reduced risk of CAD. The deletion of TCF21 in SMCs reduced fibromyocyte levels in the atherosclerotic plaques and in the fibrous caps. These findings suggest that VSMCs may acquire distinct phenotypes to promote plaque instability or stability.

1.3 Conventional mouse models of atherosclerosis

Although mice are resistant to atherosclerotic plaque development when compared to humans due to altered lipid profiles, murine models are extensively employed for investigating experimental atherosclerosis due to their ease of handling, quick reproduction, and convenience in genetic manipulation (Getz and Reardon 2012; Veseli et al. 2017; Bond and Jackson 2010). In addition, use of mice also facilitates monitoring the plaque progression in a reasonable time frame. Mice predominantly carry their plasma cholesterol in HDL particles unlike humans who mainly carry their cholesterol in LDL particles, possibly explaining their resistance to atherosclerosis (Getz and Reardon 2012; Meir and Leitersdorf 2004). Therefore, it is essential to manipulate the genes associated with lipid metabolism in mice to induce atherosclerotic plaques. The apoE- and LDLR-deficient mouse models are the two most commonly and widely employed traditional models for investigating atherogenesis (Plump et al. 1992; Piedrahita et al. 1992; Meir and Leitersdorf 2004; Veseli et al. 2017).

1.3.1 ApoE-deficient mice

ApoE is a glycoprotein (molecular size of approx. 34 kDa) that is synthesized mainly in the liver and brain (Veseli et al. 2017). It is a structural component of all lipoproteins except for LDL and serves as a ligand for lipoprotein receptors that functions to clear chylomicrons and VLDL particles (Veseli et al. 2017). Disruption of *ApoE* gene causes severe impairment in the clearance of chylomicrons and

VLDL remnants resulting in severe hypercholesterolemia in apoE KO mice (Plump et al. 1992). These mice exhibit enhanced plasma cholesterol (400-600 mg/dl) compared to wild-type mice (ranges between 75-110 mg/dl) when fed a normal diet; these plasma cholesterol levels are further increased (>1000 mg/dl) on a high-fat, Western type diet (containing 21% fat and 0.15% cholesterol) (Nakashima et al. 1994; Plump and Breslow 1995; Plump et al. 1992). Regardless of normal or high-fat diet, apoE-deficient mice develop extensive atherosclerotic plaques on both types of diets in 8-12 weeks of age (Reddick, Zhang, and Maeda 1994).

Some notable limitations of using apoE$^{-/-}$ mice includes: 1) the lipid metabolism is different between these mice and humans. ApoE KO mice possess elevated levels of plasma VLDL but increased LDL particles in circulation is a hallmark feature of atherosclerosis in humans (Plump et al. 1992). 2) In addition to lipid clearance, apoE also possesses diverse functions including cholesterol homeostasis and immunoregulation (Getz and Reardon 2009). These functions could also influence lesion formation in apoE$^{-/-}$ mice independent of plasma lipid levels. 3) Unless mechanistically induced (by placing perivascular collar) (von der Thüsen, van Berkel, and Biessen 2001), these mice do not develop plaque rupture and thrombosis, the events that are frequently seen in human atherosclerosis (Smith and Breslow 1997; Jawien, Nastalek, and Korbut 2004). Despite these drawbacks, apoE-deficient mice continue to be one of the most widely employed models in atherosclerosis due to their ability to develop atherosclerotic plaques spontaneously and diet-accelerated manner.

1.3.2 LDLR-deficient mice

LDL receptor is a membrane receptor (molecular size of 160 kDa) that facilitates the uptake of apoB-100 and apoE containing lipoproteins (Veseli et al. 2017). LDLR deficiency in mice causes a moderate increase (200-300 mg/dl) in plasma cholesterol levels and a mild increase or no changes in atherosclerotic plaque development when fed a normal diet (Ishibashi et al. 1993; Ishibashi et al. 1994). However, these mice exhibit elevated plasma cholesterol levels (>1000 mg/dl) and extensive atherosclerosis in response to a high-fat Western-type diet (Knowles and Maeda 2000; Veseli et al. 2017; Hartvigsen et al. 2007). The plasma cholesterol in LDLR KO mice is primarily carried by LDL particles, resembling human-like plasma lipid profiles (Lee et al. 2017; Hobbs et al. 1990). In addition, the disruption of the LDLR gene does not impact inflammation (Getz and Reardon 2012). Therefore, the effect of LDLR-deficiency on atherosclerosis is solely dependent on elevated plasma cholesterol levels. Despite the development of advanced lesions in a time-dependent manner on a high-fat diet, these mice also do not exhibit coronary artery occlusion, thrombosis, and myocardial infarction (Smith and Breslow 1997; Jawien, Nastalek, and Korbut 2004).

1.4 Sphingosine-1-phosphate synthesis, metabolism, and function

Sphingosine-1-phosphate (S1P), a lysosphingolipid mediator, broadly regulates multiple physiological functions by exerting its signal via five specific G-protein coupled receptors, referred to as S1PR1-5 (Sanchez and Hla 2004). Although

platelets and erythrocytes are a major source of plasma S1P, several cell types, including endothelial cells, leukocytes, and VSMC, also synthesize S1P (Dahm et al. 2006; Hänel, Andréani, and Gräler 2007). The intracellular levels of S1P are tightly regulated by the balance between its production and degradation **(Figure 1.2A)**. Inside the cells, S1P is produced from ceramide (Stunff, Milstien, and Spiegel 2004). The enzyme ceramidase catalyzes the conversion of ceramide to sphingosine, which in turn is phosphorylated to S1P by Sphingosine kinase (Sphk) 1 and 2. The synthesized S1P can be dephosphorylated to sphingosine via sphingosine phosphatases or irreversibly degraded by S1P lyase into ethanolamine phosphate and hexadecenal. In the context of atherosclerosis, genetically disrupting or manipulating metabolic enzymes involved in S1P synthesis altered S1P levels in plasma and yielded different atherogenic outcomes in murine models of atherosclerosis. For instance, inhibiting sphingosine kinase 1, an enzyme involved in S1P synthesis, caused prolonged reduction in plasma S1P and increased atherosclerotic lesions in $LDLR^{-/-}$ mice (Potì et al. 2015). However, inhibiting S1P-degrading enzyme S1P lyase raised endogenous S1P levels and drastically enhanced atherosclerosis and thrombosis in cholesterol-fed $apoE^{-/-}$ mice (Keul et al. 2022). So, the prolonged effect of raising or lowering plasma S1P on atherosclerosis is not known. The sphingolipid metabolites, S1P, and its precursors have opposing effects on cell fate. Higher levels of ceramide and sphingosine in the cell promote growth arrest and apoptosis, while increased levels of S1P promote cell growth and protect against apoptosis. The equilibrium between

S1P versus sphingosine and ceramide is crucial and often referred to as “sphingolipid rheostat” which determines the cell fate **(Figure 1.2B)**. Once synthesized within the cell, the S1P is exported outside the cell through different transporters, including spinster homolog 2 (Spns2) and Band 3 (Fukuhara et al. 2012). The majority of S1P (approx. 65%) in the circulation is known to be carried by apoM on HDL particles. Plasma S1P bound to HDL contributes to several atheroprotective functions of HDL and is inversely associated with CAD (Potì, Simoni, and Nofer 2014; Sattler et al. 2010; Keul et al. 2019). In addition, approx. 30% of plasma S1P associates with serum albumin and approx. 5 % associates with apolipoprotein B-containing lipoproteins (Kurano and Yatomi 2018). In addition, a recent study also identified ApoA4 as a novel S1P-binding protein that could activate several S1P receptors in the absence of apoM and albumin (Obinata et al. 2019).

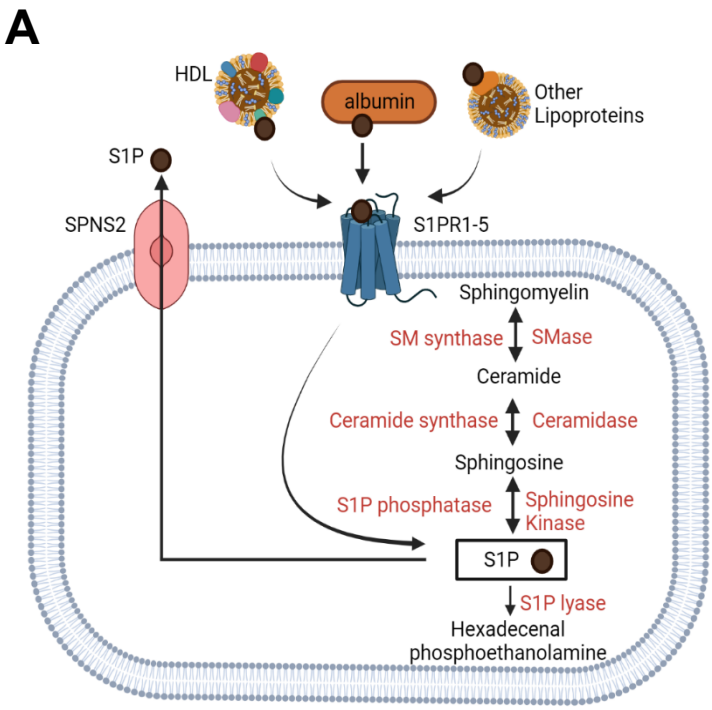
A
HDL
albumin
Other
Lipoproteins
S1P
SPNS2
S1PR1-5
Sphingomyelin
SM synthase
SMase
Ceramide
Ceramide synthase
Ceramidase
Sphingosine
S1P phosphatase
Sphingosine
Kinase
S1P
S1P lyase
Hexadecenal
phosphoethanolamine

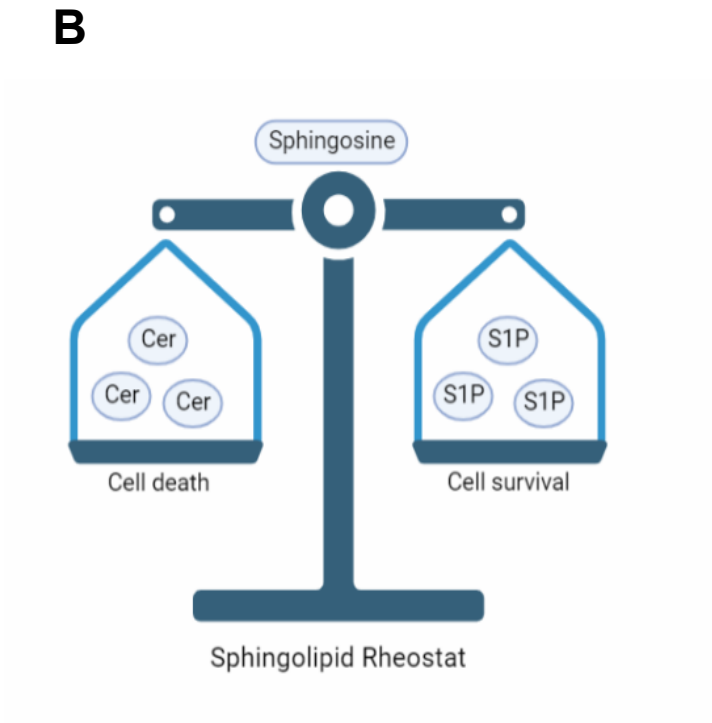
B
Sphingosine
Cer
Cer
Cer
Cell death
S1P
S1P
S1P
Cell survival
Sphingolipid Rheostat

Figure 1.2: Sphingolipid metabolism and sphingolipid rheostat

(A) The intermediate metabolite sphingosine is produced from ceramide which in turn is phosphorylated by sphingosine kinases to generate S1P. The S1P is irreversibly degraded by S1P lyase. The level of S1P is tightly regulated by sphingosine kinases, sphingosine phosphatase, and S1P lyase enzymes. Once synthesized, S1P is transported out of the cell through a sphingolipid transporter spns2. The plasma S1P is associated mainly with HDL followed by albumin. Less than 5 % of S1P also binds to other apoB-containing lipoproteins. Extracellularly, the S1P bound to these carriers signal via S1P receptors (S1PR) 1 to 5 to exert cellular functions. **(B)** The precursor ceramide and S1P have opposing roles in the cell. Ceramide regulates apoptosis whereas S1P promotes cell survival. The intracellular balance between these metabolites is referred to as sphingolipid rheostat (White et al. 2016). Created with BioRender.com

S1P signaling in cells and their effects on them may vary depending upon their association with different carriers/factors in the circulation. For example, a study by Ruiz et al (Ruiz et al. 2017) reported that at low concentrations (0.1 µmol/L) S1P associated with the apoM component of HDL decreased VCAM1 expression in the endothelial cells in response to TNF-α whereas S1P bound to albumin did not (however, both HDL- and albumin-bound S1P were equally effective at 0.5 µmol/L). Similarly, S1P carried by HDL was shown to exhibit more prolonged enhancement of endothelial cell barrier effects via S1PR1 when compared to S1P carried by albumin (Wilkerson et al. 2012). Furthermore, S1P bound to apoM-HDL was reported to enhance S1PR1-β-arrestin 2 complex formation, block NF-κB activation, and suppress ICAM-1 expression, whereas S1P bound to albumin stimulated Gi activation and caused S1PR1 endocytosis in human endothelial cells (Galvani et al. 2015). These results suggest that S1P carried by different chaperones may exert different S1P-dependent cellular responses.

In the extracellular environment, S1P associated with different carriers creates a spatial gradient activating S1PR1-5 in a paracrine and/or endocrine fashion (Cartier and Hla 2019) **(Figure 1.3)**. The activation of S1PRs induces conformational change allowing them to couple with different G proteins to recruit various downstream signaling pathways and elicit distinct cellular responses (O'Sullivan and Dev 2013). The activated receptor undergoes phosphorylation through a key regulatory enzyme GPCR kinase 2 (GRK2) which increases S1PRs

affinity to B-arrestins (B-arrestin 1 and 2), a scaffold protein that regulates receptor desensitization and internalization. S1PRs interaction with B-arrestins are critical to prevent excessive G protein-mediated signaling in cells. Among the S1PRs, S1PR1 exclusively couples with $G_{i/o}$ protein to activate PI3K, Ras, and phospholipase C pathways and inhibit adenylate cyclase which suppresses cAMP production. S1PR2-5 couples with G_q and/or $G_{12/13}$ in addition to $G_{i/o}$ protein to activate phospholipase C and Rho activation. S1P regulates a variety of cellular processes, including proliferation, migration, cytoskeleton rearrangements, and apoptosis via S1PR-mediated signaling pathways. In addition to signaling through S1PRs, S1P can signal intracellularly ie, independent of S1PRs. For instance, S1P has been shown to interact with multiple intracellular targets, including TNF receptor-associated factor 2 (Alvarez et al. 2010), histone deacetylases HDAC1 and 2 (Hait et al. 2009), and mitochondrial prohibitin 2 (Strub et al. 2011).

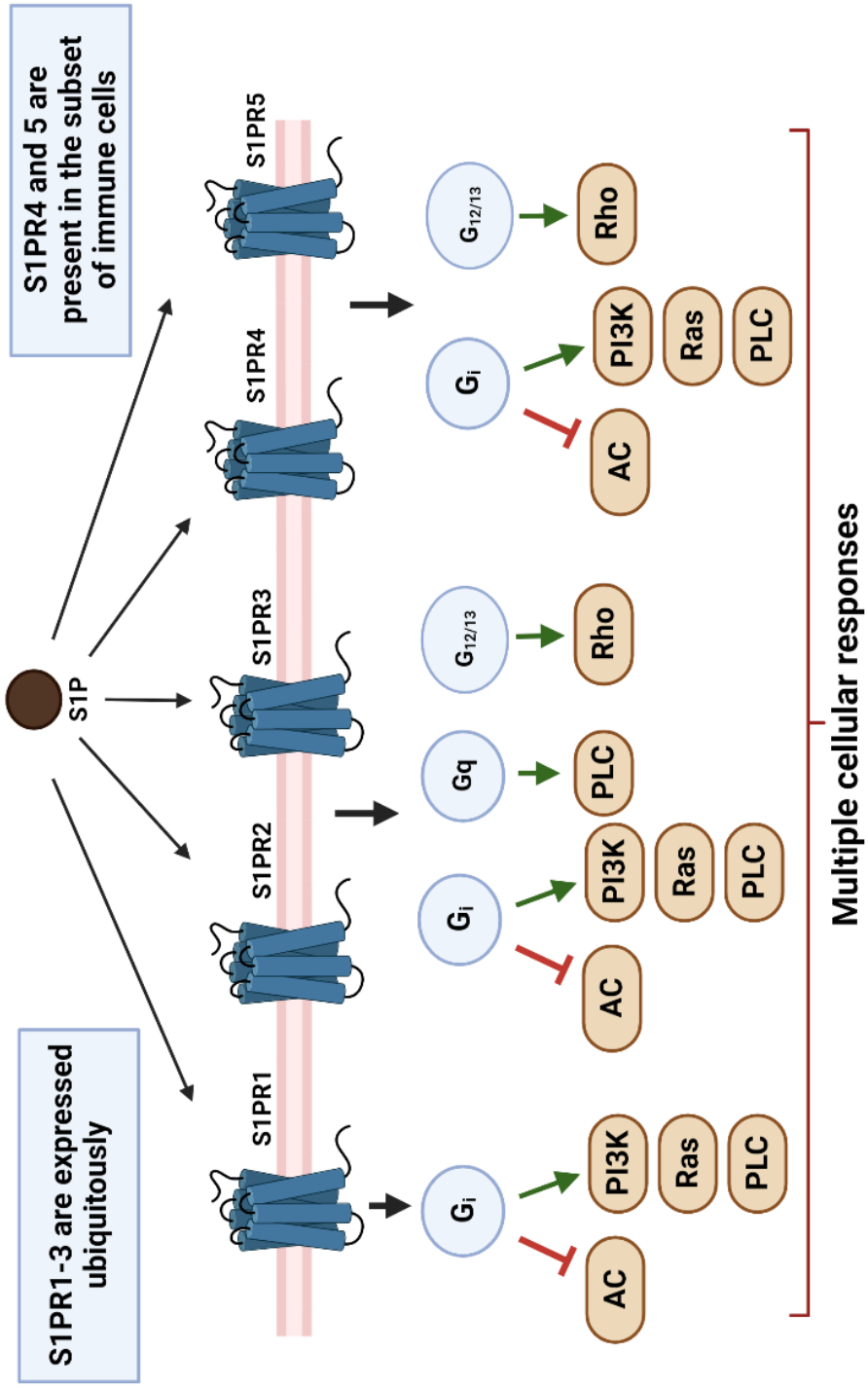
S1PR4 and 5 are present in the subset of immune cells
S1PR1-3 are expressed ubiquitously
S1P
S1PR1
S1PR2
S1PR3
S1PR4
S1PR5
Gi
Gq
G12/13
AC
PI3K
Ras
PLC
Rho
Multiple cellular responses

Figure 1.3: S1P-S1PR signaling

The bioactive lipid S1P bound to different carriers in the circulation exerts its physiological function by signaling through five different S1PRs. In response to S1P, S1PRs couple with different G-proteins to induce a series of downstream signaling pathways which in turn evoke a variety of cellular responses. S1PR1-3 are expressed ubiquitously while S1PR4 and 5 are expressed in subsets of immune cells. Created with BioRender.com

1.5 S1PR1 and its role in experimental atherosclerosis

1.5.1 S1PR1 structure, regulation, and function

S1PR1, like other G-protein coupled receptors (GPCRs), possesses seven hydrophobic transmembrane (TM) alpha helices, an extracellular N-terminus, and an intracellular C-terminus. It also possesses three extracellular loops (ECL1-3) and three intracellular loops (ICL1-3) (Parrill et al. 2000). Like other S1PRs, S1PR1 also spans approximately 400 amino acids in length. Examination of the S1PR1 crystal structure methods determined that the conserved D(E)RY and NPXXY domains in TM3 and TM7 are involved in the switch from an inactive to an active G-protein coupled form (Hanson et al. 2012). D-erytho and dihydro forms of S1P seem to have a greater affinity for S1PR1 compared to other S1P stereoisomers (O'Sullivan and Dev 2013). So far, three amino acids particularly in TM 3 and 7 (which includes Arg^{120} and Glu^{121} both in TM3 and Arg^{292} in TM7) of S1PR1 have been recognized to play a crucial role in S1P binding. Previous studies speculated that the positively charged amino acids Arg^{120} and Arg^{292} may interact with the negatively charged phosphate groups in S1P while negatively charged Glu^{121} may bind to protonated amino groups in S1P through hydrogen bonds (Rosen et al. 2013; O'Sullivan and Dev 2013).

FTY720, a synthetic mimic of S1P, binding to S1PR1 had been shown to cause receptor internalization and degradation (Mullershausen et al. 2009; Healy et al. 2013; Oo et al. 2007). Though S1P also causes internalization of S1PR1 they

subsequently recycle the receptor back to the plasma membrane (O'Sullivan and Dev 2013). The S1PR1 expression in the cell membrane is tightly regulated by activation, internalization, and degradation (Cartier and Hla 2019). A previous study showed that type II transmembrane protein CD69 interacts with the TM4 motif of S1PR1 to cause receptor internalization (Bankovich, Shiow, and Cyster 2010). Similarly, the phosphorylation of serine-rich residues in the C-terminal tail of S1PR1 by GRK2 causes β-arrestin-mediated receptor endocytosis (Oo et al. 2007); and polyubiquitination of lysine residues in the C-terminus of S1PR1 by E3 ubiquitin protein ligase 2 (WWP2) has been shown to cause S1PR1 degradation (Oo et al. 2011). In terms of function, S1PR1 plays critical roles in the vascular (promotes vascular stability and prevents vessel leakage), immune (regulates lymphocyte trafficking and survival), and central nervous systems (regulates neuroinflammation and involved in neurogenerative diseases) (Cartier and Hla 2019).

1.5.2 S1PR1 in experimental atherosclerosis

Previous studies demonstrated that FTY720 reduces atherosclerotic lesions and stimulates an anti-inflammatory response in both apoE KO and LDLR KO mice on a Western diet (Keul et al. 2007; Nofer et al. 2007b; Poti et al. 2012). Similarly, pharmacological treatment with the S1PR1 selective agonist, KRP203, substantially reduced atherosclerotic plaque development and reduced circulating lymphocyte counts in LDLR KO mice on a Western diet (Potì et al. 2013). However, another study reported that treatment with FTY720 or another S1PR1 selective

agonist, CYM5442, down-regulated macrophage pro-inflammatory cytokine production but failed to protect against diet-induced atherosclerosis in LDLR KO mice (Poti et al. 2012). Thus, pharmacological studies using S1PR1 agonists do not provide clear insight into the role of S1PR1 in experimental atherosclerosis.

1.6 Cell-specific roles of S1PR1 in atherosclerosis

The vascular wall comprises of several cell types, the most critical ones being endothelial cells, macrophages, and VSMC due to their implications in atherogenesis.

1.6.1 Role of S1PR1 in endothelial cells

S1PR1 was initially termed endothelial differentiation gene-1 (EDG1) due to its high abundance and its critical functions in the endothelial cells (Hla and Maciag 1990; Lee et al. 1998; Potì, Simoni, and Nofer 2014). S1PR1 in these cells plays a prominent role in the regulation of vascular tone, barrier integrity, and inflammatory response (Wilkerson et al. 2012; Kimura et al. 2006; Allende, Yamashita, and Proia 2003; Galvani et al. 2015; Sammani et al. 2010). The impairment of these endothelial cell functions is often associated with several vascular diseases, including atherosclerosis.

NO is a signaling molecule and a key vasodilatory substance produced by endothelial nitric oxide synthase (eNOS) (Dudzinski and Michel 2007). It regulates several physiological functions, including vascular tone in the endothelial cells. Impairment of NO generation and eNOS activity results in endothelial dysfunction,

a hallmark feature of atherosclerosis (Gimbrone Jr and García-Cardeña 2016). Previous *in-vitro* studies had reported that S1P promotes the activation of PI3K/Akt/eNOS and NO production via S1PR1 in the endothelial cells (Wilkerson et al. 2012; Kimura et al. 2006; Morales-Ruiz et al. 2001). In addition, a study by Cantalupo et al. (Cantalupo et al. 2017) directly examined the role of S1PR1 in regulating vascular tone and BP homeostasis in mice lacking S1PR1 in endothelial cells. Their results showed that knocking out S1PR1 in endothelial cells enhanced high blood pressure and suppressed flow-mediated vasodilation *in-vivo*. These findings suggest that S1PR1 signaling in endothelial cells may play a critical role in promoting vasorelaxation and in regulating vascular tone.

Endothelial-S1PR1 is also essential to maintain vascular barrier function. Genetic disruption of the *S1pr1* gene solely in endothelial cells has been shown to cause embryonic lethality in mice due to massive vascular hemorrhage and impaired vascular maturation (Allende, Yamashita, and Proia 2003). S1P-S1PR1 signaling in endothelial cells has been shown to mediate cell survival, cytoskeleton reorganization, and adherens junction assembly primarily through the Rac pathway (Lee et al. 1999; Singleton et al. 2005). Previous studies had shown that short-term administration of potent S1PR1 agonist FTY720 or selective S1PR1 agonists, (such as SEW2871) promoted vascular barrier functions and prevented vascular leakage in murine models of lung injury (Sammani et al. 2010; Camp et al. 2009). However, their extended administration has been shown to increase vessel leakage, fibrosis, and mortality after lung injury (Shea et al. 2010). This could likely

account from internalization and degradation of S1PR1 in the endothelial cells (LaMontagne et al. 2006; Oo et al. 2007; Krump-Konvalinkova, Chwalla, and Siess 2008). Thus, S1PR1 activation in endothelial cells may protect barrier integrity while their inactivation in these cells may have opposing effects.

Several *in-vitro* studies previously reported that HDL-associated S1P suppresses TNF-α-mediated enhancement of adhesion molecule expression in the endothelial cells via S1PR1 signaling pathways (Kimura et al. 2006; Ruiz et al. 2017; Galvani et al. 2015). In addition, activation of S1PR1 with S1P or selective agonist SEW2871 blocked monocyte-endothelial cell interaction (Bolick et al. 2005; Whetzel et al. 2006); while silencing S1PR1 prevented monocyte adhesion to the vascular endothelial cells in response to pro-inflammatory cytokine (Bolick et al. 2005). Furthermore, deleting *S1pr1* under the control of a tamoxifen-inducible endothelial cell-specific promoter substantially enhanced atherosclerotic plaque development in HF-diet fed apoE-deficient mice (Galvani et al. 2015). Collectively, these findings suggest that S1P-S1PR1 signaling in endothelial cells may prevent atherosclerosis by inhibiting the abundance of adhesion molecules and monocyte adhesion to the vascular endothelium.

1.6.2 Role of S1PR1 in macrophages

S1P-S1PR1 signaling has been reported to affect polarization, emigration, and apoptosis in macrophages. S1P had previously been shown to notably decrease TNF-α, MCP-1, and IL-12 secretion in response to LPS in cultured macrophages

(Hughes et al. 2008). In addition, S1P treatment also markedly reduced iNOS expression by inhibiting the NF-κB pathway and enhanced arginase 1 activity in macrophages in-vitro. A similar effect was observed when macrophages were stimulated with the S1PR1 selective agonist SEW2871, whereas opposite effects were seen with S1PR1 selective antagonist VPC44116. Furthermore, FTY720, a potent agonist for S1PRs except for S1PR2, had previously been shown to attenuate LPS-mediated classical M1 phenotype activation while enhancing IL-4-mediated alternative M2 phenotype activation in cultured macrophages (Nofer et al. 2007a). Similarly, the S1PR1 selective agonist KRP203 also inhibited macrophage activation in-vitro. KRP203 treatment has been shown to substantially lower pro-inflammatory cytokines (such as TNF-α and IL-6) and impair activation of transcription factors (NF-κB and STAT1) in cultured macrophages in response to poly(I:C) or LPS (Potì et al. 2013). Additionally, macrophages overexpressing S1PR1 exhibit increased IL-10, IL-5, and IL-1RA levels, indicating an anti-inflammatory M2 phenotype (Potì et al. 2020). Taken together, these findings suggest that S1PR1 signaling promotes anti-inflammatory M2 phenotype in macrophages.

The migratory capacity of macrophages is compromised in the atherosclerotic plaques. Both hypoxia and elevated cellular cholesterol content have been identified as factors resulting in reduced macrophage migration (Nagao et al. 2007; Park et al. 2012; Qin et al. 2006; Ramkhelawon et al. 2013). However, macrophage migration is critical for their exit from the plaque and for promoting the

regression of atherosclerotic plaques (Llodrá et al. 2004; Williams, Feig, and Fisher 2008). A previous study by Al-Jarallah reported that HDL, the S1PR1 potent agonist FTY720, and the S1PR1 selective agonist SEW2871 stimulate migration in macrophages (Al-Jarallah et al. 2014). However, these effects were blocked when macrophages were treated with the S1PR1 selective antagonist W146 or lacked the HDL receptor SR-B1. These results suggest that HDL-dependent migration in macrophages requires both SR-B1 and S1PR1 activity.

S1PR1 in macrophages has been shown to protect against atherosclerosis; specifically, the selective knockout of S1PR1 in bone marrow (BM)-derived myeloid cells was shown to enhance lesion formation, apoptotic cell accumulation within the atherosclerotic plaques, and necrotic core development in HF-diet fed LDLR KO mice (Gonzalez et al. 2017). Treatment of cultured macrophages with the S1PR1 selective agonist SEW2871 or HDL prevented ER stress or oxLDL-mediated apoptosis and these effects were blocked by S1PR1 knockout in macrophages (Gonzalez et al. 2017). Consistent with this, overexpressing S1PR1 in BM-derived myeloid cells provided protection against atherosclerotic plaque development and necrotic core formation in HF diet-fed LDLR KO mice and S1PR1 overexpressing macrophages also displayed enhanced ABCA1 and ABCG1-regulated cholesterol efflux, increased efferocytosis, and reduced apoptosis mediated by ER stress *in-vitro* (Potì et al. 2020). Collectively, these studies demonstrate that S1P-S1PR1 signaling in macrophages inhibits apoptosis and

promotes M2 polarization, migration, and cholesterol efflux, thereby mediating protection against atherosclerosis (Gonzalez et al. 2017).

1.6.3 Role of S1PR1 in VSMCs

1.6.3.1 S1P-S1PR1 signaling in VSMC proliferation and migration

VSMCs are known to express S1PR1, S1PR2, and S1PR3 (Wamhoff et al. 2008). S1P had been shown to enhance both proliferation and migration in VSMCs via S1PR1 and 3 (Kluk and Hla 2001; Shimizu et al. 2012), whereas these processes are suppressed by S1PR2 (Shimizu et al. 2007; Okamoto et al. 2000; Ryu et al. 2002).

A previous study by Hla and colleagues reported that S1PR1 coupling to Gi protein, in response to S1P, is a critical step in mediating proliferation and migration in adult medial VSMCs (Kluk and Hla 2001). In addition, several other studies have demonstrated that S1PR1 interacts with tyrosine kinase receptors, particularly PDGFR to regulate these processes in VSMCs**.** So far, three different models have been proposed for signal integration between S1PR1 and PDGFR in SMCs (Hobson et al. 2001; Rosenfeldt, Hobson, Maceyka, et al. 2001; Rosenfeldt, Hobson, Milstien, et al. 2001; Tanimoto, Lungu, and Berk 2004; Waters et al. 2003). These models are sequential, transactivation, and integrative models **(Figure 1.4)**. 1) In support of the sequential model, PDGF-PDGFR signaling has been shown to stimulate SPHK1 which in turn enhances production of S1P. This further causes S1P-mediated activation of S1PR1 which leads to Rac, focal

adhesion kinase, and c-src mediated migration (Hobson et al. 2001; Rosenfeldt, Hobson, Maceyka, et al. 2001; Rosenfeldt, Hobson, Milstien, et al. 2001). 2) In support of the transactivation model, S1P binding to S1PR1 has been shown to stimulate the transactivation of tyrosine kinase receptors, such as EGFR and PDGFR, to promote proliferation in rat aortic VSMCs (Tanimoto, Lungu, and Berk 2004). It also appears to be that S1P-mediated transactivation of EGFR and PDGFR requires intact cholesterol-rich cell membranes, proto-oncogene c-src, and ROS generation. 3) In support of the integrative model, both S1PR1 and PDGFR were shown to form complexes and co-internalize together instead of one activating/transactivating the other (Waters et al. 2003). Although these models strongly suggested cross-talk between S1PR1 and PDGFR, a different study reported that S1PR1 and PDGFR independently promote migration in response to their ligands and that S1PR1 expression is not essential for PDGF-mediated chemotaxis in VSMCs (Kluk et al. 2003).

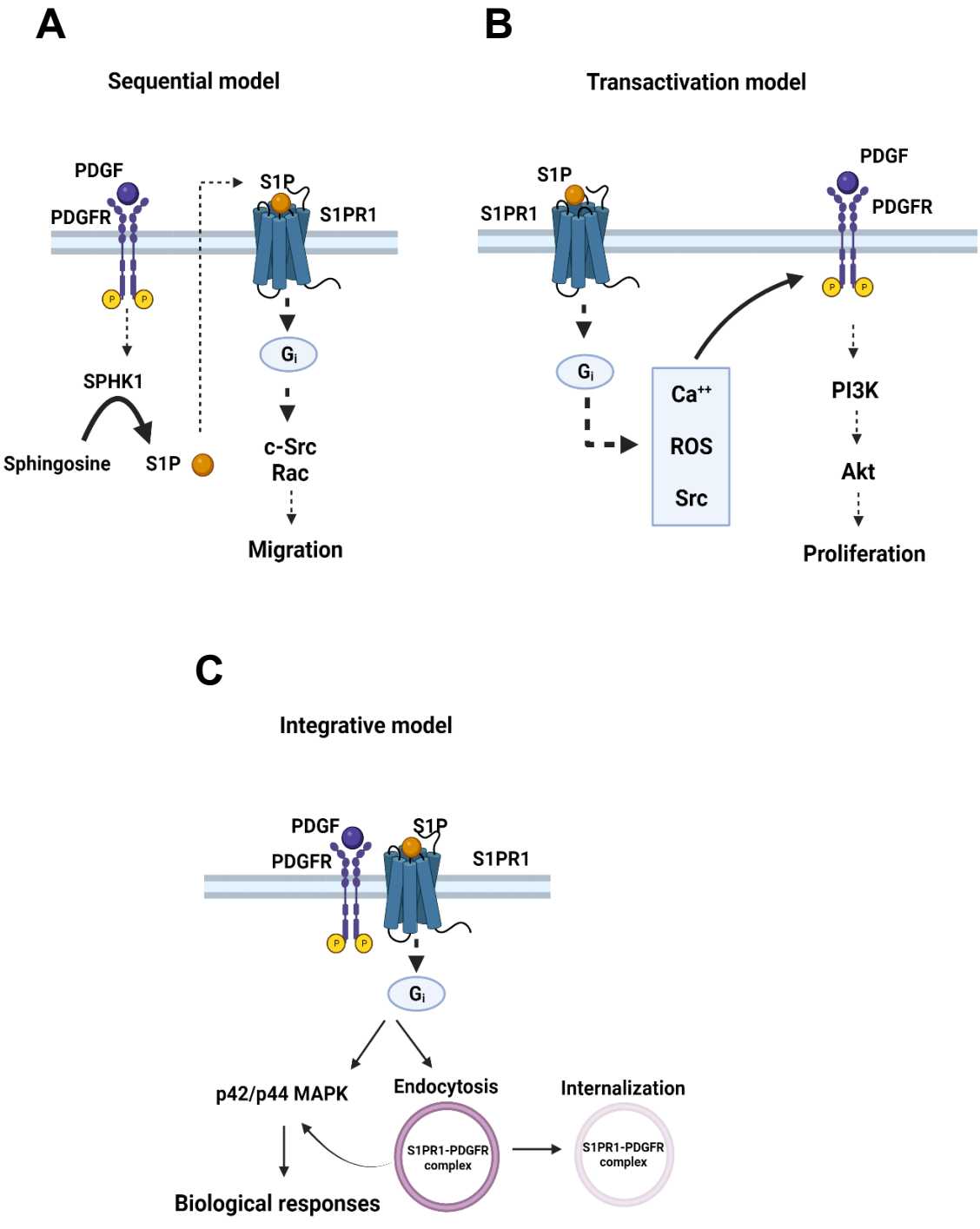
A
Sequential model
PDGF
PDGFR
S1P
S1PR1
SPHK1
Sphingosine
S1P
Gi
c-Src
Rac
Migration
B
Transactivation model
S1P
S1PR1
PDGF
PDGFR
Gi
Ca++
ROS
Src
PI3K
Akt
Proliferation
C
Integrative model
PDGF
PDGFR
S1P
S1PR1
Gi
p42/p44 MAPK
Endocytosis
Internalization
S1PR1-PDGFR complex
S1PR1-PDGFR complex
Biological responses

Figure 1.4: Cross communication between S1PR1 and PDGFR

Three models have been proposed for the functional link between S1PR1 and PDGFR. This includes **(A)** Sequential model, in which PDGF-PDGFR signaling induces sphingosine kinase levels which in turn stimulates S1P-mediated S1PR1 downstream signaling to promote cell motility. **(B)** Transactivation model, in which S1P-S1PR1 signaling transactivates PDGFR-mediated downstream signaling to induce proliferation in cells. This transactivation is dependent on Ca++, ROS, and Src. **(C)** The integrative model involves complex formation between both S1PR1 and PDGFR in response to S1P and PDGF ligands. These ligands promote the formation of endocytic vesicles containing both S1PR1 and PDGFR and their subsequent internalization. S1PR1-PDGFR complex stimulated the P42/p44 MAPK pathway to exert cellular responses. Created with BioRender.com

1.6.3.2 S1PR1 signaling in VSMC phenotype switching

Under normal circumstances, medial SMC in the arterial wall exist in the contractile phenotype, and express contractile marker genes, including *Acta2*, *Myh11*, and *Tagln* (Gomez and Owens 2012). Due to their remarkable plasticity, VSMC transforms from contractile to a highly proliferative synthetic state in response to inflammatory cues, different mitogens, and bioactive lipids. Some studies had shown that VSMC can accumulate lipid droplets, lose their lineage markers and transdifferentiate into macrophage-like cells by gaining the expression of macrophage lineage markers (such as CD68) (Rong et al. 2003; Feil et al. 2014; Matsumoto et al. 2000). A study by Wamhoff et al. (Wamhoff et al. 2008) showed that the treatment of rat aortic SMC with S1P increased the promoter activity of SMC differentiation marker genes. The authors also showed that treatment of VSMCs with FTY720, a drug that activates S1PRs except S1PR2, diminished the promoter activity of SMC differentiation marker genes. In addition, they also noticed that overexpressing S1PR1 in VSMC suppressed while overexpressing S1PR2 enhanced SMA promoter activity. Although their results suggested that the activation of S1PR1 results in down-regulation of contractile marker gene levels, a characteristic feature of SMC phenotype modulation, it is not clear if S1P-S1PR1 signaling plays a role in SMC-to-macrophage phenotype switching, and how that may impact atherosclerosis.

1.6.3.3 S1PR1 in vascular remodelling and atherosclerosis

Vascular remodelling occurs as a consequence of aberrant proliferation and migration of VSMCs, and it's one of the major causes of atherosclerosis. Although the influence of VSMC-specific S1PR1 was not directly evaluated in atherosclerosis *in-vivo*, its role in vascular remodelling was reported previously in two studies (Wamhoff et al. 2008; Kitano et al. 2019). A study by Wamhoff et al.(Wamhoff et al. 2008) assessed the effects of S1PR1 and S1PR3 antagonism on neointimal thickening in a rat carotid artery balloon injury model. While balloon injury-induced neointimal formation represents a different model compared to native atherosclerosis, their results demonstrated that the treatment with VPC44116, an antagonist for both S1PR1 and S1PR3, decreased neointimal hyperplasia by 50% while VPC01091 (an agonist for S1PR1 and antagonist for S1PR3) promoted neointimal thickness. Likewise, Kitano et al (Kitano et al. 2019) investigated the effect of overexpressing S1PR1 in VSMCs on neointimal formation in a mouse carotid artery ligation model. Their study reported that VSMC-specific S1PR1 overexpression promotes neointimal hyperplasia in response to vessel injury; and aortic SMCs isolated from these mice also exhibit enhanced IL6 expression. Together, these findings suggest that S1PR1 promotes vascular remodelling, and thus may have implications in atherosclerosis.

1.7 Overall context and objective

The role of S1PR1 has been extensively studied in endothelial cells and macrophages. In endothelial cells, S1PR1 was reported to promote barrier integrity, vascular tone, and anti-inflammatory response (Kimura et al. 2006; Wilkerson et al. 2012; Galvani et al. 2015). Similarly, this receptor has been shown to enhance M2 phenotype, anti-apoptosis, and migration in macrophages (Al-Jarallah et al. 2014; Potì et al. 2020; Nofer et al. 2007a). Indeed, conditionally knocking out this receptor in both macrophages and endothelial cells has been shown to enhance lesion formation in atherogenic mouse models (Galvani et al. 2015; Gonzalez et al. 2017). On the other hand, S1PR1 had been demonstrated to enhance proliferation and migration in aortic SMCs *in-vitro*; and overexpressing this receptor in SMCs enhanced pro-inflammatory cytokine IL6 expression and promoted neointimal thickening in carotid artery ligation model (Kitano et al. 2019). These findings suggest that S1PR1 may have a pro-atherogenic effect in VSMCs; thus, knocking out S1PR1 in VSMC may protect against atherosclerosis.

Pharmacological delivery of S1PR1 agonist FTY720 and selective agonist KRP203 abrogated lesion formation in atherogenic mice backgrounds when fed a Western diet (Nofer et al. 2007a; Potì et al. 2013; Keul et al. 2007). However, these results had not been consistently observed by other studies (Poti et al. 2012). This discrepancy in the atherosclerotic outcomes could likely be due to the dual nature of these synthetic compounds to act both as agonists and functional antagonists (due to receptor internalization and degradation) (Sykes et al. 2014). Alternatively,

the discrepant results may reflect the balance of differential outcomes of S1PR1 inhibition in different cell types.

1.8 Hypothesis

I hypothesize that inhibition of S1PR1 in VSMCs will protect against atherosclerosis in apoE-deficient mice

1.9 Specific Aims

Aim of Chapter 2

- To examine the effects of inactivating *S1pr1* gene expression in VSMCs on diet-induced atherosclerosis in *ApoE*$^{KO/KO}$ mice

Aim of Chapter 3

- To investigate the effect of pharmacological inhibition of S1PR1 using the S1PR1 selective antagonist Ex26 on atherosclerosis in *ApoE*$^{KO/KO}$ mice.

References

Abdullahi, Wazir, Dinesh Tripathi, and Patrick T Ronaldson. 2018. 'Blood-brain barrier dysfunction in ischemic stroke: targeting tight junctions and transporters for vascular protection', *American Journal of Physiology-Cell Physiology*, 315: C343-C56.

Ait-Oufella, Hafid, Vahid Pouresmail, Tabassome Simon, Olivier Blanc-Brude, Kiyoka Kinugawa, Régine Merval, Georges Offenstadt, Guy Leseche, Philip L Cohen, and Alain Tedgui. 2008. 'Defective mer receptor tyrosine kinase signaling in bone marrow cells promotes apoptotic cell accumulation and accelerates atherosclerosis', *Arteriosclerosis, thrombosis, and vascular biology*, 28: 1429-31.

Al-Jarallah, Aishah, Xing Chen, Leticia Gonzalez, and Bernardo L Trigatti. 2014. 'High density lipoprotein stimulated migration of macrophages depends on the scavenger receptor class B, type I, PDZK1 and Akt1 and is blocked by sphingosine 1 phosphate receptor antagonists', *PloS one*, 9: e106487.

Allahverdian, S., A. C. Chehroudi, B. M. McManus, T. Abraham, and G. A. Francis. 2014a. 'Contribution of intimal smooth muscle cells to cholesterol accumulation and macrophage-like cells in human atherosclerosis', *Circulation*, 129: 1551-9.

Allahverdian, Sima, Chiraz Chaabane, Kamel Boukais, Gordon A Francis, and Marie-Luce Bochaton-Piallat. 2018. 'Smooth muscle cell fate and plasticity in atherosclerosis', *Cardiovascular research*, 114: 540-50.

Allahverdian, Sima, Ali Cyrus Chehroudi, Bruce M McManus, Thomas Abraham, and Gordon A Francis. 2014b. 'Contribution of intimal smooth muscle cells to cholesterol accumulation and macrophage-like cells in human atherosclerosis', *Circulation*, 129: 1551-59.

Allende, Maria L, Tadashi Yamashita, and Richard L Proia. 2003. 'G-protein-coupled receptor S1P1 acts within endothelial cells to regulate vascular maturation', *Blood*, 102: 3665-67.

Alvarez, Sergio E, Kuzhuvelil B Harikumar, Nitai C Hait, Jeremy Allegood, Graham M Strub, Eugene Y Kim, Michael Maceyka, Hualiang Jiang, Cheng Luo, and Tomasz Kordula. 2010. 'Sphingosine-1-phosphate is a missing cofactor for the E3 ubiquitin ligase TRAF2', *Nature*, 465: 1084-88.

Arai, Satoko, John M Shelton, Mingyi Chen, Michelle N Bradley, Antonio Castrillo, Angie L Bookout, Puiying A Mak, Peter A Edwards, David J Mangelsdorf, and Peter Tontonoz. 2005. 'A role for the apoptosis inhibitory factor AIM/Spα/Api6 in atherosclerosis development', *Cell metabolism*, 1: 201-13.

Babij, Philip, Carol Kelly, and Muthu Periasamy. 1991. 'Characterization of a mammalian smooth muscle myosin heavy-chain gene: complete nucleotide and protein coding sequence and analysis of the 5'end of the gene', *Proceedings of the National Academy of Sciences*, 88: 10676-80.

Bankovich, Alexander J, Lawrence R Shiow, and Jason G Cyster. 2010. 'CD69 suppresses sphingosine 1-phosophate receptor-1 (S1P1) function through

interaction with membrane helix 4', *Journal of Biological Chemistry*, 285: 22328-37.

Björkegren, Johan LM, and Aldons J Lusis. 2022. 'Atherosclerosis: recent developments', *Cell*.

Bolick, David T, Suseela Srinivasan, Kyu W Kim, Melissa E Hatley, Jeremy J Clemens, Angela Whetzel, Nicole Ferger, Timothy L Macdonald, Michael D Davis, and Philip S Tsao. 2005. 'Sphingosine-1-phosphate prevents tumor necrosis factor-α–mediated monocyte adhesion to aortic endothelium in mice', *Arteriosclerosis, thrombosis, and vascular biology*, 25: 976-81.

Bond, Andrew R, and Christopher L Jackson. 2010. 'The fat-fed apolipoprotein E knockout mouse brachiocephalic artery in the study of atherosclerotic plaque rupture', *Journal of Biomedicine and Biotechnology*, 2011.

Bonert, Michael, Richard L Leask, Jagdish Butany, C Ross Ethier, Jerry G Myers, K Wayne Johnston, and Matadial Ojha. 2003. 'The relationship between wall shear stress distributions and intimal thickening in the human abdominal aorta', *Biomedical engineering online*, 2: 1-14.

Buschmann, Ivo, Matthias Heil, Marco Jost, and Wolfgang Schaper. 2003. 'Influence of inflammatory cytokines on arteriogenesis', *Microcirculation*, 10: 371-79.

Camp, SM, R Bittman, ET Chiang, L Moreno-Vinasco, T Mirzapoiazova, S Sammani, X Lu, C Sun, M Harbeck, and M Roe. 2009. 'Synthetic analogs of FTY720 [2-amino-2-(2-[4-octylphenyl] ethyl)-1, 3-propanediol]

differentially regulate pulmonary vascular permeability in vivo and in vitro', *Journal of Pharmacology and Experimental Therapeutics*, 331: 54-64.

Cantalupo, Anna, Antonella Gargiulo, Elona Dautaj, Catherine Liu, Yi Zhang, Timothy Hla, and Annarita Di Lorenzo. 2017. 'S1PR1 (sphingosine-1-phosphate receptor 1) signaling regulates blood flow and pressure', *Hypertension*, 70: 426-34.

Caplice, Noel M, T Jared Bunch, Paul G Stalboerger, Shaohua Wang, David Simper, Dylan V Miller, Stephen J Russell, Mark R Litzow, and William D Edwards. 2003. 'Smooth muscle cells in human coronary atherosclerosis can originate from cells administered at marrow transplantation', *Proceedings of the National Academy of Sciences*, 100: 4754-59.

Cartier, Andreane, and Timothy Hla. 2019. 'Sphingosine 1-phosphate: Lipid signaling in pathology and therapy', *Science*, 366: eaar5551.

Chen, Pei-Yu, Lingfeng Qin, Nicolas Baeyens, Guangxin Li, Titilayo Afolabi, Madhusudhan Budatha, George Tellides, Martin A Schwartz, and Michael Simons. 2015. 'Endothelial-to-mesenchymal transition drives atherosclerosis progression', *The Journal of clinical investigation*, 125: 4514-28.

Chinetti-Gbaguidi, Giulia, Morgane Baron, Mohamed Amine Bouhlel, Jonathan Vanhoutte, Corinne Copin, Yasmine Sebti, Bruno Derudas, Thérèse Mayi, Gael Bories, and Anne Tailleux. 2011. 'Human atherosclerotic plaque alternative macrophages display low cholesterol handling but high

phagocytosis because of distinct activities of the PPARγ and LXRα pathways', *Circulation research*, 108: 985-95.

Coen, Matteo, Giulio Gabbiani, and Marie-Luce Bochaton-Piallat. 2011. 'Myofibroblast-mediated adventitial remodeling: an underestimated player in arterial pathology', *Arteriosclerosis, thrombosis, and vascular biology*, 31: 2391-96.

Colin, Sophie, Giulia Chinetti-Gbaguidi, and Bart Staels. 2014. 'Macrophage phenotypes in atherosclerosis', *Immunological reviews*, 262: 153-66.

Collins, Tucker, and Myron I Cybulsky. 2001. 'NF-κB: pivotal mediator or innocent bystander in atherogenesis?', *The Journal of clinical investigation*, 107: 255-64.

Cybulsky, Myron I, Kaeko Iiyama, Hongmei Li, Suning Zhu, Mian Chen, Motoi Iiyama, Vannessa Davis, Jose-Carlos Gutierrez-Ramos, Philip W Connelly, and David S Milstone. 2001. 'A major role for VCAM-1, but not ICAM-1, in early atherosclerosis', *The Journal of clinical investigation*, 107: 1255-62.

Dahm, F, A Nocito, A Bielawska, KS Lang, P Georgiev, LM Asmis, J Bielawski, J Madon, YA Hannun, and P-A Clavien. 2006. 'Distribution and dynamic changes of sphingolipids in blood in response to platelet activation', *Journal of Thrombosis and Haemostasis*, 4: 2704-09.

Davignon, Jean, and Peter Ganz. 2004. 'Role of endothelial dysfunction in atherosclerosis', *Circulation*, 109: III-27-III-32.

Dong, Zhao Ming, Susan M Chapman, Allison A Brown, Paul S Frenette, Richard O Hynes, and Denisa D Wagner. 1998. 'The combined role of P-and E-selectins in atherosclerosis', *The Journal of clinical investigation*, 102: 145-52.

Drexler, Helmut. 1998. 'Factors involved in the maintenance of endothelial function', *American Journal of Cardiology*, 82: 3S-4S.

Duband, Jean-Loup, Mario Gimona, Marta Scatena, Saverio Sartore, and J Victor Small. 1993. 'Calponin and SM22 as differentiation markers of smooth muscle: spatiotemporal distribution during avian embryonic development', *Differentiation*, 55: 1-11.

Dubland, Joshua A, Sima Allahverdian, Katrina J Besler, Carleena Ortega, Ying Wang, Collin S Pryma, Kamel Boukais, Teddy Chan, Michael A Seidman, and Gordon A Francis. 2021. 'Low LAL (lysosomal acid lipase) expression by smooth muscle cells relative to macrophages as a mechanism for arterial foam cell formation', *Arteriosclerosis, thrombosis, and vascular biology*, 41: e354-e68.

Dudzinski, David M, and Thomas Michel. 2007. 'Life history of eNOS: partners and pathways', *Cardiovascular research*, 75: 247-60.

Duran, Edward K, and Aruna D Pradhan. 2021. 'Triglyceride-rich lipoprotein remnants and cardiovascular disease', *Clinical Chemistry*, 67: 183-96.

Eun, So Young, Young Shin Ko, Sang Won Park, Ki Churl Chang, and Hye Jung Kim. 2015. 'IL-1β enhances vascular smooth muscle cell proliferation and

migration via P2Y2 receptor-mediated RAGE expression and HMGB1 release', *Vascular pharmacology*, 72: 108-17.

Evrard, Solene M, Laura Lecce, Katherine C Michelis, Aya Nomura-Kitabayashi, Gaurav Pandey, K-Raman Purushothaman, Valentina d'Escamard, Jennifer R Li, Lahouaria Hadri, and Kenji Fujitani. 2016. 'Endothelial to mesenchymal transition is common in atherosclerotic lesions and is associated with plaque instability', *Nature communications*, 7: 11853.

Feil, Susanne, Birgit Fehrenbacher, Robert Lukowski, Frank Essmann, Klaus Schulze-Osthoff, Martin Schaller, and Robert Feil. 2014. 'Transdifferentiation of vascular smooth muscle cells to macrophage-like cells during atherogenesis', *Circulation research*, 115: 662-67.

Feng, Bo, Pin Mei Yao, Yankun Li, Cecilia M Devlin, Dajun Zhang, Heather P Harding, Michele Sweeney, James X Rong, George Kuriakose, and Edward A Fisher. 2003. 'The endoplasmic reticulum is the site of cholesterol-induced cytotoxicity in macrophages', *Nature cell biology*, 5: 781-92.

Foks, Amanda C, Daniel Engelbertsen, Felicia Kuperwaser, Noah Alberts-Grill, Ayelet Gonen, Joseph L Witztum, James Lederer, Petr Jarolim, Rosemarie H DeKruyff, and Gordon J Freeman. 2016. 'Blockade of Tim-1 and Tim-4 enhances atherosclerosis in low-density lipoprotein receptor–deficient mice', *Arteriosclerosis, thrombosis, and vascular biology*, 36: 456-65.

Frank, Philippe G., Stephanos Pavlides, and Michael P. Lisanti. 2009. ‘Caveolae and transcytosis in endothelial cells: role in atherosclerosis.’ *Cell and tissue research*, 335: 41-47.

Fukuhara, Shigetomo, Szandor Simmons, Shunsuke Kawamura, Asuka Inoue, Yasuko Orba, Takeshi Tokudome, Yuji Sunden, Yuji Arai, Kazumasa Moriwaki, and Junji Ishida. 2012. 'The sphingosine-1-phosphate transporter Spns2 expressed on endothelial cells regulates lymphocyte trafficking in mice', *The Journal of clinical investigation*, 122: 1416-26.

Gabbiani, Giulio, Erika Schmid, Stefanie Winter, Christine Chaponnier, C De Ckhastonay, Joel Vandekerckhove, Klaus Weber, and Werner W Franke. 1981. 'Vascular smooth muscle cells differ from other smooth muscle cells: predominance of vimentin filaments and a specific alpha-type actin', *Proceedings of the National Academy of Sciences*, 78: 298-302.

Galkina, Elena, Alexandra Kadl, John Sanders, Danielle Varughese, Ian J Sarembock, and Klaus Ley. 2006. 'Lymphocyte recruitment into the aortic wall before and during development of atherosclerosis is partially L-selectin dependent', *The Journal of experimental medicine*, 203: 1273-82.

Galvani, Sylvain, Marie Sanson, Victoria A Blaho, Steven L Swendeman, Hideru Obinata, Heather Conger, Björn Dahlbäck, Mari Kono, Richard L Proia, and Jonathan D Smith. 2015. 'HDL-bound sphingosine 1-phosphate acts as a biased agonist for the endothelial cell receptor S1P1 to limit vascular inflammation', *Science signaling*, 8: ra79-ra79.

Gautier, Emmanuel L, Thierry Huby, Joseph L Witztum, Betty Ouzilleau, Elizabeth R Miller, Flora Saint-Charles, Pierre Aucouturier, M John Chapman, and Philippe Lesnik. 2009. 'Macrophage apoptosis exerts divergent effects on atherogenesis as a function of lesion stage', *Circulation*, 119: 1795-804.

Gerrity, Ross G. 1981. 'The role of the monocyte in atherogenesis: I. Transition of blood-borne monocytes into foam cells in fatty lesions', *The American journal of pathology*, 103: 181.

Getz, Godfrey S, and Catherine A Reardon. 2009. 'Apoprotein E as a lipid transport and signaling protein in the blood, liver, and artery wall', *Journal of lipid research*, 50: S156-S61.

Getz, Godfrey S, and Catherine A Reardon. 2012. 'Animal models of atherosclerosis', *Arteriosclerosis, thrombosis, and vascular biology*, 32: 1104-15.

Gimbrone Jr, Michael A, and Guillermo García-Cardeña. 2016. 'Endothelial cell dysfunction and the pathobiology of atherosclerosis', *Circulation research*, 118: 620-36.

Girelli, Domenico, Nicola Martinelli, Flora Peyvandi, and Oliviero Olivieri. 2009. "Genetic architecture of coronary artery disease in the genome-wide era: implications for the emerging “golden dozen” loci." In *Seminars in thrombosis and hemostasis*, 671-82. © Thieme Medical Publishers.

Glass, Christopher K, and Joseph L Witztum. 2001. 'Atherosclerosis: the road ahead', *Cell*, 104: 503-16.

Gomez, D., and G. K. Owens. 2012. 'Smooth muscle cell phenotypic switching in atherosclerosis', *Cardiovasc Res*, 95: 156-64.

Gonzalez, Leticia, Alexander S Qian, Usama Tahir, Pei Yu, and Bernardo L Trigatti. 2017. 'Sphingosine-1-phosphate receptor 1, expressed in myeloid cells, slows diet-induced atherosclerosis and protects against macrophage apoptosis in ldlr KO mice', *International Journal of Molecular Sciences*, 18: 2721.

Grootaert, M. O. J., and M. R. Bennett. 2021. 'Vascular smooth muscle cells in atherosclerosis: time for a re-assessment', *Cardiovasc Res*, 117: 2326-39.

Hait, Nitai C, Jeremy Allegood, Michael Maceyka, Graham M Strub, Kuzhuvelil B Harikumar, Sandeep K Singh, Cheng Luo, Ronen Marmorstein, Tomasz Kordula, and Sheldon Milstien. 2009. 'Regulation of histone acetylation in the nucleus by sphingosine-1-phosphate', *Science*, 325: 1254-57.

Hänel, Petra, Paul Andréani, and Markus H Gräler. 2007. 'Erythrocytes store and release sphingosine 1-phosphate in blood', *The FASEB Journal*, 21: 1202-09.

Hanson, Michael A, Christopher B Roth, Euijung Jo, Mark T Griffith, Fiona L Scott, Greg Reinhart, Hans Desale, Bryan Clemons, Stuart M Cahalan, and Stephan C Schuerer. 2012. 'Crystal structure of a lipid G protein–coupled receptor', *Science*, 335: 851-55.

Hartvigsen, Karsten, Christoph J Binder, Lotte F Hansen, Apaïs Rafia, Joseph Juliano, Sohvi Hörkkö, Daniel Steinberg, Wulf Palinski, Joseph L Witztum,

and Andrew C Li. 2007. 'A diet-induced hypercholesterolemic murine model to study atherogenesis without obesity and metabolic syndrome', *Arteriosclerosis, thrombosis, and vascular biology*, 27: 878-85.

Healy, Luke M, Graham K Sheridan, Adam J Pritchard, Aleksandra Rutkowska, Florian Mullershausen, and Kumlesh K Dev. 2013. 'Pathway specific modulation of S1P1 receptor signalling in rat and human astrocytes', *British journal of pharmacology*, 169: 1114-29.

Hla, Timothy, and T Maciag. 1990. 'An abundant transcript induced in differentiating human endothelial cells encodes a polypeptide with structural similarities to G-protein-coupled receptors', *Journal of Biological Chemistry*, 265: 9308-13.

Hobbs, Helen H, David W Russell, Michael S Brown, and Joseph L Goldstein. 1990. 'The LDL receptor locus in familial hypercholesterolemia: mutational analysis of a membrane protein', *Annual review of genetics*, 24: 133-70.

Hobson, John P, Hans M Rosenfeldt, Larry S Barak, Ana Olivera, Samantha Poulton, Marc G Caron, Sheldon Milstien, and Sarah Spiegel. 2001. 'Role of the sphingosine-1-phosphate receptor EDG-1 in PDGF-induced cell motility', *Science*, 291: 1800-03.

Houtkamp, Mischa A, Onno J de Boer, Chris M van der Loos, Allard C van der Wal, and Anton E Becker. 2001. 'Adventitial infiltrates associated with advanced atherosclerotic plaques: structural organization suggests generation of local

humoral immune responses', *The Journal of Pathology: A Journal of the Pathological Society of Great Britain and Ireland*, 193: 263-69.

Hu, Yanhua, Zhongyi Zhang, Evelyn Torsney, Ali R Afzal, Fergus Davison, Bernhard Metzler, and Qingbo Xu. 2004. 'Abundant progenitor cells in the adventitia contribute to atherosclerosis of vein grafts in ApoE-deficient mice', *The Journal of clinical investigation*, 113: 1258-65.

Hughes, Jeniter E, Suseela Srinivasan, Kevin R Lynch, Richard L Proia, Pawel Ferdek, and Catherine C Hedrick. 2008. 'Sphingosine-1-phosphate induces an antiinflammatory phenotype in macrophages', *Circulation research*, 102: 950-58.

Ishibashi, Shun, Michael S Brown, Joseph L Goldstein, Robert D Gerard, Robert E Hammer, and Joachim Herz. 1993. 'Hypercholesterolemia in low density lipoprotein receptor knockout mice and its reversal by adenovirus-mediated gene delivery', *The Journal of clinical investigation*, 92: 883-93.

Ishibashi, Shun, Joseph L Goldstein, Michael S Brown, Joachim Herz, and Dennis K Burns. 1994. 'Massive xanthomatosis and atherosclerosis in cholesterol-fed low density lipoprotein receptor-negative mice', *The Journal of clinical investigation*, 93: 1885-93.

Jacobsen, Kevin, Marie Bek Lund, Jeong Shim, Stine Gunnersen, Ernst-Martin Füchtbauer, Mads Kjolby, Laura Carramolino, and Jacob Fog Bentzon. 2017. 'Diverse cellular architecture of atherosclerotic plaque derives from clonal expansion of a few medial SMCs', *JCI insight*, 2.

Jawien, Jacek, Pawel Nastalek, and Richard Korbut. 2004. 'Mouse models of experimental atherosclerosis', *Journal of physiology and pharmacology*, 55: 503-17.

Karunakaran, Denuja, Michele Geoffrion, Lihui Wei, Wei Gan, Laura Richards, Prakriti Shangari, Ella M DeKemp, Rachelle A Beanlands, Ljubica Perisic, and Lars Maegdefessel. 2016. 'Targeting macrophage necroptosis for therapeutic and diagnostic interventions in atherosclerosis', *Science advances*, 2: e1600224.

Kedi, Xu, Yan Ming, Wang Yongping, Yang Yi, and Zheng Xiaoxiang. 2009. 'Free cholesterol overloading induced smooth muscle cells death and activated both ER-and mitochondrial-dependent death pathway', *Atherosclerosis*, 207: 123-30.

Keul, P., A. Polzin, K. Kaiser, M. Graler, L. Dannenberg, G. Daum, G. Heusch, and B. Levkau. 2019. 'Potent anti-inflammatory properties of HDL in vascular smooth muscle cells mediated by HDL-S1P and their impairment in coronary artery disease due to lower HDL-S1P: a new aspect of HDL dysfunction and its therapy', *FASEB J*, 33: 1482-95.

Keul, Petra, Susann Peters, Karin von Wnuck Lipinski, Nathalie H Schröder, Melissa K Nowak, Dragos A Duse, Amin Polzin, Sarah Weske, Markus H Gräler, and Bodo Levkau. 2022. 'Sphingosine-1-Phosphate (S1P) Lyase Inhibition Aggravates Atherosclerosis and Induces Plaque Rupture in ApoE−/− Mice', *International Journal of Molecular Sciences*, 23: 9606.

Keul, Petra, Markus Tölle, Susann Lucke, Karin von Wnuck Lipinski, Gerd Heusch, Mirjam Schuchardt, Markus van der Giet, and Bodo Levkau. 2007. 'The sphingosine-1-phosphate analogue FTY720 reduces atherosclerosis in apolipoprotein E–deficient mice', *Arteriosclerosis, thrombosis, and vascular biology*, 27: 607-13.

Khan, Razi, Alex Agrotis, and Alex Bobik. 2007. 'Understanding the role of transforming growth factor-β1 in intimal thickening after vascular injury', *Cardiovascular research*, 74: 223-34.

Kim, Steven, Hon S Ip, Min M Lu, Cynthia Clendenin, and Michael S Parmacek. 1997. 'A serum response factor-dependent transcriptional regulatory program identifies distinct smooth muscle cell sublineages', *Molecular and cellular biology*.

Kimura, Takao, Hideaki Tomura, Chihiro Mogi, Atsushi Kuwabara, Alatangaole Damirin, Tamotsu Ishizuka, Akihiro Sekiguchi, Mitsuteru Ishiwara, Doon-Soon Im, and Koichi Sato. 2006. 'Role of scavenger receptor class B type I and sphingosine 1-phosphate receptors in high density lipoprotein-induced inhibition of adhesion molecule expression in endothelial cells', *Journal of Biological Chemistry*, 281: 37457-67.

Kinlay, Scott, Dominik Behrendt, Marco Wainstein, John Beltrame, James C Fang, Mark A Creager, Andrew P Selwyn, and Peter Ganz. 2001. 'Role of endothelin-1 in the active constriction of human atherosclerotic coronary arteries', *Circulation*, 104: 1114-18.

Kitano, T., S. Usui, S. I. Takashima, O. Inoue, C. Goten, A. Nomura, K. Yoshioka, M. Okajima, S. Kaneko, Y. Takuwa, and M. Takamura. 2019. 'Sphigosine-1-phosphate receptor 1 promotes neointimal hyperplasia in a mouse model of carotid artery injury', *Biochem Biophys Res Commun*, 511: 179-84.

Kluk, Michael J, Chantal Colmont, Ming-Tao Wu, and Timothy Hla. 2003. 'Platelet-derived growth factor (PDGF)-induced chemotaxis does not require the G protein-coupled receptor S1P1 in murine embryonic fibroblasts and vascular smooth muscle cells', *FEBS letters*, 533: 25-28.

Kluk, Michael J, and Timothy Hla. 2001. 'Role of the sphingosine 1-phosphate receptor EDG-1 in vascular smooth muscle cell proliferation and migration', *Circulation research*, 89: 496-502.

Knowles, Joshua W, and Nobuyo Maeda. 2000. 'Genetic modifiers of atherosclerosis in mice', *Arteriosclerosis, thrombosis, and vascular biology*, 20: 2336-45.

Kojima, Yoko, Kelly Downing, Ramendra Kundu, Clint Miller, Frederick Dewey, Hope Lancero, Uwe Raaz, Ljubica Perisic, Ulf Hedin, and Eric Schadt. 2019. 'Cyclin-dependent kinase inhibitor 2B regulates efferocytosis and atherosclerosis', *The Journal of clinical investigation*, 124: 1083-97.

Kreatsoulas, Catherine, and Sonia S Anand. 2010. 'The impact of social determinants on cardiovascular disease', *Canadian Journal of Cardiology*, 26: 8C-13C.

Krump-Konvalinkova, Vera, Ilona Chwalla, and Wolfgang Siess. 2008. 'FTY720 inhibits S1P-mediated endothelial healing: relationship to S1P1-receptor surface expression', *Biochemical and Biophysical Research Communications*, 370: 603-08.

Kruth, Howard S. 2011. 'Receptor-independent fluid-phase pinocytosis mechanisms for induction of foam cell formation with native LDL particles', *Current opinion in lipidology*, 22: 386.

Kuchibhotla, Sai, Difernando Vanegas, David J Kennedy, Ella Guy, George Nimako, Richard E Morton, and Maria Febbraio. 2008. 'Absence of CD36 protects against atherosclerosis in ApoE knock-out mice with no additional protection provided by absence of scavenger receptor AI/II', *Cardiovascular research*, 78: 185-96.

Kunjathoor, Vidya V, Maria Febbraio, Eugene A Podrez, Kathryn J Moore, Lorna Andersson, Stephanie Koehn, Jeongmi S Rhee, Roy Silverstein, Henry F Hoff, and Mason W Freeman. 2002. 'Scavenger receptors class AI/II and CD36 are the principal receptors responsible for the uptake of modified low density lipoprotein leading to lipid loading in macrophages', *Journal of Biological Chemistry*, 277: 49982-88.

Kurano, M., and Y. Yatomi. 2018. 'Sphingosine 1-Phosphate and Atherosclerosis', *J Atheroscler Thromb*, 25: 16-26.

Kzhyshkowska, Julia, Claudine Neyen, and Siamon Gordon. 2012. 'Role of macrophage scavenger receptors in atherosclerosis', *Immunobiology*, 217: 492-502.

LaMontagne, Kenneth, Amanda Littlewood-Evans, Christian Schnell, Terence O'Reilly, Lorenza Wyder, Teresa Sanchez, Beatrice Probst, Jeannene Butler, Alexander Wood, and Gene Liau. 2006. 'Antagonism of sphingosine-1-phosphate receptors by FTY720 inhibits angiogenesis and tumor vascularization', *Cancer research*, 66: 221-31.

Lee, Menq-Jer, Shobha Thangada, Kevin P Claffey, Nicolas Ancellin, Catherine H Liu, Michael Kluk, Mario Volpi, I Ramadan, and Timothy Hla. 1999. 'Vascular endothelial cell adherens junction assembly and morphogenesis induced by sphingosine-1-phosphate', *Cell*, 99: 301-12.

Lee, Menq-Jer, James R Van Brocklyn, Shobha Thangada, Catherine H Liu, Arthur R Hand, Ramil Menzeleev, Sarah Spiegel, and Timothy Hla. 1998. 'Sphingosine-1-phosphate as a ligand for the G protein-coupled receptor EDG-1', *Science*, 279: 1552-55.

Lee, Yee Ting, Hiu Yu Lin, Yin Wah Fiona Chan, Ka Hou Christien Li, Olivia Tsz Ling To, Bryan P Yan, Tong Liu, Guangping Li, Wing Tak Wong, and Wendy Keung. 2017. 'Mouse models of atherosclerosis: a historical perspective and recent advances', *Lipids in health and disease*, 16: 1-11.

Li, Yankun, Marie-Christine Gerbod-Giannone, Heather Seitz, Dongying Cui, Edward Thorp, Alan R Tall, Glenn K Matsushima, and Ira Tabas. 2006.

'Cholesterol-induced apoptotic macrophages elicit an inflammatory response in phagocytes, which is partially attenuated by the Mer receptor', *Journal of Biological Chemistry*, 281: 6707-17.

Li, Yankun, Robert F Schwabe, Tracie DeVries-Seimon, Pin Mei Yao, Marie-Christine Gerbod-Giannone, Alan R Tall, Roger J Davis, Richard Flavell, David A Brenner, and Ira Tabas. 2005. 'Free cholesterol-loaded macrophages are an abundant source of tumor necrosis factor-α and interleukin-6: model of NF-κB-and map kinase-dependent inflammation in advanced atherosclerosis', *Journal of Biological Chemistry*, 280: 21763-72.

Lin, Juan, Hanjie Li, Min Yang, Junming Ren, Zhe Huang, Felicia Han, Jian Huang, Jianhui Ma, Duanwu Zhang, and Zhirong Zhang. 2013. 'A role of RIP3-mediated macrophage necrosis in atherosclerosis development', *Cell reports*, 3: 200-10.

Liu, Yu–Dong, Xin Sun, Yao Zhang, Hua–Jie Wu, Hao Wang, and Rui Yang. 2019. 'Protocatechuic acid inhibits TGF-β1-induced proliferation and migration of human airway smooth muscle cells', *Journal of pharmacological sciences*, 139: 9-14.

Llodrá, Jaime, Véronique Angeli, Jianhua Liu, Eugene Trogan, Edward A Fisher, and Gwendalyn J Randolph. 2004. 'Emigration of monocyte-derived cells from atherosclerotic lesions characterizes regressive, but not progressive, plaques', *Proceedings of the National Academy of Sciences*, 101: 11779-84.

Lopes, Joshua, Eser Adiguzel, Steven Gu, Shu-Lin Liu, Guangpei Hou, Scott Heximer, Richard K Assoian, and Michelle P Bendeck. 2013. 'Type VIII collagen mediates vessel wall remodeling after arterial injury and fibrous cap formation in atherosclerosis', *The American journal of pathology*, 182: 2241-53.

Mack, Christopher P, and Gary K Owens. 1999. 'Regulation of smooth muscle α-actin expression in vivo is dependent on CArG elements within the 5′ and first intron promoter regions', *Circulation research*, 84: 852-61.

Madura, II, James A, Bram R Kaufman, David A Margolin, David M Spencer, Paul L Fox, and Linda M Graham. 1996. 'Regional differences in platelet-derived growth factor production by the canine aorta', *Journal of vascular research*, 33: 53-61.

Manning-Tobin, Jennifer J, Kathryn J Moore, Tracie A Seimon, Susan A Bell, Maia Sharuk, Jacqueline I Alvarez-Leite, Menno PJ de Winther, Ira Tabas, and Mason W Freeman. 2009. 'Loss of SR-A and CD36 activity reduces atherosclerotic lesion complexity without abrogating foam cell formation in hyperlipidemic mice', *Arteriosclerosis, thrombosis, and vascular biology*, 29: 19-26.

Matsumoto, Kengo, Ken-ichi Hirano, Shuichi Nozaki, Akiko Takamoto, Makoto Nishida, Yumiko Nakagawa-Toyama, Mohamed Yakub Janabi, Takeshi Ohya, Shizuya Yamashita, and Yuji Matsuzawa. 2000. 'Expression of macrophage (Mφ) scavenger receptor, CD36, in cultured human aortic

smooth muscle cells in association with expression of peroxisome proliferator activated receptor-γ, which regulates gain of Mφ-like phenotype in vitro, and its implication in atherogenesis', *Arteriosclerosis, thrombosis, and vascular biology*, 20: 1027-32.

Meir, Karen S, and Eran Leitersdorf. 2004. 'Atherosclerosis in the apolipoprotein E–deficient mouse: a decade of progress', *Arteriosclerosis, thrombosis, and vascular biology*, 24: 1006-14.

Miano, Joseph M, Peter Cserjesi, Keith L Ligon, Muthu Periasamy, and Eric N Olson. 1994. 'Smooth muscle myosin heavy chain exclusively marks the smooth muscle lineage during mouse embryogenesis', *Circulation research*, 75: 803-12.

Moore, Kathryn J, Frederick J Sheedy, and Edward A Fisher. 2013. 'Macrophages in atherosclerosis: a dynamic balance', *Nature Reviews Immunology*, 13: 709-21.

Morales-Ruiz, Manuel, Menq-Jer Lee, Stefan Zöllner, Jean-Philippe Gratton, Ramona Scotland, Ichiro Shiojima, Kenneth Walsh, Timothy Hla, and William C Sessa. 2001. 'Sphingosine 1-phosphate activates Akt, nitric oxide production, and chemotaxis through a Giprotein/phosphoinositide 3-kinase pathway in endothelial cells', *Journal of Biological Chemistry*, 276: 19672-77.

Mullershausen, Florian, Frédéric Zecri, Cihan Cetin, Andreas Billich, Danilo Guerini, and Klaus Seuwen. 2009. 'Persistent signaling induced by FTY720-

phosphate is mediated by internalized S1P1 receptors', *Nature chemical biology*, 5: 428-34.

Nagao, Tomokazu, Chunbo Qin, Inna Grosheva, Frederick R Maxfield, and Lynda M Pierini. 2007. 'Elevated cholesterol levels in the plasma membranes of macrophages inhibit migration by disrupting RhoA regulation', *Arteriosclerosis, thrombosis, and vascular biology*, 27: 1596-602.

Nakashima, Yutaka, Hiroshi Fujii, Shinji Sumiyoshi, Thomas N Wight, and Katsuo Sueishi. 2007. 'Early human atherosclerosis: accumulation of lipid and proteoglycans in intimal thickenings followed by macrophage infiltration', *Arteriosclerosis, thrombosis, and vascular biology*, 27: 1159-65.

Nakashima, Yutaka, Andrew S Plump, Elaine W Raines, Jan L Breslow, and Russell Ross. 1994. 'ApoE-deficient mice develop lesions of all phases of atherosclerosis throughout the arterial tree', *Arteriosclerosis and thrombosis: a journal of vascular biology*, 14: 133-40.

Nakashima, Yutaka, Elaine W Raines, Andrew S Plump, Jan L Breslow, and Russell Ross. 1998. 'Upregulation of VCAM-1 and ICAM-1 at atherosclerosis-prone sites on the endothelium in the ApoE-deficient mouse', *Arteriosclerosis, thrombosis, and vascular biology*, 18: 842-51.

Nakashima, Yutaka, Thomas N Wight, and Katsuo Sueishi. 2008. 'Early atherosclerosis in humans: role of diffuse intimal thickening and extracellular matrix proteoglycans', *Cardiovascular research*, 79: 14-23.

Newby, Andrew C, and Alla B Zaltsman. 1999. 'Fibrous cap formation or destruction—the critical importance of vascular smooth muscle cell proliferation, migration and matrix formation', *Cardiovascular research*, 41: 345-60.

Newman, Alexandra AC, Vlad Serbulea, Richard A Baylis, Laura S Shankman, Xenia Bradley, Gabriel F Alencar, Katherine Owsiany, Rebecca A Deaton, Santosh Karnewar, and Sohel Shamsuzzaman. 2021. 'Multiple cell types contribute to the atherosclerotic lesion fibrous cap by PDGFRβ and bioenergetic mechanisms', *Nature metabolism*, 3: 166-81.

Nofer, J. R., M. Bot, M. Brodde, P. J. Taylor, P. Salm, V. Brinkmann, T. van Berkel, G. Assmann, and E. A. Biessen. 2007a. 'FTY720, a synthetic sphingosine 1 phosphate analogue, inhibits development of atherosclerosis in low-density lipoprotein receptor-deficient mice', *Circulation*, 115: 501-8.

Nofer, Jerzy-Roch, Martine Bot, Martin Brodde, Paul J Taylor, Paul Salm, Volker Brinkmann, Theo van Berkel, Gerd Assmann, and Erik AL Biessen. 2007b. 'FTY720, a synthetic sphingosine 1 phosphate analogue, inhibits development of atherosclerosis in low-density lipoprotein receptor–deficient mice', *Circulation*, 115: 501-08.

O'Sullivan, Catherine, and Kumlesh K Dev. 2013. 'The structure and function of the S1P1 receptor', *Trends in pharmacological sciences*, 34: 401-12.

Obinata, Hideru, Andrew Kuo, Yukata Wada, Steven Swendeman, Catherine H Liu, Victoria A Blaho, Rieko Nagumo, Kenichi Satoh, Takashi Izumi, and

Timothy Hla. 2019. 'Identification of ApoA4 as a sphingosine 1-phosphate chaperone in ApoM-and albumin-deficient mice', *Journal of lipid research*, 60: 1912-21.

Okamoto, Hiroyuki, Noriko Takuwa, Takehiko Yokomizo, Naotoshi Sugimoto, Soutaro Sakurada, Hiroshi Shigematsu, and Yoh Takuwa. 2000. 'Inhibitory regulation of Rac activation, membrane ruffling, and cell migration by the G protein-coupled sphingosine-1-phosphate receptor EDG5 but not EDG1 or EDG3', *Molecular and cellular biology*, 20: 9247-61.

Oo, Myat Lin, Sung-Hee Chang, Shobha Thangada, Ming-Tao Wu, Karim Rezaul, Victoria Blaho, Sun-Il Hwang, David K Han, and Timothy Hla. 2011. 'Engagement of S1P 1-degradative mechanisms leads to vascular leak in mice', *The Journal of clinical investigation*, 121: 2290-300.

Oo, Myat Lin, Shobha Thangada, Ming-Tao Wu, Catherine H Liu, Timothy L Macdonald, Kevin R Lynch, Chen-Yong Lin, and Timothy Hla. 2007. 'Immunosuppressive and anti-angiogenic sphingosine 1-phosphate receptor-1 agonists induce ubiquitinylation and proteasomal degradation of the receptor', *Journal of Biological Chemistry*, 282: 9082-89.

Pan, H., C. Xue, B. J. Auerbach, J. Fan, A. C. Bashore, J. Cui, D. Y. Yang, S. B. Trignano, W. Liu, J. Shi, C. O. Ihuegbu, E. C. Bush, J. Worley, L. Vlahos, P. Laise, R. A. Solomon, E. S. Connolly, A. Califano, P. A. Sims, H. Zhang, M. Li, and M. P. Reilly. 2020. 'Single-Cell Genomics Reveals a Novel Cell State During Smooth Muscle Cell Phenotypic Switching and Potential Therapeutic

Targets for Atherosclerosis in Mouse and Human', *Circulation*, 142: 2060-75.

Park, Young Mi, Judith A Drazba, Amit Vasanji, Thomas Egelhoff, Maria Febbraio, and Roy L Silverstein. 2012. 'Oxidized LDL/CD36 interaction induces loss of cell polarity and inhibits macrophage locomotion', *Molecular biology of the cell*, 23: 3057-68.

Parrill, Abby L, De-an Wang, Debra L Bautista, James R Van Brocklyn, Zsolt Lorincz, David J Fischer, Daniel L Baker, Karoly Liliom, Sarah Spiegel, and Gabor Tigyi. 2000. 'Identification of Edg1 receptor residues that recognize sphingosine 1-phosphate', *Journal of Biological Chemistry*, 275: 39379-84.

Piedrahita, Jorge A, Sunny H Zhang, John R Hagaman, Paula M Oliver, and Nobuyo Maeda. 1992. 'Generation of mice carrying a mutant apolipoprotein E gene inactivated by gene targeting in embryonic stem cells', *Proceedings of the National Academy of Sciences*, 89: 4471-75.

Plump, Andrew S, and Jan L Breslow. 1995. 'Apolipoprotein E and the apolipoprotein E-deficient mouse', *Annual review of nutrition*, 15: 495-518.

Plump, Andrew S, Jonathan D Smith, Tony Hayek, Katriina Aalto-Setälä, Annemarie Walsh, Judy G Verstuyft, Edward M Rubin, and Jan L Breslow. 1992. 'Severe hypercholesterolemia and atherosclerosis in apolipoprotein E-deficient mice created by homologous recombination in ES cells', *Cell*, 71: 343-53.

Pober, Jordan S, and Ramzi S Cotran. 1990. 'The role of endothelial cells in inflammation', *Transplantation*, 50: 537-44.

Pober, Jordan S, and William C Sessa. 2007. 'Evolving functions of endothelial cells in inflammation', *Nature Reviews Immunology*, 7: 803-15.

Potì, F, E Scalera, R Feuerborn, J Fischer, L Arndt, G Varga, E Pardali, M Seidl, G Liebisch, and F Rosenbauer. 2020. 'Sphingosine 1-phosphate (S1P) receptor type 1 signaling induces an anti-atherogenic phenotype in macrophages and attenuates atherosclerosis in LDL-receptor-deficient mice', *Atherosclerosis*, 315: e12.

Potì, Francesco, Uta Ceglarek, Ralph Burkhardt, Manuela Simoni, and Jerzy-Roch Nofer. 2015. 'SKI-II–a sphingosine kinase 1 inhibitor–exacerbates atherosclerosis in low-density lipoprotein receptor-deficient (LDL-R−/−) mice on high cholesterol diet', *Atherosclerosis*, 240: 212-15.

Poti, Francesco, Sara Costa, Valeria Bergonzini, Margherita Galletti, Elisa Pignatti, Christian Weber, Manuela Simoni, and Jerzy-Roch Nofer. 2012. 'Effect of sphingosine 1-phosphate (S1P) receptor agonists FTY720 and CYM5442 on atherosclerosis development in LDL receptor deficient (LDL-R−/−) mice', *Vascular pharmacology*, 57: 56-64.

Potì, Francesco, Fabio Gualtieri, Sandro Sacchi, Gabriele Weißen-Plenz, Georg Varga, Martin Brodde, Christian Weber, Manuela Simoni, and Jerzy-Roch Nofer. 2013. 'KRP-203, sphingosine 1-phosphate receptor type 1 agonist,

ameliorates atherosclerosis in LDL-R−/− mice', *Arteriosclerosis, thrombosis, and vascular biology*, 33: 1505-12.

Potì, Francesco, Manuela Simoni, and Jerzy-Roch Nofer. 2014. 'Atheroprotective role of high-density lipoprotein (HDL)-associated sphingosine-1-phosphate (S1P)', *Cardiovascular research*, 103: 395-404.

Qin, Chunbo, Tomokazu Nagao, Inna Grosheva, Frederick R Maxfield, and Lynda M Pierini. 2006. 'Elevated plasma membrane cholesterol content alters macrophage signaling and function', *Arteriosclerosis, thrombosis, and vascular biology*, 26: 372-78.

Radeva, MY, and J Waschke. 2018. 'Mind the gap: mechanisms regulating the endothelial barrier', *Acta physiologica*, 222: e12860.

Ramkhelawon, Bhama, Yuan Yang, Janine M van Gils, Bernd Hewing, Katey J Rayner, Sajesh Parathath, Liang Guo, Scott Oldebeken, Jessica L Feig, and Edward A Fisher. 2013. 'Hypoxia induces netrin-1 and Unc5b in atherosclerotic plaques: mechanism for macrophage retention and survival', *Arteriosclerosis, thrombosis, and vascular biology*, 33: 1180-88.

Rayner, Katey J. 2017. 'Cell death in the vessel wall: the good, the bad, the ugly', *Arteriosclerosis, thrombosis, and vascular biology*, 37: e75-e81.

Reddick, Robert L, Sunny H Zhang, and Nobuyo Maeda. 1994. 'Atherosclerosis in mice lacking apo E. Evaluation of lesional development and progression', *Arteriosclerosis and thrombosis: a journal of vascular biology*, 14: 141-47.

Regan, Christopher P, Paul J Adam, Cort S Madsen, and Gary K Owens. 2000. 'Molecular mechanisms of decreased smooth muscle differentiation marker expression after vascular injury', *The Journal of clinical investigation*, 106: 1139-47.

Rong, James X, Mark Shapiro, Eugene Trogan, and Edward A Fisher. 2003. 'Transdifferentiation of mouse aortic smooth muscle cells to a macrophage-like state after cholesterol loading', *Proceedings of the National Academy of Sciences*, 100: 13531-36.

Rosen, Hugh, Raymond C Stevens, Michael Hanson, Edward Roberts, and Michael BA Oldstone. 2013. 'Sphingosine-1-phosphate and its receptors: structure, signaling, and influence', *Annual review of biochemistry*, 82: 637-62.

Rosenfeldt, Hans M, John P Hobson, Michael Maceyka, Ana Olivera, Victor E Nava, Sheldon Milstien, and Sarah Spiegel. 2001. 'EDG-1 links the PDGF receptor to Src and focal adhesion kinase activation leading to lamellipodia formation and cell migration', *The FASEB Journal*, 15: 2649-59.

Rosenfeldt, HM, JP Hobson, S Milstien, and S Spiegel. 2001. "The sphingosine-I-phosphate receptor EDG-I is essential for platelet-derived growth factor-induced cell motility." In.: Portland Press Ltd.

Ruiz, Mario, Cecilia Frej, Andreas Holmér, Li J Guo, Sinh Tran, and Björn Dahlbäck. 2017. 'High-density lipoprotein–associated apolipoprotein M limits endothelial inflammation by delivering sphingosine-1-phosphate to the

sphingosine-1-phosphate receptor 1', *Arteriosclerosis, thrombosis, and vascular biology*, 37: 118-29.

Ryu, Yasuji, Noriko Takuwa, Naotoshi Sugimoto, Sotaro Sakurada, Soichiro Usui, Hiroyuki Okamoto, Osamu Matsui, and Yoh Takuwa. 2002. 'Sphingosine-1-phosphate, a platelet-derived lysophospholipid mediator, negatively regulates cellular Rac activity and cell migration in vascular smooth muscle cells', *Circulation research*, 90: 325-32.

Sammani, Saad, Liliana Moreno-Vinasco, Tamara Mirzapoiazova, Patrick A Singleton, Eddie T Chiang, Carrie L Evenoski, Ting Wang, Biji Mathew, Aliya Husain, and Jaideep Moitra. 2010. 'Differential effects of sphingosine 1–phosphate receptors on airway and vascular barrier function in the murine lung', *American journal of respiratory cell and molecular biology*, 43: 394-402.

Sanchez, Teresa, and Timothy Hla. 2004. 'Structural and functional characteristics of S1P receptors', *Journal of cellular biochemistry*, 92: 913-22.

Sano, Hideto, Tetsuo Sudo, Masayuki Yokode, Toshinori Murayama, Hiroshi Kataoka, Nobuyuki Takakura, Satomi Nishikawa, Shin-Ichi Nishikawa, and Toru Kita. 2001. 'Functional blockade of platelet-derived growth factor receptor-β but not of receptor-α prevents vascular smooth muscle cell accumulation in fibrous cap lesions in apolipoprotein E–deficient mice', *Circulation*, 103: 2955-60.

Sata, Masataka, Akio Saiura, Atsushi Kunisato, Akihiro Tojo, Seiji Okada, Takeshi Tokuhisa, Hisamaru Hirai, Masatoshi Makuuchi, Yasunobu Hirata, and Ryozo Nagai. 2002. 'Hematopoietic stem cells differentiate into vascular cells that participate in the pathogenesis of atherosclerosis', *Nature medicine*, 8: 403-09.

Sattler, K. J., S. Elbasan, P. Keul, M. Elter-Schulz, C. Bode, M. H. Graler, M. Brocker-Preuss, T. Budde, R. Erbel, G. Heusch, and B. Levkau. 2010. 'Sphingosine 1-phosphate levels in plasma and HDL are altered in coronary artery disease', *Basic Res Cardiol*, 105: 821-32.

Schober, Andreas, and Alma Zernecke. 2007. 'Chemokines in vascular remodeling', *Thrombosis and haemostasis*, 97: 730-37.

Scull, Christopher M, and Ira Tabas. 2011. 'Mechanisms of ER stress-induced apoptosis in atherosclerosis', *Arteriosclerosis, thrombosis, and vascular biology*, 31: 2792-97.

Shai, Shaw-Yung, Sergiy Sukhanov, Yusuke Higashi, Charlotte Vaughn, James Kelly, and Patrice Delafontaine. 2010. 'Smooth muscle cell–specific insulin-like growth factor-1 overexpression in Apoe−/− mice does not alter atherosclerotic plaque burden but increases features of plaque stability', *Arteriosclerosis, thrombosis, and vascular biology*, 30: 1916-24.

Shankman, Laura S, Delphine Gomez, Olga A Cherepanova, Morgan Salmon, Gabriel F Alencar, Ryan M Haskins, Pamela Swiatlowska, Alexandra AC Newman, Elizabeth S Greene, and Adam C Straub. 2015. 'KLF4-dependent

phenotypic modulation of smooth muscle cells has a key role in atherosclerotic plaque pathogenesis', *Nature medicine*, 21: 628-37.

Shea, Barry S, Sarah F Brooks, Benjamin A Fontaine, Jerold Chun, Andrew D Luster, and Andrew M Tager. 2010. 'Prolonged exposure to sphingosine 1–phosphate receptor-1 agonists exacerbates vascular leak, fibrosis, and mortality after lung injury', *American journal of respiratory cell and molecular biology*, 43: 662-73.

Shi, Yi, James E O'Brien, Ali Fard, and Andrew Zalewski. 1996. 'Transforming growth factor-β1 expression and myofibroblast formation during arterial repair', *Arteriosclerosis, thrombosis, and vascular biology*, 16: 1298-305.

Shimizu, T., A. De Wispelaere, M. Winkler, T. D'Souza, J. Caylor, L. Chen, F. Dastvan, J. Deou, A. Cho, A. Larena-Avellaneda, M. Reidy, and G. Daum. 2012. 'Sphingosine-1-phosphate receptor 3 promotes neointimal hyperplasia in mouse iliac-femoral arteries', *Arterioscler Thromb Vasc Biol*, 32: 955-61.

Shimizu, Takuya, Tatsu Nakazawa, Aesim Cho, Frank Dastvan, Dustin Shilling, Günter Daum, and Michael A Reidy. 2007. 'Sphingosine 1-phosphate receptor 2 negatively regulates neointimal formation in mouse arteries', *Circulation research*, 101: 995-1000.

Singleton, Patrick A, Steven M Dudek, Eddie T Chiang, and Joe GN Garcia. 2005. 'Regulation of sphingosine 1-phosphate-induced endothelial cytoskeletal

rearrangement and barrier enhancement by S1P1 receptor, PI3 kinase, Tiam1/Rac1, and α-actinin', *The FASEB Journal*, 19: 1646-56.

Sluiter, Thijs J, Jaap D van Buul, Stephan Huveneers, Paul HA Quax, and Margreet R de Vries. 2021. 'Endothelial barrier function and leukocyte transmigration in atherosclerosis', *Biomedicines*, 9: 328.

Smith, JD, and JL Breslow. 1997. 'The emergence of mouse models of atherosclerosis and their relevance to clinical research', *Journal of internal medicine*, 242: 99-109.

Sowers, James R. 2002. "Hypertension, angiotensin II, and oxidative stress." In, 1999-2001. Mass Medical Soc.

Strub, Graham M, Melanie Paillard, Jie Liang, Ludovic Gomez, Jeremy C Allegood, Nitai C Hait, Michael Maceyka, Megan M Price, Qun Chen, and David C Simpson. 2011. 'Sphingosine-1-phosphate produced by sphingosine kinase 2 in mitochondria interacts with prohibitin 2 to regulate complex IV assembly and respiration', *The FASEB Journal*, 25: 600.

Stunff, Hervé Le, Sheldon Milstien, and Sarah Spiegel. 2004. 'Generation and metabolism of bioactive sphingosine-1-phosphate', *Journal of cellular biochemistry*, 92: 882-99.

Sykes, David A, Darren M Riddy, Craig Stamp, Michelle E Bradley, Neil McGuiness, Afrah Sattikar, Danilo Guerini, Ines Rodrigues, Albrecht Glaenzel, and Mark R Dowling. 2014. 'Investigating the molecular

mechanisms through which FTY 720-P causes persistent S1P1 receptor internalization', *British journal of pharmacology*, 171: 4797-807.

Tanimoto, Tatsuo, Andreea O Lungu, and Bradford C Berk. 2004. 'Sphingosine 1-phosphate transactivates the platelet-derived growth factor β receptor and epidermal growth factor receptor in vascular smooth muscle cells', *Circulation research*, 94: 1050-58.

Tellides, George, and Jordan S Pober. 2015. 'Inflammatory and immune responses in the arterial media', *Circulation research*, 116: 312-22.

Tigges, Ulrich, Masanobu Komatsu, and William B Stallcup. 2013. 'Adventitial pericyte progenitor/mesenchymal stem cells participate in the restenotic response to arterial injury', *Journal of vascular research*, 50: 134-44.

Topouzis, Stavros, and Mark W Majesky. 1996. 'Smooth muscle lineage diversity in the chick embryo: two types of aortic smooth muscle cell differ in growth and receptor-mediated transcriptional responses to transforming growth factor-β', *Developmental biology*, 178: 430-45.

Trigueros-Motos, Laia, José M González-Granado, Christine Cheung, Patricia Fernández, Fátima Sánchez-Cabo, Ana Dopazo, Sanjay Sinha, and Vicente Andrés. 2013. 'Embryological-origin–dependent differences in homeobox expression in adult aorta: role in regional phenotypic variability and regulation of NF-κB activity', *Arteriosclerosis, thrombosis, and vascular biology*, 33: 1248-56.

Van der Loop, FT, Gert Schaart, ED Timmer, FC Ramaekers, and GJ Van Eys. 1996. 'Smoothelin, a novel cytoskeletal protein specific for smooth muscle cells', *The Journal of cell biology*, 134: 401-11.

Van Gils, Janine M, Merran C Derby, Luciana R Fernandes, Bhama Ramkhelawon, Tathagat D Ray, Katey J Rayner, Sajesh Parathath, Emilie Distel, Jessica L Feig, and Jacqueline I Alvarez-Leite. 2012. 'The neuroimmune guidance cue netrin-1 promotes atherosclerosis by inhibiting the emigration of macrophages from plaques', *Nature immunology*, 13: 136-43.

Veseli, Besa Emini, Paola Perrotta, Gregory RA De Meyer, Lynn Roth, Carole Van der Donckt, Wim Martinet, and Guido RY De Meyer. 2017. 'Animal models of atherosclerosis', *European journal of pharmacology*, 816: 3-13.

von der Thüsen, Jan H, Theo JC van Berkel, and Erik AL Biessen. 2001. 'Induction of rapid atherogenesis by perivascular carotid collar placement in apolipoprotein E–deficient and low-density lipoprotein receptor–deficient mice', *Circulation*, 103: 1164-70.

Wamhoff, B. R., K. R. Lynch, T. L. Macdonald, and G. K. Owens. 2008. 'Sphingosine-1-phosphate receptor subtypes differentially regulate smooth muscle cell phenotype', *Arterioscler Thromb Vasc Biol*, 28: 1454-61.

Wang, Haidong, Mohsen Naghavi, Christine Allen, Ryan M Barber, Zulfiqar A Bhutta, Austin Carter, Daniel C Casey, Fiona J Charlson, Alan Zian Chen, and Matthew M Coates. 2016. 'Global, regional, and national life expectancy, all-cause mortality, and cause-specific mortality for 249 causes

of death, 1980–2015: a systematic analysis for the Global Burden of Disease Study 2015', *The lancet*, 388: 1459-544.

Wang, Ying, Joshua A Dubland, Sima Allahverdian, Enyinnaya Asonye, Basak Sahin, Jen Erh Jaw, Don D Sin, Michael A Seidman, Nicholas J Leeper, and Gordon A Francis. 2019. 'Smooth muscle cells contribute the majority of foam cells in ApoE (Apolipoprotein E)-deficient mouse atherosclerosis', *Arteriosclerosis, thrombosis, and vascular biology*, 39: 876-87.

Waters, Catherine, Balwinder Sambi, Kok-Choi Kong, Dawn Thompson, Stuart M Pitson, Susan Pyne, and Nigel J Pyne. 2003. 'Sphingosine 1-phosphate and platelet-derived growth factor (PDGF) act via PDGFβ receptor-sphingosine 1-phosphate receptor complexes in airway smooth muscle cells', *Journal of Biological Chemistry*, 278: 6282-90.

Westerterp, Marit, and Alan R Tall. 2020. 'A new pathway of macrophage cholesterol efflux', *Proceedings of the National Academy of Sciences*, 117: 11853-55.

Whetzel, Angela M, David T Bolick, Suseela Srinivasan, Timothy L Macdonald, Margaret A Morris, Klaus Ley, and Catherine C Hedrick. 2006. 'Sphingosine-1 phosphate prevents monocyte/endothelial interactions in type 1 diabetic NOD mice through activation of the S1P1 receptor', *Circulation research*, 99: 731-39.

White, Christopher, Heba Alshaker, Colin Cooper, Matthias Winkler, and Dmitri Pchejetski. 2016. 'The emerging role of FTY720 (Fingolimod) in cancer treatment', *Oncotarget*, 7: 23106.

Wilkerson, Brent A, G Daniel Grass, Shane B Wing, W Scott Argraves, and Kelley M Argraves. 2012. 'Sphingosine 1-phosphate (S1P) carrier-dependent regulation of endothelial barrier: high density lipoprotein (HDL)-S1P prolongs endothelial barrier enhancement as compared with albumin-S1P via effects on levels, trafficking, and signaling of S1P1', *Journal of Biological Chemistry*, 287: 44645-53.

Williams, Kevin Jon, Jonathan E Feig, and Edward A Fisher. 2008. 'Rapid regression of atherosclerosis: insights from the clinical and experimental literature', *Nature clinical practice Cardiovascular medicine*, 5: 91-102.

Wirka, R. C., D. Wagh, D. T. Paik, M. Pjanic, T. Nguyen, C. L. Miller, R. Kundu, M. Nagao, J. Coller, T. K. Koyano, R. Fong, Y. J. Woo, B. Liu, S. B. Montgomery, J. C. Wu, K. Zhu, R. Chang, M. Alamprese, M. D. Tallquist, J. B. Kim, and T. Quertermous. 2019. 'Atheroprotective roles of smooth muscle cell phenotypic modulation and the TCF21 disease gene as revealed by single-cell analysis', *Nat Med*, 25: 1280-89.

Xie, Wei-Bing, Zuguo Li, Ning Shi, Xia Guo, Junming Tang, Wenjun Ju, Jun Han, Tengfei Liu, Erwin P Bottinger, and Yang Chai. 2013. 'Smad2 and myocardin-related transcription factor B cooperatively regulate vascular

smooth muscle differentiation from neural crest cells', *Circulation research*, 113: e76-e86.

Yusuf, Salim, Steven Hawken, Stephanie Ôunpuu, Tony Dans, Alvaro Avezum, Fernando Lanas, Matthew McQueen, Andrzej Budaj, Prem Pais, and John Varigos. 2004. 'Effect of potentially modifiable risk factors associated with myocardial infarction in 52 countries (the INTERHEART study): case-control study', *The lancet*, 364: 937-52.

Yvan-Charvet, Laurent, Nan Wang, and Alan R Tall. 2010. 'Role of HDL, ABCA1, and ABCG1 transporters in cholesterol efflux and immune responses', *Arteriosclerosis, thrombosis, and vascular biology*, 30: 139-43.

Zhou, Ji, Šárka Lhoták, Brooke A Hilditch, and Richard C Austin. 2005. 'Activation of the unfolded protein response occurs at all stages of atherosclerotic lesion development in apolipoprotein E–deficient mice', *Circulation*, 111: 1814-21.

Zorc-Pleskovič, Ruda, Aleš Pleskovič, Olga Vraspir-Porenta, Metka Zorc, and Aleksandra Milutinović. 2018. 'Immune cells and vasa vasorum in the tunica media of atherosclerotic coronary arteries', *Bosnian Journal of Basic Medical Sciences*, 18: 240.

Chapter 2: Sphingosine-1-phosphate receptor 1 deletion in smooth muscle cells protects against atherosclerosis in apoE-deficient mice by reducing cell proliferation and lipid droplet formation.

Narmadaa Thyagarajan, Wei Wang, Alex Qian, Jennifer Nouanesengsy, Usama Tahir, Darren Sam, Leticia Gonzalez, Yuan Qui and Bernardo L. Trigatti

Foreword

This manuscript examines the effect of inactivating S1PR1 deletion in smooth muscle cells on atherosclerotic plaque development in apoE-deficient mice. We demonstrate herein that deleting S1PR1 under the control of SMC promoter Tagln substantially reduces high-fat diet-induced atherosclerotic lesion formation, together with reduced cell proliferation within the atherosclerotic plaques, without affecting plasma lipid levels or circulating leukocyte levels in apoE-deficient mice. Furthermore, we also notice that S1PR1 deletion in VSMC reduces their ability to proliferate and accumulate lipid droplets in culture in response to S1PR1 selective agonist SEW2871. These results suggest that S1PR1 may play a pro-atherogenic role in VSMCs.

This manuscript will be submitted to Atherosclerosis, Thrombosis, and Vascular Biology for publication in 2024. This manuscript was written by Narmadaa Thyagarajan under the guidance of Dr. Bernardo L. Trigatti. This project was designed by Narmadaa Thyagarajan and Bernardo L. Trigatti. All in-vivo experiments, except *LysM$^{cre/cre}$; S1pr1$^{lox/lox}$; ApoE$^{KO/KO}$* studies, was performed by Narmadaa Thyagarajan. *LysM$^{cre/cre}$; S1pr1$^{lox/lox}$; ApoE$^{KO/KO}$* studies were performed

by previous undergraduate students Usama Tahir and Darren Sam under the guidance of Dr. Letecia Gonzalez. VSMC cholesterol loading experiment, immunofluorescence staining for CD45, Mac3, and SMA was carried out and analyzed by postdoctoral researcher Wei Wang. An in-vitro cell proliferation assay was performed by Wei Wang and an undergraduate student Jennifer Nouanesengsy. *S1pr1* expression in macrophages was assessed by Alex Qian. Atherosclerotic plaque development in *LysM*$^{cre/cre}$*; S1pr1*$^{lox/lox}$*; LDLR*$^{KO/KO}$ male mice was assessed by Yuan Qui.

2.1 Abstract

Objective: The sphingosine 1 phosphate (S1P) receptor 1 (S1PR1), one of the five G-protein coupled receptors for S1P, controls several cellular processes and thus implicated in atherosclerosis. Although S1PR1 deletion in macrophages and endothelial cells had shown to enhance atherosclerotic plaque development *in-vivo*, the role of S1PR1 in vascular smooth muscle cells in atherosclerosis is not yet clear.

Approach and results: In an attempt to investigate the cell-specific effect of deleting S1PR1 on atherosclerosis, we unexpectedly observed that introducing *S1pr1*$^{lox/lox}$ allele alone (in the absence of cre-mediated excision) reduces atherosclerotic lesions in the aortic sinus cross-sections of *ApoE*$^{KO/KO}$ mice compared to *S1pr1*$^{WT/WT}$*; ApoE*$^{KO/KO}$ controls after feeding them a high-fat (HF)-diet for eight weeks. The presence of *S1pr1*$^{lox/lox}$ allele alone in mice significantly reduced *S1pr1* expression in select cell types, such as macrophages and vascular smooth muscle cells, compared to *S1pr1*$^{WT/WT}$ mice. Furthermore, reciprocal bone marrow transplantation between *S1pr1*$^{WT/WT}$*; ApoE*$^{KO/KO}$ and *S1pr1*$^{lox/lox}$*; ApoE*$^{KO/KO}$ mice demonstrated that the *S1pr1*$^{lox/lox}$ mutation in a non-bone marrow-derived cell type was responsible for the reduced atherosclerotic plaque development. We hypothesized that this cell type might be the vascular smooth muscle cell. Therefore, we generated *Tagln-cre*^{TG}*; S1pr1*$^{lox/lox}$*; ApoE*$^{KO/KO}$ mice in which cre is expressed under the control of the promoter of the smooth muscle cell-specific Transgelin gene in order to completely eliminate *S1pr1* expression in vascular

smooth muscle cells. Our data showed that complete inactivation of S1PR1 in vascular smooth muscle cells reduced diet-induced atherosclerosis by approx. 50% compared to *S1pr1*$^{lox/lox}$*; ApoE*$^{KO/KO}$ controls without affecting plasma lipid levels or absolute leukocyte counts in circulation. A synthetic S1PR1 selective agonist (SEW2871) was able to stimulate the proliferation (when added alone) and to enhance the platelet derived growth factor-stimulated proliferation of cultured primary aortic smooth muscle cells isolated from *S1pr1*$^{WT/WT}$*; ApoE*$^{KO/KO}$ mice and these effects were reduced in primary aortic smooth muscle cells from *S1pr1*$^{lox/lox}$*; ApoE*$^{KO/KO}$ mice and eliminated in primary aortic smooth muscle cells from *Tagln-cre*^{TG}*; S1pr1*$^{lox/lox}$*; ApoE*$^{KO/KO}$ mice, mirroring levels of *S1pr1* expression. Similarly, we detected progressively reduced proliferation in atherosclerotic plaques from mice that were *S1pr1*$^{WT/WT}$*; ApoE*$^{KO/KO}$ > *S1pr1*$^{lox/lox}$*; ApoE*$^{KO/KO}$ > *Tagln-cre*^{TG}*; S1pr1*$^{lox/lox}$*; ApoE*$^{KO/KO}$ genotypes, mirroring the levels of expression of S1PR1 in cultured primary aortic smooth muscle cells. Finally, SEW2871 enhanced cholesterol-induced lipid droplet formation and *Cd68* gene expression but suppressed *Acta2* gene expression in cultured primary aortic smooth muscle cells from *S1pr1*$^{WT/WT}$*; ApoE*$^{KO/KO}$ mice and this was attenuated in primary aortic smooth muscle cells from *S1pr1*$^{lox/lox}$*; ApoE*$^{KO/KO}$ mice and lost in aortic smooth muscle cells from *Tagln-cre*^{TG}*; S1pr1*$^{lox/lox}$*; ApoE*$^{KO/KO}$ mice.

Conclusions: Our data demonstrates that knocking out S1PR1 in vascular smooth muscle cells protects *ApoE*$^{KO/KO}$ mice against atherosclerosis by reducing proliferation and foam cell formation in vascular smooth muscle cells.

2.2 Introduction

Atherosclerosis is a multifaceted disease involving a complex interplay between lipids and multiple cell types, including endothelial cells, immune cells such as monocyte-derived macrophages, and vascular smooth muscle cells (VSMC) in the arterial wall (Tabas, García-Cardeña, and Owens 2015; Hegele 1996). The dysfunction of vascular endothelial cells lining the atherosclerotic lesion-prone regions of arteries and the recruitment of blood-borne monocytes into the subendothelial space are key early events in the pathobiology of murine atherosclerosis (Gimbrone Jr and García-Cardeña 2016). Monocyte-derived macrophages retained in the intima participate in sustained inflammatory responses and take up modified lipoproteins becoming lipid-laden foam cells (Moore, Sheedy, and Fisher 2013). In addition, the medial VSMCs also undergoes proliferation and migration into the intima in response to cytokines and growth factors secreted by macrophages and endothelial cells (Newby and Zaltsman 1999). For several decades, macrophages were presumed to be athero-promoting by considering their role in apoptosis and necrotic core formation (Gonzalez and Trigatti 2017), whereas VSMCs were thought to be atheroprotective due to their role in forming a plaque stabilizing-fibrous cap (Bennett, Sinha, and Owens 2016). However, loading the aortic smooth muscle cells (SMC) with cholesterol resulted in the formation of lipid droplets in culture. In addition, the lipid loading also caused these cells to lose their lineage marker genes (such as *Acta2* and *Myh11*) and gain macrophage marker genes (*Cd68* and *Mac2*), resulting in SMC-to-macrophage

transdifferentiation (Rong et al. 2003). Similar observations were made in atherosclerotic plaques of apoE-deficient mice using lineage tracing and fate mapping studies (Feil et al. 2014). Furthermore, previous studies have also identified that intimal SMCs give rise to a huge proportion of foam cells in both murine and human atherosclerotic plaques (Wang et al. 2019; Allahverdian et al. 2014).

Sphingosine-1-phosphate receptor (S1PR) 1, one of the five G-protein coupled receptor S1PR1-5, regulates vascular and immune functions in response to bioactive lysosphingolipid S1P (Rivera, Proia, and Olivera 2008; O'Sullivan and Dev 2013). S1PR1 expression is ubiquitous, with higher levels of expression observed in endothelial cells, macrophages, and proliferating VSMCs (Daum, Grabski, and Reidy 2009; Liu et al. 2018). Previous studies showed that S1PR1 signaling in endothelial cells reduced vascular permeability, promoted anti-inflammatory responses, including reduced vascular adhesion molecules, and protected against atherosclerotic plaque development in apoE KO mice (Galvani et al. 2015; Kimura et al. 2006; Argraves et al. 2008). S1PR1 signaling in macrophages also reduced apoptosis, increased migration, and protected against atherosclerosis (Al-Jarallah et al. 2014; Gonzalez et al. 2017). Thus, S1PR1 seems to be beneficial in endothelial cells and macrophages. However, S1P-S1PR1 signaling in cultured aortic smooth muscle cells (SMC) independently or synergistically with platelet-derived growth factor (PDGF) had been shown to enhance cell proliferation, migration, and cytoskeleton rearrangements (Kluk et al.

2003; Kluk and Hla 2001; Tanimoto, Lungu, and Berk 2004; Rosenfeldt et al. 2001). S1PR1 has been shown to play a role in neointimal hyperplasia, a form of vascular remodeling that occurs due to uncontrolled SMC proliferation and migration. Vascular remodeling is a key characteristic feature of atherosclerosis. An *in-vivo* study by Wamhoff et al. (Wamhoff et al. 2008) demonstrated that pharmacologically inhibiting S1PR1 and 3 receptors suppressed S1P-mediated proliferation in cultured rat aortic SMCs and reduced neointimal thickening by approx. 50% in a rat carotid artery injury model. Furthermore, overexpression of S1PR1 under the control of *Acta2* promoter enhanced neointimal hyperplasia and neointimal cell proliferation in carotid artery ligation mouse model (Kitano et al. 2019). The VSMCs overexpressing S1PR1 also exhibited higher pro-inflammatory IL6 expression (Kitano et al. 2019). These findings suggest that S1PR1 may play a pro-atherogenic role in VSMC.

In this study, we report that $ApoE^{KO/KO}$ mice homozygous for a knockout-ready $S1pr1^{lox/lox}$ conditional allele ($S1pr1^{lox/lox}; ApoE^{KO/KO}$ mice) in the absence of cre recombinase, unanticipatedly exhibit about 50% reduced high fat diet induced atherosclerotic plaque development compared to control $S1pr1^{WT/WT}; ApoE^{KO/KO}$ mice. The SMC selective expression of Cre recombinase resulted in a further 50% reduction in high fat diet induced atherosclerotic plaque development in the $S1pr1^{lox/lox}; ApoE^{KO/KO}$ mice. We demonstrate that homozygosity for the S1PR1 lox mutant allele resulted in approximately 50% reduction in *S1pr1* gene expression in aortic SMCs and peritoneal macrophages and other tissues and that the

introduction of the Tagln-Cre transgene completely eliminated *S1pr1* gene expression in aortic SMCs but not macrophages. Finally, the synthetic S1PR1 specific agonist SEW2871 stimulated the proliferation, enhanced the PDGF-stimulated proliferation and enhanced cholesterol induced lipid droplet formation and *Cd68* gene expression and suppression of *Acta2* gene expression in primary aortic SMCs from *S1pr1*$^{WT/WT}$*; ApoE*$^{KO/KO}$ mice while these effects were attenuated in primary aortic SMCs from *S1pr1*$^{lox/lox}$*; ApoE*$^{KO/KO}$ mice and absent from primary aortic SMCs from *Tagln-cre*^{TG}*; S1pr1*$^{lox/lox}$*; ApoE*$^{KO/KO}$ mice. These results demonstrate that S1PR1 in aortic SMCs promotes atherosclerosis development, and that selective inhibition of S1PR1 in SMCs effectively protects against atherosclerotic plaque formation by attenuating VSMC proliferation and foam cell formation.

2.3 Materials and Methods

2.3.1 Mice

All mouse procedures were performed in the David Braley Research Institute Animal Facility at McMaster University following Canadian Council of Animal Care guidelines and after approval from the Animal Research Ethics Board of McMaster University. Mice were bred and housed in ventilated cages with free access to a food and automated watering on a 12 hr light/12 hr dark cycle. *ApoE*$^{KO/KO}$, *Ldlr*$^{KO/KO}$, wild-type (WT) C57BL6, LysM-cre (where cre recombinase is inserted into the first ATG codon of Lysozyme 2 gene), and Tagln-cre^{TG} (Cre recombinase is expressed under the control of mouse Transgelin promoter) mouse founders were purchased from Jackson Laboratories. *S1pr1*$^{lox/lox}$ mice were bred from founders originally generously provided by Professor Richard Proia (National Institute of Diabetes and Digestive and Kidney Diseases, Bethesda, MD, USA). *S1pr1*$^{lox/lox}$ mice were bred with either *LysM*$^{cre/cre}$ or *Tagln-cre*^{TG} mice to generate myeloid-specific S1PR1 KO (*LysM*$^{cre/cre}$ *S1pr1*$^{lox/lox}$) mice or SMC-specific S1PR1 KO mice (*Tagln-cre*^{TG}*; S1pr1*$^{lox/lox}$). For atherosclerosis studies, *LysM*$^{cre/cre}$*; S1pr1*$^{lox/lox}$ mice and *Tagln-cre*^{TG}*; S1pr1*$^{lox/lox}$ mice were crossed with *ApoE*$^{KO/KO}$ mice to generate *LysM*$^{cre/cre}$*; S1pr1*$^{lox/lox}$*; ApoE*$^{KO/KO}$ and *Tagln-cre*^{TG}*; S1pr1*$^{lox/lox}$*; ApoE*$^{KO/KO}$ mice as well as *S1pr1*$^{lox/lox}$*; ApoE*$^{KO/KO}$ and control *S1pr1*$^{WT/WT}$*; ApoE*$^{KO/KO}$ mice with the unaltered (WT) *S1pr1* gene. To induce accelerated atherosclerosis development, mice starting at 10 weeks of age were fed with a high fat diet (HFD containing 21% butter fat and 0.15% cholesterol) for 8 weeks.

2.3.2 Bone marrow transplantation

Bone marrow (BM) transplantation was performed as described previously with some modifications (Covey et al. 2003; Pei et al. 2013; Yu et al. 2018; Gonzalez et al. 2017; Kluck et al. 2023). Bone marrow recipients (eight weeks of age) were exposed to 2 doses (667 and 333 rad) of irradiation with a 3 hrs rest between doses, using a ^{137}Cs source using a Gammacel 3000 small animal irradiator (Best Theratronics, Ottawa, ON, Canada) to induce bone marrow aplasia. BM donor mice were humanely euthanized, and BM cells were collected by flushing their femurs and tibias with Iscove's Modified Dulbecco's media (Gibco, Thermo Fisher, Ottawa, ON, Canada) containing 2% heat-inactivated fetal bovine serum (FBS) supplemented with 2mM L-Glutamine, 50 U/mL penicillin, and 50 mg/mL streptomycin. BM cells were disaggregated and passed through 100um mesh prior to intra venous injection into the retro-orbital venous plexus of irradiated recipient mice (9 x 10^6 cells per recipient). Recipient mice were allowed to recover for four weeks before blood was collected and genotyped to confirm BM engraftment and commencing HFD feeding to induce atherosclerosis.

2.3.3 In-vitro cell culture

Aortic SMCs were isolated from mice (5-8 weeks old C57BL6, *S1pr1*$^{lox/lox}$, *S1pr1*$^{WT/WT}$; *ApoE*$^{KO/KO}$, *S1pr1*$^{lox/lox}$; *ApoE*$^{KO/KO}$, and *Tagln-cre*^{TG}; *S1pr1*$^{lox/lox}$; *ApoE*$^{KO/KO}$) as described previously by others with slight modifications (Shen et al. 2018). Briefly, the mouse was anesthetized using isoflurane and sprayed with 70% ethanol. During surgery, inhalant anesthesia was continuously provided to the

mouse under the dissecting lamp. The blood was collected by cardiac puncture and the heart was perfused with sterile PBS. Except the heart, all other organs were removed to get a clear view of the aorta. Next, the whole aorta was collected and cleaned under a dissecting microscope with sterile PBS containing 50 U/mL penicillin, and 50 mg/mL streptomycin. The aorta was incubated in a freshly prepared cocktail of enzymes (1 mg/ml collagenase II, 1 mg/ml soybean trypsin inhibitor, and 0.744 U/ml elastase) in 1X Hanks Balanced Salt Solution (HBSS; Thermo Fisher Scientific) with 50 U/mL penicillin and 50 mg/mL streptomycin for 10 min at 37 °C. After removing the adventitia, the aorta was chopped into small pieces. The final digestion step was performed by incubating them in a freshly prepared enzyme cocktail (see above) at 37 °C for 1 hr. When the tissue fragments were dissolved, the cells were washed once and cultured in DMEM/F12 supplemented with 20% FBS, 2mM L-Glutamine, 50 U/mL penicillin, and 50 mg/mL streptomycin.

Peritoneal macrophages were elicited by intraperitoneal injection of 1 ml of 10% thioglycolate. After 4 days, mice were anesthetized with isoflurane and euthanized using CO_2 asphyxiation and cells were collected by peritoneal lavage using 10 ml PBS containing 5 mM EDTA. The cells were centrifuged at 250 *x g* for 5 min and resuspended in DMEM media containing 10% FBS, 2 mM L-Glutamine, 50 U/mL penicillin, and 50 mg/mL streptomycin.

2.3.4 Cell Proliferation

The primary aortic SMCs were seeded at a cell density of 5 x 10^3 cells/chamber in Lab-TekTM 8-well chamber slides in DMEM/F12 media supplemented with 20% heat-inactivated FBS, 2 mM L-Glutamine, 50 U/mL penicillin and 50 mg/mL streptomycin and incubated for 48 hrs at 37°C and 5% CO_2. Cells were washed twice and serum-starved in DMEM/F12 media containing 3% newborn calf lipoprotein deficient serum (NCLPDS), 2 mM L-glutamine, 50 U/mL penicillin and 50 mg/mL streptomycin for 24 hrs and then treated with no addition or SEW2871 (10 μM) in the presence or absence of PDGF-BB (50 ng/ml) as above for 24 hrs. The cells were fixed with 4% PFA for 20 min after 2x washes with plain DMEM/F12 media, permeabilized with 0.1% Triton X-100 in PBS for 5 min after 2x wash with PBS, and blocked with 3% goat serum in PBS-T for 1 hr at RT. Then cells were incubated with rabbit anti-Ki67 antibody (# ab15580, Abcam) diluted 1:50 with 3% goat serum in PBS-T solution at 4°C overnight, washed 3x with PBS-T, and incubated with goat anti-rabbit Alexa Fluor™ 488 secondary antibody (Thermo Fisher Scientific, catalog No. A-11008) diluted at 1:500 with 3% goat serum in PBS-T solution) at RT for 1 hr. Samples were stained with nuclear DNA 4’,6-diamidino-2-phenylindole dihydrochloride (DAPI; 300 nM) mounted and imaged with a STELLARIS confocal microscope (Leica Microsystems, Wetzlar, Germany). Alternatively, primary aortic SMCs were seeded at a cell density of 2 x 10^3 cells/ well in a 96-well plate for 3-(4,5-dimethylthiazol-2-yl)-2,5-diphenyltetrazolium bromide (MTT) assay; and seeded 2 x 10^4 cells/ well in a 6- well place for cell

proliferation assay. The cells were grown in the media described above for 48 hrs. At that point the media was replaced with fresh media without in serum and cells were cultured for 24 hrs, prior to the addition of fresh serum-free media without or with recombinant PDGF-BB (50 ng/ml) or SEW2871 (10 µM). For the MTT assay, the cells were incubated with 0.5 mg/ml MTT solution (Cayman Chemical Company, Ann Arbor, Michigan, USA) for 4 hrs. The formazan crystals produced in the cells were dissolved with crystal dissolving solution and the absorbance was measured at 570 nm using a Spectramax plus microplate reader (Molecular Devises, Sunnyvale, CA, USA). For proliferation assay, cells were released from each well by treatment with trypsin and counted in a hemocytometer at times 0 (corresponding to the addition of PDGF and/or SEW2871), 1, and 2 days.

2.3.5 Cholesterol Loading

Primary aortic SMCs were seeded at a cell density of 5 x 10^4 cells/chamber in Lab-TekTM 8-well chamber slides or 2 x 10^5 cells/well in 6-well plates and grown in the media described above for 24 hrs. Cells were washed twice and serum-starved in DMEM/F12 media containing 0.2% BSA, 2 mM L-glutamine, 50 U/mL penicillin, and 50 mg/mL streptomycin for 20 hrs. Afterwards, cells were treated with no addition or SEW2871 (10 µM) in the presence or absence of 10 µg/ml of cholesterol complexed with methyl-β-cyclodextrin (Molar ratio- 1:6 cholesterol/cyclodextrin; Sigma-Aldrich) for 72 hrs. The corresponding treatment media were changed every 24 hrs. The concentration of cholesterol/cyclodextrin complex used here was based on cholesterol weight, as reported previously (Rong et al. 2003). Cells

cultured on chamber slides were stained with 0.3% w/v Oil Red O and visualized by fluorescence microscopy, while cells seeded in 6-well plates were utilized for RT-PCR analyses (see below).

For Oil Red O staining, cells were fixed with 4% PFA for 20 min after 2x washes with plain DMEM/F12 media, permeabilized with 0.1% Triton X-100 in PBS for 5 min after 2x wash with PBS, and blocked with 3% goat serum in PBS-T for 1 hr at RT. Then cells were incubated with anti-alpha SMA primary antibody (Abcam, catalog No. ab5694) diluted at 1:200 with 3% goat serum in PBS-T solution at 4°C overnight, washed 3x with PBS-T, and incubated with goat anti-rabbit Alexa Fluor™ 488 secondary antibody (Thermo Fisher Scientific, catalog No. A-11008) diluted at 1:500 with 3% goat serum in PBS-T solution at RT for 1 hr. After 3x washes in PBS-T, cells were stained with 0.3 % w/v Oil Red O solution at RT for 18 min in Coplin Jar, washed 3x in PBS-T, cells were counterstained for nuclear DNA DAPI, mounted and imaged using a STELLARIS confocal microscope (Leica Microsystems, Wetzlar, Germany).

2.3.6 RT-PCR

RNA was isolated from the tissue samples, peritoneal macrophages, and VSMCs (*in vitro*) using RNeasy Mini Kit (Qiagen, Toronto, ON, Canada) according to the Manufacturer's instructions. cDNA was synthesized from 500-1000 ng of RNA samples using a High-Capacity cDNA Reverse Transcription kit (Invitrogen Life Technologies Inc., Burlington, ON, Canada). Quantitative RT-PCR was performed using Platinum SYBR green dye (Invitrogen) on 10 ng cDNA per 20 ul cDNA

synthesis reaction mix using Applied Biosystems StepOnePlus Real-Time PCR System (Thermo Fisher Scientific, Ottawa, ON, Canada). The mouse primers and probe sequences for sphingosine 1 phosphate receptors (*S1pr*) 1, 2, and 3, *Acta2*, and the cluster of differentiation 68 (*Cd68*) are listed in major resource table. All target genes were normalized to the reference gene *Gapdh*. All RT-PCR reactions was performed in duplicates. The transcript levels were calculated by the $2^{-\Delta\Delta Ct}$ method (Livak and Schmittgen 2001) and expressed as fold-change over the controls.

2.3.7 Plasma lipid analysis

Blood was collected from anesthetized mice by cardiac puncture prior to sacrifice. All samples were spun at 775 x *g* for 10 min to obtain plasma. Enzymatic assay kits were used to quantify total cholesterol (Cholesterol Infinity kit, Thermo Scientific, Ottawa, ON, Canada), HDL-C (HDL-cholesterol E kit, Wako Diagnostics, Mountain View, CA, USA) and triglycerides (Triglyceride, Wako Diagnostics, Mountain View, CA, USA). Absorbance was measured with a Spectramaxplus microplate reader (Molecular Devises, Sunnyvale, CA, USA) using SoftMax Pro software. Non-HDL cholesterol was calculated as the difference between plasma total cholesterol and HDL-C values for each sample.

2.3.8 Flow cytometry analysis

Fresh blood was incubated with appropriate fluorochrome-conjugated antibodies for CD3, CD4, CD8, NK1.1, CD11b, and Ly6G to label different leukocytes. Next, the red blood cells were lysed and fixed with a 1-step fix/lyse solution (1X) (# 00-

5333, Thermo Fisher Scientific). The 123count eBeads (#01-1234-42, Thermo Fisher Scientific) were added to each sample, and results were acquired on a BD FACSCalibur Flow Cytometry system (BD Biosciences, Mississauga, Ontario, Canada). The data were analyzed using FlowJo v10 software.

2.3.9 Analysis of atherosclerotic plaque sizes

For atherosclerosis studies, hearts were excised from anesthetized mice upon sacrifice and embedded in the Tissue-Tek® OCT compound. Serial 10 µm thick cryosections from the appearance to the disappearance of aortic valve leaflets were collected on microscopic slides. The sections were stained with ORO for neutral lipids and counterstained with Meyer's Hematoxylin for cell nuclei. Images were obtained using a Zeiss Axiovert 200M fluorescence microscope (Carl Zeiss Canada Ltd. Toronto, ON, Canada) at 5X magnification. Atherosclerotic plaque cross sectional areas were measured in each of 7 sections taken at 100 µm intervals, spanning a total of 600 µm of the aortic sinus. Atherosclerotic plaque volumes were calculated as the areas under the curve of atherosclerotic plaque cross sectional area versus distance.

2.3.10 Immunofluorescence analyses of atherosclerotic plaques

Sections of atherosclerotic plaques were fixed by 4% PFA , permeabilized with 0.1% Triton X-100 and incubated with the following primary antibodies: rabbit anti-Ki67 antibody (1:50 dilution, # ab15580, Abcam), rat anti-mouse CD107b (Mac3) antibody (1:50 dilution, # 553322, BD biosciences), and anti-alpha SMA primary antibody (1:200, #ab5694, Abcam) at 4°C overnight followed by goat anti-rabbit

Alexa Fluor™ 488 or 594 secondary antibody or goat anti-rat Alexa Fluor™ 488 secondary antibody (1:500 dilution, Thermo Fisher Scientific) at RT for 1 hr. The leukocyte (CD45) content was detected using Alexa Fluor™ 594 anti-mouse CD45.2 Antibody (#109850, BioLegend). Slides were then stained with DAPI (as described earlier) for 10 min at room temperature and mounted with PermafluorTM aqueous mounting medium (Fisher Scientific). All images were captured using a STELLARIS confocal microscope (Leica Microsystems, Wetzlar, Germany) with a 63X objective. Ki67+ cells within the atherosclerotic lesions were normalized to DAPI counts. Total area of CD45, Mac3, and SMA staining within the atherosclerotic plaques was normalized to total plaque area.

2.3.11 Statistical Analysis

We confirmed the normal distribution and tested the difference between the variances using Shapiro-Wilk normality test and F-test, respectively. To compare two independent groups, we used Welch's t-test when sample variances were unequal or Student's t-test when sample variances were equal. Unless otherwise stated, we used one-way ANOVA with Tukey's multiple comparison test to compare three or more groups with one independent variable, and Two-way ANOVA with Tukey's multiple comparison test to compare multiple groups with two or more independent variables. All data are represented as mean± standard error mean (SEM). Statistical analyses were performed using GraphPad Prism 9.

2.4 Results

2.4.1 Reduced atherosclerosis in *S1pr1$^{lox/lox}$; ApoE$^{KO/KO}$* mice in the absence of Cre recombinase

To allow us to analyze the effects of conditional deletion of S1PR1 on atherosclerosis in apoE-deficient mice, we first generated *S1pr1$^{lox/lox}$; ApoE$^{KO/KO}$* and control *S1pr1$^{WT/WT}$; ApoE$^{KO/KO}$* mice. We fed these mice a high fat diet for 8 weeks and analyzed atherosclerotic plaque cross sectional areas in several sections along 600 µm of the aortic sinus. Surprisingly, we found that atherosclerosis development in the aortic sinus was significantly reduced, in the absence of Cre recombinase expression, in both male ($1.86 \pm 0.45 \times 10^7$ µm^3 versus $6.25 \pm 0.73 \times 10^7$ µm^3; $P<0.0001$; **Figure 2.1A-D**) and female ($4.38 \pm 0.60 \times 10^7$ µm^3 versus $9.19 \pm 0.75 \times 10^7$ µm^3; $P<0.0001$; **Figure 2.1E-H**) *S1pr1$^{lox/lox}$; ApoE$^{KO/KO}$* mice compared to control *S1pr1$^{WT/WT}$; ApoE$^{KO/KO}$* mice. In contrast, there were no statistically significant differences in the average plasma levels of total, HDL- and non-HDL cholesterol, or triglycerides, although towards reductions in total and non-HDL cholesterol were noted in males (**Supplementary Figure 2.7A-D**)

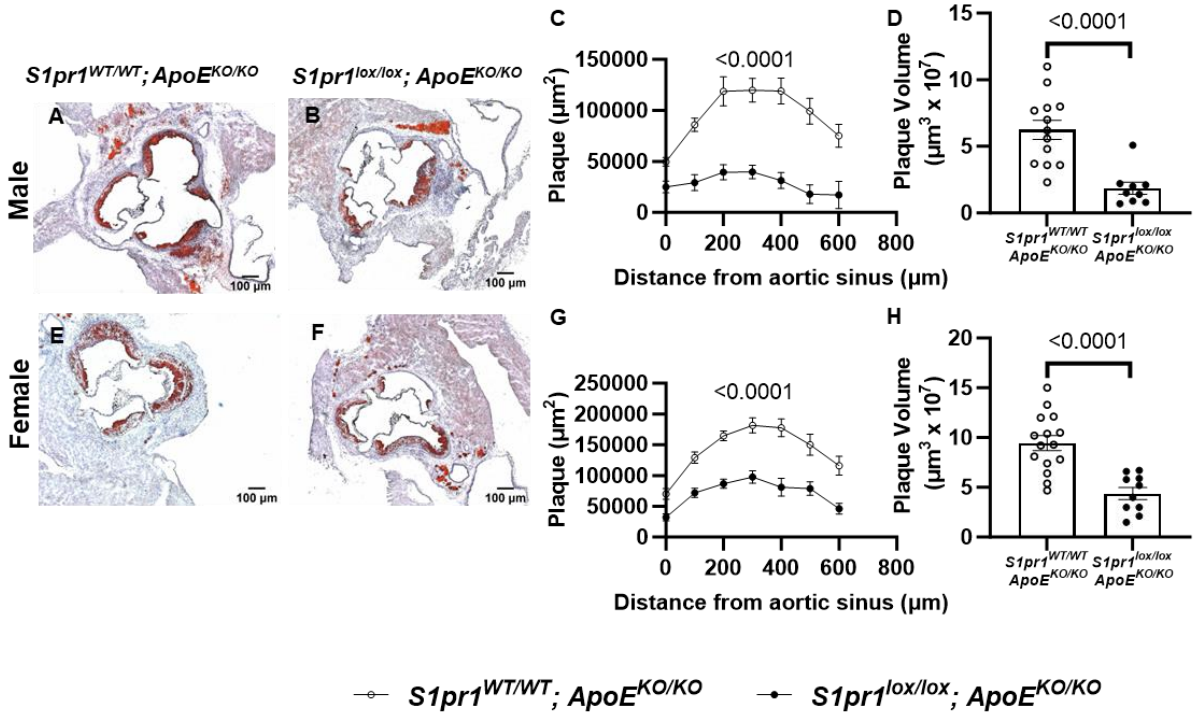

Figure 2.1: *S1pr1*$^{lox/lox}$ mutation alone independent of cre recombinase protects against diet-induced atherosclerosis

The atherosclerotic plaques in *S1pr1*$^{lox/lox}$*; ApoE*$^{KO/KO}$ mice littermates were quantified in comparison to *S1pr1*$^{WT/WT}$*; ApoE*$^{KO/KO}$ controls. The mice were fed a normal diet for 10 weeks and HFD for 8 weeks. The plaques were visualized using Oil Red O. **A, B** are representative images of the atherosclerotic plaques in the aortic-sinus cross-sections for the male *S1pr1*$^{WT/WT}$*; ApoE*$^{KO/KO}$ and *S1pr1*$^{lox/lox}$*; ApoE*$^{KO/KO}$ mice (n=13, 9). **C, the** plaque cross-sectional area along 600 µm of the aortic sinus. **D**, total plaque volume of each group of male mice, measured by calculating the area under the curve of the plaque cross-sectional area versus distance. **1E and F** are representative images of each group for the female mice (n=15, 10). **1G** and **H** represent the plaque cross-sectional area and total plaque volume of each group of female mice. Scale bars= 100 µm. Statistical analysis was performed using a two-way ANOVA for the line graph and an unpaired t-test for the bar graph, respectively. All data are representative of mean± SEM from biological replicates.

2.4.2 The effect of the *S1pr1$^{lox/lox}$* allele on *S1pr1* expression

We wondered if this reduction of atherosclerosis in *S1pr1$^{lox/lox}$; ApoE$^{KO/KO}$* mice might be due to altered levels of *S1pr1* expression in one or more tissues/ cell types in these mice. S1PR1 expression levels are reportedly high in brain, lung, aorta, and spleen of the adult mice, and moderate in the heart (Chae, Proia, and Hla 2004). We, therefore, quantified *S1pr1* gene expression by RT-PCR in these tissues. No significant changes in the *S1pr1* mRNA levels were detected in brains, hearts, lungs, and aortas except spleen **(Figure 2.2A-E)**. On the other hand, *S1pr1* expression levels were statistically significantly reduced by approximately 50 % in cultured aortic SMC and macrophages isolated from *S1pr1$^{lox/lox}$* mice compared to those isolated from *S1pr1$^{WT/WT}$* mice (**Figure 2.2F and G).** This suggests that that insertion of the LoxP sites into the *S1pr1* gene locus (Allende et al. 2003) may have resulted in hypomorphic *S1pr1* expression, at least in some tissues/cell types.

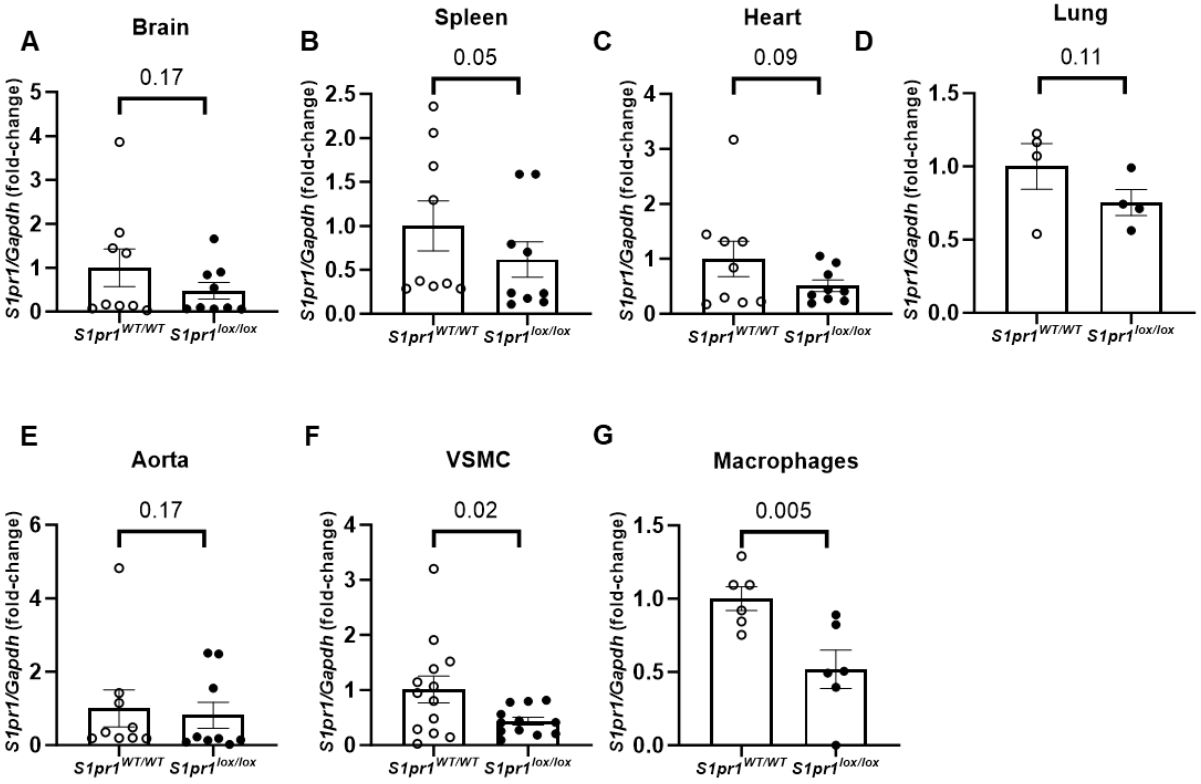

Figure 2.2: The effect of the S1pr1$^{lox/lox}$ allele on altering *S1pr1* expression levels in different tissues/ cell types

We examined the effects of the *S1pr1$^{lox/lox}$* allele on modulating S1pr1 expression levels in different tissues/ cell types. Select tissues were harvested from female mice that harbor the *S1pr1$^{lox/lox}$* and *S1pr1$^{WT/WT}$* gene at 10 weeks of age. The mRNA transcript levels of *S1pr1* were quantified in the **(A)** brain (n=9, 9); **(B)** spleen (n=9, 9); **(C)** heart (n=9, 9); **(D)** lung (n=4, 4); and **(E)** aorta (n=9, 9). The VSMCs were isolated from the aortas of these mice using the protease digestion method at 6-8 weeks of age. **F** represents *S1pr1* mRNA level in aortic VSMCs of *S1pr1$^{lox/lox}$* mice compared to *S1pr1$^{WT/WT}$* mice (n=13, 12). In addition, the peritoneal macrophages were also isolated using thioglycolate from each group of male mice at 8 weeks. **G** represents *S1pr1* gene expression in macrophages of *S1pr1$^{lox/lox}$* mice in comparison to *S1pr1$^{WT/WT}$* mice (n=6, 6). All data were normalized to GAPDH. All data are representative of mean± SEM from biological replicates.

2.4.3 The presence of the *S1pr1$^{lox/lox}$* mutation in a non-BM derived cell type protects apoE-deficient mice against HF diet-induced atherosclerosis

We have previously reported that knockout of S1PR1 in bone marrow-derived myeloid cells accelerated high fat diet induced atherosclerosis development in LDLR-deficient mice (Gonzalez et al. 2017). We, therefore, used reciprocal bone marrow transplantation to generate *ApoE$^{KO/KO}$* mice with the homozygous *S1pr1$^{lox/lox}$* mutation either exclusively in bone marrow-derived or in non-bone marrow-derived cells **(***S1pr1$^{WT/WT}$; ApoE$^{KO/KO}$* donors→ *S1pr1$^{lox/lox}$; ApoE$^{KO/KO}$* recipients and *S1pr1$^{lox/lox}$; ApoE$^{KO/KO}$* donors→ *S1pr1$^{WT/WT}$; ApoE$^{KO/KO}$* recipients). As we observed reduction in atherosclerotic plaques in both male and female *S1pr1$^{lox/lox}$; ApoE$^{KO/KO}$* mice compared to *S1pr1$^{WT/WT}$; ApoE$^{KO/KO}$* mice, we opted to utilize male mice for reciprocal bone marrow transplantation experiment. We performed genotyping for *S1pr1^{lox}* and *S1pr1^{WT}* alleles in the blood cells of the recipients to confirm the success of BMT from donor mice **(Supplementary Figure 2.8A)**. As controls for the bone marrow transplantation, we transplanted bone marrow from *S1pr1$^{WT/WT}$; ApoE$^{KO/KO}$* donors into *S1pr1$^{WT/WT}$; ApoE$^{KO/KO}$* recipients and from *S1pr1$^{lox/lox}$; ApoE$^{KO/KO}$* donors into *S1pr1$^{lox/lox}$; ApoE$^{KO/KO}$* recipients. These mice were allowed to recover for four weeks and then fed a HFD for eight weeks. Analysis of atherosclerosis in the aortic sinus revealed that atherosclerosis was reduced when the recipient mice were *S1pr1$^{lox/lox}$; ApoE$^{KO/KO}$* compared to *S1pr1$^{WT/WT}$; ApoE$^{KO/KO}$*, regardless of whether the bone marrow was from *S1pr1$^{WT/WT}$; ApoE$^{KO/KO}$* or *S1pr1$^{lox/lox}$; ApoE$^{KO/KO}$* donors, whereas there were no

statistically significant effects of transplanting *S1pr1$^{lox/lox}$; ApoE$^{KO/KO}$* versus *S1pr1$^{WT/WT}$; ApoE$^{KO/KO}$* bone marrow into either group of recipients (**Figure 2.3A-F**). This suggests that the protection against atherosclerosis development conferred by the *S1pr1$^{lox/lox}$* genotype is due to its presence in one or more types of non-bone marrow derived cells. As further support for this, we saw virtually identical results when we generated *LysM$^{cre/cre}$; S1pr1$^{lox/lox}$; ApoE$^{KO/KO}$* mice and control *LysM$^{cre/cre}$; S1pr1$^{WT/WT}$; ApoE$^{KO/KO}$* mice and analyzed HF diet-induced atherosclerosis without reciprocal bone marrow transplantation **(**Male: $1.44\times10^7 \pm 0.26$ μm^3 versus $4.63\times10^7 \pm 0.76$ μm^3, P=0.001; Female: $1.77\times10^7 \pm 0.37$ μm^3 versus $8.37\times10^7 \pm 0.79$ μm^3, P<0.0001; **Supplementary Figure 2.9A-H).** Analysis of leukocyte populations in the *S1pr1$^{WT/WT}$; ApoE$^{KO/KO}$* and *S1pr1$^{lox/lox}$; ApoE$^{KO/KO}$* mice receiving reciprocal or autologous BM transplantations, revealed that *S1pr1$^{lox/lox}$; ApoE$^{KO/KO}$* mice exhibited lower CD3+, CD8+ and B220+ cells, compared to *S1pr1$^{WT/WT}$; ApoE$^{KO/KO}$* mice, but that these were largely restored by transplantation of BM from *S1pr1$^{WT/WT}$; ApoE$^{KO/KO}$* donors **(Supplementary Figure 2.10)**. On the other hand, *S1pr1$^{lox/lox}$; ApoE$^{KO/KO}$* mice also exhibited trends towards reduced levels of NK, NKT, CD11b+ and Ly6G+ cells which were not restored by transplantation of BM from *S1pr1$^{WT/WT}$; ApoE$^{KO/KO}$* donors **(Supplementary Figure 2.10)**. Importantly, these alterations in circulating leukocyte counts did not correlate with changes in atherosclerosis, suggesting that the reduced atherosclerosis in the recipient *S1pr1$^{lox/lox}$; ApoE$^{KO/KO}$* mice was not likely the consequence of reductions in circulating levels of any of these leukocytes.

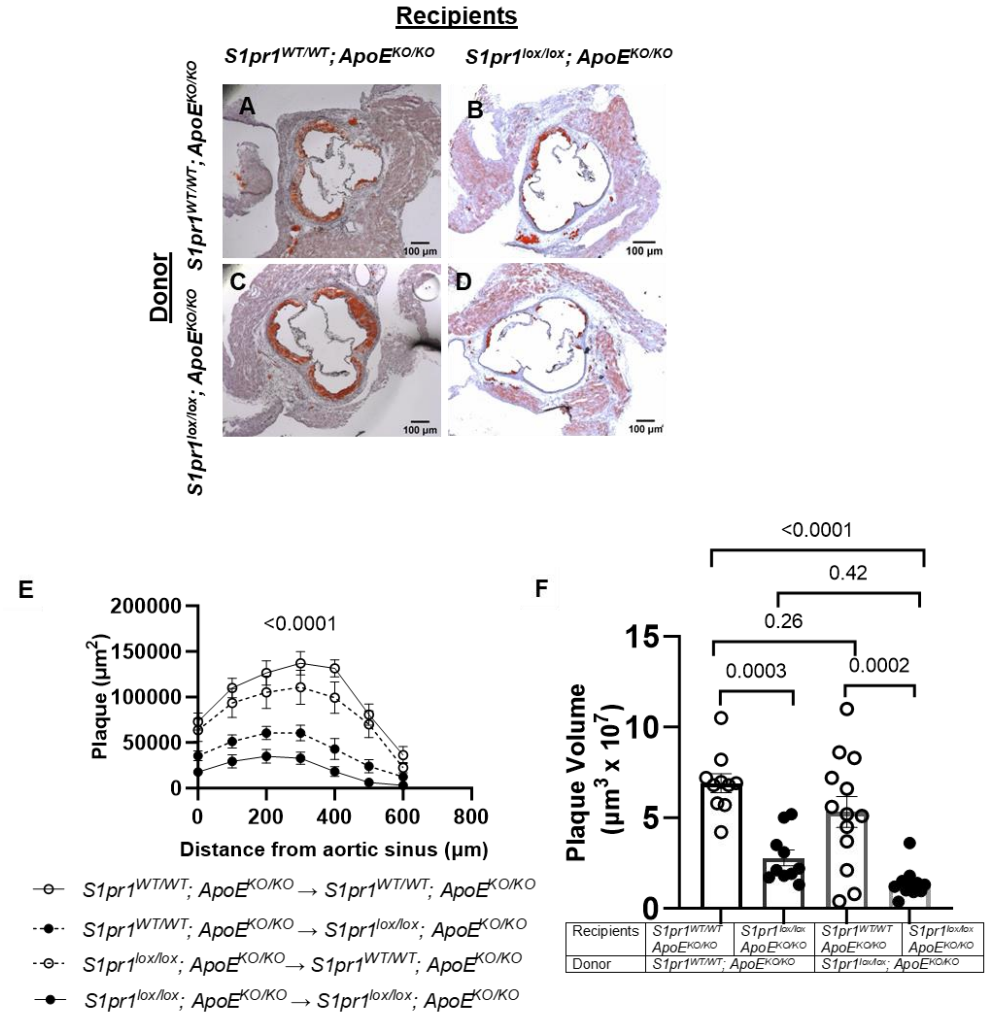
Recipients
S1pr1WT/WT; ApoEKO/KO
S1pr1lox/lox; ApoEKO/KO
Donor
S1pr1WT/WT; ApoEKO/KO
S1pr1lox/lox; ApoEKO/KO
A
B
C
D
100 µm
E
Plaque (µm2)
200000
150000
100000
50000
0
<0.0001
0
200
400
600
800
Distance from aortic sinus (µm)
S1pr1WT/WT; ApoEKO/KO → S1pr1WT/WT; ApoEKO/KO
S1pr1WT/WT; ApoEKO/KO → S1pr1lox/lox; ApoEKO/KO
S1pr1lox/lox; ApoEKO/KO → S1pr1WT/WT; ApoEKO/KO
S1pr1lox/lox; ApoEKO/KO → S1pr1lox/lox; ApoEKO/KO
F
<0.0001
0.42
0.26
0.0003
0.0002
Plaque Volume (µm3 x 10^7)
15
10
5
0
Recipients
S1pr1WT/WT ApoEKO/KO
S1pr1lox/lox ApoEKO/KO
S1pr1WT/WT ApoEKO/KO
S1pr1lox/lox ApoEKO/KO
Donor
S1pr1WT/WT; ApoEKO/KO
S1pr1lox/lox; ApoEKO/KO

Figure 2.3: The presence of the *S1pr1$^{lox/lox}$* allele in a non-BM derived cell type reduces atherosclerotic plaque development

Reciprocal BMT was performed in *S1pr1$^{WT/WT}$; ApoE$^{KO/KO}$* mice and *S1pr1$^{lox/lox}$; ApoE$^{KO/KO}$* male mice at 8 weeks of age. The recipient mice were lethally irradiated with 1000 RAD and transplanted with donor BM cells. The mice were allowed to recover for 4 weeks. Atherosclerotic plaque size was assessed in the cross-sections of the aortic sinus of *S1pr1$^{WT/WT}$; ApoE$^{KO/KO}$* and *S1pr1$^{lox/lox}$; ApoE$^{KO/KO}$* recipient mice fed with 8 weeks of HFD. Cryosections were stained with Oil Red O to visualize plaques. **A & B** are the representative images of *S1pr1$^{WT/WT}$; ApoE$^{KO/KO}$* and *S1pr1$^{lox/lox}$; ApoE$^{KO/KO}$* recipients transplanted with *S1pr1$^{WT/WT}$; ApoE$^{KO/KO}$* BM donor cells. **C & D** are representative images of *S1pr1$^{WT/WT}$; ApoE$^{KO/KO}$* and *S1pr1$^{lox/lox}$; ApoE$^{KO/KO}$* recipients transplanted with *S1pr1$^{lox/lox}$; ApoE$^{KO/KO}$* BM donor cells. **E** and **F** represent plaque cross-sectional area and total plaque volume for all four reciprocal BMT groups. N=10,10,13, and 11. Scale bars = 100 µm. Plaque cross-sectional areas were analyzed by the two-way ANOVA. For the bar graph, the statistical analysis was performed by the one-way ANOVA with the Tukey Post hoc test. All results are denoted as mean± SEM. Statistical analyses and graphical representations were made in GraphPad Prism.

2.4.4 Selective deletion of S1PR1 in VSMC attenuates atherosclerosis development

The observations that the presence of the *S1pr1*$^{lox/lox}$ genotype was associated with reduced *S1pr1* expression in isolated aortic SMCs together with previous reports that selective inactivation of S1PR1 in endothelial cells or bone marrow derived myeloid cells increased atherosclerosis development, an effect opposite to reduced atherosclerosis we observed in *S1pr1*$^{lox/lox}$*; ApoE*$^{KO/KO}$ mice (**Figures 2.1** and **2.3**), led us to speculate that the reduced atherosclerosis may be a consequence of reduced S1PR1 in VSMCs. To test this, we evaluated the direct effect of knocking out S1PR1 in VSMCs by generating *Tagln-cre*^{TG}*; S1pr1*$^{lox/lox}$*; ApoE*$^{KO/KO}$ mice (in which *S1pr1* expression is driven by Transgelin promoter). We first isolated and cultured primary aortic SMCs from *Tagln-cre*^{TG}*; S1pr1*$^{lox/lox}$*; ApoE*$^{KO/KO}$ (N=5) and *S1pr1*$^{lox/lox}$*; ApoE*$^{KO/KO}$ (control; N=4) male mice and analyzed transcript levels of *S1pr1*, *S1pr2* and *S1pr3* to confirm selective S1PR1 deletion. Our data showed 95% reduction of *S1pr1* mRNA transcript levels (0.05±0.03 versus 1±0.24; *P*=0.02) while no compensatory changes in *S1pr2* (1.06±0.30 versus 1±0.15; *P*=0.99) or *S1pr3* (1.2±0.30 versus 1±0.11 vs; *P*=0.92) expression in aortic SMCs of *Tagln-cre*^{TG}*; S1pr1*$^{lox/lox}$ *; ApoE*$^{KO/KO}$ mice compared to control cre-negative *S1pr1*$^{lox/lox}$*; ApoE*$^{KO/KO}$ mice (**Figure 2.4 A**). In addition, we also quantified *S1pr1* expression in peritoneal macrophages of the same strains. As expected, S1PR1 transcript levels were not altered in peritoneal macrophages (1.08±0.12 versus 1±0.14; *P*=0.67, **Figure 2.4 B**) of *Tagln-cre*^{TG}; *S1pr1*$^{lox/lox}$*;*

ApoE$^{KO/KO}$ compared to cre-negative *S1pr1*$^{lox/lox}$*; ApoE*$^{KO/KO}$ mice. These results confirm the cre-dependent selective inactivation of S1PR1 in aortic SMCs.

To test the effect of inactivating S1PR1 in VSMC on atherosclerosis, we compared levels of atherosclerosis in *Tagln-cre*^{TG}; *S1pr1*$^{lox/lox}$*; ApoE*$^{KO/KO}$ and cre-negative *S1pr1*$^{lox/lox}$*; ApoE*$^{KO/KO}$ littermates that were fed the HF diet for 8 weeks. For both male and female mice, fasting plasma cholesterol levels were similar between *Tagln-cre*^{TG}; *S1pr1*$^{lox/lox}$*; ApoE*$^{KO/KO}$ and cre-negative *S1pr1*$^{lox/lox}$*; ApoE*$^{KO/KO}$ mice **(Supplementary Figure 2.11)**. In addition, we also quantified the levels of circulating leukocytes using flow cytometry. Both male and female *Tagln-cre*^{TG}; *S1pr1*$^{lox/lox}$*; ApoE*$^{KO/KO}$ mice exhibited similar levels of circulating leukocytes in comparison to corresponding cre-negative *S1pr1*$^{lox/lox}$*; ApoE*$^{KO/KO}$ mice **(Supplementary Figure 2.12)**. Oil red O/hematoxylin staining of atherosclerotic plaques in the aortic sinuses revealed that both male and female *Tagln-cre*^{TG}; *S1pr1*$^{lox/lox}$*; ApoE*$^{KO/KO}$ mice exhibited approx. 50% reductions in diet-induced atherosclerosis compared to corresponding cre-negative *S1pr1*$^{lox/lox}$*; ApoE*$^{KO/KO}$ controls (Male-0.90±0.17×10^7 μm^3 vs 1.61±0.17×10^7 μm^3, P=0.01, N=11, 8. Female- 1.56±0.24×10^7 μm^3 vs 2.86±0.53×10^7 μm^3, *P*= 0.03, N=9, 10. **Figure 2.4 C-J**). No significant changes in the abundance of CD45- and Mac3-positive cells in the atherosclerotic plaques were observed between corresponding *S1pr1*$^{WT/WT}$*; ApoE*$^{KO/KO}$, cre-negative *S1pr1*$^{lox/lox}$*; ApoE*$^{KO/KO}$, and *Tagln-cre*^{TG}; *S1pr1*$^{lox/lox}$*; ApoE*$^{KO/KO}$ mice. Although there was a trend towards increased α-SMA-positive staining atherosclerotic lesions of *Tagln-cre*^{TG}; *S1pr1*$^{lox/lox}$*; ApoE*$^{KO/KO}$ mice this did

not reach statistical significance **(Supplementary Figure 2.13)**. Some studies have reported Tagln promoter activity in hematopoietic cells (Yu et al. 2011), raising the possibility that differences in atherosclerosis between the cre-negative *S1pr1*$^{lox/lox}$*; ApoE*$^{KO/KO}$ and *Tagln-cre*^{TG}; *S1pr1*$^{lox/lox}$*; ApoE*$^{KO/KO}$ mice may reflect cre-mediated inactivation of S1PR1 in hematopoietic rather than SMCs. To rule this out, we transplanted BM from cre-negative *S1pr1*$^{WT/WT}$*; ApoE*$^{KO/KO}$ male donor mice into cre-negative *S1pr1*$^{lox/lox}$*; ApoE*$^{KO/KO}$ or *Tagln-cre*^{TG}; *S1pr1*$^{lox/lox}$*; ApoE*$^{KO/KO}$ male recipient mice. Analysis of aortic sinus atherosclerosis revealed the same, approximately 50 % reduction in HF diet induced atherosclerosis in the *Tagln-cre*^{TG}; *S1pr1*$^{lox/lox}$*; ApoE*$^{KO/KO}$ compared to the cre-negative *S1pr1*$^{lox/lox}$*; ApoE*$^{KO/KO}$ recipient mice ($1.1\pm0.18\times10^7$ μm^3 vs $2.7\pm0.57\times10^7$ μm^3, P=0.01, N=15, 13, **Supplementary Figure 2.14**). This is consistent with the reduced atherosclerosis being due to S1PR1 inactivation in VSMCs.

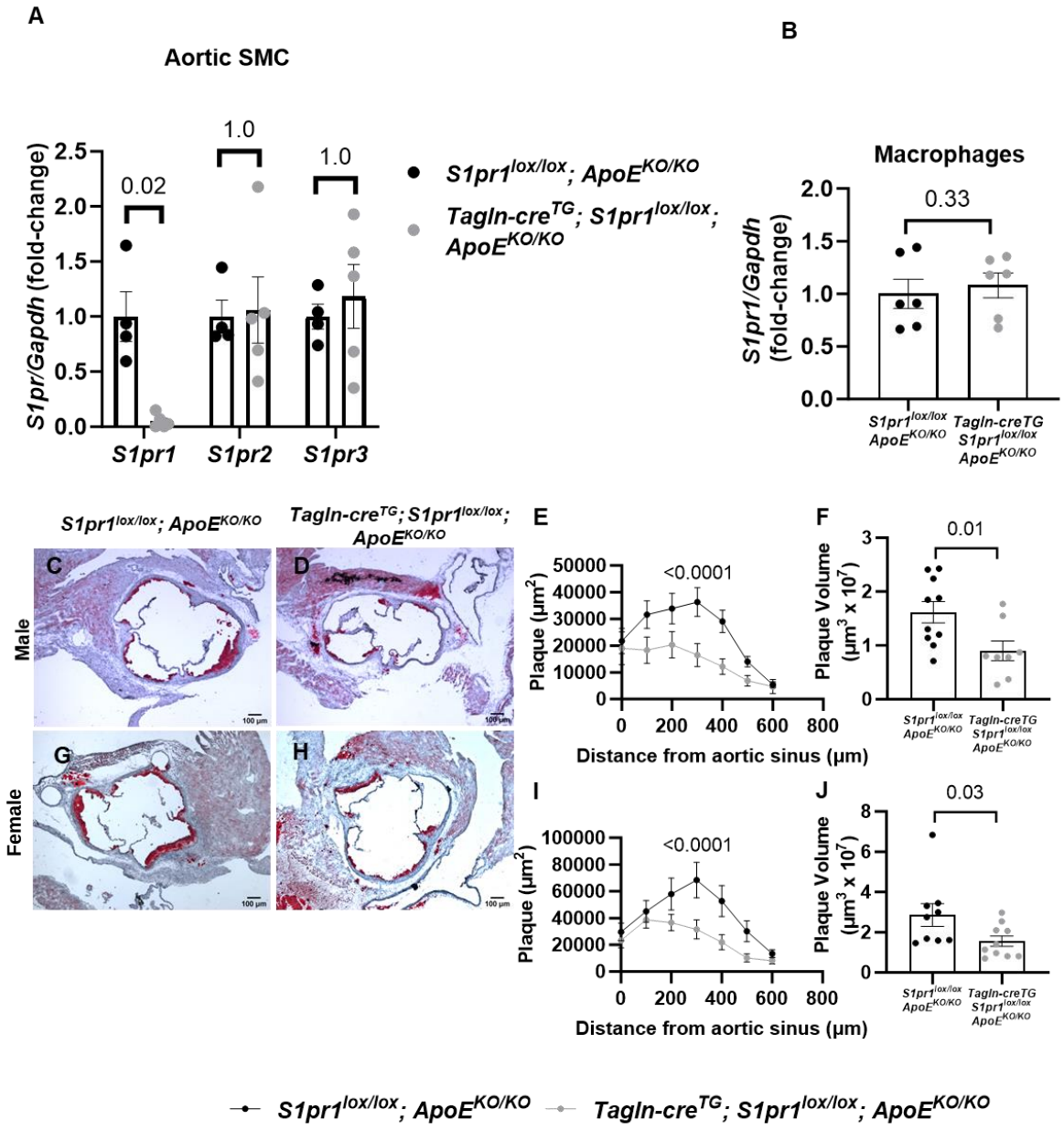
A
Aortic SMC
S1pr/Gapdh (fold-change)
0.02
1.0
1.0
S1pr1
S1pr2
S1pr3
S1pr1lox/lox; ApoEKO/KO
Tagln-creTG; S1pr1lox/lox; ApoEKO/KO
B
Macrophages
S1pr1/Gapdh (fold-change)
0.33
S1pr1lox/lox ApoEKO/KO
Tagln-creTG S1pr1lox/lox ApoEKO/KO
S1pr1lox/lox; ApoEKO/KO
Tagln-creTG; S1pr1lox/lox; ApoEKO/KO
Male
Female
C
D
G
H
E
Plaque (μm2)
<0.0001
Distance from aortic sinus (μm)
F
Plaque Volume (μm3 x 107)
0.01
I
<0.0001
J
0.03

Figure 2.4: The absence of S1PR1 in VSMC renders protection against atherosclerosis

SMC-specific S1PR1 KO (*Tagln-cre^{TG}; S1pr1$^{lox/lox}$*) mice were generated in an apoE KO background. To confirm specific S1PR1 deletion, VSMC from the aortas of male *Tagln-cre^{TG}; S1pr1$^{lox/lox}$; ApoE$^{KO/KO}$* mice and *S1pr1$^{lox/lox}$; ApoE$^{KO/KO}$* littermates were isolated using the protease digestion method. The RNA was isolated from these cells for RT-PCR analysis. **(A)** The mRNA transcript levels of *S1pr1*, *S1pr2*, and *S1pr3* in VSMCs from *Tagln-cre^{TG}; S1pr1$^{lox/lox}$; ApoE$^{KO/KO}$* mice compared to *S1pr1$^{lox/lox}$; ApoE$^{KO/KO}$* mice. N=4, 5 (each biological replicate denotes isolates from different mice). Data were analyzed using two-way ANOVA followed by Sidak's multiple comparisons test. In addition, the mRNA transcript levels of *S1pr1* were also quantified in **(B)** peritoneal macrophages isolated from *Tagln-cre^{TG}; S1pr1$^{lox/lox}$; ApoE$^{KO/KO}$* and *S1pr1$^{lox/lox}$; ApoE$^{KO/KO}$* female mice. N=6, biological replicates. All data were normalized to GAPDH. Data were analyzed using an unpaired *t*-test. For atherosclerosis studies, *Tagln-cre^{TG}; S1pr1$^{lox/lox}$; ApoE$^{KO/KO}$* and *S1pr1$^{lox/lox}$; ApoE$^{KO/KO}$* controls were fed an HFD for 8 weeks. The plaques were visualized using oil-red O staining. **C, D, G, and H** are the representative images for the atherosclerotic plaques (red) in the aortic sinus cross-sections of both male and female *S1pr1$^{lox/lox}$; ApoE$^{KO/KO}$* and *Tagln-cre^{TG}; S1pr1$^{lox/lox}$; ApoE$^{KO/KO}$* mice. **E and I** represent the average plaque cross-sectional area through the aortic sinus and ascending aorta for each group of male and female mice. **F and J** represent the total plaque volume for each group of male and female mice. Males-n=11, 8; Females-n=9, 10. Scale bars = 100 μm. Plaque cross-sectional areas were analyzed by the two-way ANOVA and plaque volume was assessed using an unpaired *t*-test or Welch's t-test based on testing for normality and equal variance. All results are denoted as mean± SEM.

2.4.5 S1PR1 inactivation in VSMC reduces cell proliferation both in culture and in atherosclerotic lesions

To understand the effect of partial/complete loss of S1PR1 in VSMC on cell proliferation, we stimulated primary aortic SMCs from *S1pr1*$^{WT/WT}$*; ApoE*$^{KO/KO}$, cre-negative *S1pr1*$^{lox/lox}$*; ApoE*$^{KO/KO}$ mice and *Tagln-cre*^{TG}; *S1pr1*$^{lox/lox}$*; ApoE*$^{KO/KO}$ mice with PDGF and/or the S1PR1 selective agonist SEW2871 for 24 hours and carried out immunofluorescence for Ki67 as a marker of cell proliferation. Treatment of aortic SMCs from *S1pr1*$^{WT/WT}$*; ApoE*$^{KO/KO}$ mice with either PDGF or SEW2871 alone increased the proportions of Ki67-positive cells by 2-fold and addition of both PDGF and SEW2871 increased the proportions of Ki67-positive cells by approx. 4.5-fold compared to untreated controls **(Figure 2.5 A)**. SEW2871- but not PDGF-stimulated increases in cell proliferation measured by Ki67 staining appeared to be reduced in aortic SMCs from cre-negative *S1pr1*$^{lox/lox}$*; ApoE*$^{KO/KO}$ mice, **(Figure 2.5 B)** consistent with the reduced average level of S1PR1 expression (Figure 2F). In contrast, when aortic SMCs from *Tagln-cre*^{TG}**;** *S1pr1*$^{lox/lox}$*; ApoE*$^{KO/KO}$ mice were treated with either PDGF, SEW2871 or both, no increases in proportions of Ki67-positive cells were observed. **(Figure 2.5 C)**. Similar results were observed when cell proliferation was measured using an MTT asay **(Supplementary Figure 2.15 A-C).** Likewise, when cell proliferation was assessed by counting cells over the course of 2 days, SEW2871 was unable to induce proliferation in aortic SMCs from *Tagln-cre*^{TG}; *S1pr1*$^{lox/lox}$*; ApoE*$^{KO/KO}$ compared to those from cre-negative *S1pr1*$^{lox/lox}$*; ApoE*$^{KO/KO}$ mice even though PDGF stimulation appeared largely

unaffected (**Supplementary Figure 2.15 D)**. Immunofluorescence for Ki67 was used as a marker for cell proliferation in aortic sinus atherosclerotic plaques of *S1pr1*$^{WT/WT}$*; ApoE*$^{KO/KO}$, cre-negative *S1pr1*$^{lox/lox}$*; ApoE*$^{KO/KO}$ and *Tagln-cre*^{TG}; *S1pr1*$^{lox/lox}$*; ApoE*$^{KO/KO}$ mice (**Figure 2.5 D**). This analysis revealed the highest proportion of Ki67 positive nuclei in plaques from the *S1pr1*$^{WT/WT}$*; ApoE*$^{KO/KO}$ with an approximately 50% reduction in the proportion of Ki67 positive nuclei in plaques from the cre-negative *S1pr1*$^{lox/lox}$*; ApoE*$^{KO/KO}$ mice and a further >50% reduction in the proportion of Ki67 positive nuclei in plaques from the *Tagln-cre*^{TG}; *S1pr1*$^{lox/lox}$*; ApoE*$^{KO/KO}$ mice (**Figure 2.5 E**). These effects are consistent with the differences in S1PR1 expression levels in primary aortic SMCs isolated from these mice and on the levels of SEW2871 stimulated proliferation of the aortic SMCs analyzed in vitro. These findings suggest that deletion of S1PR1 in VSMCs reduces their proliferation in the context of atherosclerosis.

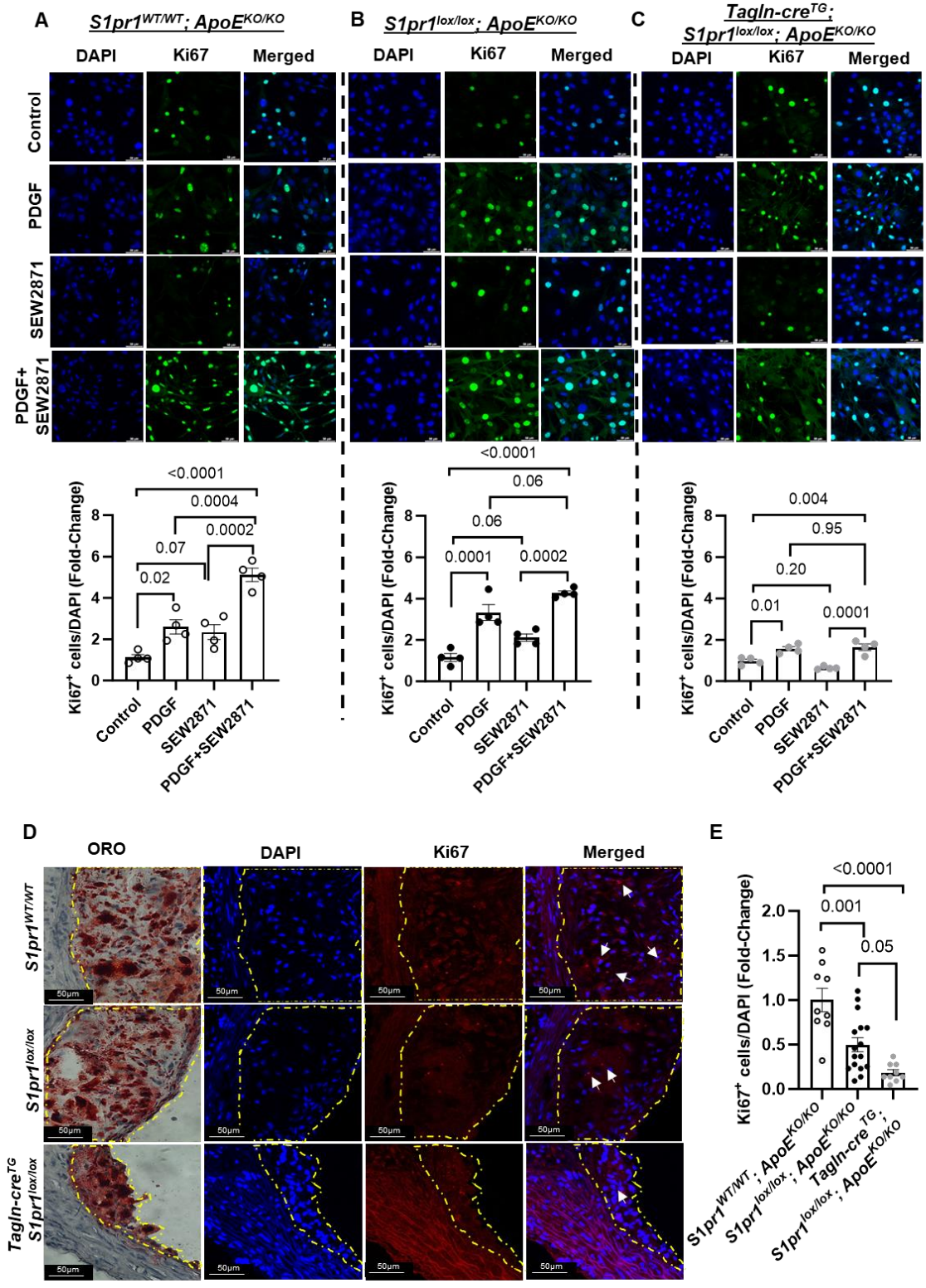
A
S1pr1WT/WT; ApoEKO/KO
B
S1pr1lox/lox; ApoEKO/KO
C
Tagln-creTG; S1pr1lox/lox; ApoEKO/KO
DAPI
Ki67
Merged
Control
PDGF
SEW2871
PDGF+ SEW2871
Ki67+ cells/DAPI (Fold-Change)
<0.0001
0.0004
0.0002
0.07
0.02
0.06
0.0001
0.004
0.95
0.20
0.01
Control
PDGF
SEW2871
PDGF+SEW2871
D
ORO
S1pr1WT/WT
S1pr1lox/lox
Tagln-creTG S1pr1lox/lox
50µm
E
0.001
0.05
S1pr1WT/WT; ApoEKO/KO
S1pr1lox/lox; ApoEKO/KO
Tagln-creTG; S1pr1lox/lox; ApoEKO/KO

Figure 2.5: Partial or complete loss of S1PR1 in VSMC reduces cell proliferation

The aortic VSMCs were isolated from less than 8 weeks old *S1pr1$^{WT/WT}$; ApoE$^{KO/KO}$*, *S1pr1$^{lox/lox}$; ApoE$^{KO/KO}$*, and *Tagln-cre^{TG}; S1pr1$^{lox/lox}$; ApoE$^{KO/KO}$* male mice. The cells were stimulated with no addition control, PDGF with/without SEW2871 for 24 hrs. The fixed cells were stained with cell proliferation marker Ki67 and counterstained with DAPI for cell nuclei (blue). Panel **A-C** shows representative images and semi-quantitative measurements of Ki67+ cells (green) in *S1pr1$^{WT/WT}$; ApoE$^{KO/KO}$*, *S1pr1$^{lox/lox}$; ApoE$^{KO/KO}$*, and *Tagln-cre^{TG}; S1pr1$^{lox/lox}$; ApoE$^{KO/KO}$* VSMCs. Next, Ki67+ cells were also assessed in the atherosclerotic plaques in the aortic sinus cross-sections of HF-diet fed *S1pr1$^{WT/WT}$; ApoE$^{KO/KO}$*, *S1pr1$^{lox/lox}$; ApoE$^{KO/KO}$*, and *Tagln-cre^{TG}; S1pr1$^{lox/lox}$; ApoE$^{KO/KO}$* female mice. The aortic sinus cross-sections with the atherosclerotic plaques were stained with Oil Red O. The adjacent sections were stained with cell proliferation marker Ki67 (red) and counterstained with DAPI for cell nuclei (blue). **D,** Immunofluorescent staining detected Ki67^{+} cells (white arrow) within atherosclerotic plaques in the aortic sinus cross-sections of *Tagln-cre^{TG}; S1pr1$^{lox/lox}$; ApoE$^{KO/KO}$* mice, *S1pr1$^{lox/lox}$; ApoE$^{KO/KO}$* mice and *S1pr1$^{WT/WT}$; ApoE$^{KO/KO}$* mice. (**E**) Semi-quantitative measurement of Ki67+ cells (fold-change) showed reduced SMC proliferation in *Tagln-cre^{TG}; S1pr1$^{lox/lox}$; ApoE$^{KO/KO}$* mice in comparison to *S1pr1$^{lox/lox}$; ApoE$^{KO/KO}$* mice and *S1pr1$^{WT/WT}$; ApoE$^{KO/KO}$* controls. The images were taken at 63X magnification using a STELLARIS confocal microscope. Scale bars=50µm. N=4. Statistical analyses and graphical representations were made in GraphPad Prism. Data are represented as mean± SEM. Statistical analysis was performed using One-way ANOVA with Tukey's multiple comparisons test.

2.4.6 S1PR1 enhances cholesterol loading-induced lipid accumulation and phenotype switching of aortic SMCs

We tested if S1PR1 impacted the degree of lipid droplet formation and phenotypic switching as characterized by the loss of expression of the SMC marker *Acta2* and gain of the macrophage marker, *Cd68*. These processes can be driven in cultured SMCs by incubation with cholesterol complexed with methyl-b-cyclodextrin (Rong et al. 2003). Cholesterol loading of aortic SMCs from *S1pr1*$^{WT/WT}$*; ApoE*$^{KO/KO}$ increased lipid droplet formation as analyzed by ORO staining and triggered reduced *Acta2* and a trend towards increased *Cd68* expression as has previously been described (Rong et al. 2003) Simultaneous treatment with the S1PR1 selective agonist SEW2871 increased the extent of lipid droplet formation and *Cd68* gene expression (**Figure 2.6A and B**). The degree to which SEW2871 was able to enhance cholesterol loading-induced lipid droplet formation and *Cd68* gene expression was reduced in aortic SMCs from cre-negative *S1pr1*$^{lox/lox}$*; ApoE*$^{KO/KO}$ mice and eliminated in aortic SMCs from *Tagln-cre*^{TG}; *S1pr1*$^{lox/lox}$*; ApoE*$^{KO/KO}$ mice **(Figure 2.6C-F)**. These results suggest that S1PR1 activation increases VSMC proliferation and enhances lipid droplet formation and the expression of *Cd68*, hallmarks of SMC foam cell formation which contribute to atherosclerotic plaque development, and that these processes can be suppressed by inhibition of S1PR1 in vascular SMCs.

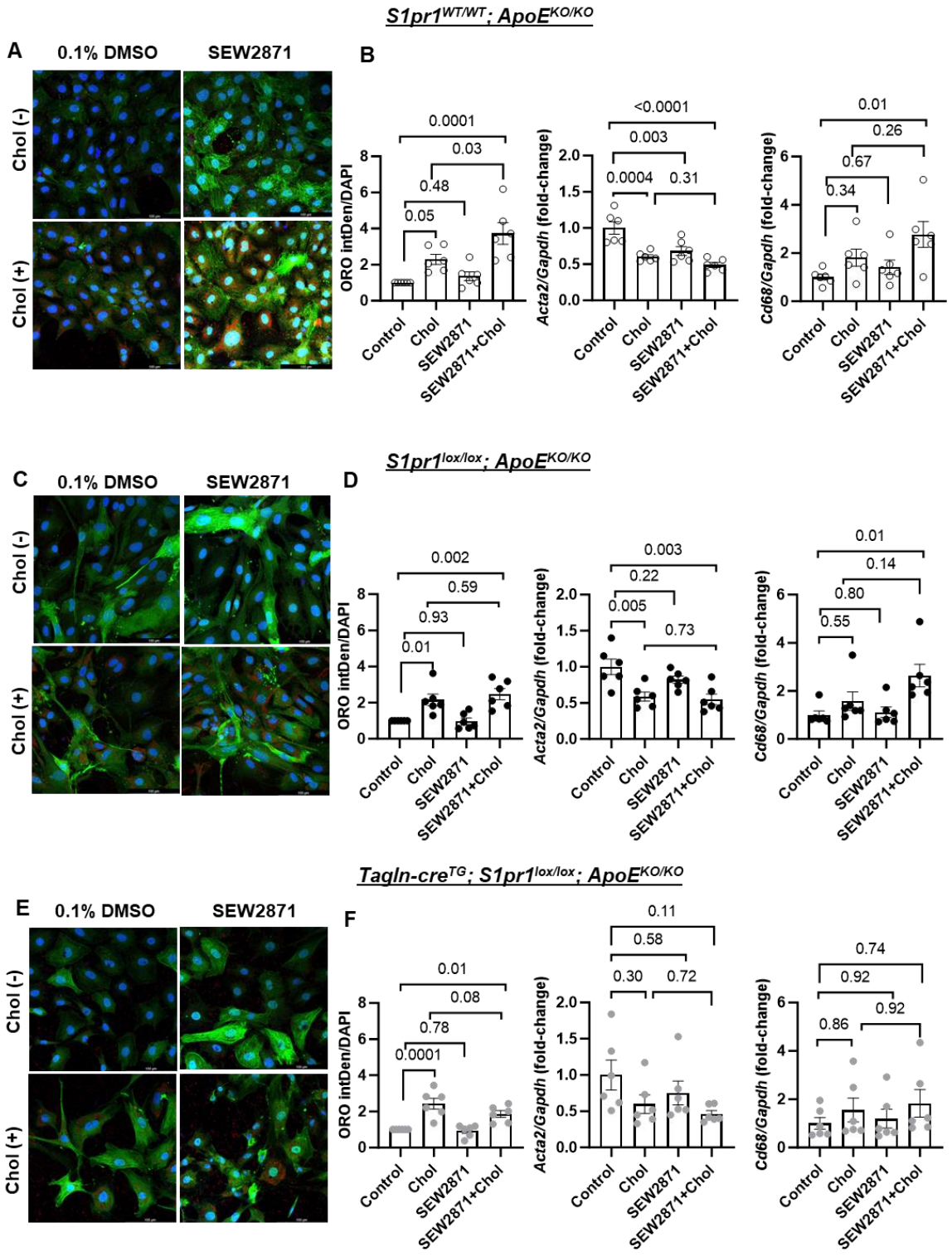
S1pr1WT/WT; ApoEKO/KO
A
0.1% DMSO
SEW2871
Chol (-)
Chol (+)
B
ORO intDen/DAPI
0.0001
0.03
0.48
0.05
Acta2/Gapdh (fold-change)
<0.0001
0.003
0.0004
0.31
Cd68/Gapdh (fold-change)
0.01
0.26
0.67
0.34
Control
Chol
SEW2871
SEW2871+Chol
S1pr1lox/lox; ApoEKO/KO
C
D
0.002
0.59
0.93
0.01
0.003
0.22
0.005
0.73
0.14
0.80
0.55
Tagln-creTG; S1pr1lox/lox; ApoEKO/KO
E
F
0.11
0.58
0.30
0.72
0.74
0.92
0.86
0.08
0.78
0.0001

Figure 2.6: S1PR1 mediates lipid droplet formation in aortic SMC
We isolated VSMC from the aortas of *S1pr1$^{WT/WT}$; ApoE$^{KO/KO}$*, *S1pr1$^{lox/lox}$; ApoE$^{KO/KO}$*, and *Tagln-cre^{TG}; S1pr1$^{lox/lox}$; ApoE$^{KO/KO}$* male mice at less than 8 weeks of age. The sub-confluent cells at the seeding density 5 x 10^4 cells/ chamber were stimulated with/without SEW2871 in the presence or absence of cholesterol-cyclodextrin complex (Chol) for 72 hrs to measure lipid droplet formation, *Acta2* expression, and *Cd68* expression. **A**, **C**, and **E** are representative images of VSMCs (isolated from all three strains) subjected to different treatments and stained with anti-alpha SMA antibody for SMC (green), Oil red O for lipid droplet (red), and counterstained with DAPI for cell nuclei (blue). Scale bars=100 µm. **B, D, and F,** Semi-quantitative measurements of lipid droplets, *Acta2* mRNA, and *Cd68* transcript levels in aortic SMCs isolated from *S1pr1$^{WT/WT}$; ApoE$^{KO/KO}$*, *S1pr1$^{lox/lox}$; ApoE$^{KO/KO}$*, and *Tagln-cre^{TG}; S1pr1$^{lox/lox}$; ApoE$^{KO/KO}$* mice. N=6 (biological replicates). Results were analyzed using One-way ANOVA followed by *the Holm-Šídák test.* All results are denoted as mean± SEM.

2.5 Discussion

The S1P-S1PR1 signaling in vascular and immune cells mediates several cellular responses in the arterial wall and is thus considered to play a critical role in vascular pathophysiology. A previous study from our lab evaluated the effects of myeloid-specific S1PR1 inactivation on atherosclerosis (Gonzalez et al. 2017). That study was performed by transplanting the BM cells from donor *Lys2$^{cre/cre}$; S1pr1$^{lox/lox}$* and *Lys2$^{cre/cre}$; S1pr1$^{WT/WT}$* control mice into LDLR$^{-/-}$ recipient mice. Those controls were chosen to control for potential effects of inactivation of the *Lys2* gene due to the cre transgene knockin. That study demonstrated that S1PR1 knockout in BM-derived myeloid cells promoted HFD-induced atherosclerosis and cellular apoptosis in atherosclerotic plaques in LDLR-deficient mice. However, in this study, when we crossed *Lys2$^{cre/cre}$; S1pr1$^{lox/lox}$* and control Lys2$^{cre/cre}$; S1pr1$^{WT/WT}$ mice with either *apoE$^{KO/KO}$* or *LDLR$^{KO/KO}$* mice and analyzed atherosclerosis in the resulting *Lys2$^{cre/cre}$; S1pr1$^{lox/lox}$; ApoE$^{KO/KO}$* and *Lys2$^{cre/cre}$; S1pr1$^{lox/lox}$; LDLR$^{KO/KO}$* and corresponding *S1pr1$^{WT/WT}$* controls, we observed dramatically reduced atherosclerosis in the mice which were homozygous for the *S1pr1$^{lox/lox}$* allele compared to those with the *S1pr1$^{WT/WT}$* allele. Analysis of atherosclerosis in *S1pr1$^{lox/lox}$; ApoE$^{KO/KO}$* and control *S1pr1$^{WT/WT}$; ApoE$^{KO/KO}$* mice lacking any cre-transgene revealed that the reduction in atherosclerosis was due to the *S1pr1$^{lox/lox}$* genotype and was independent of cre recombinase. Several studies have reported that the retention of neo cassette while constructing floxed alleles could lead to hypomorphic phenotypes characterized by reduced expression of the floxed gene

(Dora et al. 2016; Jacks et al. 1994; Levin and Meisler 2004). Consistent with this, we detected approximately 50% reductions in average expression levels of *S1pr1* in primary elicited peritoneal macrophages and aortic SMCs, and trends towards reduced *S1pr1* expression (which did not reach statistical significance) in a number of tissues from *S1pr1*$^{lox/lox}$ compared to *S1pr1*$^{WT/WT}$ mice.

Reciprocal BM transplantation between *S1pr1*$^{lox/lox}$*; ApoE*$^{KO/KO}$ and *S1pr1*$^{WT/WT}$*; ApoE*$^{KO/KO}$ mice revealed that the reduced atherosclerosis was associated with the *S1pr1*$^{lox/lox}$ genotype in the BM-recipients, and not the donors, making it unlikely that the reduced S1PR1 expression in BM-derived macrophages was responsible for the reduced atherosclerosis in the *S1pr1*$^{lox/lox}$*; ApoE*$^{KO/KO}$ mice. Our data revealed that the presence of the *S1pr1*$^{lox/lox}$ allele in non-BM-derived tissues/cell types resulted in reduced aortic-sinus atherosclerosis in our recipients. Although *S1pr1*$^{lox/lox}$ locus suppressed *S1pr1* expression by approx. 50% in macrophages, our BMT results confirmed that *S1pr1*$^{lox/lox}$ allele in BM-derived myeloid cells failed to reduce atherosclerotic lesion size in apoE-deficient mice. One interpretation of the atherosclerosis analyses in the reciprocal BM-transplanted mice is that the *S1pr1*$^{lox/lox}$ genotype in one or more type of non-BM derived cell present in the artery wall may be responsible for the reduced atherosclerosis. The arterial wall comprises several non-BM-derived cell types, including endothelial cells and VSMCs which are key contributors to atherosclerosis. Hla and colleagues previously reported that endothelial cell specific inducible *S1pr1* knockout increased atherosclerotic plaque development

in apoE-deficient mice (Galvani et al. 2015). Therefore, we considered it unlikely that the reduced atherosclerosis observed in mice with the *S1pr1*$^{lox/lox}$ compared to the *S1pr1*$^{WT/WT}$ genotype would be the result of reduced *S1pr1* expression in endothelial cells. Therefore, we turned our attention to VSMCs. We observed a 50% reduction in the average level of *S1pr1* expression in primary aortic SMCs from *S1pr1*$^{lox/lox}$ compared to *S1pr1*$^{WT/WT}$ mice. The introduction of the Tagln-cre^{TG} resulted in the virtual complete suppression of *S1pr1* gene expression in primary aortic SMCs of *S1pr1*$^{lox/lox}$*; ApoE*$^{KO/KO}$ mice without affecting S1PR1 expression in elicited peritoneal macrophages. Atherosclerotic plaque sizes in *Tagln-cre*^{TG}; *S1pr1*$^{lox/lox}$*; ApoE*$^{KO/KO}$ mice were reduced a further 2.5-fold compared to those in cre-negative *S1pr1*$^{lox/lox}$*; ApoE*$^{KO/KO}$ mice, revealing that eliminating *S1pr1* gene expression in VSMCs protects against experimental atherosclerosis. This is consistent with the detrimental effects reported for overexpression of S1PR1 in VSMCs on other forms of vascular pathology. For example, a previous study reported that FVB mouse strain that expresses higher levels of *S1pr1* in SMC compared to C57BL/6 mouse strain develops a larger neointima after acute vascular injury (Inoue et al. 2007). Similarly, another study observed transient increase in *S1pr1* mRNA expression levels in VSMCs in a rat carotid artery model of acute balloon injury and that inhibiting *S1pr1* and *3* reduced neointimal hyperplasia in injured carotid arteries (Wamhoff et al. 2008). Similarly, transgenic mice overexpressing *S1pr1* under the control of *Acta2* promoter develop increased ligation-induced neointimal hyperplasia concomitant with enhanced intimal cell

proliferation in carotid arteries compared to controls non-transgenic mice (Kitano et al. 2019). In all of these studies, S1PR1 activity or expression levels have been linked to increased VSMC proliferation or migration (Wamhoff et al. 2008; Kitano et al. 2019; Inoue et al. 2007). Our study is the first to test the role of S1PR1 in VSMCs on native atherosclerotic plaque development. Our data clearly demonstrate that selective S1PR1 inactivation in VSMC protects against experimental, HF-diet induced atherosclerosis and links this protection to reduced VSMC proliferation and foam cell formation.

A caveat of our study is that SMC early differentiation marker genes, including *Tagln*, are not only expressed by medial VSMC but also, to some extent, by myeloid-derived cells and cre-transgene activity has been reported in some leukocyte populations in *Tagln-cre*^{TG} mice (Shen et al. 2012) and thus add to further complexity in identifying the origin of SMC marker-positive cells in atherosclerotic plaque development (Sata et al. 2002; Caplice et al. 2003; Iwata et al. 2010; Yu et al. 2011). However, we ruled out the potential contribution of *S1pr1* inactivation in Tagln-cre expressing BM-derived cells by demonstrating that atherosclerosis was reduced in *Tagln-cre*^{TG}; *S1pr1*$^{lox/lox}$*; ApoE*$^{KO/KO}$ compared to cre-negative *S1pr1*$^{lox/lox}$*; ApoE*$^{KO/KO}$ mice when both had been transplanted with BM from cre-negative *S1pr1*$^{WT/WT}$*; ApoE*$^{KO/KO}$ donors, since the resulting BM-chimeric mice did not have either Tagln-driven cre expression or recombination-ready floxed *S1pr1* in any BM-derived cell. Instead, our data demonstrates that S1PR1 inactivation in VSMC protects against atherosclerosis, suggesting that

S1PR1 in VSMCs normally plays a role in promoting atherosclerotic plaque development. The impacts on atherosclerosis of inactivating S1PR1 in VSMCs are, therefore, opposite of the impacts of inactivating S1PR1 in endothelial cells or BM-derived myeloid cells which have previously been shown to protect against atherosclerosis (Galvani et al. 2015; Gonzalez et al. 2017), apparently reflecting different impacts of S1PR1 signaling in the different cell types. In endothelial cells, S1PR1 signaling plays an important role in inflammation, by regulating endothelial cell activation and leukocyte extravasation from lymph nodes into the blood, and in endothelial cell proliferation and migration and maintenance of endothelial integrity. In macrophages, S1PR1 signaling protects against macrophage apoptosis and stimulates migration, which may potentially impact macrophage egress from plaques.

The proliferation and migration of VSMCs also impact atherosclerosis development, but apparently in a detrimental manner. Several *in-vitro* studies reported that S1P signaling (via S1PR1 and S1PR3) synergizes with PDGFR signaling to promote proliferation and migration of VSMC (Kluk and Hla 2001; Kluk et al. 2003; Tanimoto, Lungu, and Berk 2004; Mousseau, Mollard, Faucher-Durand, et al. 2012). We examined migration in human and mouse aortic SMCs after stimulating them with PDGF and/or SEW2871 (data not shown). While PDGF and SEW2871 each independently enhanced migration of human aortic SMCs, we did not observe a synergistic effect of combining PDGF and SEW2871 (data not shown). However, in contrast, PDGF (at the concentration tested) did not stimulate

the migration of the primary aortic SMCs that we isolated from wild type mice, contrary to what others have reported previously (Myllärniemi et al. 1997; Jalvy et al. 2007). Furthermore S1PR1 signaling has been reported by others to predominantly stimulate PDGFR induced proliferation while S1PR3 signaling predominantly stimulates PDGFR induced migration of VSMCs (Mousseau, Mollard, Richard, et al. 2012). Therefore, we focussed on cell proliferation rather than migration. Our findings that the S1PR1 agonist SEW2871 potentiates PDGF-stimulated aortic SMC proliferation and that this, along with proliferation of cells within atherosclerotic plaques are substantially reduced in cells/mice that are *Tagln-cre*^{TG}; *S1pr1*$^{lox/lox}$*; ApoE*$^{KO/KO}$ supports the important role played by S1PR1 in VSMC proliferation.

In addition to clonal expansion, medial SMC in the arterial wall undergo lineage reprogramming into macrophage-like cells during atherosclerotic plaque development (Feil et al. 2014). Transcriptional repression of SMC differentiation marker genes (such as *Acta2*, *MYH11*, and *Tagln*) and an increase in macrophage markers (such as CD68 and MAC-2) are hallmark features of SMC-to macrophage transdifferentiation (Rong et al. 2003). The SMCs transdifferentiated into macrophage-like cells also acquire lipid droplets, taking on the appearance of foam cells in culture (Matsumoto et al. 2000). These processes can be driven in culture by artificially loading VSMCs with cholesterol (Rong et al. 2003) It has previously been shown that the treatment of rat aortic SMC with S1P increased the promoter activity of SMC differentiation marker genes, however overexpression of S1PR1

suppressed while overexpression of S1PR2 enhanced *Acta2* promoter activity (Wamhoff et al. 2008). We demonstrate that the S1PR1 agonist SEW2871 enhanced the cholesterol-loading driven lipid droplet accumulation and CD68 expression in aortic SMCs and that this was lost when S1PR1 expression was inactivated. In contrast, we did not observe SEW2871-dependent potentiation of the cholesterol loading-induced reduction in *Acta2* gene expression. Nevertheless, our findings suggest that inactivation of S1PR1 in VSMCs may potentially impair both clonal expansion (i.e. proliferation) and reprogramming to macrophage-like foam cells. Although we artificially cholesterol-loaded aortic SMCs cells using cyclodextrin-cholesterol complexes, it remains to be determined whether S1PR1 activation and inactivation would have the same effects on more physiologically relevant pathways of cholesterol loading, such as incubation with aggregated LDL, very low-density lipoprotein or oxidized LDL. Nevertheless, our data suggest a possible mechanism that accounts for reduced aortic sinus atherosclerosis observed in mice in which S1PR1 is selectively knocked out in VSMCs; namely, the reduced proliferation and transdifferentiation of VSMCs to foam cells.

In summary, our findings demonstrate that S1PR1 in VSMCs promotes pro-atherogenic responses including cell proliferation and foam cell formation and targeting S1PR1 in VSMCs protects against atherosclerotic plaque development by suppressing these responses. The role that SMC phenotype switching to-macrophage-like foam cells plays in atherosclerotic plaque formation in both humans and mouse model systems is becoming increasingly better appreciated.

Further elucidating how the S1P-S1PR1 signaling axis regulates phenotype switching in VSMCs will provide greater insight into the potential benefits of inhibiting this pathway in VSMCs for protection against atherosclerosis.

2.6 References

Al-Jarallah, Aishah, Xing Chen, Leticia Gonzalez, and Bernardo L Trigatti. 2014. 'High density lipoprotein stimulated migration of macrophages depends on the scavenger receptor class B, type I, PDZK1 and Akt1 and is blocked by sphingosine 1 phosphate receptor antagonists', *PloS one*, 9: e106487.

Allahverdian, Sima, Ali Cyrus Chehroudi, Bruce M McManus, Thomas Abraham, and Gordon A Francis. 2014. 'Contribution of intimal smooth muscle cells to cholesterol accumulation and macrophage-like cells in human atherosclerosis', *Circulation*, 129: 1551-59.

Argraves, Kelley M, Patrick J Gazzolo, Eric M Groh, Brent A Wilkerson, Bryan S Matsuura, Waleed O Twal, Samar M Hammad, and W Scott Argraves. 2008. 'High density lipoprotein-associated sphingosine 1-phosphate promotes endothelial barrier function', *Journal of Biological Chemistry*, 283: 25074-81.

Bennett, M. R., S. Sinha, and G. K. Owens. 2016. 'Vascular Smooth Muscle Cells in Atherosclerosis', *Circ Res*, 118: 692-702.

Caplice, Noel M, T Jared Bunch, Paul G Stalboerger, Shaohua Wang, David Simper, Dylan V Miller, Stephen J Russell, Mark R Litzow, and William D Edwards. 2003. 'Smooth muscle cells in human coronary atherosclerosis can originate from cells administered at marrow transplantation', *Proceedings of the National Academy of Sciences*, 100: 4754-59.

Chae, Sung-Suk, Richard L Proia, and Timothy Hla. 2004. 'Constitutive expression of the S1P1 receptor in adult tissues', *Prostaglandins & other lipid mediators*, 73: 141-50.

Covey, Scott D, Monty Krieger, Wei Wang, Marsha Penman, and Bernardo L Trigatti. 2003. 'Scavenger receptor class B type I–mediated protection against atherosclerosis in LDL receptor–negative mice involves its expression in bone marrow–derived cells', *Arteriosclerosis, thrombosis, and vascular biology*, 23: 1589-94.

Daum, G., A. Grabski, and M. A. Reidy. 2009. 'Sphingosine 1-phosphate: a regulator of arterial lesions', *Arterioscler Thromb Vasc Biol*, 29: 1439-43.

Dora, Natalie J, Aaron JF Crookshanks, Karen KY Leung, T Ian Simpson, John O Mason, David J Price, and John D West. 2016. 'Analysis of compound heterozygotes reveals that the mouse floxed Pax6 tm1Ued allele produces abnormal eye phenotypes', *Transgenic research*, 25: 679-92.

Feil, Susanne, Birgit Fehrenbacher, Robert Lukowski, Frank Essmann, Klaus Schulze-Osthoff, Martin Schaller, and Robert Feil. 2014. 'Transdifferentiation of vascular smooth muscle cells to macrophage-like cells during atherogenesis', *Circulation research*, 115: 662-67.

Galvani, Sylvain, Marie Sanson, Victoria A Blaho, Steven L Swendeman, Hideru Obinata, Heather Conger, Björn Dahlbäck, Mari Kono, Richard L Proia, and Jonathan D Smith. 2015. 'HDL-bound sphingosine 1-phosphate acts as a

biased agonist for the endothelial cell receptor S1P1 to limit vascular inflammation', *Science signaling*, 8: ra79-ra79.

Gimbrone Jr, Michael A, and Guillermo García-Cardeña. 2016. 'Endothelial cell dysfunction and the pathobiology of atherosclerosis', *Circulation research*, 118: 620-36.

Gonzalez, Leticia, Alexander S Qian, Usama Tahir, Pei Yu, and Bernardo L Trigatti. 2017. 'Sphingosine-1-phosphate receptor 1, expressed in myeloid cells, slows diet-induced atherosclerosis and protects against macrophage apoptosis in ldlr KO mice', *International Journal of Molecular Sciences*, 18: 2721.

Gonzalez, Leticia, and Bernardo Louis Trigatti. 2017. 'Macrophage apoptosis and necrotic core development in atherosclerosis: a rapidly advancing field with clinical relevance to imaging and therapy', *Canadian Journal of Cardiology*, 33: 303-12.

Hegele, Robert A. 1996. 'The pathogenesis of atherosclerosis', *Clinica chimica acta*, 246: 21-38.

Inoue, S., T. Nakazawa, A. Cho, F. Dastvan, D. Shilling, G. Daum, and M. Reidy. 2007. 'Regulation of arterial lesions in mice depends on differential smooth muscle cell migration: a role for sphingosine-1-phosphate receptors', *J Vasc Surg*, 46: 756-63.

Iwata, Hiroshi, Ichiro Manabe, Katsuhito Fujiu, Tetsufumi Yamamoto, Norifumi Takeda, Kosei Eguchi, Akiko Furuya, Makoto Kuro-o, Masataka Sata, and

Ryozo Nagai. 2010. 'Bone marrow–derived cells contribute to vascular inflammation but do not differentiate into smooth muscle cell lineages', *Circulation*, 122: 2048-57.

Jacks, Tyler, T Shane Shih, Earlene M Schmitt, Roderick T Bronson, Andre Bernards, and Robert A Weinberg. 1994. 'Tumour predisposition in mice heterozygous for a targeted mutation in Nf1', *Nature genetics*, 7: 353-61.

Jalvy S, Renault MA, Leen LL, Belloc I, Bonnet J, Gadeau AP, Desgranges C. 2007. 'Autocrine expression of osteopontin contributes to PDGF-mediated arterial smooth muscle cell migration'. Cardiovascular research. 75:738-47.

Kimura, Takao, Hideaki Tomura, Chihiro Mogi, Atsushi Kuwabara, Alatangaole Damirin, Tamotsu Ishizuka, Akihiro Sekiguchi, Mitsuteru Ishiwara, Doon-Soon Im, and Koichi Sato. 2006. 'Role of scavenger receptor class B type I and sphingosine 1-phosphate receptors in high density lipoprotein-induced inhibition of adhesion molecule expression in endothelial cells', *Journal of Biological Chemistry*, 281: 37457-67.

Kitano, T., S. Usui, S. I. Takashima, O. Inoue, C. Goten, A. Nomura, K. Yoshioka, M. Okajima, S. Kaneko, Y. Takuwa, and M. Takamura. 2019. 'Sphigosine-1-phosphate receptor 1 promotes neointimal hyperplasia in a mouse model of carotid artery injury', *Biochem Biophys Res Commun*, 511: 179-84.

Kluck, George EG, Alexander S Qian, Emmanuel H Sakarya, Henry Quach, Yak D Deng, and Bernardo L Trigatti. 2023. 'Apolipoprotein A1 Protects Against Necrotic Core Development in Atherosclerotic Plaques: PDZK1-Dependent

High-Density Lipoprotein Suppression of Necroptosis in Macrophages', *Arteriosclerosis, thrombosis, and vascular biology*, 43: 45-63.

Kluk, Michael J, Chantal Colmont, Ming-Tao Wu, and Timothy Hla. 2003. 'Platelet-derived growth factor (PDGF)-induced chemotaxis does not require the G protein-coupled receptor S1P1 in murine embryonic fibroblasts and vascular smooth muscle cells', *FEBS letters*, 533: 25-28.

Kluk, Michael J, and Timothy Hla. 2001. 'Role of the sphingosine 1-phosphate receptor EDG-1 in vascular smooth muscle cell proliferation and migration', *Circulation research*, 89: 496-502.

Levin, Stephen I, and Miriam H Meisler. 2004. 'Floxed allele for conditional inactivation of the voltage-gated sodium channel Scn8a (Nav1. 6)', *genesis*, 39: 234-39.

Liu, Hui, Hongjun Jin, Junbin Han, Xuyi Yue, Hao Yang, Mohamed A Zayed, Robert J Gropler, and Zhude Tu. 2018. 'Upregulated sphingosine 1-phosphate receptor 1 expression in human and murine atherosclerotic plaques', *Molecular imaging and biology*, 20: 448-56.

Livak, Kenneth J, and Thomas D Schmittgen. 2001. 'Analysis of relative gene expression data using real-time quantitative PCR and the 2− ΔΔCT method', *methods*, 25: 402-08.

Matsumoto, Kengo, Ken-ichi Hirano, Shuichi Nozaki, Akiko Takamoto, Makoto Nishida, Yumiko Nakagawa-Toyama, Mohamed Yakub Janabi, Takeshi Ohya, Shizuya Yamashita, and Yuji Matsuzawa. 2000. 'Expression of

macrophage (Mφ) scavenger receptor, CD36, in cultured human aortic smooth muscle cells in association with expression of peroxisome proliferator activated receptor-γ, which regulates gain of Mφ-like phenotype in vitro, and its implication in atherogenesis', *Arteriosclerosis, thrombosis, and vascular biology*, 20: 1027-32.

Moore, Kathryn J, Frederick J Sheedy, and Edward A Fisher. 2013. 'Macrophages in atherosclerosis: a dynamic balance', *Nature Reviews Immunology*, 13: 709-21.

Mousseau, Yoanne, Séverine Mollard, Karine Faucher-Durand, Laurence Richard, Angélique Nizou, Jeanne Cook-Moreau, Yasser Baaj, Hao Qiu, Xavier Plainard, and Laurent Fourcade. 2012. 'Fingolimod potentiates the effects of sunitinib malate in a rat breast cancer model', *Breast cancer research and treatment*, 134: 31-40.

Mousseau, Yoanne, Séverine Mollard, Laurence Richard, Angélique Nizou, Karine Faucher-Durand, Jeanne Cook-Moreau, Hao Qiu, Yasser Baaj, Benoit Funalot, and Laurent Fourcade. 2012. 'Fingolimod inhibits PDGF-B-induced migration of vascular smooth muscle cell by down-regulating the S1PR1/S1PR3 pathway', *Biochimie*, 94: 2523-31.

Myllärniemi M, Calderon L, Lemström K, Buchdunger E, Häyry P. 1997. ‘Inhibition of platelet-derived growth factor receptor tyrosine kinase inhibits vascular smooth muscle cell migration and proliferation’. 11:1119-26.

Newby, Andrew C, and Alla B Zaltsman. 1999. 'Fibrous cap formation or destruction—the critical importance of vascular smooth muscle cell proliferation, migration and matrix formation', *Cardiovascular research*, 41: 345-60.

O'Sullivan, Catherine, and Kumlesh K Dev. 2013. 'The structure and function of the S1P1 receptor', *Trends in pharmacological sciences*, 34: 401-12.

Pei, Ying, Xing Chen, Dina Aboutouk, Mark T Fuller, Omid Dadoo, Pei Yu, Elizabeth J White, Suleiman A Igdoura, and Bernardo L Trigatti. 2013. 'SR-BI in bone marrow derived cells protects mice from diet induced coronary artery atherosclerosis and myocardial infarction', *PloS one*, 8: e72492.

Rivera, Juan, Richard L Proia, and Ana Olivera. 2008. 'The alliance of sphingosine-1-phosphate and its receptors in immunity', *Nature Reviews Immunology*, 8: 753-63.

Rong, James X, Mark Shapiro, Eugene Trogan, and Edward A Fisher. 2003. 'Transdifferentiation of mouse aortic smooth muscle cells to a macrophage-like state after cholesterol loading', *Proceedings of the National Academy of Sciences*, 100: 13531-36.

Rosenfeldt, Hans M, John P Hobson, Michael Maceyka, Ana Olivera, Victor E Nava, Sheldon Milstien, and Sarah Spiegel. 2001. 'EDG-1 links the PDGF receptor to Src and focal adhesion kinase activation leading to lamellipodia formation and cell migration', *The FASEB Journal*, 15: 2649-59.

Sata, Masataka, Akio Saiura, Atsushi Kunisato, Akihiro Tojo, Seiji Okada, Takeshi Tokuhisa, Hisamaru Hirai, Masatoshi Makuuchi, Yasunobu Hirata, and Ryozo Nagai. 2002. 'Hematopoietic stem cells differentiate into vascular cells that participate in the pathogenesis of atherosclerosis', *Nature medicine*, 8: 403-09.

Shen, Mengcheng, Mei Hu, Paul WM Fedak, Gavin Y Oudit, and Zamaneh Kassiri. 2018. 'Cell-specific functions of ADAM17 regulate the progression of thoracic aortic aneurysm', *Circulation research*, 123: 372-88.

Shen, Zhuxia, Chao Li, Ryan A Frieler, Alena S Gerasimova, Soo Jung Lee, Jing Wu, Michael M Wang, Carey N Lumeng, Frank C Brosius III, and Sheng Zhong Duan. 2012. 'Smooth muscle protein 22 alpha-Cre is expressed in myeloid cells in mice', *Biochemical and Biophysical Research Communications*, 422: 639-42.

Tabas, Ira, Guillermo García-Cardeña, and Gary K Owens. 2015. 'Recent insights into the cellular biology of atherosclerosis', *Journal of Cell Biology*, 209: 13-22.

Tanimoto, Tatsuo, Andreea O Lungu, and Bradford C Berk. 2004. 'Sphingosine 1-phosphate transactivates the platelet-derived growth factor β receptor and epidermal growth factor receptor in vascular smooth muscle cells', *Circulation research*, 94: 1050-58.

Wamhoff, B. R., K. R. Lynch, T. L. Macdonald, and G. K. Owens. 2008. 'Sphingosine-1-phosphate receptor subtypes differentially regulate smooth muscle cell phenotype', *Arterioscler Thromb Vasc Biol*, 28: 1454-61.

Wang, Ying, Joshua A Dubland, Sima Allahverdian, Enyinnaya Asonye, Basak Sahin, Jen Erh Jaw, Don D Sin, Michael A Seidman, Nicholas J Leeper, and Gordon A Francis. 2019. 'Smooth muscle cells contribute the majority of foam cells in ApoE (Apolipoprotein E)-deficient mouse atherosclerosis', *Arteriosclerosis, thrombosis, and vascular biology*, 39: 876-87.

Yu, Haixiang, Victoria Stoneman, Murray Clarke, Nichola Figg, Hong-Bo Xin, Michael Kotlikoff, Trevor Littlewood, and Martin Bennett. 2011. 'Bone marrow–derived smooth muscle–like cells are infrequent in advanced primary atherosclerotic plaques but promote atherosclerosis', *Arteriosclerosis, thrombosis, and vascular biology*, 31: 1291-99.

Yu, Pei, Alexander S Qian, Kevin M Chathely, and Bernardo L Trigatti. 2018. 'PDZK1 in leukocytes protects against cellular apoptosis and necrotic core development in atherosclerotic plaques in high fat diet fed ldl receptor deficient mice', *Atherosclerosis*, 276: 171-81.

2.7 Supplementary Figures

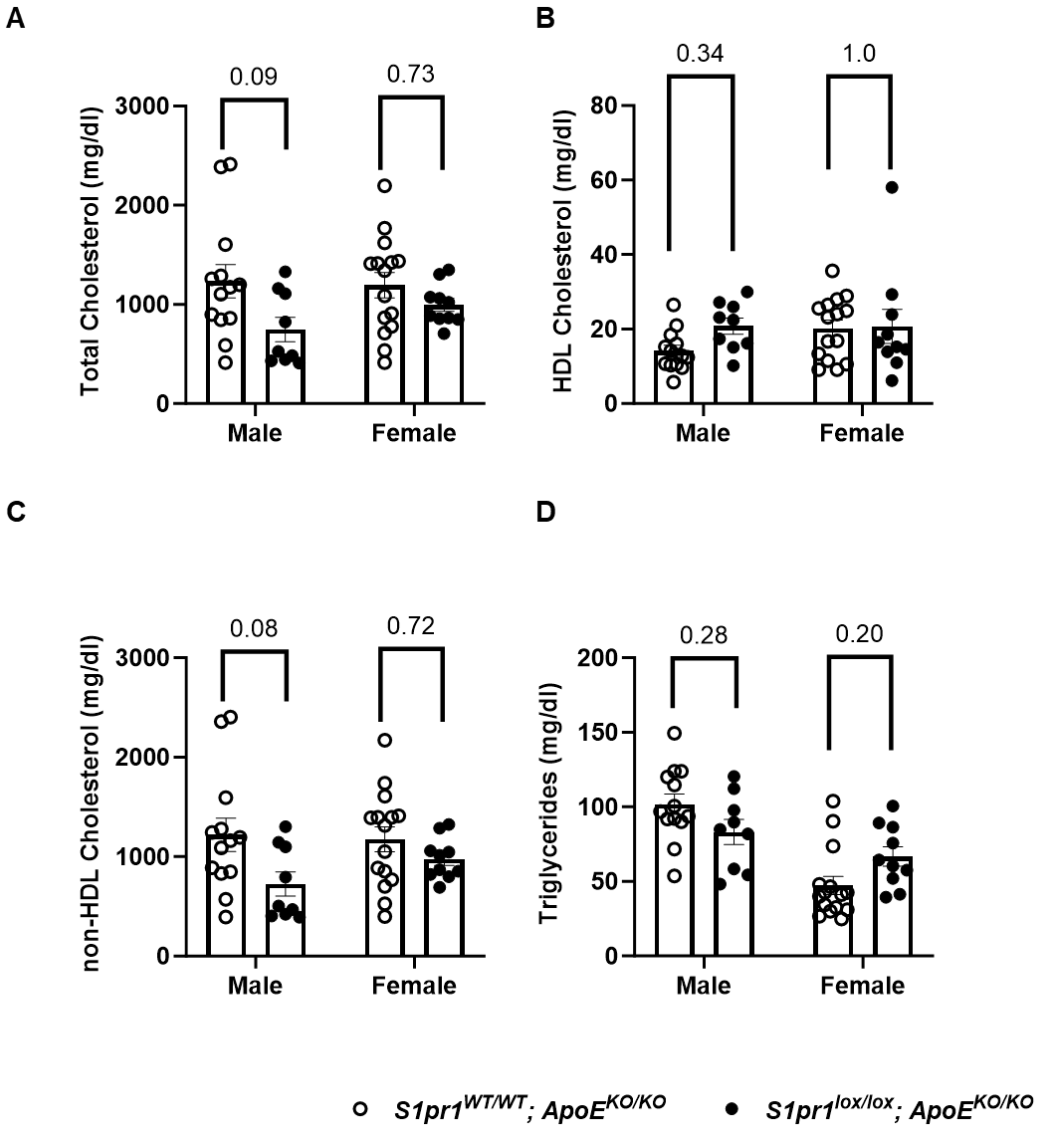

Figure 2.7: *S1pr1*$^{lox/lox}$ conditional allele did not affect plasma lipid and lipoprotein levels

The *S1pr1*$^{WT/WT}$*; ApoE*$^{KO/KO}$ and *S1pr1*$^{lox/lox}$*; ApoE*$^{KO/KO}$ mice were fed with an HFD for 8 weeks starting at 10 weeks of age and harvested at 18 weeks of age. The plasma was separated from the blood samples by centrifugation at 775 x *g* for 10 min. Enzymatic assays were performed on the plasma to measure (**A**) total cholesterol, **(B)** HDL cholesterol, **(C)** non-HDL cholesterol, and (**D**) Triglyceride levels in each group of male and female mice. Values represent mean± SEM. Data were assessed using two-way ANOVA with the Tukey's multiple comparison test.

A

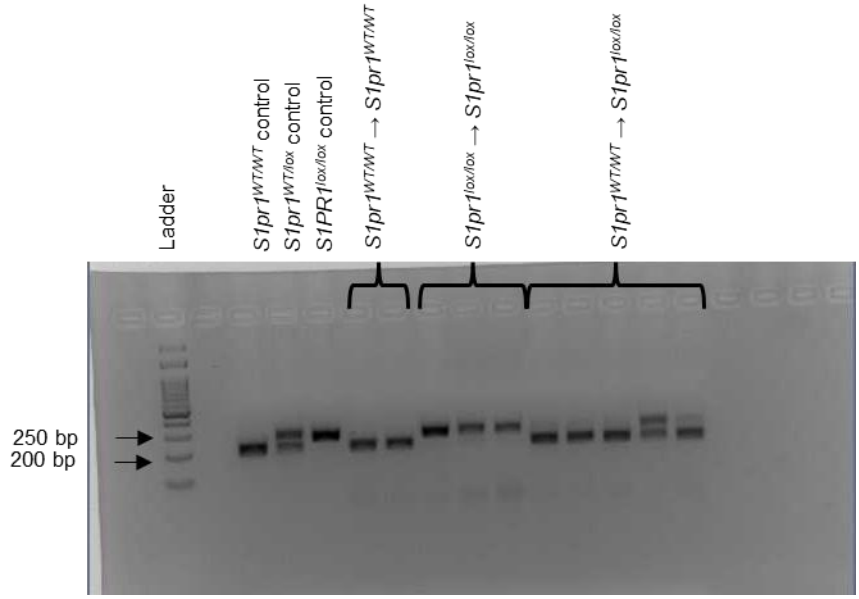

Figure 2.8: Representative PCR genotyping results for BM transplantation

Reciprocal BMT was performed in *S1pr1*$^{WT/WT}$*; ApoE*$^{KO/KO}$ mice and *S1pr1*$^{lox/lox}$*; ApoE*$^{KO/KO}$ male mice at 8 weeks of age. The recipient mice were lethally irradiated with 1000 RAD and transplanted with donor BM cells. After 4 weeks of recovery, all the recipients were fed an HFD for 8 weeks. The blood samples were collected from each mouse during the time of harvest. The DNA from blood samples was genotyped to confirm the success of BMT in recipient mice. **A**. PCR products were separated using 3% agarose gel (250 bp for the lox/lox allele band and 200 bp for the WT/WT allele band). BP-base pair. Each lane represents individual samples from BM recipients. The DNA templates from S1PR1-wt/wt, S1PR1-lox/wt (heterozygous), and S1PR1-lox/lox (homozygous) mice were used as controls. The recipients were only included in the study when the BMs from donor mice were fully restored (ie, *S1pr1*$^{WT/WT}$ or *S1pr1*$^{lox/lox}$ band); and were excluded when the *S1pr1* gene was partially restored (*S1pr1*$^{WT/lox}$). Marker: 100 bp DNA ladder.

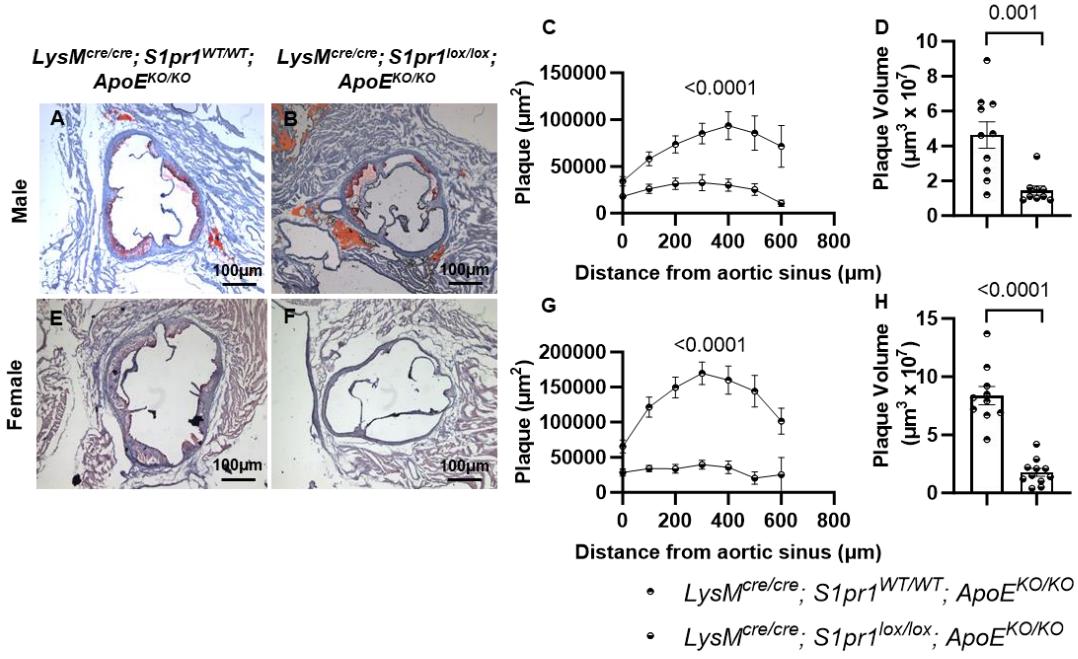
LysM cre/cre; S1pr1 WT/WT; ApoE KO/KO
LysM cre/cre; S1pr1 lox/lox; ApoE KO/KO
Male
Female
A
B
E
F
100µm
C
G
Plaque (µm2)
<0.0001
Distance from aortic sinus (µm)
D
H
Plaque Volume (µm3 x 10^7)
0.001
<0.0001
LysM cre/cre; S1pr1 WT/WT; ApoE KO/KO
LysM cre/cre; S1pr1 lox/lox; ApoE KO/KO

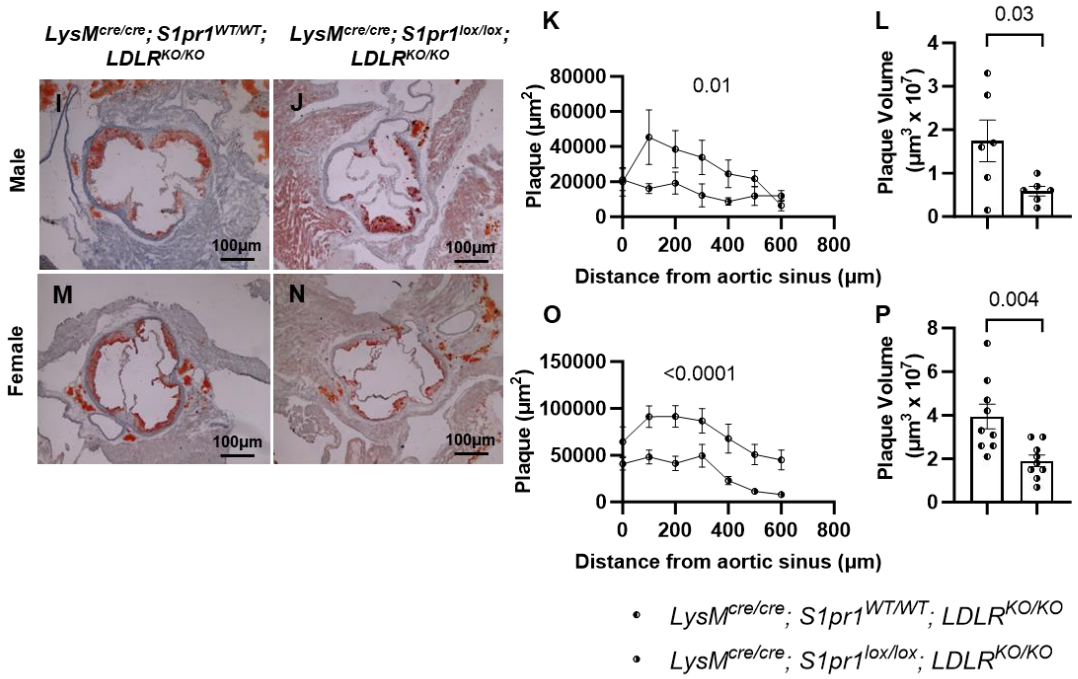
LysM cre/cre; S1pr1 WT/WT; LDLR KO/KO
LysM cre/cre; S1pr1 lox/lox; LDLR KO/KO
Male
Female
I
J
M
N
100µm
K
O
Plaque (µm2)
0.01
<0.0001
Distance from aortic sinus (µm)
L
P
Plaque Volume (µm3 x 10^7)
0.03
0.004
LysM cre/cre; S1pr1 WT/WT; LDLR KO/KO
LysM cre/cre; S1pr1 lox/lox; LDLR KO/KO

Figure 2.9: The effect of *LysM$^{cre/cre}$; S1pr1$^{lox/lox}$* allele on atherosclerotic plaque development

LysM$^{cre/cre}$ S1pr1$^{WT/WT}$ and *LysM$^{cre/cre}$ S1pr1$^{lox/lox}$* mice were generated in both *ApoE$^{KO/KO}$* and *LDLR$^{KO/KO}$* backgrounds. The plaques were visualized using Oil Red O. **A, B, E and F** are representative images of the atherosclerotic plaques in the aortic-sinus cross-sections for the male and female LysM$^{cre/cre}$ apoE$^{KO/KO}$ and LysM$^{cre/cre}$ S1PR1$^{lox/lox}$ apoE$^{KO/KO}$ mice in response to 8 weeks HFD (n= 10, 9). **C** and **G,** the plaque cross-sectional area along 600 µm of the aortic sinus of each group of male and female mice. **D and H**, the total plaque volume of each group of male and female mice, measured by calculating the area under the curve of the plaque cross-sectional area versus distance. Male-n=10, 9; Female-n=10, 11. represent the plaque cross-sectional area and total plaque volume of each group of male mice. **I, J, M, and N** are representative images of the atherosclerotic plaques in the aortic-sinus cross-sections for the male and female *LysM$^{cre/cre}$ Ldlr$^{KO/KO}$* and *LysM$^{cre/cre}$ S1pr1$^{lox/lox}$ Ldlr$^{KO/KO}$* mice in response to 9 weeks HFD. **K, L, O**, and **P** represent the plaque cross-sectional area and total plaque volume of each group of male and female mice. Male-n=6, 6; Female-n=9, 9. Scale bars-100 µm. Plaque cross-sectional areas were analyzed by the two-way ANOVA and plaque volume was assessed using an unpaired *t*-test or Welch's t-test based on testing for normality and equal variance. All results are denoted as mean± SEM.

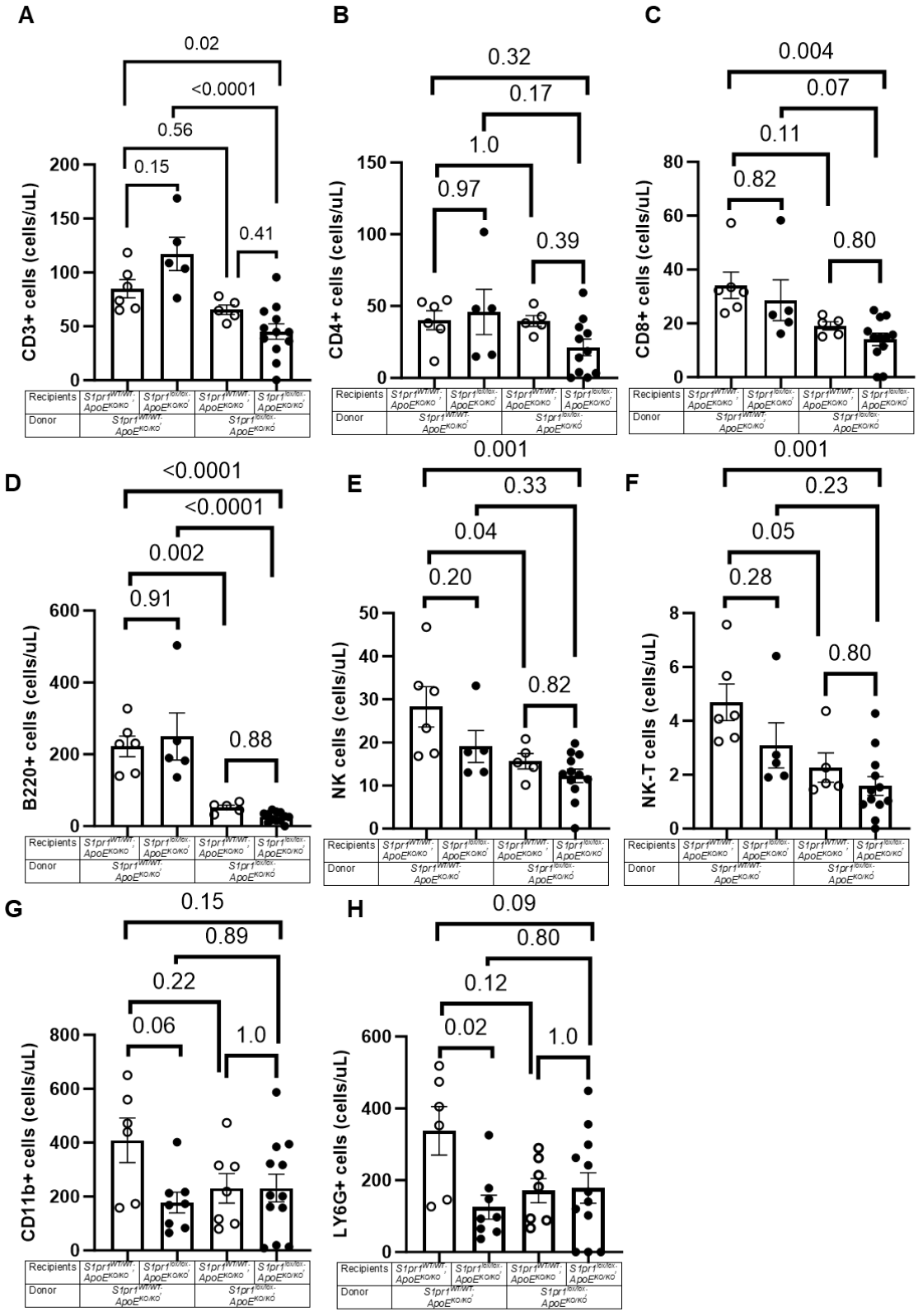
A
CD3+ cells (cells/uL)
0.02
<0.0001
0.56
0.15
0.41
B
CD4+ cells (cells/uL)
0.32
0.17
1.0
0.97
0.39
C
CD8+ cells (cells/uL)
0.004
0.07
0.11
0.82
0.80
D
B220+ cells (cells/uL)
<0.0001
<0.0001
0.002
0.91
0.88
E
NK cells (cells/uL)
0.001
0.33
0.04
0.20
0.82
F
NK-T cells (cells/uL)
0.001
0.23
0.05
0.28
0.80
G
CD11b+ cells (cells/uL)
0.15
0.89
0.22
0.06
1.0
H
LY6G+ cells (cells/uL)
0.09
0.80
0.12
0.02
1.0
Recipients
Donor
S1pr1WT/WT; ApoEKO/KO
S1pr1lox/lox; ApoEKO/KO
S1pr1WT/WT; ApoEKO/KO
S1pr1lox/lox; ApoEKO/KO
S1pr1WT/WT; ApoEKO/KO
S1pr1lox/lox; ApoEKO/KO

Figure 2.10: The effect of *S1pr1*-lox/lox locus in BM- and non-BM-derived cells in modulating lymphocyte and myeloid cell levels in circulation

Reciprocal BMT was carried out in male *S1pr1*$^{WT/WT}$*; ApoE*$^{KO/KO}$ and *S1pr1*$^{lox/lox}$*; ApoE*$^{KO/KO}$ mice. The recipient mice were transplanted with BM donor cells at 8 weeks of age. After 4 weeks of recovery, the recipients were fed with an HFD for 8 weeks. The lymphocyte counts, such as (**A**) CD3+ cells, (**B**) CD4+ cells, (**C**) CD8+ cells, (**D**) B220+ cells, (**E**) NK cells, and (**F**) NK-T cells were measured using flow cytometry in all four groups. N= 6, 5, 5, and 12. The samples were also stained with different antibodies to detect **(G)** CD11b+ and **(H)** Ly6G+ levels in all four groups. N=6, 8, 7, and 12. Data were analyzed by the One-way ANOVA with Tukey's multiple comparison test. Values represent mean± SEM.

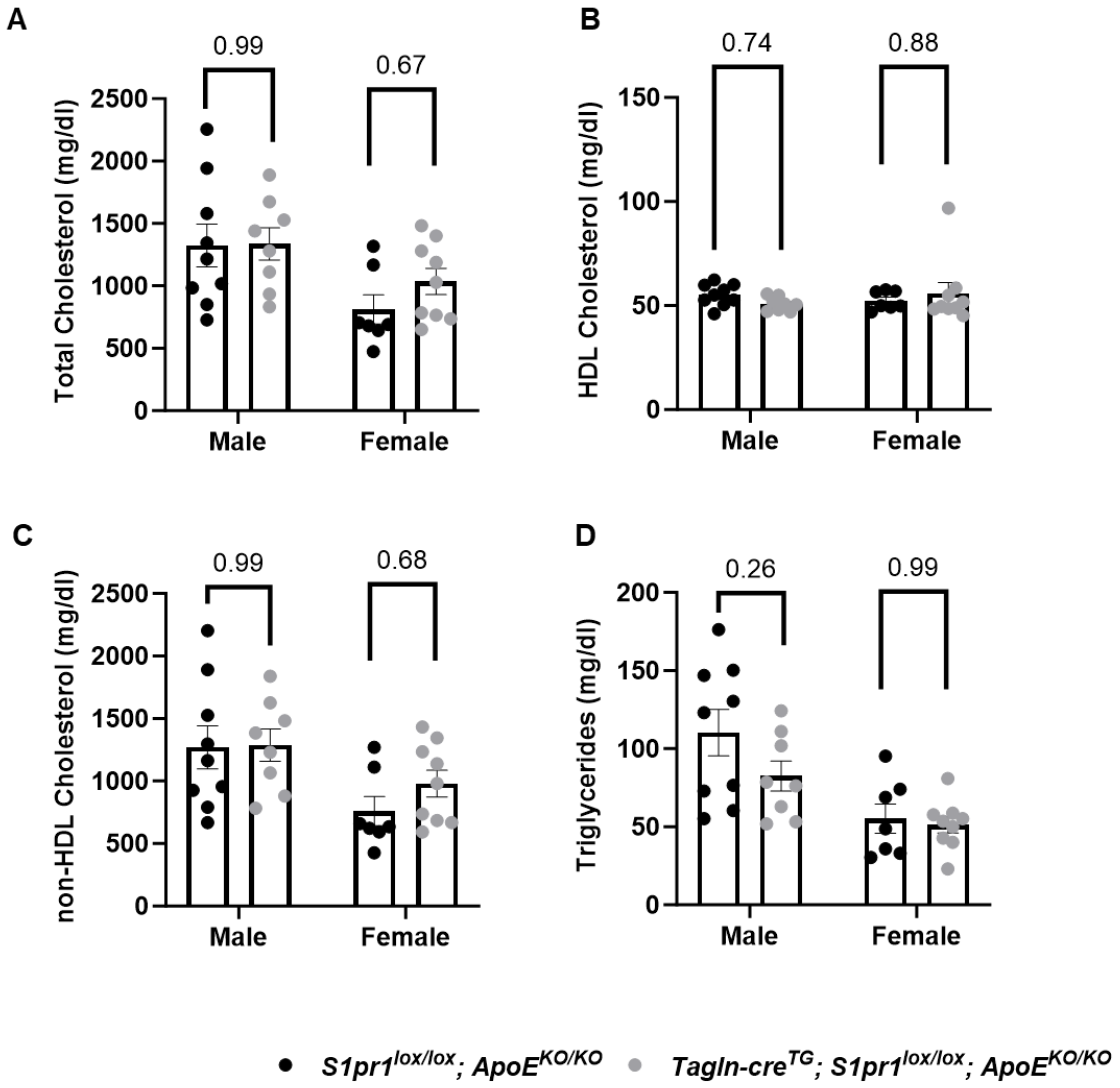

Figure 2.11: S1PR1 deletion in VSMC did not affect plasma lipid and lipoprotein levels

Tagln-cre^{TG}; S1pr1$^{lox/lox}$; ApoE$^{KO/KO}$ mice and *S1pr1$^{lox/lox}$; ApoE$^{KO/KO}$* controls were fed an HFD for 8 weeks. The plasma was isolated from the blood samples collected from each group of male and female mice during the time of harvest. Enzymatic assays were performed on the plasma to measure (**A**) Total Cholesterol, (**B**) HDL-Cholesterol, (**C**) non-HDL-Cholesterol, and (**D**) Triglycerides in male and female *Tagln-cre^{TG}; S1pr1$^{lox/lox}$; ApoE$^{KO/KO}$* mice in comparison to corresponding *S1pr1$^{lox/lox}$; ApoE$^{KO/KO}$* controls. Data is denoted as mean± SEM using Two-way ANOVA with Tukey's multiple comparison test.

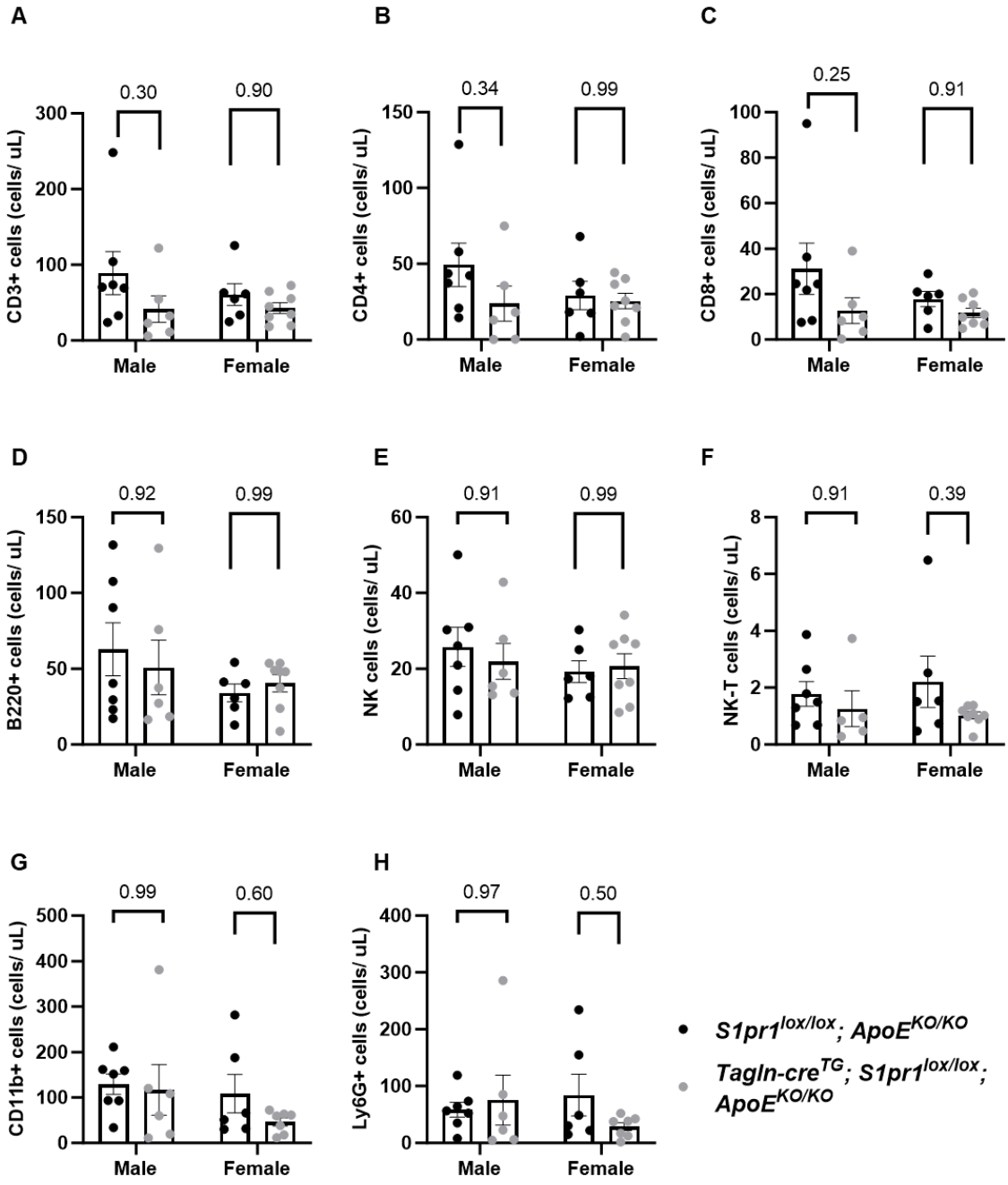
A
CD3+ cells (cells/ uL)
0.30
0.90
Male
Female
B
CD4+ cells (cells/ uL)
0.34
0.99
C
CD8+ cells (cells/ uL)
0.25
0.91
D
B220+ cells (cells/ uL)
0.92
0.99
E
NK cells (cells/ uL)
0.91
0.99
F
NK-T cells (cells/ uL)
0.91
0.39
G
CD11b+ cells (cells/ uL)
0.99
0.60
H
Ly6G+ cells (cells/ uL)
0.97
0.50
S1pr1lox/lox; ApoEKO/KO
Tagln-creTG; S1pr1lox/lox; ApoEKO/KO

Figure 2.12: Inactivating S1PR1 in VSMC did not modulate circulating leukocyte levels

Tagln-cre^{TG}*; S1pr1*$^{lox/lox}$*; ApoE*$^{KO/KO}$ mice and *S1pr1*$^{lox/lox}$*; ApoE*$^{KO/KO}$ controls were fed an HFD for 8 weeks. The flow cytometry analysis was performed on the blood samples to detect circulating lymphocyte and myeloid cell levels from these strains. The samples were stained with different antibodies to detect **(A)** CD3+, **(B)** CD4+, **(C)**CD8+, **(D)** B220+, **(E)** NK1.1 cells, **(F)** NK-T cells, **(G)** CD11b+, and **(H)** Ly6G+ cells. Male-n=7, 6; Female-n=6, 8. Statistical analyses and graphical representations were made in GraphPad Prism. Data is represented as mean± SEM using Two-way ANOVA with Tukey post hoc test.

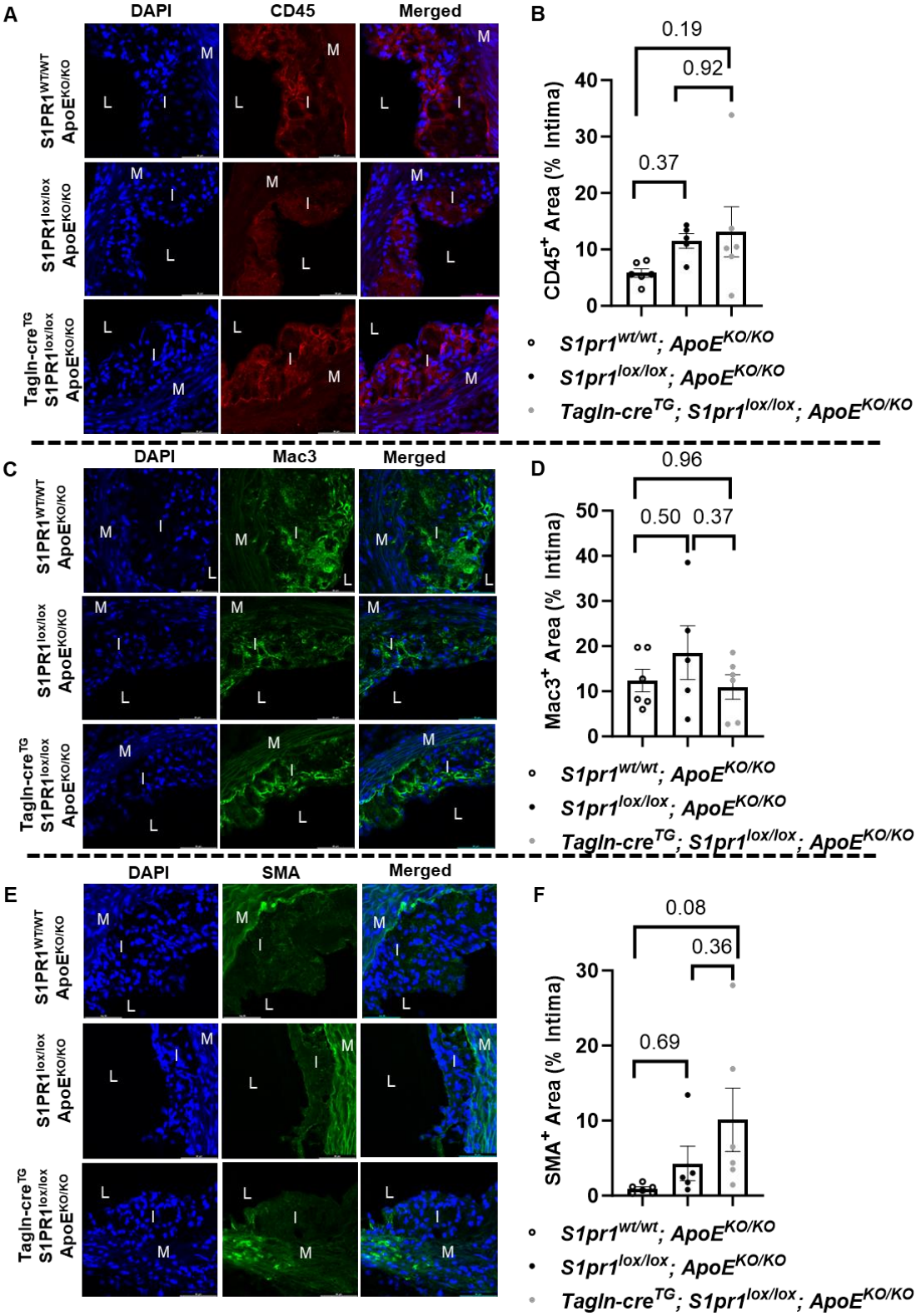
A
DAPI
CD45
Merged
S1PR1WT/WT ApoEKO/KO
S1PR1lox/lox ApoEKO/KO
Tagln-creTG S1PR1lox/lox ApoEKO/KO
B
0.19
0.92
0.37
CD45+ Area (% Intima)
S1pr1wt/wt; ApoEKO/KO
S1pr1lox/lox; ApoEKO/KO
Tagln-creTG; S1pr1lox/lox; ApoEKO/KO
C
DAPI
Mac3
Merged
D
0.96
0.50
0.37
Mac3+ Area (% Intima)
E
DAPI
SMA
Merged
F
0.08
0.36
0.69
SMA+ Area (% Intima)

Figure 2.13: Immunofluorescent staining of CD45, Mac3, and SMA in the atherosclerotic plaques in aortic sinus cross-sections

S1pr1$^{WT/WT}$*; ApoE*$^{KO/KO}$, *S1pr1*$^{lox/lox}$*; ApoE*$^{KO/KO}$, and *Tagln-cre*^{TG}*; S1pr1*$^{lox/lox}$*; ApoE*$^{KO/KO}$ female mice were fed an HFD for 8 weeks. The aortic sinus cross-sections from these mice were stained with CD45 (for leukocytes), Mac3 (for macrophages), and α-SMA (for SMCs) and counterstained with Dapi (for cell nuclei; blue). **Panel A, C, and E**- Representative images of anti-CD45 (red), anti-Mac3 (green), and anti-SMA (green) immunofluorescence staining in the atherosclerotic plaques in the aortic sinus cross-sections from three different mice strains. **Panel B, D, and F-** Quantitative measurements of CD45, Mac3, and SMA content in the atherosclerotic plaques. Scale bars = 50 μm. Data represents mean± SEM using the One-way ANOVA with Tukey's multiple comparison test. L: Lumen, I: Intima, and M: Media.

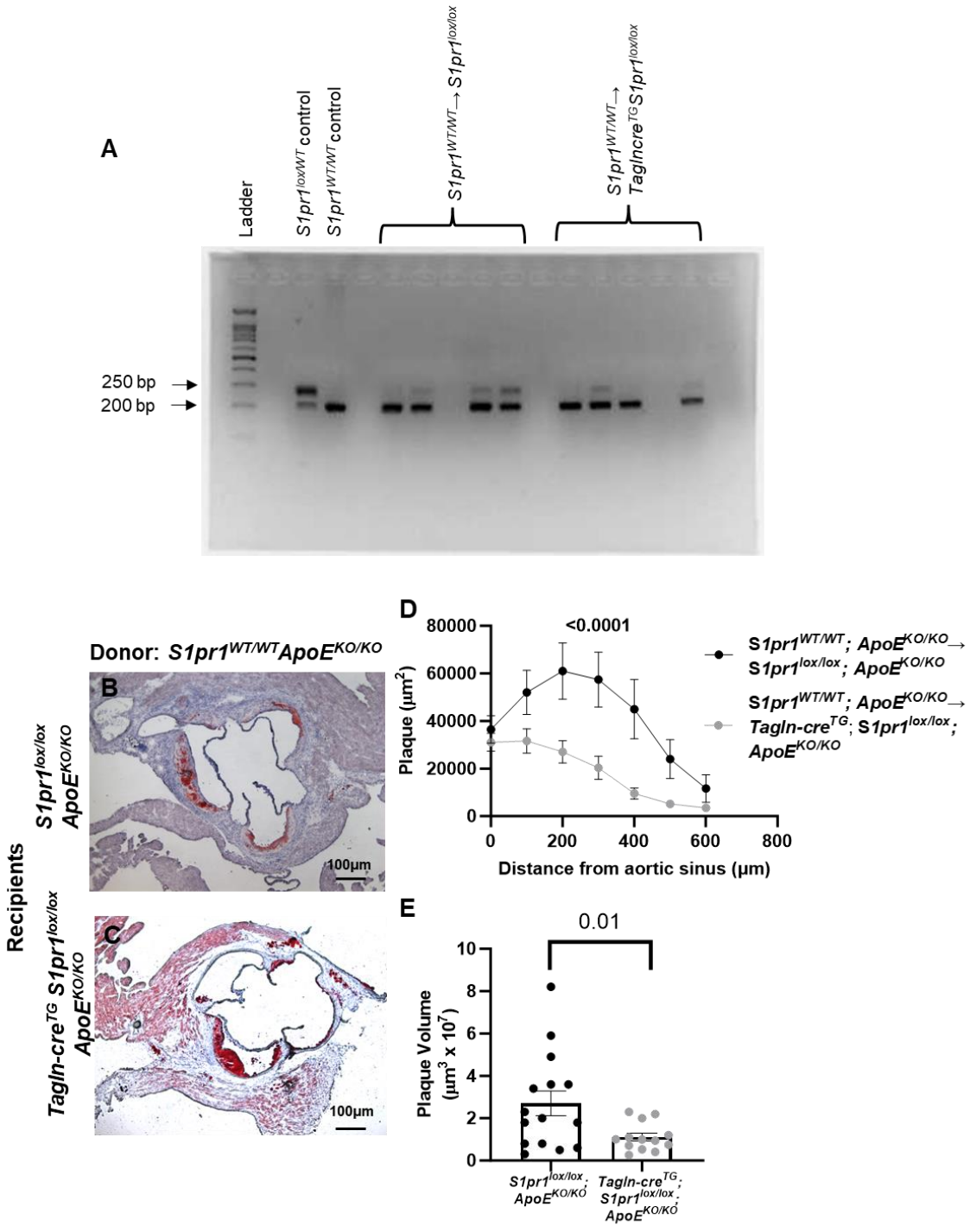
A
Ladder
S1pr1lox/WT control
S1pr1WT/WT control
S1pr1WT/WT→ S1pr1lox/lox
S1pr1WT/WT→ Taglncre^TG S1pr1lox/lox
250 bp
200 bp
Donor: S1pr1WT/WT ApoEKO/KO
Recipients
S1pr1lox/lox ApoEKO/KO
Tagln-cre^TG S1pr1lox/lox ApoEKO/KO
B
C
100μm
100μm
D
<0.0001
Plaque (μm2)
Distance from aortic sinus (μm)
S1pr1WT/WT; ApoEKO/KO→ S1pr1lox/lox; ApoEKO/KO
S1pr1WT/WT; ApoEKO/KO→ Tagln-creTG; S1pr1lox/lox; ApoEKO/KO
E
0.01
Plaque Volume (μm3 x 10^7)
S1pr1lox/lox; ApoEKO/KO
Tagln-creTG; S1pr1lox/lox; ApoEKO/KO

Figure 2.14: Introducing WT-S1PR1 gene in BM-derived cells of *Tagln-cre^{TG}; S1pr1$^{lox/lox}$; ApoE$^{KO/KO}$* mice reduce atherosclerosis

To identify if the atheroprotective effects observed in *Tagln-cre^{TG}; S1pr1$^{lox/lox}$; ApoE$^{KO/KO}$* **mice** are due to the absence of S1PR1 in host VSMC, we transplanted BM cells from *S1pr1$^{WT/WT}$; ApoE$^{KO/KO}$* male mice into *S1pr1$^{lox/lox}$; ApoE$^{KO/KO}$* controls and *Tagln-cre^{TG}; S1PR1$^{lox/lox}$; ApoE$^{KO/KO}$* recipients at 8 weeks of age. After 4 weeks of the recovery period, the recipients were fed an HFD for 8 weeks and harvested at 20 weeks of age. The DNA from blood samples was genotyped to confirm the success of BMT in recipient mice. **A**. PCR products were separated using 3% agarose gel (250 bp for the lox/lox allele band and 200 bp for the WT/WT allele band). BP-base pair. Each lane represents individual samples from BM recipients. The DNA templates from S1PR1-wt/wt and S1PR1-lox/wt (heterozygous) were used as controls. The recipients were only included in the study when the BMs from donor mice were fully restored (ie, *S1pr1$^{WT/WT}$* band); and were excluded when the *S1pr1* gene was partially restored (*S1pr1$^{WT/lox}$*). Marker: 100 bp DNA ladder. **B and C** are representative images of Oil red O-stained atherosclerotic plaques in the aortic-sinus cross-sections from *S1pr1$^{lox/lox}$; ApoE$^{KO/KO}$* and *Tagln-cre^{TG}; S1pr1$^{lox/lox}$; ApoE$^{KO/KO}$* male recipients. The average total plaque cross-sectional area was calculated along a 100-micron distance between each image. **D and E** represent the average plaque cross-sectional area and plaque volume of each group of male mice. Scale bars = 100 μm. Data represents mean± SEM using Welch's unpaired t-test.

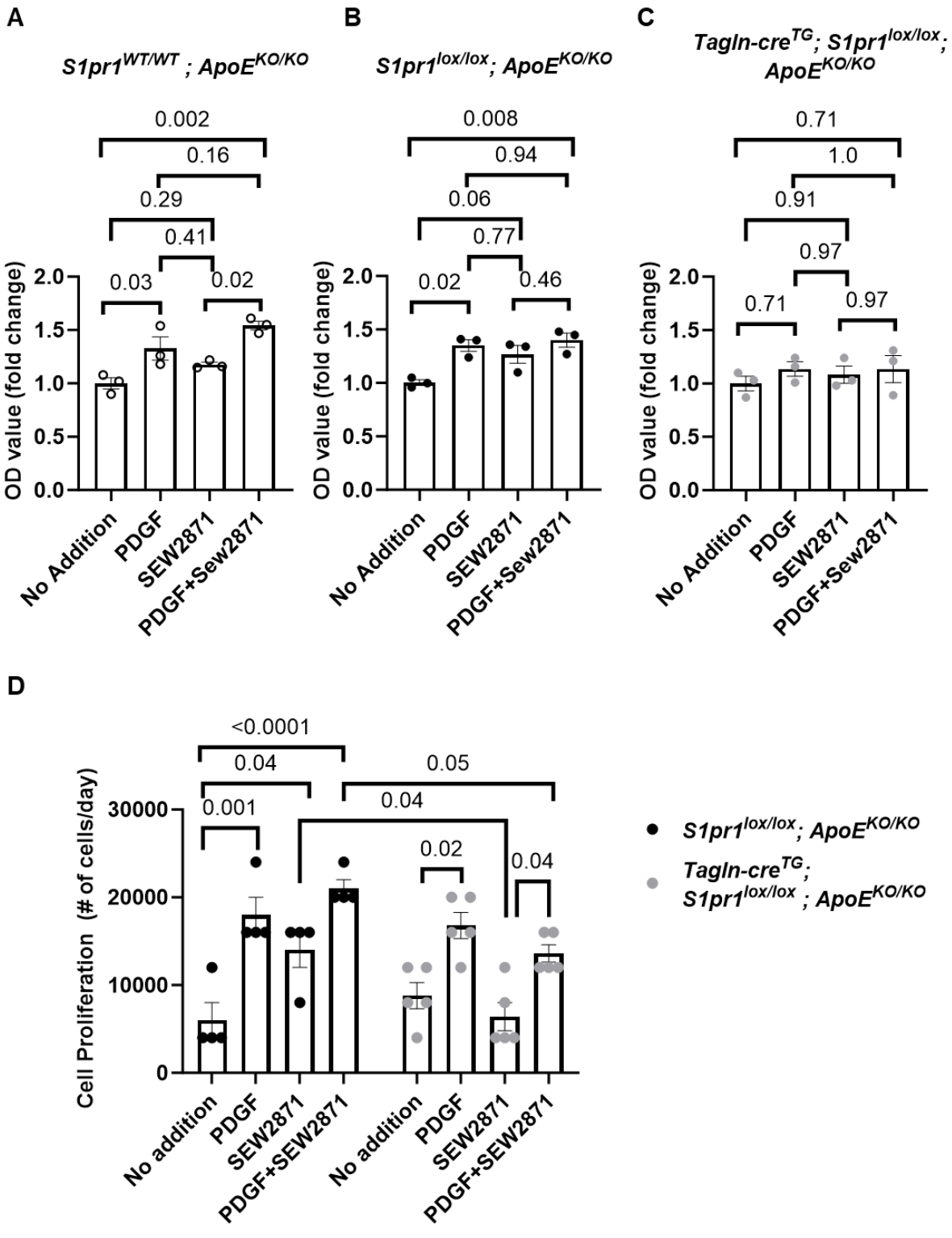
A
S1pr1WT/WT ; ApoEKO/KO
0.002
0.16
0.29
0.41
0.03
0.02
OD value (fold change)
2.0
1.5
1.0
0.5
0.0
No Addition
PDGF
SEW2871
PDGF+Sew2871
B
S1pr1lox/lox; ApoEKO/KO
0.008
0.94
0.06
0.77
0.02
0.46
C
Tagln-creTG; S1pr1lox/lox; ApoEKO/KO
0.71
1.0
0.91
0.97
0.71
0.97
D
<0.0001
0.04
0.05
0.001
0.04
0.02
0.04
Cell Proliferation (# of cells/day)
30000
20000
10000
0
No addition
PDGF
SEW2871
PDGF+SEW2871
S1pr1lox/lox; ApoEKO/KO
Tagln-creTG; S1pr1lox/lox ; ApoEKO/KO

Figure 2.15: S1PR1 inactivation in VSMC hinders PDGF and SEW2871-mediated proliferation

A-C: MTT assay results from *S1pr1$^{WT/WT}$; ApoE$^{KO/KO}$*, *S1pr1$^{lox/lox}$; ApoE$^{KO/KO}$*, and *Tagln-cre^{TG}; S1pr1$^{lox/lox}$; ApoE$^{KO/KO}$* VSMCs (seeded at the density 2 x 10^3 cells/ well) stimulated with no additional control, 50 ng/mL PDGF-B and/or 10 uM SEW2871 for 24 hours. N=3 (each biological replicate denotes isolates from different mice). Statistical analyses were performed using One-way ANOVA with Tukey's multiple comparison test. **(D)** The proliferation rates of *S1pr1$^{lox/lox}$; ApoE$^{KO/KO}$* mice and *Tagln-cre^{TG}; S1pr1$^{lox/lox}$; ApoE$^{KO/KO}$* VSMCs (seeded at the density 2 x 10^4 cells/well) in response to PDGF and SEW2871 on day 0, 1, and 2 of proliferation. N=4, 5 (biological replicates). Statistical analyses were done using Two-way ANOVA with Tukey's multiple comparison test. All results are denoted as mean± SEM.

Chapter 3: Selective S1PR1 antagonist Ex26 provides protection against atherosclerotic plaque development in apoE-deficient mice by inhibiting S1PR1 activity in vascular smooth muscle cells

Narmadaa Thyagarajan, Wei Wang, Jennifer Nouanesengsy, and Bernardo L. Trigatti

Foreword

This manuscript examines the mechanism by which S1PR1 antagonist Ex26 protects against atherosclerosis. In this study, we demonstrated that Ex26 treatment reduced circulating B cells and aortic-sinus atherosclerosis without affecting plasma lipid levels or causing pulmonary edema in HF-diet fed apoE KO mice. To understand if this reduction in atherosclerosis is due to inhibition of S1PR1 in VSMC, we also delivered Ex26 to SMC-specific S1PR1/apoE double KO mice (*Tagln-cre^{TG}; S1pr1$^{lox/lox}$; ApoE$^{KO/KO}$* mice). Our results showed that Tagln-cre^{TG} *S1pr1$^{lox/lox}$; ApoE$^{KO/KO}$* mice treated with Ex26 exhibited similar levels of atherosclerotic lesion size in comparison to DMSO vehicle control. Interestingly, S1PR1-WT VSMCs treated with Ex26 reduced S1PR1 agonist SEW2871-mediated cell growth and SMC lipid droplet formation compared to corresponding controls. These data suggest that S1PR1 antagonist Ex26 may render atheroprotection by mainly inhibiting S1PR1 activity in VSMCs.

This manuscript will be submitted to the Journal of Arteriosclerosis, Thrombosis, and Vascular Biology in 2024. This manuscript was written by

Narmadaa Thyagarajan under the guidance of Dr. Bernardo. L. Trigatti. All *in-vivo* experiments were performed and analyzed by Narmadaa Thyagarajan. Immunofluorescence staining on the atherosclerotic plaques was performed by Wei Wang and the data was analyzed by Narmadaa Thyagarajan. The SMC phenotype switching experiment was carried out and analyzed by Wei Wang, and the proliferation assay was conducted and analyzed by Jennifer Nouanesengsy.

3.1 Abstract

Background:

S1PR1 signaling in different types of cells appears to have pleiotropic effects on atherosclerosis. The deletion of S1PR1 in endothelial cells and macrophages, increases atherosclerotic plaque development, while the inactivation of S1PR1 in VSMCs reduces atherosclerosis. The effects of global inactivation of S1PR1 on atherosclerosis are difficult to evaluate using genetic tools because global inactivation of S1PR1 leads to embryonic lethality. Our objective in this study was to investigate the effects of pharmacological inhibition of S1PR1 on atherosclerosis in adult *apoE*$^{KO/KO}$ mice to evaluate the potential for S1PR1 as a target for inhibition to reduce atherosclerosis.

Methods and Results:

Apolipoprotein E-deficient mice were treated subcutaneously with Ex26, an S1PR1-specific antagonist. Mice were fed a high-fat diet for 6 weeks. Control mice were treated with DMSO vehicle. Prolonged treatment with Ex26 decreased diet-induced atherosclerosis by approximately 55% and reduced average macrophage and leukocyte content within the plaques, without causing pulmonary edema or altering plasma lipid levels in *apoE*$^{KO/KO}$ mice. Ex26 treatment reduced circulating B-cell levels by approx. 63% but did not affect T-cells, NK cells, CD11b+ cells, or neutrophil levels in *apoE*$^{KO/KO}$ mice compared to mice treated with DMSO. In contrast, Ex26 treatment did not affect atherosclerotic plaque sizes or leukocyte

or macrophage content in atherosclerotic plaques in *Tagln-cre^{TG}; S1pr1$^{lox/lox}$; ApoE$^{KO/KO}$* mice which have S1PR1 knocked out selectively in SMCs. Lymphocyte counts were considerably lower in the *Tagln-cre^{TG}; S1pr1$^{lox/lox}$; ApoE$^{KO/KO}$* mice than the *ApoE$^{KO/KO}$* mice and Ex26 treatment reduced CD4+ T cells further but not total B or T cells. Stimulation of cultured aortic SMCs with the S1PR1 agonist SEW2871 potentiated PDGF-induced proliferation and this was inhibited by Ex26. Treatment of primary murine aortic SMCs with SEW2871 similarly potentiated cholesterol induced lipid droplet accumulation and this was similarly inhibited by Ex26.

Conclusions:

Our findings suggest that the S1PR1 antagonist, Ex26, protects against atherosclerosis in a manner that is dependent on S1PR1 expression in VSMCs and its involvement in VSMC proliferation and lipid accumulation.

3.2 Introduction

Atherosclerosis, a chronic inflammatory disease condition and an underlying pathological process in CVD, is mainly characterized by the accumulation of cholesterol-overloaded cells (also referred as foam cells) in the arterial wall. Studies of atherosclerosis development using murine models have led to the idea that foam cells primarily originate from monocyte-derived macrophages. However, recent studies challenge this belief by identifying SMCs as a key contributor to foam cell formation in both murine and human atherosclerosis (Wang et al. 2019; Allahverdian et al. 2014). SMC can play dual roles in atherosclerosis. On the one hand, these cells secrete extracellular matrix to form thick fibrous caps that protect plaque rupture (Ross 1993). On the other hand, the SMCs undergo phenotype switching to macrophage-like foam cells contributing to the progression of atherosclerosis (Feil et al. 2014; Shankman et al. 2015). Depending on the acquired phenotype, these cells can either contribute to plaque stability or instability (Alencar et al. 2020; Pan et al. 2020; Wirka et al. 2019). Over several years, prolonged lipid accumulation, defective macrophage egress, enhanced accumulation of apoptotic bodies, impaired efferocytosis (engulfment of apoptotic bodies), and necrotic core formation causes thinning of fibrous caps resulting in plaque vulnerability and rupture (Tabas 2010; Hansson 2005; Björkegren and Lusis 2022).

Sphingosine-1-phosphate (S1P) receptor 1 (S1PR1) is one of five G-protein coupled receptors (GPCRs) for the bioactive lipid mediator S1P (O'Sullivan and

Dev 2013). As part of the class A family of GPCRs, S1PR1 binds to Gi protein in response to S1P to activate phosphoinositide 3-kinase, and mitogen-activated protein kinase pathways and inhibit adenylyl cyclase. The principal role of S1PR1 signaling in vascular development, lymphocyte egress from lymph nodes, and inflammation makes it a potent target for numerous diseases, including atherosclerosis (Liu et al. 2000; Allende et al. 2004; Allende, Yamashita, and Proia 2003; Matloubian et al. 2004; Galvani et al. 2015). The S1P-S1PR1 signaling axis can have different effects on endothelial cells, macrophages, and vascular smooth muscle cells (VSMCs)- major cell types in the vasculature that contribute to atherosclerotic plaque development. S1PR1 signaling in vascular endothelial cells regulates several processes including barrier function, migration, and cell survival (Burg et al. 2018; Kimura et al. 2003). Similarly, S1PR1 activity in macrophages has also been shown to mediate anti-atherogenic responses, such as enhanced migration, M2 polarization, and reduced apoptosis and pro-inflammatory cytokine production (Gonzalez et al. 2017; Al-Jarallah et al. 2014; Hughes et al. 2008). Consequently, selective inactivation of S1PR1 in either endothelial cells or myeloid cells including macrophages enhances atherosclerosis development in mouse models (Galvani et al. 2015; Gonzalez et al. 2017). On the other hand, S1PR1 signaling in VSMC regulates their proliferation, migration and phenotype switching to foam cells, (Wamhoff et al. 2008; Mousseau et al. 2012) and selective in activation of S1PR1 in SMCs reduces atherosclerosis development [Thyagarajan and Trigatti, manuscript in preparation].

Fingolimod (FTY720), a synthetic analog of S1P, is an orally active immunomodulatory drug approved by the US Food and Drug Administration for the treatment of relapsing-remitting multiple sclerosis (Kappos et al. 2010; Brinkmann et al. 2010). FTY720 serves as a high-affinity agonist for S1PR1 and S1PR3-5 (Mandala et al. 2002). Some studies reported that FTY720 reduced atherosclerosis development in experimental mice by reducing lymphocytes and macrophages (Nofer et al. 2007b; Keul et al. 2007). In contrast, other studies reported that FTY720 treatment reduced blood lymphocyte counts and macrophage function without impacting diet-induced atherosclerosis (Poti et al. 2012). Similarly, others reported that FTY720 treatment improved left ventricular (LV) function and prolonged the lifespan without impacting atherosclerosis development in either the aortic sinus or coronary arteries in a mouse model of high fat diet-induced coronary heart disease (Wang et al. 2014; Luk et al. 2016). Similarly, different studies of S1PR1-specific agonists, such as KRP203 and CYM5442, also reported different effects on atherosclerosis development, with some reporting reduced atherosclerotic plaque sizes and others reporting no effects (Poti et al. 2012; Potì et al. 2013). It is important to note, however, that these agents serve both as agonists of S1PR1 over the short term, and as functional antagonists of S1PR1, with prolonged treatment (Sykes et al. 2014). The functional antagonism arises due to internalization and/or degradation of the S1PR1 (Sykes et al. 2014). Whether this dual nature of S1PR1 agonists contributes to the discrepant outcomes on atherosclerosis development is not clear. Likewise, it is also unclear if the

protection against atherosclerosis, when it was observed, was due to S1PR1 agonism or due to functional antagonism. Finally, it is not clear of the overall effect of inhibiting S1PR1 signaling, given the opposing effects of S1PR1 inhibition in endothelial and myeloid cells (increased atherosclerosis) versus VSMCs (reduced atherosclerosis).

In our present study, we hypothesized that pharmacological inhibition of S1PR1 using a receptor-selective antagonist will reduce atherosclerotic plaque development in *apoE*$^{KO/KO}$ mice, mainly via antagonizing S1PR1 activity in VSMC. We demonstrate that treatment of *apoE*$^{KO/KO}$ mice with the S1PR1 selective antagonist Ex26 led to a substantial reduction in high fat diet induced atherosclerotic plaque development and that this effect was lost in mice with a VSMC-selective knockout of S1PR1. We demonstrate that the S1PR1 selective agonist SEW2871 potentiated PDGF induced proliferation and cholesterol-loading induced lipid accumulation in aortic SMCs and that both of these were impaired by Ex26. These findings demonstrate that inhibiting S1PR1 with Ex26 may hold promise as a therapeutic approach to reducing atherosclerosis development.

3.3 Materials and Methods

3.3.1 Animals

All mouse procedures were performed in the David Braley Research Institute Animal Facility at McMaster University following Canadian Council of Animal Care guidelines and after approval from the Animal Research Ethics Board of McMaster University. Mice were bred and housed in ventilated cages with free access to a food and automated watering on a 12-hr light/12 hr dark cycle. *ApoE*$^{KO/KO}$ and *Tagln-cre*^{TG} (Cre recombinase is expressed under the control of mouse Transgelin promoter) mouse founders were purchased from Jackson Laboratories. *S1pr1*$^{lox/lox}$ mice were bred from founders originally generously provided by Professor Richard Proia (National Institute of Diabetes and Digestive and Kidney Diseases, Bethesda, MD, USA). *S1pr1*$^{lox/lox}$ mice were mated with *Tagln-cre*^{TG} mice to generate SMC-specific S1PR1 KO mice (*Tagln-cre*^{TG}*; S1pr1*$^{lox/lox}$). For atherosclerosis studies, *Tagln-cre*^{TG}*; S1pr1*$^{lox/lox}$ mice were crossed with *ApoE*$^{KO/KO}$ mice for multiple generations to generate *Tagln-cre*^{TG}*; S1pr1*$^{lox/lox}$*; ApoE*$^{KO/KO}$ mice.

3.3.2 Mini-osmotic pump surgery

The S1PR1 antagonist Ex26 (catalogue No: 5833, Tocris, Bristol, UK) was delivered using Alzet mini-osmotic pumps (model 2006, Durect Corporation, Cupertino, CA, USA). A controlled dose of 0.1 mg/kg/hour of Ex26 was delivered continuously via the minipump for a period of six weeks. In brief, 11-week-old female mice were anesthetized with isoflurane and 0.1 ml of the non-steroidal anti-

inflammatory agent carprofen (5 mg/kg) was administered subcutaneously. The fur on the back of the mouse was clipped and the surgical site was cleaned with 10% povidone-iodine scrub, 70% isopropyl alcohol, and 7.5% povidone-iodine solution. A mid-scapular incision in the skin was made, and a pocket was created large enough to accommodate one pump. Osmotic pumps were filled with either Ex26 (16 mg/ml in DMSO) or DMSO vehicle control. Following the subcutaneous insertion of the pump, the wound was closed with a wound clip. Mice were immediately placed on a high-fat diet (HFD) for six weeks. Carprofen (5 mg/kg dose) was injected subcutaneously daily for the two days following surgery. The mice were fasted for 12 hrs prior to sacrifice.

3.3.3 Lipid analysis and pulmonary edema measurement

Blood was collected from anesthetized mice by cardiac puncture prior to sacrifice. All samples were spun at 775 x *g* for 10 min to obtain plasma. Enzymatic assay kits were used to quantify total cholesterol (Cholesterol Infinity kit, Thermo Scientific, Ottawa, ON, Canada), HDL-C (HDL-cholesterol E kit, Wako Diagnostics, Mountain View, CA, USA) and triglycerides (Triglyceride, Wako Diagnostics, Mountain View, CA, USA). Absorbance was measured with a Spectramax plus microplate reader (Molecular Devises, Sunnyvale, CA, USA) using SoftMax Pro software. Non-HDL cholesterol was calculated as the difference between plasma total cholesterol and HDL-C values for each sample. The lungs were harvested during the time of harvest, wet weights were collected, and lungs were then dried

for 72 hours at 50°C to for measurement of dry weights. The lung wet-to-dry weight ratio was calculated as a measure of pulmonary edema.

3.3.4 Flow cytometry analysis

Flow cytometry was performed on fresh blood samples collected from mice at harvest. Blood cells were labeled by incubation with fluorochrome-conjugated antibodies for 30 minutes. The antibodies used are as follows: FITC-CD3 (BD Biosciences, # 555274, Mississauga, Ontario, Canada), BV510-CD45 (Biolegend, # 103138, San Diego, California, USA), PerCP-Cyanine5.5-CD45R (B220) (eBioscience, # 45-0452-80, San Diego, California, USA), PE-Cy5-CD4 (BD Biosciences, # 553050), PE-Cy7-CD8a (BD Biosciences, # 552877), PE-NK1.1 (BD Biosciences, # 553165), PE CD11b (M1/70.15) (Thermo Fisher Scientific, # RM2805), PE-Cy7-Ly6C (Biolegend, # 128018), and PE-Dazzle-594-Ly6G (Biolegend, # 127648(BLG)). Fluorochrome-conjugated antibodies were used either singly or in various combinations (Myeloid cells: FITC-CD3, BV510-CD45, PerCP-Cyanine5.5-CD45R, PE CD11b, PE-Cy7-Ly6C, and PE-Dazzle-594-Ly6G; Lymphocytes: FITC-CD3, BV510-CD45, PerCP-Cyanine5.5-CD45R, PE-Cy5-CD4, PE-Cy7-CD8a, and PE-NK1.1). After incubation with antibodies, leukocytes were fixed and red blood cells were lysed with a 1-step fix/lyse solution 1X (Thermo Fisher Scientific, # 00-5333) for 15 minutes in the dark at room temperature. Flow cytometry was performed on a BD FACSCalibur instrument (BD Biosciences) on samples spiked with 123count eBeads (Thermo Fisher Scientific, #01-1234-42). Analysis of the data was performed with FlowJo v10 software (BD Biosciences).

3.3.5 Quantification of aortic-sinus atherosclerosis

For atherosclerosis studies, hearts were excised from anesthetized mice upon sacrifice and embedded in the Tissue-Tek® OCT compound. Serial 10 µm thick cryosections from the appearance to the disappearance of aortic valve leaflets were collected on microscopic slides. The sections were stained with ORO for neutral lipids and counterstained with Meyer's Hematoxylin for cell nuclei. Images were obtained using a Zeiss Axiovert 200M fluorescence microscope (Carl Zeiss Canada Ltd. Toronto, ON, Canada) at 5X magnification. Atherosclerotic plaque cross sectional areas were measured in each of 7 sections taken at 100 µm intervals, spanning a total of 600 µm of the aortic sinus. Atherosclerotic plaque volumes were calculated as the areas under the curve of atherosclerotic plaque cross sectional area versus distance.

3.3.6 Immunofluorescence analyses of atherosclerotic plaques

The leukocyte (CD45) and macrophage (Mac3) content in the atherosclerotic plaques within the aortic sinus were detected using following antibodies: Alexa Fluor™ 594 anti-mouse CD45.2 Antibody (#109850, BioLegend) for CD45, rat anti-mouse CD107b antibody (1:50 dilution, # 553322, BD biosciences) followed by Alexa Fluor™ 488-conjugated goat anti-rat secondary antibody (1:500 dilution, # A-11006, Invitrogen) for Mac3 staining. Lastly, the slides were stained with DAPI for 10 min at room temperature and mounted with PermafluorTM aqueous mounting medium (Fisher Scientific). All images were captured using a STELLARIS confocal microscope (Leica Microsystems, Wetzlar, Germany) with a

63X objective. Total area of CD45 and Mac3 staining within the atherosclerotic plaques was normalized to total plaque area.

3.3.7 In-vitro cell culture

Human aortic smooth muscle cells (HASMC; Thermo Scientific, #C0075C) were cultured in Medium 231 (Invitrogen, # M-231-500) supplemented with 5% smooth muscle growth supplement (SMGS; Thermo Fisher Scientific, #S00725), 50 U/mL penicillin and 50 mg/mL streptomycin and incubated at 37°C in an atmosphere of 95% air and 5% CO_2.

Aortic smooth muscle cells were isolated from mice 5-8 weeks old female C57BL6/J as described previously by others with slight modifications (Shen et al. 2018). Briefly, the mouse was anesthetized using isoflurane and sprayed with 70% ethanol. During surgery, inhalant anesthesia was continuously provided to the mouse under the dissecting lamp. The blood was collected by cardiac puncture and the heart was perfused with sterile PBS. Except the heart, all other organs were removed to get a clear view of the aorta. Next, the whole aorta was collected and cleaned under a dissecting microscope with sterile PBS containing 50 U/mL penicillin, and 50 mg/mL streptomycin. The aorta was incubated in a freshly prepared cocktail of enzymes (1 mg/ml collagenase II, 1 mg/ml soybean trypsin inhibitor, and 0.744 U/ml elastase) in 1X Hanks Balanced Salt Solution (HBSS; Thermo Fisher Scientific) with 50 U/mL penicillin and 50 mg/mL streptomycin for 10 min at 37 °C. After removing the adventitia, the aorta was chopped into small pieces. The final digestion step was performed by incubating them in a freshly

prepared enzyme cocktail (see above) at 37 °C for 1 hr. When the tissue fragments were dissolved, the cells were washed once and cultured in DMEM/F12 supplemented with 20% FBS, 2mM L-Glutamine, 50 U/mL penicillin, and 50 mg/mL streptomycin.

3.3.8 Cell proliferation

For proliferation assays, HASMCs were seeded in 6-well plates at 2 x 10^4 cells/well in Medium 231 supplemented with SMGS, 50 U/mL penicillin and 50 mg/mL streptomycin and incubated at 37°C and 5% CO2 for 24 hours. Cells were then serum-starved for 24 hrs. Cells were released from one set of wells by incubation with trypsin and counted to establish cell numbers at time 0. Cell proliferation was induced in the other wells by adding recombinant PDGF-BB (50 ng/ml; Biolegend, San Deigo, California, USA) together with SEW2871 (1 µM; Cayman Chemicals, Ann Arbor, Michigan, USA), and Ex26 (10 µM), either alone or in combination. Cells were released from the remaining wells by incubation with trypsin at times 48 and 96 hours after addition of PDGF-BB. Cells released from wells were immediately counted with a Bright Line Hemocytometer. Total cell numbers per well were plotted versus time to determine rates of proliferation.

3.3.9 Cholesterol Loading

Cholesterol loading was carried out using a complex of cholesterol/methyl-β-cyclodextrin (chol/MCD; Millipore Sigma, Oakville ON, Canada, catalogue # C4951-30MG; molar ratio of 0.14) as originally described by others (Rong et al. 2003). All treatment concentrations involving chol/MCD were based on cholesterol weight. In brief, the VSMCs (from C57BL6/J female mice) were seeded in Lab-TekTM 8-well chamber slides at a density of 5 x 10^4 cells per chamber and allowed to grow for 24 hours. After two washes, the cells were starved in DMEM/F12 media containing 50 U/mL penicillin, and 50 mg/mL streptomycin, 2 mM L-glutamine, and 0.2% filtered BSA for 20 hrs. The following day, the cells were treated with 0.1% DMSO vehicle, chol/MCD (10 µg cholesterol/ml), SEW2871 (10 µM) and Ex26 (10 µM) individually or in combination for 72 hours. The corresponding treatment media were changed every 24 hrs.

Next, the cells were fixed with 4% PFA for 20 min after 2x washes with plain DMEM/F12 media, permeabilized with 0.1% Triton X-100 in PBS for 5 min after 2x wash with PBS, and blocked with 3% goat serum in PBS-T for 1 hr at RT. Then cells were incubated with anti-alpha SMA primary antibody (Abcam, catalog No. ab5694) diluted at 1:200 with 3% goat serum in PBS-T solution at 4°C overnight, washed 3x with PBS-T, and incubated with goat anti-rabbit Alexa Fluor™ 488 secondary antibody (Thermo Fisher Scientific, catalog No. A-11008) diluted at 1:500 with 3% goat serum in PBS-T solution at RT for 1 hr. After 3x washes in PBS-T, cells were stained with 0.3 % w/v Oil Red O solution at RT for 18 min in

Coplin Jar, washed 3x in PBS-T, cells were counterstained for nuclear DNA DAPI, mounted and imaged using a STELLARIS confocal microscope (Leica Microsystems, Wetzlar, Germany).

3.3.10 Statistical analysis

We confirmed the normal distribution and tested the difference between the variances using Shapiro-Wilk normality test and F-test, respectively. To compare two independent groups, we used Welch's t-test when sample variances were unequal or Student's t-test when sample variances were equal. Unless otherwise stated, we used one-way ANOVA with Tukey's multiple comparison test to compare three or more groups with one independent variable, and Two-way ANOVA with Tukey's multiple comparison test to compare multiple groups with two or more independent variables. All data are represented as mean± standard error mean (SEM). Statistical analyses were performed using GraphPad Prism 9.

3.4 Results

3.4.1 Prolonged S1PR1 antagonist treatment renders protections against atherosclerosis

To investigate if S1PR1 inhibition provides protection against diet-induced atherosclerosis in *ApoE*$^{KO/KO}$ mice, we subcutaneously administered Ex26, a highly potent S1PR1 antagonist, to female *ApoE*$^{KO/KO}$ mice using Alzet osmotic minipumps at a dosage of 0.1 mg/kg/hour. Control mice received osmotic pumps containing the DMSO vehicle alone. Pumps were implanted when mice were 11 weeks of age and mice were switched to high fat diet feeding, which was maintained for 6 weeks, after which mice were fasted and humanely euthanized for analyses of atherosclerosis in the aortic sinus. Since female *ApoE*$^{KO/KO}$ mice develop diet-induced atherosclerosis more rapidly than males we elected to use female mice for these studies to maximize the extent of aortic sinus atherosclerosis development during the 6 week treatment period, Our results showed that Ex26 treatment did not alter the body or heart weights of *ApoE*$^{KO/KO}$ mice compared to DMSO vehicle (**Supplementary Figure 3.8 A and B**). Because S1PR1 plays an important role in endothelial barrier integrity, and other reports of S1PR1 inhibition have reported lung edema (Sammani et al. 2010), we examined the ratio of lung wet/dry weights in Ex26 versus DMSO treated mice. Under the conditions (dose/duration) used, and in agreement with other reports (Cahalan et al. 2013) Ex26 treatment did not change lung wet/dry weight ratio compared to DMSO vehicle treatment in *ApoE*$^{KO/KO}$ mice (**Supplementary Figure 3.8 C**). As circulating

lipid levels can influence the development of atherosclerotic plaques, we also measured plasma lipids and lipoprotein levels of Ex26- and DMSO-treated *ApoE*$^{KO/KO}$ mice. Our results showed no significant changes in total cholesterol, triglyceride, HDL cholesterol, and non-HDL cholesterol levels between Ex26- and DMSO-treated mice (**Supplementary Figure 3.9**). In contrast, Ex26 treatment significantly reduced (by almost 60%) atherosclerotic plaque development in the aortic sinus of *ApoE*$^{KO/KO}$ mice in comparison to mice treated with the DMSO vehicle control (3.76 ±0.68 x 10^7 versus 9±1.12 x 10^7 μm^3; *P*=0.001; N=9,9, **Figure 3.1**). Immunofluorescence staining analysis of atherosclerotic plaques revealed a trend (which did not reach statistical significance) towards a reduction in the average extent of staining for CD45, a marker of leukocytes that have infiltrated into plaques **(Figure 3.2 A)** and a statistically significant reduction in the average extent of staining for Mac3 a commonly used marker for macrophages **(Figure 3.2 B)**. Because previous studies have shown that prolonged S1PR1 antagonism results in profound lymphopenia (Cahalan et al. 2013; Tarrasón et al. 2011), we analyzed circulating lymphocyte and myeloid cell levels in blood of HF-diet fed apoE KO mice treated with either Ex26 or DMSO vehicle. B220+ cells were significantly reduced (by 63%; 102.1±36.9 versus 277.85±46.6 cells/uL, *P*=0.005) in Ex26 compared to DMSO treated mice, no differences were observed in concentrations of CD3+ (T cells), CD4+ or CD8+ T cells, NK cells, and NK-T (NK1.1/CD3 double positive) cells, monocytic cells (CD11b+) or neutrophils (Ly6G+)(**Figure 3.3**). These results suggest that Ex26 treatment protects against

atherosclerotic plaque development, in part by reducing the content of macrophage-like cells within atherosclerotic plaques.

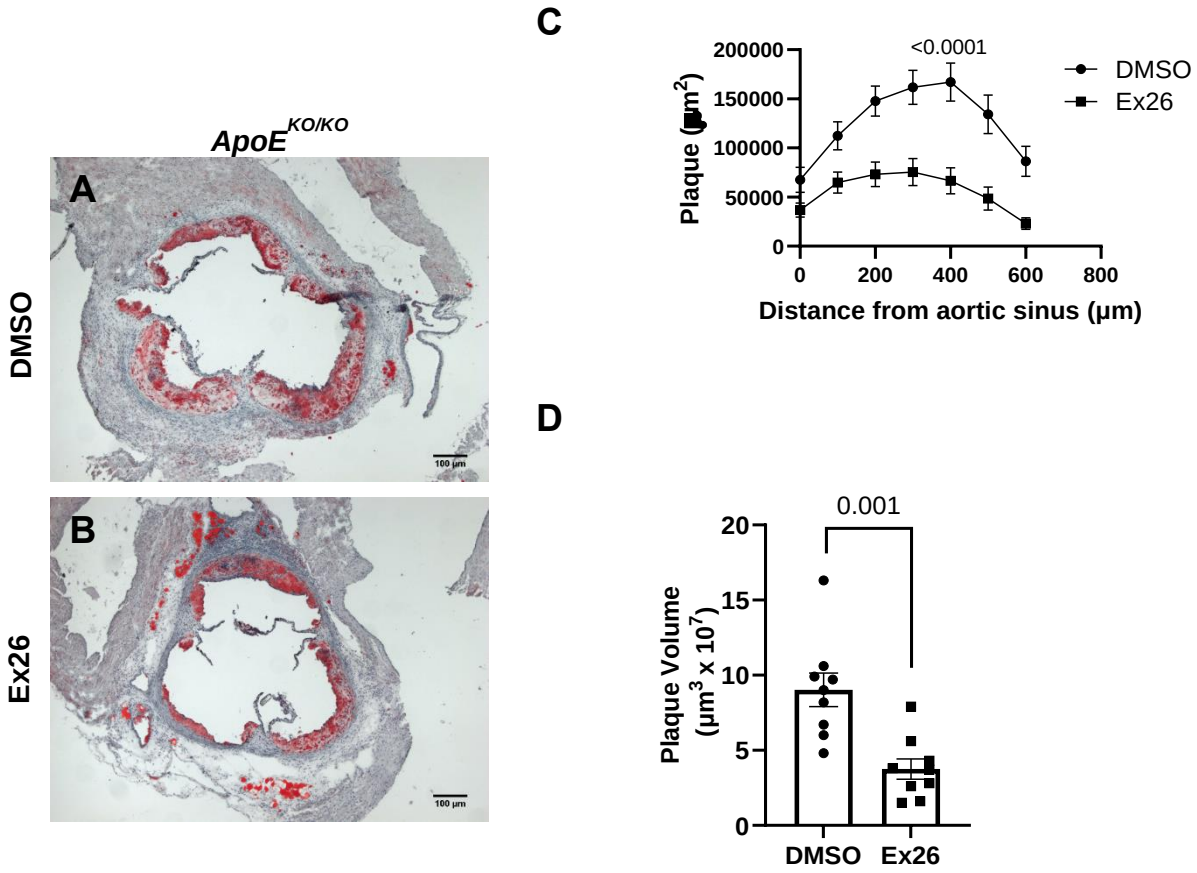

Figure 3.1: The S1PR1 selective antagonist, Ex26, reduced diet-induced atherosclerosis development in *ApoE*$^{KO/KO}$ mice

Alzet osmotic pumps containing S1PR1 antagonist Ex26 (at 0.1 mg/kg/hr) or vehicle control DMSO were inserted subcutaneously into at 11 week-old female *ApoE*$^{KO/KO}$ mice. The mice were fed HFD 6 weeks and harvested at 17 weeks of age. Aortic sinus cross-sections were stained with oil red O and hematoxylin to visualize atherosclerotic plaques. Representative images are shown in panels **A and B**. Atherosclerotic plaque cross sectional areas were analyzed in sections collected every 100 µm along the aortic sinus, starting at the base of the aortic valve pouches, covering a distance of 600 µm. **C:** Average plaque cross-sectional areas (± standard error of the mean) versus distance along the aortic sinus. **D:** Plaque volumes determined from the areas under the curves of plaque cross-sectional area versus distance for individual mice. Each point represents data from an individual mouse. Bars represent averages and error bars represent standard errors of the mean. N=9 mice per group. Scale bars = 100 µm. Statistical analyses were performed by 2-way ANOVA in C and unpaired *t*-test in D.

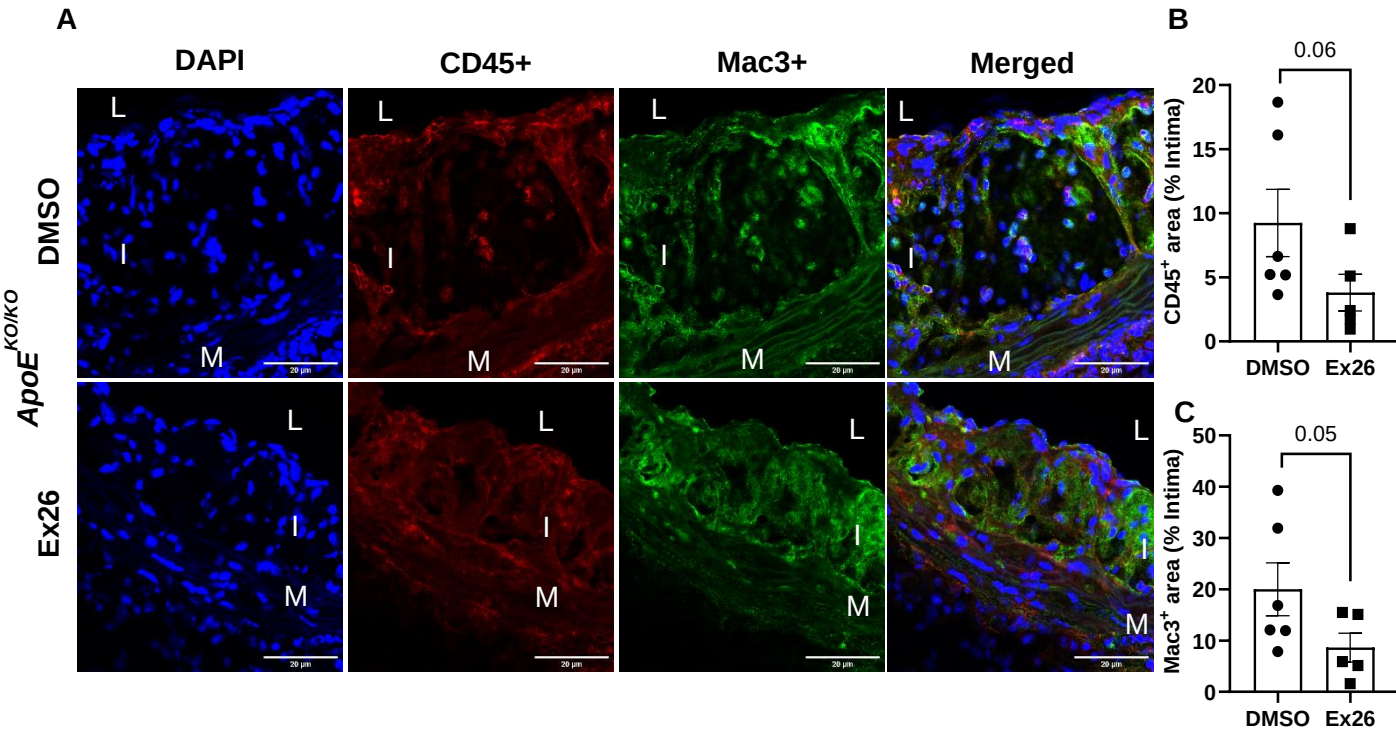

Figure 3.2: Effects of Ex26 on leukocyte and macrophage content in atherosclerotic plaques in aortic sinus cross-sections of *ApoE$^{KO/KO}$* mice

The aortic sinus cross-sections Ex26 or DMSO-treated female *ApoE$^{KO/KO}$* mice were stained for leukocytes (**A, B**: anti-CD45.2 conjugated to Alexa Fluor™ 594; red fluorescence) or macrophages (**A, C**: Mac3: rat anti-CD107b antibody followed by Alexa Fluor™ 488-conjugated goat anti-rat secondary antibody; green fluorescence) and nuclei were counterstained with DAPI (blue fluorescence). **(A)** Representative images (scale bars = 20 μm) and **B,C)** quantification of anti-CD45 **(A,B)** and anti-Mac3 **(A,C)** staining in the atherosclerotic plaques. Each point in B and D represents data from an individual mouse. Bars represent averages and error bars represent standard errors of the means. N=6 DMSO treated and N=5 Ex26 treated mice. Statistical analysis was performed using an unpaired Student's *t* test. L: Lumen, I: Intima, and M-Media.

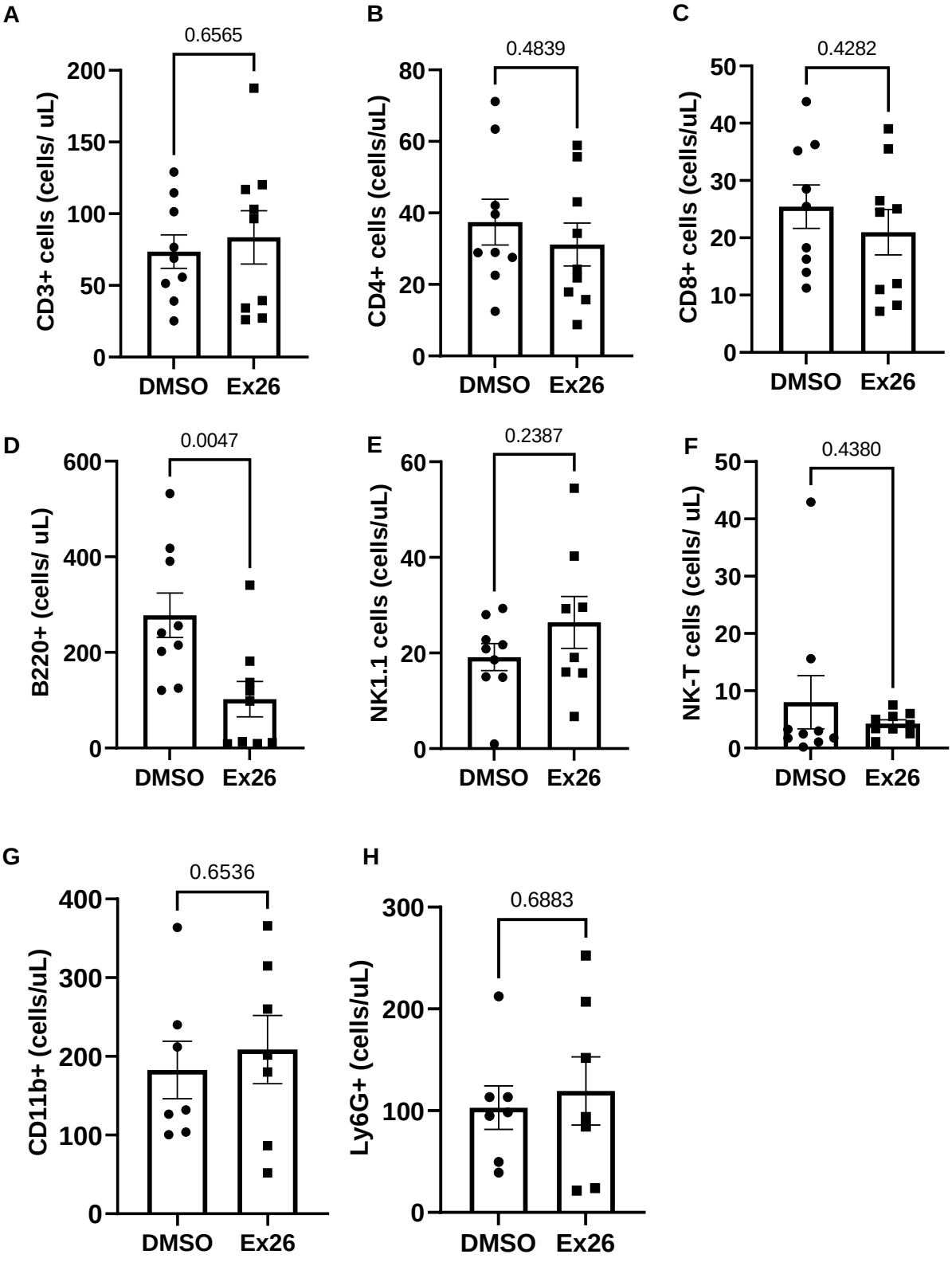
A
0.6565
CD3+ cells (cells/ uL)
200
150
100
50
0
DMSO
Ex26
B
0.4839
CD4+ cells (cells/uL)
80
60
40
20
0
DMSO
Ex26
C
0.4282
CD8+ cells (cells/uL)
50
40
30
20
10
0
DMSO
Ex26
D
0.0047
B220+ (cells/ uL)
600
400
200
0
DMSO
Ex26
E
0.2387
NK1.1 cells (cells/uL)
60
40
20
0
DMSO
Ex26
F
0.4380
NK-T cells (cells/ uL)
50
40
30
20
10
0
DMSO
Ex26
G
0.6536
CD11b+ (cells/uL)
400
300
200
100
0
DMSO
Ex26
H
0.6883
Ly6G+ (cells/uL)
300
200
100
0
DMSO
Ex26

Figure 3.3: Effects of Ex26 treatment on the abundance of leukocytes in blood of *ApoE*$^{KO/KO}$ mice

Flow cytometry was performed on blood samples from Ex26 or DMSO-treated *ApoE*$^{KO/KO}$ mice to detect circulating leucocyte levels. **(A)** CD3+ cells; **(B)** CD4+ cells; **(C)** CD8+ cells; **(D)** B220+ cells; **(E)** NK cells; **(F)** NK-T cells; **(G)** CD11b+ cells; and **(H)** Ly6G+ cells. N=9 (A-F) or 7 (G, H). Each symbol represents data from a single mouse. Bars represent averages and error bars represent standard errors of the means. Statistical analyses were performed using unpaired *t*-tests.

3.4.2 S1PR1 antagonist mediates atheroprotection by inhibiting S1PR1 in VSMCs

We have recently found that selective genetic knockout of *S1pr1* in VSMC protects *ApoE*$^{KO/KO}$ mice against atherosclerosis [Thyagarajan and Trigatti, manuscript in preparation], whereas we and others have reported that selective S1PR1 knockout either in bone marrow derived myeloid cells or in endothelial cells promotes atherosclerosis development in mice (Galvani et al. 2015; Gonzalez et al. 2017). To test if the protective effect of Ex26 treatment might depend on *S1pr1* expression in VSMCs, we treated female *Tagln-cre*^{TG}*; S1pr1*$^{lox/lox}$*; ApoE*$^{KO/KO}$ mice, which lack *S1pr1* expression in VSMCs, with Ex26 or DMSO vehicle control for 6 weeks while mice were fed a HF diet. After 6 weeks of HF diet feeding, we found that as we had previously reported, the extent of atherosclerosis in the DMSO treated *Tagln-cre*^{TG}*; S1pr1*$^{lox/lox}$*; ApoE*$^{KO/KO}$ mice was substantially lower **(Figure 3.4)** than the correspondingly treated *ApoE*$^{KO/KO}$ mice **(Figure 3.1)**. Unlike the *ApoE*$^{KO/KO}$ mice, Ex26 treatment did not result in any further reduction in atherosclerosis in the *Tagln-cre*^{TG}*; S1pr1*$^{lox/lox}$*; ApoE*$^{KO/KO}$ mice ($1.7\pm0.24\times10^7$ μm^3 versus $1.29\pm0.28\times10^7$ μm^3, P=0.13; N=9,8; **Figure 3.4**). Furthermore, Ex26 treatment did not impact the extent of staining for either Mac3 or CD45, indicating that it did not impact macrophage or leukocyte content in plaques of *Tagln-cre*^{TG}*; S1pr1*$^{lox/lox}$*; ApoE*$^{KO/KO}$ mice **(Figure 3.5 A-D)**. Flow cytometry analysis of blood cells revealed lower blood concentrations of some leukocyte fractions, including B220+ cells, in DMSO control treated *Tagln-cre*^{TG}*; S1pr1*$^{lox/lox}$*; ApoE*$^{KO/KO}$ mice than similarly treated *ApoE*$^{KO/KO}$

mice (compare Figure 3D with Figure 6D). Ex26 treated versus DMSO treated *Tagln-cre^{TG}; S1pr1$^{lox/lox}$; ApoE$^{KO/KO}$* mice exhibited slightly lower blood counts for CD3+, CD4+, CD8+ and B220+ cells but this only reached statistical significance for CD4+ cells **(Figure 3.6 A-D)**. No statistically significant differences were observed in other classes of leukocytes in Ex26 versus DMSO treated *Tagln-cre^{TG}; S1pr1$^{lox/lox}$; ApoE$^{KO/KO}$* mice **(Figure 3.6 E-H)**. These results suggest that the effects of Ex26 on the concentrations of leukocytes in blood do not involve S1PR1 expression in VSMCs and are consistent with previous reports that effects of S1PR1 on blood lymphocyte levels are due to its role in endothelial cells in regulating lymphocyte egress from lymph nodes (Wei et al. 2005).

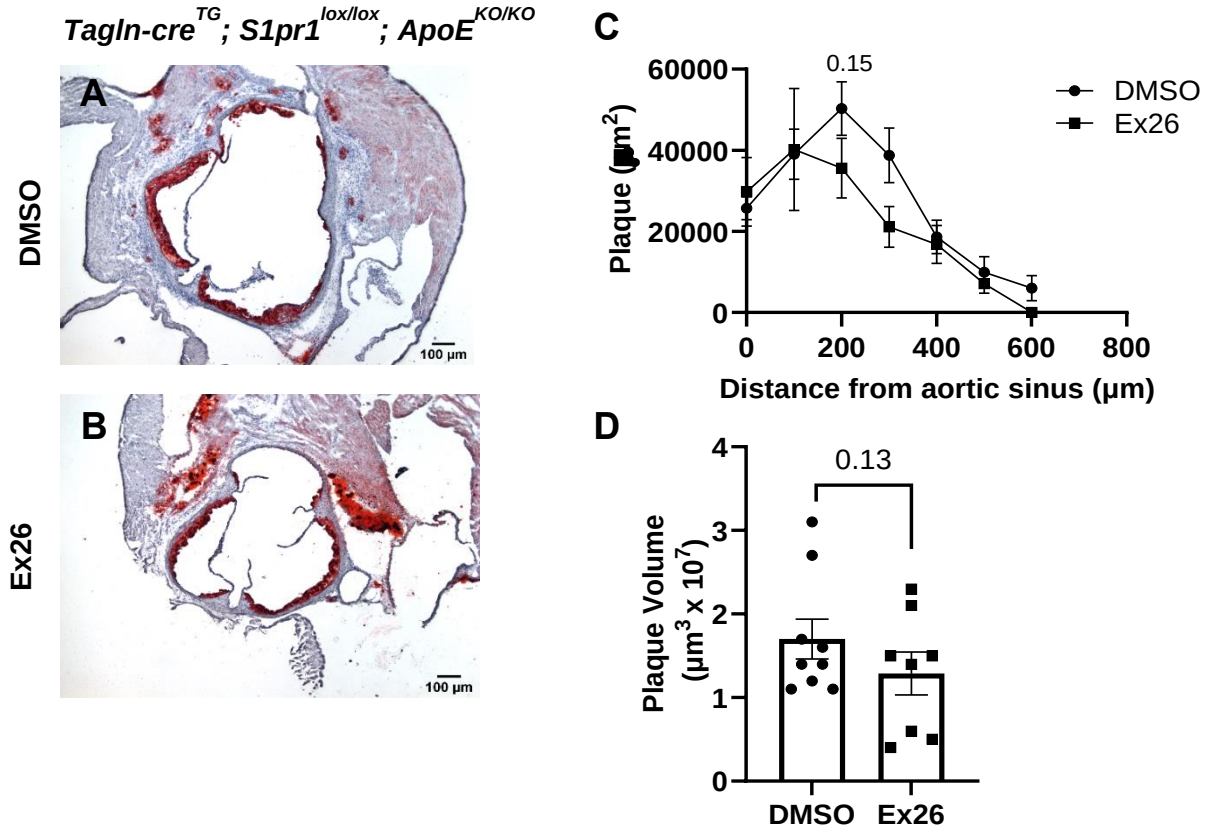

Figure 3.4: Ex26 treatment does not affect atherosclerotic plaque development *ApoE*$^{KO/KO}$ mice with S1PR1 inactivated in VSMCs

Female *Tagln-cre*^{TG}*; S1pr1*$^{lox/lox}$*; ApoE*$^{KO/KO}$ mice were treated subcutaneously, beginning at 11 weeks of age, with either Ex26 (at 0.1 mg/kg/hr in DMSO) or DMSO vehicle control, using Alzet osmotic pumps and were fed the HFD 6 weeks, and were harvested at 17 weeks of age. Atherosclerotic plaques were analyzed as described in the legend to Figure 1. Representative images are shown in panels **A and B**. Atherosclerotic plaque cross sectional areas were analyzed in sections collected every 100 µm along the aortic sinus, starting at the base of the aortic valve pouches, covering a distance of 600 µm. **C:** Average plaque cross-sectional areas (± standard error of the mean) versus distance along the aortic sinus. **D:** Plaque volumes determined from the areas under the curves of plaque cross-sectional area versus distance for individual mice. Each point represents data from an individual mouse. Bars represent averages and error bars represent standard errors of the mean. N=9 (DMSO) and 8 (Ex26) mice per group. Scale bars = 100 µm. Statistical analyses were performed by 2-way ANOVA in C and unpaired t-test in D.

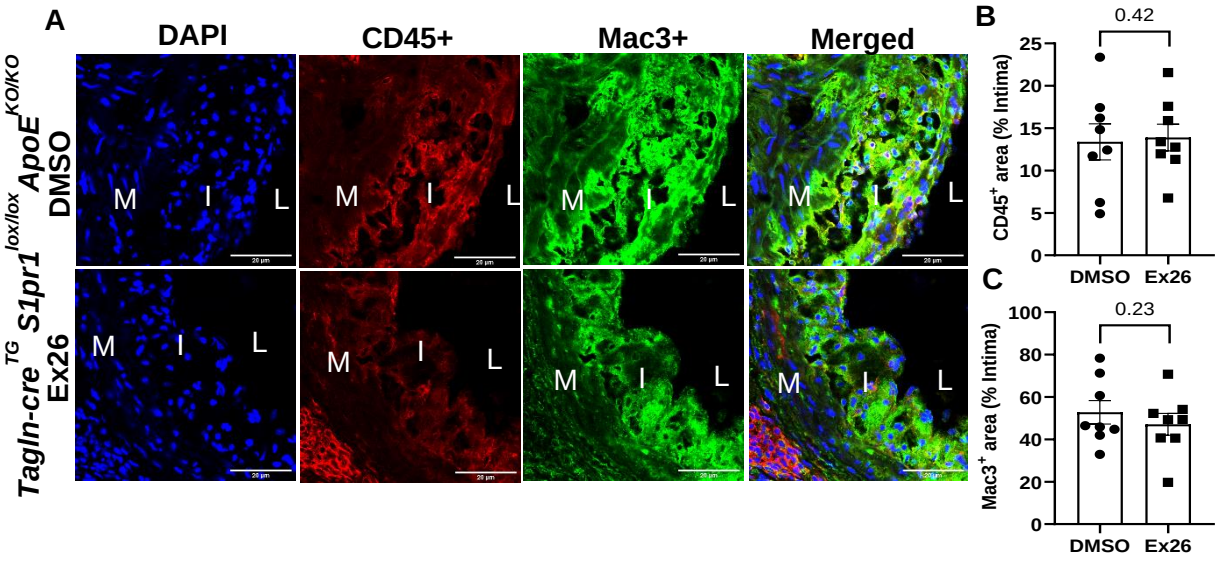

Figure 3.5: Ex26 does not impact leukocyte or macrophage content in atherosclerotic plaques in *ApoE$^{KO/KO}$* mice with S1PR1 inactivated in VSMCs

The aortic sinus cross-sections Ex26 or DMSO-treated female *Tagln-cre^{TG}; S1pr1$^{lox/lox}$; ApoE$^{KO/KO}$* mice were stained for leukocytes (**A, B**: anti-CD45.2 conjugated to Alexa Fluor™ 594; red fluorescence) or macrophages (**A, C**: Mac3: rat anti-CD107b antibody followed by Alexa Fluor™ 488-conjugated goat anti-rat secondary antibody; green fluorescence) and nuclei were counterstained with DAPI (blue fluorescence). **: A)** Representative images (scale bars = 20 μm) and **B,C)** quantification of anti-CD45 **(A,B)** and anti-Mac3 **(A,C)** staining in the atherosclerotic plaques. Each point in B and D represents data from an individual mouse. Bars represent averages and error bars represent standard errors of the means. N=8 mice per group. Statistical analysis was performed using an unpaired Student's *t* test. L: Lumen, I: Intima, and M-Media.

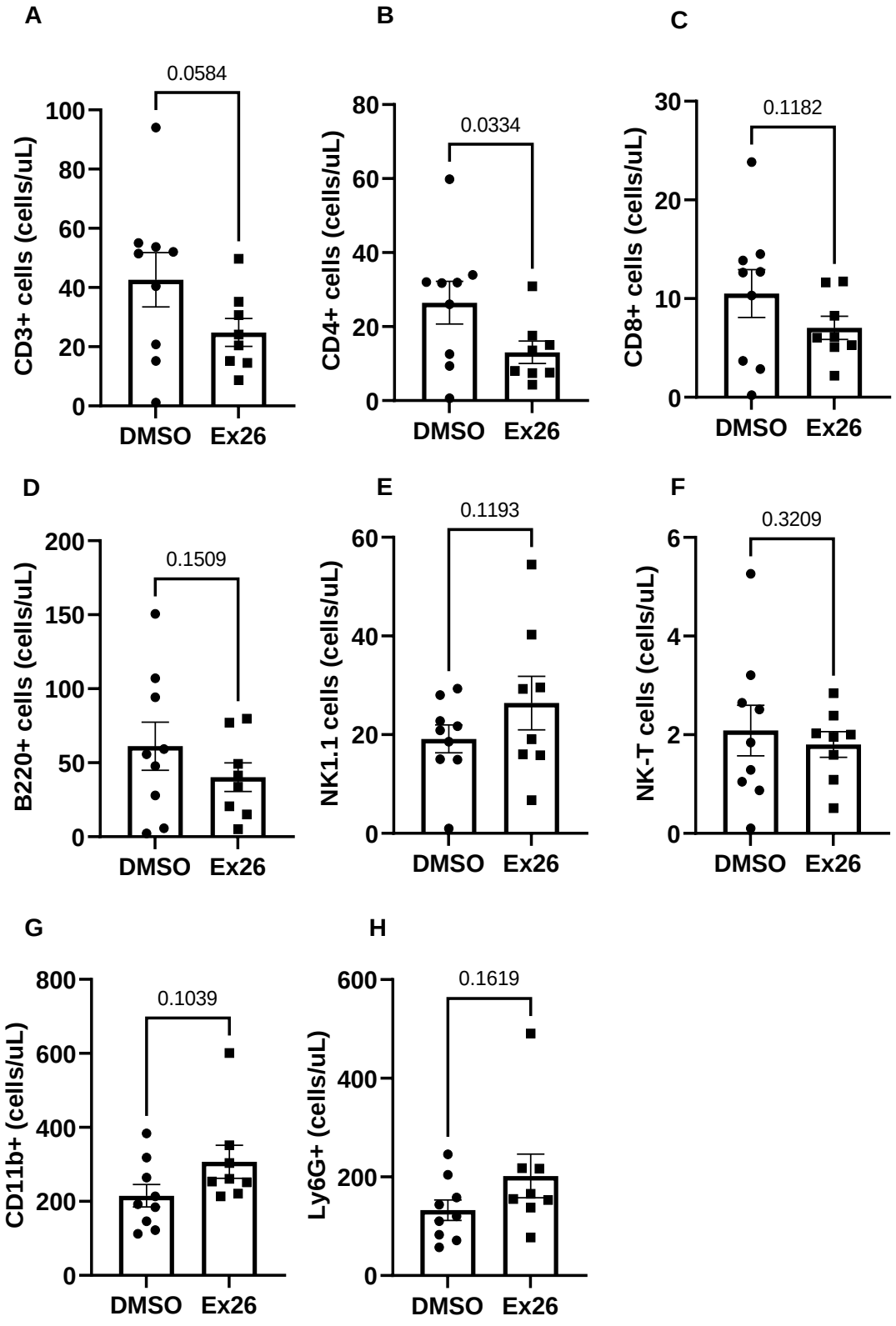
A
0.0584
CD3+ cells (cells/uL)
100
80
60
40
20
0
DMSO
Ex26
B
0.0334
CD4+ cells (cells/uL)
80
60
40
20
0
DMSO
Ex26
C
0.1182
CD8+ cells (cells/uL)
30
20
10
0
DMSO
Ex26
D
0.1509
B220+ cells (cells/uL)
200
150
100
50
0
DMSO
Ex26
E
0.1193
NK1.1 cells (cells/uL)
60
40
20
0
DMSO
Ex26
F
0.3209
NK-T cells (cells/uL)
6
4
2
0
DMSO
Ex26
G
0.1039
CD11b+ (cells/uL)
800
600
400
200
0
DMSO
Ex26
H
0.1619
Ly6G+ (cells/uL)
600
400
200
0
DMSO
Ex26

Figure 3.6: Effects of Ex26 treatment on the abundance of leukocytes in blood of *ApoE$^{KO/KO}$* mice with S1PR1 inactivated in VSMCs

Flow cytometry was performed on blood samples from Ex26 or DMSO-treated *Tagln-cre^{TG}; S1pr1$^{lox/lox}$; ApoE$^{KO/KO}$* mice to detect circulating leucocyte levels. **(A)** CD3+ cells; **(B)** CD4+ cells; **(C)** CD8+ cells; **(D)** B220+ cells; **(E)** NK cells; **(F)** NK-T cells; **(G)** CD11b+ cells; and **(H)** Ly6G+ cells. N=9 (DMSO) and 8 (Ex26). Each symbol represents data from a single mouse. Bars represent averages and error bars represent standard errors of the means. Statistical analyses were performed using unpaired *t*-tests.

3.4.3 S1PR1 inhibition blocks the effects of S1PR1 activation on aortic SMC proliferation and lipid accumulation

Treatment of HASMCs with the S1PR1-specific SEW2871 alone resulted in a significant increase in cell proliferation **(Figure 3.7 A and B)**. Treatment with PDGF, a known mitogen that acts through the PDGF receptor, resulted in a greater degree of proliferation of HASMCs **(Figure 3.7 A and B)**. Treatment of HASMCs with both PDGF and SEW2871 lead to an even greater increase in cell proliferation, suggesting that SEW2871 potentiated the effect of PDGF **(Figure 3.7 A and B)**, consistent with reports that S1PR1 and the PDGF receptor interact functionally (Hobson et al. 2001; Rosenfeldt, Hobson, Maceyka, et al. 2001; Waters et al. 2003; Waters et al. 2006; Tanimoto, Lungu, and Berk 2004). Ex26 treatment, however, attenuated cell proliferation in response to either SEW2871 or PDGF or both (**Figure 3.7A and B**). Treatment of primary murine aortic SMCs with chol/MCD resulted in the accumulation of neutral lipid droplets detected by staining with oil red O **(Figure 3.7 C and D)**. Including the S1PR1-selective agonist, SEW2871, increased the level of chol/MCD-induced lipid droplet accumulation **(Figure 3.7 C and D)**. Similar results were observed using primary aortic SMCs from male mice (**Figure 2.6A, B**). Ex26 prevented the SEW2871 mediated increase in lipid droplet formation **(Figure 3.7 C and D)**. These findings confirm a role for S1PR1 in aortic SMCs in potentiating proliferation in response to PDGF and lipid droplet formation in response to cholesterol loading and demonstrate that the S1PR1 antagonist, Ex26, suppresses these pro-atherogenic processes.

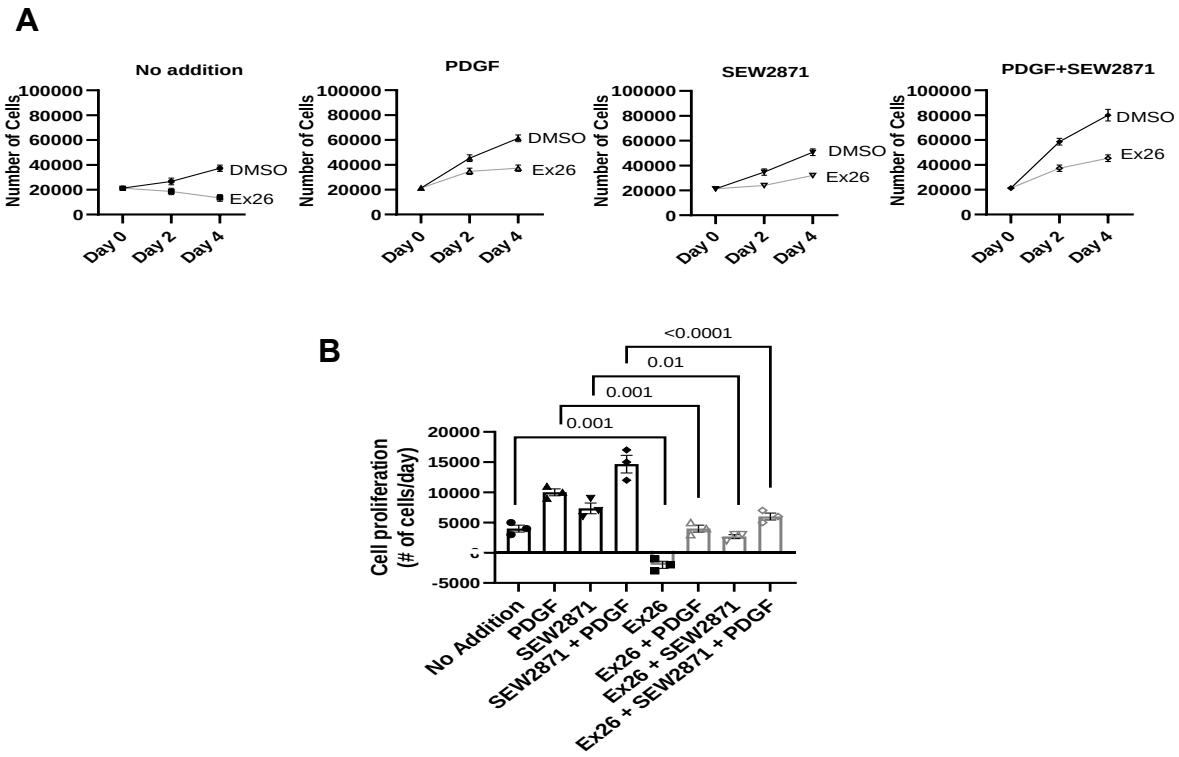
A
No addition
PDGF
SEW2871
PDGF+SEW2871
Number of Cells
100000
80000
60000
40000
20000
0
DMSO
Ex26
Day 0
Day 2
Day 4
B
<0.0001
0.01
0.001
0.001
Cell proliferation
(# of cells/day)
20000
15000
10000
5000
0
-5000
No Addition
PDGF
SEW2871
SEW2871 + PDGF
Ex26
Ex26 + PDGF
Ex26 + SEW2871
Ex26 + SEW2871 + PDGF
C
DMSO
chol/MCD
Ex26+
chol/MCD
SEW2871+
chol/MCD
SEW2871+Ex26+
chol/MCD
D
ORO intensity/DAPI numbers
25
20
15
10
5
0
0.02
0.01
0.0004
chol/MCD - + + + +
Ex26 - - + - +
SEW2871 - - - + +

Figure 3.7: Ex26 treatment reduced S1PR1 agonist-mediated proliferation and lipid droplet formation in cultured aortic SMC

HASMCs (20,000 cells/well) were either treated with DMSO vehicle or Ex26 (10 μM in DMSO) alone or in combination with PDGF-BB (50 ng/mL), and/or SEW2871 (1 μM), as indicated. **A:** Time course of cell proliferation over 4 days. **B:** Cell proliferation rates. Mouse aortic SMCs were cultured for 72 hours without or with cholesterol (10 μg/ml) complexed with methyl-β-cyclodextrin, together with SEW2871 (10 μM), Ex26 (10 μM) (each added in DMSO) or DMSO (vehicle control to final DMSO concentration of 0.1% for all samples) either alone or in combination as indicated. **C:** Representative merged fluorescence images of control and treated cells stained with Oil red O for lipid droplets (red), anti-alpha SMA antibody (green), and DAPI for nuclei (blue). Scale bars = 100 μm. **D:** Quantification of oil red O staining intensity normalized to numbers of nuclei across 5 fields of view per well for 3-5 independent cultures of cells, representing cell isolates from 3 different female mice. Each symbol represents an independent culture of cells. Bars represent averages and error bars represent standard errors of the mean. Statistical analysis was carried out using a one-way ANOVA with Tukey's multiple comparison test.

3.5 Discussion

Previous studies reported that the treatment of mice with the S1PR1 agonists FTY720 (activates S1PR1 and S1PRs 3-5), and KRP203 (selective for S1PR1), protected mice against HF-diet induced atherosclerosis (Nofer et al. 2007b; Potì et al. 2013; Keul et al. 2007). However, other studies of the effects of these/other S1PR1 agonists (including FTY720 and CYM5442, itself an S1PR1 selective agonist) reported little-to-no effect on atherosclerosis development (Poti et al. 2012; Wang et al. 2014; Luk et al. 2016). These studies reported lymphopenia in mice treated with these S1PR1 agonists (Nofer et al. 2007a; Keul et al. 2007; Potì et al. 2013; Poti et al. 2012), an outcome that reflects S1PR1 agonist effect on endothelial cells (Wei et al. 2005). These S1PR1 agonists can also act as functional antagonists, as exemplified by the well-studied effects of FTY720, which, upon long term treatment, triggers S1PR1 internalization and degradation, and thus leading to shutdown of S1PR1 signaling (Gräler and Goetzl 2004; Gonzalez-Cabrera, Hla, and Rosen 2007; Gonzalez-Cabrera et al. 2008). This complicates interpretation of studies reporting effects of these agents on atherosclerosis since it is not clear if the protection observed in some of the studies is the result of activation or functional antagonism of S1PR1 signaling. We and others reported different atherogenic outcomes of inactivating S1PR1 in different cell types: Inactivation of S1PR1 in either endothelial cells or bone marrow derived myeloid cells increases atherosclerosis development, consistent with a protective role for S1PR1 signaling in these cell types, promoting cell migration, cell survival and

suppressing inflammatory activation (Galvani et al. 2015; Gonzalez et al. 2017; Burg et al. 2018; Kimura et al. 2003; Al-Jarallah et al. 2014; Hughes et al. 2008). On the other hand, inactivation of *S1pr1* gene expression in VSMCs reduces atherosclerotic plaque development, consistent with a role for S1PR1 in VSMCs in promoting atherosclerosis development, for example, by promoting VSMC proliferation and lipid accumulation [Thyagarajan and Trigatti manuscript in preparation]. As a result of these differential effects of the genetic inactivation of *S1pr1* in endothelial cells and/or myeloid cells versus VSMCs, it was not clear whether overall inhibition of S1PR1 would lead to increased atherosclerosis development (reflecting a predominant role for endothelial and/or myeloid cell S1PR1 on atherosclerosis) or reduce atherosclerosis development (reflecting a predominant role for S1PR1 in promoting atherosclerosis as exemplified by its role in VSMC). Therefore, we wanted to investigate the direct effects of inhibition of S1PR1 on experimental atherosclerosis by using Ex26, a potent and selective S1PR1 antagonist with no reported ability to activate S1PR1 signaling. Cahalan et al. (Cahalan et al. 2013) reported that continuous administration of Ex26 at a dose of 0.1 mg/ kg/ hr caused lymphocyte sequestration within lymph notes and reduced splenic B-cells and T-cells and that a higher dose (30 mg/kg/day), attenuated autoimmune encephalomyelitis. Ex26 reportedly inhibited S1PR1 internalization and polyubiquitylation *in vitro* (Cahalan et al. 2013), demonstrating that it acted as a direct antagonist rather than a functional antagonist of S1PR1 signaling.

S1PR1 signaling is crucial for the stabilization of inter endothelial junctions to preserve endothelial barrier function and to prevent micro vessel leakiness. For instance, administration of S1P or treatment with the S1PR1 agonist SEW2871, but not the inverse agonist SB649146, protected C57BL6 mice against LPS-induced lung injury and vascular permeability (Sammani et al. 2010). Ex26 treatment reportedly also triggers transient lung edema in a dose and time-dependent manner with no effects reported in mice treated continuously with 0.1 mg/kg/hr, but transient lung edema (resolved within 24 hrs) observed after a single 3 mg/kg injection (Cahalan et al. 2013). Consistent with these findings, we observed no evidence of pulmonary edema in *ApoE*$^{KO/KO}$ mice treated continuously with Ex26 at a dose of 0.1 mg/kg/hr for 42 days.

Ex26 treatment substantially reduced HF-diet induced atherosclerotic plaque development in apoE-deficient mice without affecting plasma lipid levels. It also lowered the accumulation of cells expressing the macrophage marker Mac3, and there was a trend towards a reduction in the content of leukocytes (detected by staining for CD45, a marker of blood derived leukocytes) in atherosclerotic plaques, but the latter did not reach statistical significance. These observations are similar to those studies that observed reductions in atherosclerosis in apoE or LDLR-deficient mice treated with the S1PR1 agonists FTY720 and KRP203 (Nofer et al. 2007a; Potì et al. 2013; Keul et al. 2007). Whether the observed reductions in Mac3 and/or CD45 staining in atherosclerotic plaques of Ex26 treated *ApoE*$^{KO/KO}$ mice reflect an impact of S1PR1 inhibition on leukocyte recruitment at the level of

endothelial or other vascular cells in the atherosclerotic plaque, endothelial cells in lymphatic organs impacting cell egress into blood or impacts on leukocytes themselves remains to be determined. We did observe reductions in blood concentrations of certain leukocytes, namely B220+ cells, consistent with the known effect of S1PR1 inhibition on triggering lymphopenia. However, we also noted that the extent of Mac3 staining in plaques was greater than the extent of CD45 staining suggesting that a significant proportion of Mac3+ cells were not derived from circulating leukocytes recruited to plaques from the blood. This is consistent with evolving research findings demonstrating that a significant proportion of cells exhibiting macrophage surface markers and other characteristics are derived from cells resident in the artery wall, including smooth muscle cells which have transdifferentiated, losing expression of smooth muscle specific genes and gaining expression of macrophage associated genes, macrophage characteristics such as the ability to phagocytose, and macrophage phenotypes like the accumulation of lipid droplets and the ability to form foam cells (Rong et al. 2003; Feil et al. 2014; Dubland et al. 2021). Ex26 did not impact atherosclerotic plaque sizes, or Mac3 content within atherosclerotic plaques in mice in which S1PR1 was in activated in VSMCs, lending support to the notion that Ex26's ability to protect against atherosclerosis development might be mediated through inhibition of S1PR1 activity in VSMCs.

Previous studies have demonstrated that S1PR1 in VSMCs promotes cell proliferation and migration, in part through cross-talk with PDGFR. For example, it

has been reported that S1PR1 and PDGFR interact both functionally and biochemically to reciprocally trans-activate each other in smooth muscle cells (Tanimoto, Lungu, and Berk 2004; Waters et al. 2003; Waters et al. 2006), whereas others have reported this is not the case for cell migration (Kluk et al. 2003). Others have reported sequential potentiation of S1PR1 signaling by PDGFR activation, occurring through a PDGF-mediated induction of the intracellular synthesis of S1P, the ligand for S1PR1 (Hobson et al. 2001; Rosenfeldt, Hobson, Milstien, et al. 2001; Rosenfeldt, Hobson, Maceyka, et al. 2001). Pharmacological inhibition of S1PR1 and 3 using the dual active antagonist VPC25239 reduced neointimal hyperplasia (Wamhoff et al. 2008) while overexpressing S1PR1 in VSMCs enhanced IL6 expression in cultured cells and promoted vascular remodelling in rodent models of vascular injury (Kitano et al. 2019). Consistent with these findings, we found that the S1PR1-specific agonist SEW2871 potentiated PDGF induced proliferation of human aortic SMCs and cholesterol-loading induced lipid droplet formation in primary mouse aortic SMCs, and that Ex26 treatment prevented these effects. We also recently demonstrated that smooth muscle selective knockout of S1PR1, like Ex26 treatment, reduced atherosclerotic plaque formation in apoE-deficient mice and demonstrate here that the ability of Ex26 to protect against atherosclerosis is lost when S1PR1 is knocked out in VSMCs. This suggests that Ex26 mediated protection against atherosclerosis may reflect its inhibition of S1PR1 in VSMCs leading to reduced proliferation and lipid droplet formation within

the plaque. However, these impacts of Ex26 observed in cultured aortic SMCs remain to be demonstrated in vivo.

It is important to point out that we cannot rule out the possibility that the reduced blood lymphocytes count observed in Ex26 treated mice might contribute, at least in part, to the reduced atherosclerosis development. Importantly we also observed lower levels of B220+ cells in the blood of mice in which S1PR1 was selectively inactivated in VSMCs, consistent with a role for and therefore reduced recruitment of lymphocytes into plaques.

In conclusion, our study demonstrates that pharmacological inhibition of S1PR1 protects against atherosclerosis development in apoE-deficient mice. The S1PR1 selective antagonist Ex26 protected against atherosclerosis development mainly by inhibiting S1PR1 activity in VSMCs. This involved inhibition of S1PR1 agonist induced SMC proliferation and lipid droplet formation. As a result of our findings, we propose that S1PR1 antagonism may be a promising therapeutic approach to preventing atherosclerosis.

3.6 References

Al-Jarallah, Aishah, Xing Chen, Leticia Gonzalez, and Bernardo L Trigatti. 2014. 'High density lipoprotein stimulated migration of macrophages depends on the scavenger receptor class B, type I, PDZK1 and Akt1 and is blocked by sphingosine 1 phosphate receptor antagonists', *PloS one*, 9: e106487.

Alencar, Gabriel F, Katherine M Owsiany, Santosh Karnewar, Katyayani Sukhavasi, Giuseppe Mocci, Anh T Nguyen, Corey M Williams, Sohel Shamsuzzaman, Michal Mokry, and Christopher A Henderson. 2020. 'Stem cell pluripotency genes Klf4 and Oct4 regulate complex SMC phenotypic changes critical in late-stage atherosclerotic lesion pathogenesis', *Circulation*, 142: 2045-59.

Allahverdian, Sima, Ali Cyrus Chehroudi, Bruce M McManus, Thomas Abraham, and Gordon A Francis. 2014. 'Contribution of intimal smooth muscle cells to cholesterol accumulation and macrophage-like cells in human atherosclerosis', *Circulation*, 129: 1551-59.

Allende, Maria L, Jennifer L Dreier, Suzanne Mandala, and Richard L Proia. 2004. 'Expression of the sphingosine 1-phosphate receptor, S1P1, on T-cells controls thymic emigration', *Journal of Biological Chemistry*, 279: 15396-401.

Allende, Maria L, Tadashi Yamashita, and Richard L Proia. 2003. 'G-protein-coupled receptor S1P1 acts within endothelial cells to regulate vascular maturation', *Blood*, 102: 3665-67.

Björkegren, Johan LM, and Aldons J Lusis. 2022. 'Atherosclerosis: recent developments', *Cell*.

Brinkmann, Volker, Andreas Billich, Thomas Baumruker, Peter Heining, Robert Schmouder, Gordon Francis, Shreeram Aradhye, and Pascale Burtin. 2010. 'Fingolimod (FTY720): discovery and development of an oral drug to treat multiple sclerosis', *Nature reviews Drug discovery*, 9: 883-97.

Burg, Nathalie, Steven Swendeman, Stefan Worgall, Timothy Hla, and Jane E Salmon. 2018. 'Sphingosine 1-Phosphate Receptor 1 Signaling Maintains Endothelial Cell Barrier Function and Protects Against Immune Complex–Induced Vascular Injury', *Arthritis & Rheumatology*, 70: 1879-89.

Cahalan, Stuart M, Pedro J Gonzalez-Cabrera, Nhan Nguyen, Miguel Guerrero, Elizabeth A George Cisar, Nora B Leaf, Steven J Brown, Edward Roberts, and Hugh Rosen. 2013. 'Sphingosine 1-phosphate receptor 1 (S1P1) upregulation and amelioration of experimental autoimmune encephalomyelitis by an S1P1 antagonist', *Molecular Pharmacology*, 83: 316-21.

Dubland, Joshua A, Sima Allahverdian, Katrina J Besler, Carleena Ortega, Ying Wang, Collin S Pryma, Kamel Boukais, Teddy Chan, Michael A Seidman,

and Gordon A Francis. 2021. 'Low LAL (lysosomal acid lipase) expression by smooth muscle cells relative to macrophages as a mechanism for arterial foam cell formation', *Arteriosclerosis, thrombosis, and vascular biology*, 41: e354-e68.

Feil, Susanne, Birgit Fehrenbacher, Robert Lukowski, Frank Essmann, Klaus Schulze-Osthoff, Martin Schaller, and Robert Feil. 2014. 'Transdifferentiation of vascular smooth muscle cells to macrophage-like cells during atherogenesis', *Circulation research*, 115: 662-67.

Galvani, Sylvain, Marie Sanson, Victoria A Blaho, Steven L Swendeman, Hideru Obinata, Heather Conger, Björn Dahlbäck, Mari Kono, Richard L Proia, and Jonathan D Smith. 2015. 'HDL-bound sphingosine 1-phosphate acts as a biased agonist for the endothelial cell receptor S1P1 to limit vascular inflammation', *Science signaling*, 8: ra79-ra79.

Gonzalez-Cabrera, Pedro J, Timothy Hla, and Hugh Rosen. 2007. 'Mapping pathways downstream of sphingosine 1-phosphate subtype 1 by differential chemical perturbation and proteomics', *Journal of Biological Chemistry*, 282: 7254-64.

Gonzalez-Cabrera, Pedro J, Euijung Jo, M Germana Sanna, Steven Brown, Nora Leaf, David Marsolais, Marie-Therese Schaeffer, Jacqueline Chapman, Michael Cameron, and Miguel Guerrero. 2008. 'Full pharmacological

efficacy of a novel S1P1 agonist that does not require S1P-like headgroup interactions', *Molecular Pharmacology*, 74: 1308-18.

Gonzalez, Leticia, Alexander S Qian, Usama Tahir, Pei Yu, and Bernardo L Trigatti. 2017. 'Sphingosine-1-phosphate receptor 1, expressed in myeloid cells, slows diet-induced atherosclerosis and protects against macrophage apoptosis in ldlr KO mice', *International Journal of Molecular Sciences*, 18: 2721.

Gräler, Markus H, and Edward J Goetzl. 2004. 'The immunosuppressant FTY720 down-regulates sphingosine 1-phosphate G protein-coupled receptors', *The FASEB Journal*, 18: 551-53.

Hansson, Göran K. 2005. 'Inflammation, atherosclerosis, and coronary artery disease', *New England Journal of Medicine*, 352: 1685-95.

Hobson, John P, Hans M Rosenfeldt, Larry S Barak, Ana Olivera, Samantha Poulton, Marc G Caron, Sheldon Milstien, and Sarah Spiegel. 2001. 'Role of the sphingosine-1-phosphate receptor EDG-1 in PDGF-induced cell motility', *Science*, 291: 1800-03.

Hughes, Jeniter E, Suseela Srinivasan, Kevin R Lynch, Richard L Proia, Pawel Ferdek, and Catherine C Hedrick. 2008. 'Sphingosine-1-phosphate induces an antiinflammatory phenotype in macrophages', *Circulation research*, 102: 950-58.

Kappos, Ludwig, Ernst-Wilhelm Radue, Paul O'Connor, Chris Polman, Reinhard Hohlfeld, Peter Calabresi, Krzysztof Selmaj, Catherine Agoropoulou, Malgorzata Leyk, and Lixin Zhang-Auberson. 2010. 'A placebo-controlled trial of oral fingolimod in relapsing multiple sclerosis', *New England Journal of Medicine*, 362: 387-401.

Keul, Petra, Markus Tölle, Susann Lucke, Karin von Wnuck Lipinski, Gerd Heusch, Mirjam Schuchardt, Markus van der Giet, and Bodo Levkau. 2007. 'The sphingosine-1-phosphate analogue FTY720 reduces atherosclerosis in apolipoprotein E–deficient mice', *Arteriosclerosis, thrombosis, and vascular biology*, 27: 607-13.

Kimura, Takao, Koichi Sato, Enkhzol Malchinkhuu, Hideaki Tomura, Kenichi Tamama, Atsushi Kuwabara, Masami Murakami, and Fumikazu Okajima. 2003. 'High-density lipoprotein stimulates endothelial cell migration and survival through sphingosine 1-phosphate and its receptors', *Arteriosclerosis, thrombosis, and vascular biology*, 23: 1283-88.

Kitano, T., S. Usui, S. I. Takashima, O. Inoue, C. Goten, A. Nomura, K. Yoshioka, M. Okajima, S. Kaneko, Y. Takuwa, and M. Takamura. 2019. 'Sphigosine-1-phosphate receptor 1 promotes neointimal hyperplasia in a mouse model of carotid artery injury', *Biochem Biophys Res Commun*, 511: 179-84.

Kluk, Michael J, Chantal Colmont, Ming-Tao Wu, and Timothy Hla. 2003. 'Platelet-derived growth factor (PDGF)-induced chemotaxis does not require the G

protein-coupled receptor S1P1 in murine embryonic fibroblasts and vascular smooth muscle cells', *FEBS letters*, 533: 25-28.

Liu, Yujing, Ryuichi Wada, Tadashi Yamashita, Yide Mi, Chu-Xia Deng, John P Hobson, Hans M Rosenfeldt, Victor E Nava, Sung-Suk Chae, and Menq-Jer Lee. 2000. 'Edg-1, the G protein–coupled receptor for sphingosine-1-phosphate, is essential for vascular maturation', *The Journal of clinical investigation*, 106: 951-61.

Luk, Fu Sang, Roy Y Kim, Kang Li, Daniel Ching, David K Wong, Sunil K Joshi, Isabella Imhof, Norman Honbo, Holly Hoover, and Bo-Qing Zhu. 2016. 'Immunosuppression with FTY720 Reverses Cardiac Dysfunction in Hypomorphic ApoE Mice Deficient in SR-BI Expression that Survive: Myocardial Infarction Caused by Coronary Atherosclerosis', *Journal of cardiovascular pharmacology*, 67: 47.

Mandala, Suzanne, Richard Hajdu, James Bergstrom, Elizabeth Quackenbush, Jenny Xie, James Milligan, Rosemary Thornton, Gan-Ju Shei, Deborah Card, and CarolAnn Keohane. 2002. 'Alteration of lymphocyte trafficking by sphingosine-1-phosphate receptor agonists', *Science*, 296: 346-49.

Matloubian, Mehrdad, Charles G Lo, Guy Cinamon, Matthew J Lesneski, Ying Xu, Volker Brinkmann, Maria L Allende, Richard L Proia, and Jason G Cyster. 2004. 'Lymphocyte egress from thymus and peripheral lymphoid organs is dependent on S1P receptor 1', *Nature*, 427: 355-60.

Mousseau, Yoanne, Séverine Mollard, Laurence Richard, Angélique Nizou, Karine Faucher-Durand, Jeanne Cook-Moreau, Hao Qiu, Yasser Baaj, Benoit Funalot, and Laurent Fourcade. 2012. 'Fingolimod inhibits PDGF-B-induced migration of vascular smooth muscle cell by down-regulating the S1PR1/S1PR3 pathway', *Biochimie*, 94: 2523-31.

Nofer, J. R., M. Bot, M. Brodde, P. J. Taylor, P. Salm, V. Brinkmann, T. van Berkel, G. Assmann, and E. A. Biessen. 2007a. 'FTY720, a synthetic sphingosine 1 phosphate analogue, inhibits development of atherosclerosis in low-density lipoprotein receptor-deficient mice', *Circulation*, 115: 501-8.

Nofer, Jerzy-Roch, Martine Bot, Martin Brodde, Paul J Taylor, Paul Salm, Volker Brinkmann, Theo van Berkel, Gerd Assmann, and Erik AL Biessen. 2007b. 'FTY720, a synthetic sphingosine 1 phosphate analogue, inhibits development of atherosclerosis in low-density lipoprotein receptor–deficient mice', *Circulation*, 115: 501-08.

O'Sullivan, Catherine, and Kumlesh K Dev. 2013. 'The structure and function of the S1P1 receptor', *Trends in pharmacological sciences*, 34: 401-12.

Pan, H., C. Xue, B. J. Auerbach, J. Fan, A. C. Bashore, J. Cui, D. Y. Yang, S. B. Trignano, W. Liu, J. Shi, C. O. Ihuegbu, E. C. Bush, J. Worley, L. Vlahos, P. Laise, R. A. Solomon, E. S. Connolly, A. Califano, P. A. Sims, H. Zhang, M. Li, and M. P. Reilly. 2020. 'Single-Cell Genomics Reveals a Novel Cell State During Smooth Muscle Cell Phenotypic Switching and Potential Therapeutic

Targets for Atherosclerosis in Mouse and Human', *Circulation*, 142: 2060-75.

Poti, Francesco, Sara Costa, Valeria Bergonzini, Margherita Galletti, Elisa Pignatti, Christian Weber, Manuela Simoni, and Jerzy-Roch Nofer. 2012. 'Effect of sphingosine 1-phosphate (S1P) receptor agonists FTY720 and CYM5442 on atherosclerosis development in LDL receptor deficient (LDL-R−/−) mice', *Vascular pharmacology*, 57: 56-64.

Potì, Francesco, Fabio Gualtieri, Sandro Sacchi, Gabriele Weißen-Plenz, Georg Varga, Martin Brodde, Christian Weber, Manuela Simoni, and Jerzy-Roch Nofer. 2013. 'KRP-203, sphingosine 1-phosphate receptor type 1 agonist, ameliorates atherosclerosis in LDL-R−/− mice', *Arteriosclerosis, thrombosis, and vascular biology*, 33: 1505-12.

Rong, James X, Mark Shapiro, Eugene Trogan, and Edward A Fisher. 2003. 'Transdifferentiation of mouse aortic smooth muscle cells to a macrophage-like state after cholesterol loading', *Proceedings of the National Academy of Sciences*, 100: 13531-36.

Rosenfeldt, Hans M, John P Hobson, Michael Maceyka, Ana Olivera, Victor E Nava, Sheldon Milstien, and Sarah Spiegel. 2001. 'EDG-1 links the PDGF receptor to Src and focal adhesion kinase activation leading to lamellipodia formation and cell migration', *The FASEB Journal*, 15: 2649-59.

Rosenfeldt, HM, JP Hobson, S Milstien, and S Spiegel. 2001. "The sphingosine-I-phosphate receptor EDG-I is essential for platelet-derived growth factor-induced cell motility." In.: Portland Press Ltd.

Ross, Russell. 1993. 'The pathogenesis of atherosclerosis: a perspective for the 1990s', *Nature*, 362: 801-09.

Sammani, Saad, Liliana Moreno-Vinasco, Tamara Mirzapoiazova, Patrick A Singleton, Eddie T Chiang, Carrie L Evenoski, Ting Wang, Biji Mathew, Aliya Husain, and Jaideep Moitra. 2010. 'Differential effects of sphingosine 1–phosphate receptors on airway and vascular barrier function in the murine lung', *American journal of respiratory cell and molecular biology*, 43: 394-402.

Shankman, Laura S, Delphine Gomez, Olga A Cherepanova, Morgan Salmon, Gabriel F Alencar, Ryan M Haskins, Pamela Swiatlowska, Alexandra AC Newman, Elizabeth S Greene, and Adam C Straub. 2015. 'KLF4-dependent phenotypic modulation of smooth muscle cells has a key role in atherosclerotic plaque pathogenesis', *Nature medicine*, 21: 628-37.

Shen, Mengcheng, Mei Hu, Paul WM Fedak, Gavin Y Oudit, and Zamaneh Kassiri. 2018. 'Cell-specific functions of ADAM17 regulate the progression of thoracic aortic aneurysm', *Circulation research*, 123: 372-88.

Sykes, David A, Darren M Riddy, Craig Stamp, Michelle E Bradley, Neil McGuiness, Afrah Sattikar, Danilo Guerini, Ines Rodrigues, Albrecht

Glaenzel, and Mark R Dowling. 2014. 'Investigating the molecular mechanisms through which FTY 720-P causes persistent S1P1 receptor internalization', *British journal of pharmacology*, 171: 4797-807.

Tabas, Ira. 2010. 'Macrophage death and defective inflammation resolution in atherosclerosis', *Nature Reviews Immunology*, 10: 36-46.

Tanimoto, Tatsuo, Andreea O Lungu, and Bradford C Berk. 2004. 'Sphingosine 1-phosphate transactivates the platelet-derived growth factor β receptor and epidermal growth factor receptor in vascular smooth muscle cells', *Circulation research*, 94: 1050-58.

Tarrasón, Gema, Mariona Aulí, Sanam Mustafa, Vladislav Dolgachev, Maria Teresa Domènech, Neus Prats, María Domínguez, Rosa López, Nuria Aguilar, and Marta Calbet. 2011. 'The sphingosine-1-phosphate receptor-1 antagonist, W146, causes early and short-lasting peripheral blood lymphopenia in mice', *International immunopharmacology*, 11: 1773-79.

Wamhoff, B. R., K. R. Lynch, T. L. Macdonald, and G. K. Owens. 2008. 'Sphingosine-1-phosphate receptor subtypes differentially regulate smooth muscle cell phenotype', *Arterioscler Thromb Vasc Biol*, 28: 1454-61.

Wang, Guanying, Roy Y Kim, Isabella Imhof, Norman Honbo, Fu Sang Luk, Kang Li, Nikit Kumar, Bo-Qing Zhu, Delphine Eberlé, and Daniel Ching. 2014. 'The immunosuppressant FTY720 prolongs survival in a mouse model of diet-

induced coronary atherosclerosis and myocardial infarction', *Journal of cardiovascular pharmacology*, 63: 132.

Wang, Ying, Joshua A Dubland, Sima Allahverdian, Enyinnaya Asonye, Basak Sahin, Jen Erh Jaw, Don D Sin, Michael A Seidman, Nicholas J Leeper, and Gordon A Francis. 2019. 'Smooth muscle cells contribute the majority of foam cells in ApoE (Apolipoprotein E)-deficient mouse atherosclerosis', *Arteriosclerosis, thrombosis, and vascular biology*, 39: 876-87.

Waters, Catherine M, Jaclyn Long, Irina Gorshkova, Yuko Fujiwara, Michelle Connell, Kristen E Belmonte, Gabor Tigyi, Viswanathan Natarajan, Susan Pyne, and Nigel J Pyne. 2006. 'Cell migration activated by platelet-derived growth factor receptor is blocked by an inverse agonist of the sphingosine 1-phosphate receptor-1', *The FASEB Journal*, 20: 509-11.

Waters, Catherine, Balwinder Sambi, Kok-Choi Kong, Dawn Thompson, Stuart M Pitson, Susan Pyne, and Nigel J Pyne. 2003. 'Sphingosine 1-phosphate and platelet-derived growth factor (PDGF) act via PDGFβ receptor-sphingosine 1-phosphate receptor complexes in airway smooth muscle cells', *Journal of Biological Chemistry*, 278: 6282-90.

Wei, Sindy H, Hugh Rosen, Melanie P Matheu, M Germana Sanna, Sheng-Kai Wang, Euijung Jo, Chi-Huey Wong, Ian Parker, and Michael D Cahalan. 2005. 'Sphingosine 1-phosphate type 1 receptor agonism inhibits

transendothelial migration of medullary T cells to lymphatic sinuses', *Nature immunology*, 6: 1228-35.

Wirka, R. C., D. Wagh, D. T. Paik, M. Pjanic, T. Nguyen, C. L. Miller, R. Kundu, M. Nagao, J. Coller, T. K. Koyano, R. Fong, Y. J. Woo, B. Liu, S. B. Montgomery, J. C. Wu, K. Zhu, R. Chang, M. Alamprese, M. D. Tallquist, J. B. Kim, and T. Quertermous. 2019. 'Atheroprotective roles of smooth muscle cell phenotypic modulation and the TCF21 disease gene as revealed by single-cell analysis', *Nat Med*, 25: 1280-89.

3.7 Supplementary Figures

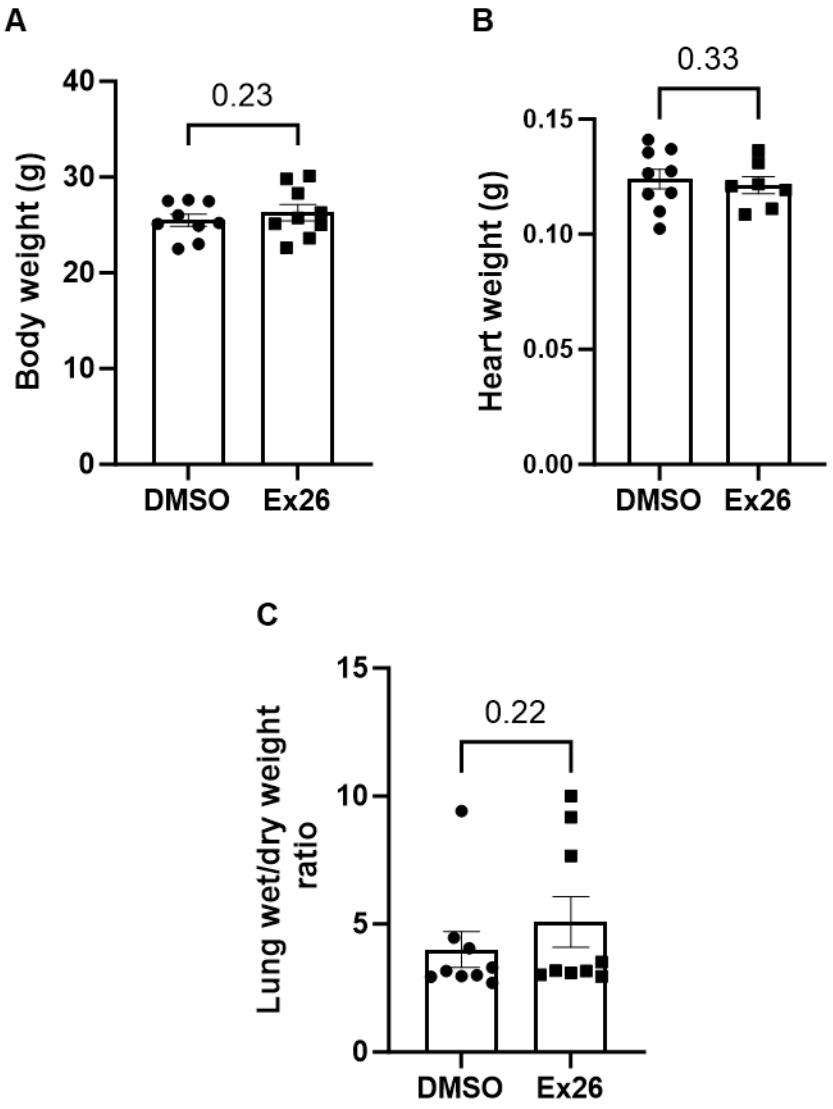

Supplementary Figure 3.8: Ex26 treatment did not affect body or heart weights and or induce pulmonary edema in *ApoE*$^{KO/KO}$ mice

A: Body weights; B: heart weights; C Lung wet/dry weights for female *ApoE* $^{KO/KO}$ mice treated with either Ex26 or DMSO vehicle and fed a HF diet for 6 weeks, beginning at 11 weeks of age. N=9 mice/group. Individual data points represent individual mice, bars represent averages and error bars represent standard errors of the mean. Statistical analyses were done using an unpaired *t*-test.

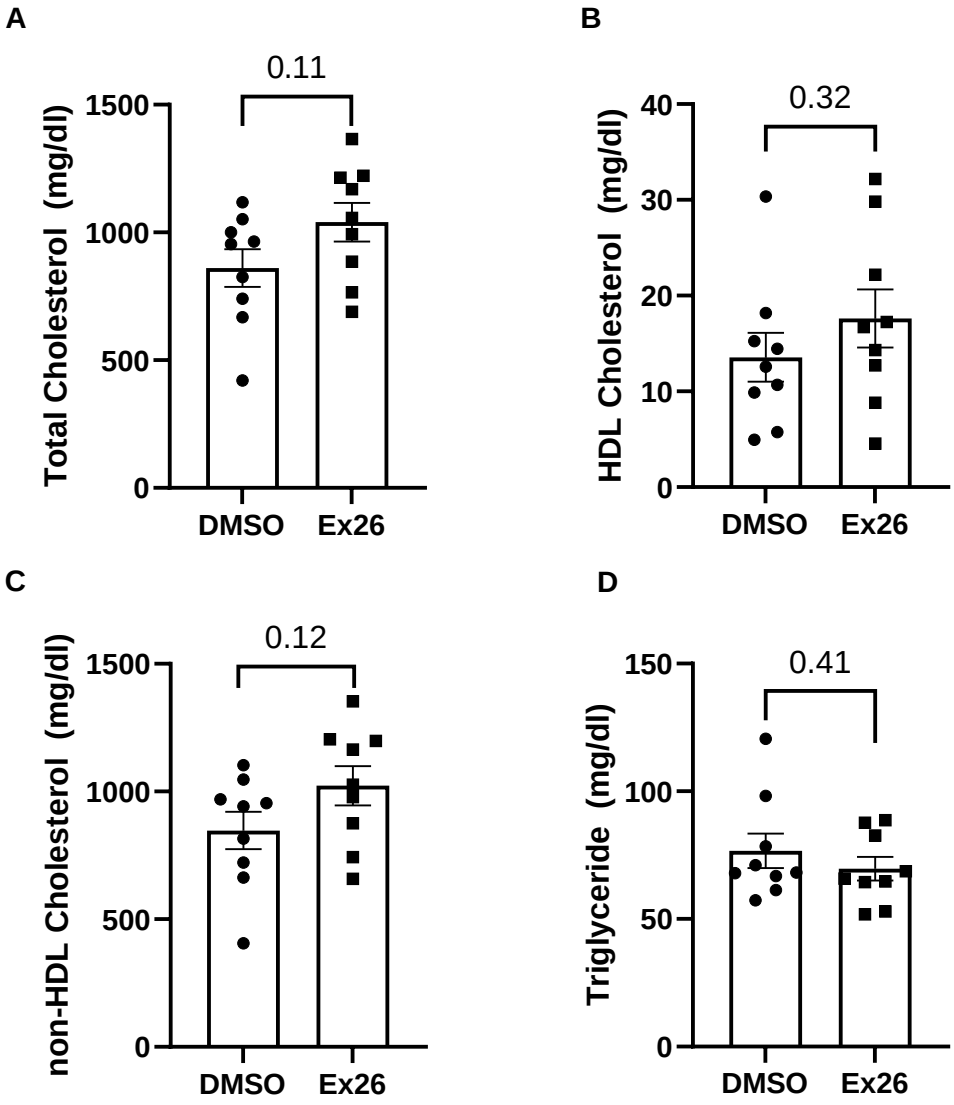

Supplementary Figure 3.9: Ex26 treatment does not impact plasma lipid levels in *ApoE*$^{KO/KO}$ mice

Plasma was collected from female *ApoE*$^{KO/KO}$ mice after 6 weeks of treatment with either DMSO or Ex26 and HF diet feeding. **(A)** total cholesterol, **(B)** HDL cholesterol, **(C)** non-HDL cholesterol (calculated as the difference between total- and HDL-cholesterol levels), and **(D)** triglyceride levels. Each symbol represents data from an individual mouse. Bars represent averages and error bars represent standard errors of the mean. Statistical analyses were done using an unpaired *t*-test.

Chapter 4: Discussion

4.1 Summary of Results in Chapter 2 and 3

This thesis examines the role of S1PR1 in arterial SMC in atherosclerotic plaque development. In Chapter 2, we unexpectedly observed partial suppression of *S1pr1* expression levels in select cell types, such as macrophages and VSMCs, in *S1pr1*-lox/lox mice compared to controls. In an attempt to understand whether the presence of the *S1pr1*-lox/lox allele alone affects atherosclerosis, we generated *S1pr1*-lox/lox mice on an apoE-deficient mice background. To our surprise, our data showed that the *S1pr1*-lox/lox mutation, in the absence of cre recombinase, significantly reduced atherosclerotic plaque development in apoE KO mice compared to controls. The plasma lipid levels were similar between $S1pr1^{lox/lox}$; $ApoE^{KO/KO}$ and $S1pr1^{WT/WT}$; $ApoE^{KO/KO}$ mice. In addition, performing reciprocal BMT in $ApoE^{KO/KO}$ mice in the presence or absence of *S1pr1*-lox/lox allele also demonstrated that the presence of *S1pr1*-lox/lox allele in non-BM derived tissues/cell types reduces atherosclerosis. In contrast, this mutation in BM-derived tissues/cell types did not alter plaque development in $ApoE^{KO/KO}$ mice. Interestingly, the presence of the *S1pr1*-lox/lox allele in both BM- and non-BM-derived cells also caused lymphocyte sequestration in the recipient mice compared to their counterparts that harbored the *S1pr1*-WT gene in all cell types. Previous studies reported that inactivating S1PR1 in endothelial cells and macrophages promotes lesion formation in atherogenic mouse models (Galvani et al. 2015; Gonzalez et al. 2017). Therefore, it is unlikely that the hypomorphic reduction of

S1pr1 expression in these cell types may result in atheroprotection in *S1pr1*$^{lox/lox}$*; ApoE*$^{KO/KO}$ mice. On the other hand, although the role of VSMC-specific S1PR1 on atherosclerosis is not examined before, the overexpression of S1PR1 under the control of SMA promoter had previously been shown to enhance pro-inflammatory cytokine expression and promote intimal thickening in a carotid artery ligation mouse model (Kitano et al. 2019). Hence, we suspected that the *S1pr1*-lox/lox allele in VSMC may contribute to reduced atherosclerosis in *S1pr1*$^{lox/lox}$*; ApoE*$^{KO/KO}$ mice.

In Chapter 2, we investigated the direct impact of deleting S1PR1 in VSMC on atherosclerosis. In this study, the *Tagln-cre*^{TG}*; S1pr1*$^{lox/lox}$*; ApoE*$^{KO/KO}$ (in which the *S1pr1* gene is inactivated under the control of SMC promoter Tagln) and *S1pr1*$^{lox/lox}$*; ApoE*$^{KO/KO}$ control littermates were fed an HFD for 8 weeks to measure aortic sinus-atherosclerotic plaque development. When S1PR1 was inactivated in VSMC of apoE-deficient mice, the lesions and Ki67+ cells (but not CD45+, Mac3+, and SMA+ cells) in atherosclerotic plaques were significantly reduced compared to controls. Plasma lipid levels and circulating leukocyte counts were similar between both groups. Furthermore, to identify how Tagln-cre-mediated S1PR1 deletion reduces atherosclerosis, we examined cell proliferation and phenotype switching in arterial SMCs isolated from *Tagln-cre*^{TG}*; S1pr1*$^{lox/lox}$*; ApoE*$^{KO/KO}$ mice, *S1pr1*$^{lox/lox}$*; ApoE*$^{KO/KO}$ mice, and *S1pr1*$^{WT/WT}$*; ApoE*$^{KO/KO}$ controls. We observed an incremental effect on proliferation and cholesterol accumulation when adding the *S1pr1*-WT/WT or *S1pr1*-lox/lox with/ without Tagln-cre allele (i.e, *S1pr1*$^{WT/WT}$*;*

ApoE$^{KO/KO}$ VSMCs > *S1pr1*$^{lox/lox}$; *ApoE*$^{KO/KO}$ VSMCs > *Tagln-cre*^{TG}; *S1pr1*$^{lox/lox}$; *ApoE*$^{KO/KO}$ VSMCs), when stimulated with SEW2871 (S1PR1 selective agonist). Together, our data demonstrated that knocking out S1PR1 in VSMC protects against the onset of atherosclerosis by reducing VSMC proliferation and phenotype switching.

In Chapter 3, we examined the effects of pharmacologically inhibiting S1PR1, using the selective S1PR1 antagonist Ex26, on HF-diet-induced atherosclerosis in *S1pr1*$^{WT/WT}$; *ApoE*$^{KO/KO}$ mice. Our results showed that Ex26 substantially reduced aortic sinus atherosclerosis and decreased CD45+ and Mac3+ cell content within the atherosclerotic plaques without causing pulmonary edema and affecting plasma lipid levels in these mice. Ex26 delivery caused lymphopenia but did not alter circulating myeloid cell levels in *S1pr1*$^{WT/WT}$; *ApoE*$^{KO/KO}$ mice. In addition, we also investigated the effects of Ex26 on diet-induced atherosclerosis in *Tagln-cre*^{TG}; *S1pr1*$^{lox/lox}$; *ApoE*$^{KO/KO}$ mice. We noticed that Ex26 failed to reduce atherosclerosis and decrease CD45+ and Mac3+ cell content within the atherosclerotic plaques when S1PR1 was deleted in VSMCs. Furthermore, to understand how Ex26 exerts its atheroprotective effects on VSMCs, we also measured cell proliferation (after stimulating them with SEW2871 and PDGF with/without EX26) and lipid loading (after stimulating them with SEW2871 and/or EX26 with/without cholesterol) in S1PR1-WT VSMCs. We observed that treatment with SEW2871 enhanced PDGF-mediated cell proliferation and cholesterol loading in VSMCs, however adding Ex26 to this

mixture reduced cell proliferation and cholesterol loading in VSMCs. Collectively, our results from Chapter 3 demonstrate that pharmacological inhibition of S1PR1 protects against atherosclerosis by mainly inhibiting S1PR1 in VSMCs.

4.2 Implications of results from chapter 2 and 3

4.2.1 Can the impact of *S1pr1*-lox/lox mutation on atherosclerosis be the effect of passenger gene effect?

The cre-lox system is a most powerful genetic tool that has been widely used to date to inactivate the target gene in specific tissues/cell types. Our study found that introducing the *S1pr1*-lox/lox allele alone, without cre recombinase, reduced *S1pr1* expression in select cell types and reduced aortic sinus atherosclerosis in an apoE-deficient background. Indeed, this protection against atherosclerosis in $S1pr1^{lox/lox}$; $ApoE^{KO/KO}$ mice is attributed primarily to the presence of the S1PR1-lox/lox allele in non-BM-derived tissues/cell types. These findings raise a critical question of whether the unexpected atheroprotection observed in $S1pr1^{lox/lox}$; $ApoE^{KO/KO}$ mice may be due to passenger genes. The passenger gene effect is a phenomenon whereby undesirable alleles concomitantly with mutant allele of interest are transferred from a donor to a recipient strain despite of backcrossing several times (Ackert-Bicknell and Rosen 2016). If the region flanking the selected locus is not removed by recombination, the flanking DNA (ie, the passenger gene) is expected to be retained in recipient strain even after several backcrosses (Lusis, Yu, and Wang 2007). Flaherty et al. (Flaherty 1981) previously reported that the probability

of passenger genes located 5 centimorgan genetic distance from the selected locus being retained is approx. 63% even after backcrossing 10 generations. There are several instances where a null mutation in certain genes that are well known to increase/decrease atherosclerosis had shown to yield opposite outcomes. For example, studies from three different laboratories that investigated the role of ATP Binding Cassette Subfamily G Member 1 (ABCG1) in atherosclerosis reported different atherogenic outcomes. The ABCG1 cholesterol transporter transports excess cholesterol from the cells to HDL, which subsequently carries it to the liver for bile secretion. Thus, ABCG1 inactivation in BM-derived macrophages is expected to increase plaque development. In one study, LDLR-deficient mice transplanted with ABCG1$^{-/-}$ BM donor cells developed moderately more atherosclerotic plaques (Out et al. 2006), whereas the other two studies that used the same procedure noticed a reduction in atherosclerosis (Baldán et al. 2006; Ranalletta et al. 2006). These discrepancies could likely arise due to differences in genetic background strains (Curtiss 2006; Lusis, Yu, and Wang 2007). Such passenger genetic variations could affect the phenotypes under study which may result in drawing misleading conclusions.

In our current study, pharmacologically inhibiting S1PR1 with Ex26 also substantially reduced atherosclerosis in apoE-deficient background; and this protection rendered by Ex26 was lost when S1PR1 was deleted in VSMCs of apoE KO mice. These results were in agreement with the reduced atherosclerosis noticed in *S1pr1*$^{lox/lox}$*; ApoE*$^{KO/KO}$ mice and *Tagln-cre*^{TG}*; S1pr1*$^{lox/lox}$*; ApoE*$^{KO/KO}$

mice. Thus, we suspect that the atheroprotective effects of *S1pr1*-lox/lox allele could likely arise from partial suppression of *S1pr1* expression in VSMC and not due to passenger genes. Indeed, there are several instances in which inserting loxP sites to the gene of interest, independent of cre recombinase, has been shown to reduce gene expression and sometimes lead to a severe hypomorphism in mouse models (Zisman et al. 2000; Abel et al. 2001; Dora et al. 2016; Jacks et al. 1994). This hypomorphic effect of the lox/lox allele could likely arise due to several factors, such as the retention of neo cassettes and the disruption of regulatory elements in the target gene flanked by loxP sites. Nevertheless, other alternative approaches could be used to validate our results and effectively address issues related to passenger genes in our studies. For instance, we could investigate if overexpression of S1PR1 in VSMC promotes diet-induced atherosclerosis in apoE KO mice. This complementary study will provide confirmation that the reduced atherosclerosis observed in *Tagln-cre^{TG}; S1pr1$^{lox/lox}$; ApoE$^{KO/KO}$* mice is not an artifact. In our lab, we have recently generated *Tagln-cre^{TG}; S1pr1$^{lox/stop/lox}$; ApoE$^{KO/KO}$* mice model. The *S1pr1*-lox/stop/lox mice carry a lox-poly(A)/STOP-loxP cassette upstream of *S1pr1* transgene knocked into the Rosa 26 locus. The loxP-poly(A)/STOP sequence prevents the transcription of the *S1pr1* gene, while overexpression of S1PR1 occurs following the Cre-mediated excision of the poly(A)/STOP sequence between the loxP sites. We could perform atherosclerosis studies in *Tagln-cre^{TG}; S1pr1$^{lox/stop/lox}$; ApoE$^{KO/KO}$* mice and *S1pr1$^{lox/stop/lox}$; ApoE$^{KO/KO}$* control mice. Interestingly, Ohkura et al. (Ohkura et al. 2017) generated

transgenic (Tg) mice that overexpressed S1PR1 under the control of the human α-smooth muscle actin promoter to study the effect of S1PR1 in fibroblasts for cardiac remodeling. Their data showed that Tg mice overexpressing S1PR1 had increased levels of angiotensin-converting enzyme and interleukin-6 further leading to cardiac hypertrophy. In our case, we suspect that the over-expression of S1PR1 in VSMCs may promote diet-induced atherosclerosis in apoE KO mice.

4.2.2 Tagln cre-mediated S1PR1 deletion and their effects on atherosclerosis

SMCs, critical components of the vascular wall, exhibit remarkable plasticity for their functional versatility. Although SMC phenotypic plasticity promotes wound healing and remodelling processes, the development of SMC-targeting cre driver lines identified their role in neointima formation, fibrous cap, and foam cell formation in the atherosclerotic plaques (Bennett, Sinha, and Owens 2016). In SMC-expressing cre driver lines, the cre recombinase is driven under the control of SMC differential marker genes, the most popular ones being SMA, Tagln, and MYH11 (Bennett, Sinha, and Owens 2016; Alexander and Owens 2012). However, one major challenge of expressing cre under the control of these promoters is that they are not only expressed by SMC lineage but are also expressed by other cell types (Chakraborty et al. 2019). In our present study, we used tagln-cre driver line to delete S1PR1 gene within SMCs. Tagln is an actin-binding protein that functions as an early indicator of SMC differentiation (Assinder, Stanton, and Prasad 2009). Despite being extensively used for gene deletion in SMCs, it's now acknowledged that the tagln promoter is also active in different non-SMC cell types, including

neutrophils, monocytes, and platelets (Chakraborty et al. 2019; Shen et al. 2012; Smith et al. 2013). Since Tagln-cre expression has been observed in some BM-derived cells, the reduced atherosclerosis that we noticed in *Tagln-cre^{TG}; S1pr1$^{lox/lox}$; ApoE$^{KO/KO}$* mice might possibly be the result of tagln-cre mediated S1PR1 deletion within the BM-derived cells. In order to rule out this possibility, we conducted BM transplantation in *Tagln-cre^{TG}; S1pr1$^{lox/lox}$; ApoE$^{KO/KO}$* and *S1pr1$^{lox/lox}$; ApoE$^{KO/KO}$* control mice with the BM donor cells from *S1pr1$^{WT/WT}$; ApoE$^{KO/KO}$* mice. Despite abolishing Tagln activity in BM-derived cells in both groups, *Tagln-cre^{TG}; S1pr1$^{lox/lox}$; ApoE$^{KO/KO}$* mice still exhibited a substantial reduction in atherosclerosis compared to *S1pr1$^{lox/lox}$; ApoE$^{KO/KO}$* mice. This data confirmed that the protective effects against atherosclerosis observed in *Tagln-cre^{TG}; S1pr1$^{lox/lox}$; ApoE$^{KO/KO}$* mice is attributed to tagln activity within the host cells. Previous studies have also noticed tagln expression in adipocytes and myofibroblasts (Ehler, Babiychuk, and Draeger 1996; Chang et al. 2012). This intricate expression pattern complicates the identification of whether the impact of tagln-cre mediated S1PR1 deletion stems from tagln activity in VSMC or from its expression in other non-SMCs.

Likewise, several studies that employed SMA-cre driver lines observed that cre activity is not confined solely to visceral and vascular SMC; it is also found in fibroblast, myofibroblast, myoepithelial cells, arterioles-associated pericytes, and cardiomyocytes (Wendling et al. 2009; Hill et al. 2015; Chakraborty et al. 2019). Among all SMC differentiation marker genes, MYH11 is so far considered to be the

most specific marker for the SMC lineage (Chakraborty et al. 2019). Several studies had previously employed tamoxifen-inducible MYH11-creER^{T2} transgenic mouse model to investigate the fate of SMCs in atherogenesis (Chappell et al. 2016; Shankman et al. 2015). One major drawback of using this model is that the MYH11-creER^{T2} transgene was originally inserted into the Y chromosome which confined the investigations to male mice only. Although this limitation has now been overcome by introducing the transgene into the X chromosome (Liao et al. 2017), making it inheritable by both the genders, this line was not commercially available when we begun our experiments. Thus, we opted for the tagln-cre driver line to delete S1PR1 in SMCs. Although MYH11 is widely accepted to be specific for SMC among all commercially available SMC-cre driver lines, some recent studies observed MYH11 expression in SMC-like cells, such as pericytes, in the lungs (Murgai et al. 2017; Sheikh, Lighthouse, and Greif 2014). This finding has led to question the true specificity of MYH11 for SMCs as well.

Another disadvantage of using the aforementioned SMC-cre driver lines is that they label both visceral and vascular SMCs (Chakraborty et al. 2019). Using these drivers to delete or over-express certain genes under the control of SMC promoters may result in unexpected phenotypes in nonvascular SMCs. This may result in unexpected complications in tissues/organs related to the respiratory, gastrointestinal, and urogenital systems. These issues may hinder our ability to accurately evaluate the influence of target genes specifically within the vasculature. Although tagln-cre mediated S1PR1 deletion in our study did not cause any visible

outcomes in visceral SMCs, inactivating this gene specifically in vascular SMCs will allow us to differentiate their role within arterial walls and uncover their contributions to atherosclerotic lesion development. Recently, Miano and colleagues generated an itga8-CreERT2 mouse model in which inducible cre is driven by an alpha 8 integrin (itga8) promoter (Miano, Fisher, and Majesky 2021). This model has been demonstrated to display preferential activity in VSMCs. Although they are not commercially available yet, leveraging cre under the control of promoters specific for VSMC will allow us to identify the particular role of VSMC S1PR1 in experimental atherosclerosis.

4.2.3 S1PR1 inhibition as a potential therapeutic strategy against atherosclerosis

Some studies reported that potent S1PR1 agonist FTY720 and selective S1PR1 agonist KRP20 reduced lesion formation in atherogenic mouse models (Keul et al. 2007; Potì et al. 2013; Nofer et al. 2007). However, these synthetic compounds act as both agonists and functional antagonists. Thus, it is unclear if these synthetic compounds provide atheroprotection by activating or inactivating this receptor. In our study, we directly tested the effects of S1PR1 selective antagonist Ex26 on diet-induced atherosclerosis. Our results demonstrated that pharmacologically inhibiting S1PR1 mediates protection against atherosclerotic plaque development in apoE-deficient mice.

Although the S1P-S1PR1 signaling axis appears to play similar roles across all cell types (such as promoting cell growth and migration), their consequences and implications for atherosclerosis appear to be distinct. For instance, the inactivation of S1PR1 specifically in endothelial cells and macrophages promoted lesion formation in murine atherosclerosis models (Galvani et al. 2015; Gonzalez et al. 2017). On the other hand, our data in this thesis demonstrated that S1PR1 deletion in arterial SMCs substantially reduced lesion formation in apoE KO mice. Indeed, pharmacological inhibition of S1PR1 with Ex26 also protected against atherosclerosis. However, this protection was completely lost when S1PR1 was deleted in VSMCs of apoE KO mice. Therefore, these results collectively suggest that knocking out S1PR1 in VSMC provides atheroprotection that outweighs the effect of inactivating S1PR1 in macrophage and endothelial cells that promotes atherosclerosis. Identifying a means to inhibit S1PR1 only in VSMCs, instead of all cell types, will prevent the adverse effects of antagonising S1PR1 in endothelial cells and macrophages.

Lymphocyte sequestration is a hallmark feature of any S1PR1 functional/selective antagonist (Cahalan et al. 2013; Potì et al. 2013; Nofer et al. 2007). In our studies, we also observed that Ex26 treatment significantly reduced circulating lymphocyte counts in apoE KO mice. Although our results strongly suggest that Ex26 mediates atheroprotection mainly by inhibiting S1PR1 in VSMCs, we cannot rule out the possibility that Ex26-mediated lymphocyte sequestration could at least partly account for this atheroprotection. One way to

test if the protection seen upon Ex26 treatment is independent of lymphocytes, is to deliver Ex26 to *ApoE*$^{KO/KO}$ mice that lacks recombination activating gene 1 (Rag1), a gene that's responsible for producing mature T- and B-cells. In general, Rag1/apoE DKO mice are usually smaller in size compared to apoE-deficient mice. Thus, it is technically difficult to implant bigger osmotic pumps into these mice directly. To avoid this technical issue, we could transplant the BM donor cells from Rag1/apoE DKO mice into apoE KO recipients at 8 weeks of age. After 4 weeks of recovery, the osmotic pumps carrying Ex26 (dosage of 0.1 mg/ kg/ hr) or DMSO (vehicle control) could be implanted subcutaneously for 6 weeks and also be fed an HFD over this time period. We suspect that Ex26 will still provide protection against atherosclerosis in the absence of Rag1 in the BM-derived cells of *ApoE*$^{KO/KO}$ mice. This speculation is based on our observation that the presence of S1PR1-lox/lox hypomorphic allele in BM-derived cells alone exhibited reduced circulating lymphocytes but failed to reduce atherosclerosis in *ApoE*$^{KO/KO}$ recipients compared to mice that harbors *S1pr1*-WT allele in their BM-derived cells. This prospective experiment will allow us to determine whether Ex26 can still reduce atherosclerosis, even when there are no B- and T-cells in circulation.

Although pharmacological treatment of S1PR1 selective agonists consistently reduced lymphocyte counts, their effect on atherosclerosis was contradictory. For instance, treatment with the selective agonist KRP-203 reduced lesion formation and lymphocyte count in LDLR KO mice (Potì et al. 2013). However, treatment with another selective agonist CYM5442 altered circulating

lymphocyte levels but failed to protect against atherosclerosis in LDLR KO mice (Poti et al. 2012). This suggests that lymphocyte sequestration itself does not appear to be sufficient to protect against atherosclerosis. In light of this, it is important to confirm if the atheroprotection induced by Ex26 is a general phenomenon. Therefore, testing the effects of other selective antagonists (such as W146) on atherosclerotic plaque development will help us identify whether pharmacological inhibition of S1PR1 could serve as a potential therapeutic strategy against atherosclerosis.

4.3 Limitations and Future Directions

The S1P-S1PR1 signaling axis regulates various cellular processes and is implicated in vascular disease pathogenesis. In particular, S1PR1 was observed to promote anti-atherogenic responses in endothelial cells and macrophages (Potì et al. 2013; Kimura et al. 2006; Galvani et al. 2015; Hughes et al. 2008; Al-Jarallah et al. 2014; Gonzalez et al. 2017). Inactivating S1PR1 in these cell types enhanced lesion formation in mouse models of atherosclerosis (Galvani et al. 2015; Gonzalez et al. 2017). However, our current study has demonstrated that S1PR1 signaling in arterial SMCs has the opposite effects, promoting atherosclerosis development. S1PR1 deletion in SMCs reduced atherosclerotic plaque development in apoE-deficient mice in response to a high fat, high cholesterol diet. A critical question raised by our study that has not yet been resolved is how S1P-S1PR1 signaling in SMCs differs from that in endothelial cells and macrophages. Physiologically, the

bioactive ligand S1P is predominantly transported by HDL in the circulation. Multiple studies have linked the atheroprotective abilities of HDL to its S1P cargo (Potì, Simoni, and Nofer 2014), and the atheroprotective effects of S1P appear to be dependent on its being carried by HDL. While S1PR1, S1PR2, and S1PR3 are found on all the cell types in the arterial wall, endothelial cells and macrophages predominantly express S1PR1 and S1PR3 whereas VSMC's mainly express S1PR2 and S1PR3, and express S1PR1 to lesser extent. Several studies have previously reported that HDL-bound S1P imparts its anti-atherogenic effects mainly through S1PR1 and S1PR3 in endothelial cells (Potì, Simoni, and Nofer 2014; Nofer et al. 2004; Kimura et al. 2006; Kimura et al. 2010). Similarly, HDL and S1P had been shown to exert atheroprotective effects in macrophages (Al-Jarallah et al. 2014; Gonzalez et al. 2017). On the other hand, the S1P cargo in HDL had been demonstrated to mediate atheroprotective effects in VSMC primarily via S1PR2 (Keul et al. 2019). Thus, it is highly probable that the impact of S1PR1 on atherogenesis may depend upon their abundance in these specific cell types. Another possible explanation for diverse atherosclerotic outcomes could arise from a particular receptor with which S1PR1 interacts. For instance, HDL signaling has been found to rely on S1PR1 and the HDL receptor SR-B1 in order to facilitate atheroprotective effects in endothelial cells and macrophages (Kimura et al. 2006; Al-Jarallah et al. 2014; Al-Jarallah and Trigatti 2010). Notably, a recent study from our lab showed that there is a complex formation between S1PR1 and SR-B1, both in cultured macrophages and within atherosclerotic plaques (Unpublished, Bassila

et al.). Also, this was shown by others in a cell culture model overexpressing SR-B1 and S1PR1 (Lee et al. 2017). Conversely, S1P associated with HDL has been demonstrated to govern inhibitory effects on PDGF-mediated migration via S1PR2 (Tamama et al. 2005). S1P signaling has been observed to promote proliferation and migration via S1PR1. Indeed, S1PR1 has been found to interact with PDGFR physically and functionally in VSMCs. This leads to two fascinating hypotheses: 1) HDL-bound S1P signaling may mediate anti-atherogenic effects in VSMCs through S1PR2 and SR-B1; 2) S1PR1 in VSMCs may interact with PDGFR, rather than SR-B1, to exert pro-atherogenic effects. But this remains to be demonstrated experimentally, that S1PR1 interacts with different receptors in different cell types (with SR-B1 in macrophages but with PDGFR in VSMC's) and that SR-B1 interaction with different S1P receptors in different cell types (S1PR1 in macrophages but S1PR2 in VSMC's) despite the receptors all being expressed. If this is the case, the mechanisms by which such a differential interaction occurs are unknown and remain to be explored. An in-depth understanding of how HDL-bound S1P signaling axis functions within VSMCs and the intricate interaction of S1PR1 with other receptors will open doors for new therapeutic opportunities tailored to specific cell populations.

While our studies have demonstrated that inhibiting S1PR1 in VSMC reduces atherosclerosis by decreasing proliferation and accumulation of lipids, the downstream signaling pathways through which S1PR1 mediates it's pro-atherogenic effect has not been investigated here. The role of S1PR1 in regulating

proliferation and migration has been well established. Several studies reported that S1PR1 works synergically with PDGF to promote SMC proliferation while others showcased the independent action of S1PR1 in enhancing proliferation (Kluk et al. 2003; Waters et al. 2003; Rosenfeldt et al. 2001). Both PDGFR-β and S1PR1 have been found to regulate proliferation and migration through distinct signaling pathways, notably the Ras-MAPK-ERK pathways and PI3K/AKT pathway (Nelson et al. 1998; Xiao et al. 2017; Tanimoto, Lungu, and Berk 2004). Since, in our studies, the isolated VSMCs from *Tagln-cre^{TG}; S1pr1$^{lox/lox}$; ApoE$^{KO/KO}$* mice exhibited reduced proliferation in response to both PDGF and SEW2871, it is conceivable that downstream signaling pathways such as Ras and PI3K pathways could be similarly affected. Importantly, our investigations have also revealed a novel role of S1PR1 in VSMC lipid droplet formation and phenotype switching. However, the manner in which S1PR1 facilitates lipid loading and SMC to macrophage-like cells transdifferentiation has not been examined in this thesis. Recent studies have identified kruppel-like factor 4 (KLF4), a zinc finger transcription factor, as a critical molecular switch governing the transdifferentiation of VSMC to macrophage-like cells and foam cell formation (Yang et al. 2021). KLF4 has been associated with the Ras/ERK and PI3K pathways either upstream or downstream, thereby exerting control over proliferation and differentiation in several cell types, including VSMCs (Zheng et al. 2009; Riverso, Montagnani, and Stecca 2017). Additionally, a recent study has identified B-cell lymphoma 2-associated transcription factor 1 (BCLAF1) as a potential regulator of cell survival

and SMC-to-macrophage-like cell transdifferentiation in human carotid SMCs (Rykaczewska et al. 2022). Hence, examining the expression levels of select genes in VSMCs *in-vitro* and within atherosclerotic plaques *in-vivo* from *Tagln-cre^{TG}; S1pr1$^{lox/lox}$; ApoE$^{KO/KO}$* mice will provide insights into the molecular mechanism by which S1PR1 regulates proliferation and SMC-to-macrophage-like cells transdifferentiation.

In this current study, we only examined the effects of S1PR1 antagonist Ex26 on lesion development in the aortic-sinus cross-sections of apoE-deficient mice. This may not necessarily reflect the effect of S1PR1 antagonism on atherosclerosis in other locations. Indeed, the key sites for atherosclerotic disease in humans are the coronary arteries. Plaque progression in coronary arteries eventually results in thrombotic events and myocardial infarctions. Mice deficient in apoE or LDLR do not develop clinically relevant plaques in the coronary arteries in response to HFD. Studies have reported that SR-B1 KO mice generated in apoE (KO or hypomorphic) or LDLR KO backgrounds develop coronary artery occlusions, myocardial infarctions, and cardiac dysfunction spontaneously or in response to atherogenic diets (Trigatti et al. 1999; Braun et al. 2002; Fuller et al. 2014; Zhang et al. 2005; Luk et al. 2016). Using these mouse models, we may be able to test the effects of pharmacologically inhibiting S1PR1 on myocardial coronary atherosclerosis in the future.

4.4 Conclusion

In summary, our data shows that S1PR1 plays a pro-atherogenic role in arterial SMCs (**Figure 4.1**). Our findings demonstrated that unanticipated suppression of S1PR1 caused due to the presence of *S1pr1*-lox/lox hypomorphic allele in non-BM derived cells, likely VSMC, provided protection against plaque development in apoE-deficient mice. Our research revealed that directly knocking out S1PR1 in SMC using a tagln-cre driver line, promotes anti-atherosclerosis potentially through reducing proliferation and SMC phenotype switching to macrophage-like cells. Additionally, we also showed that pharmacologically inhibiting S1PR1 using S1PR1 selective antagonist renders atheroprotection mainly by inhibiting S1PR1 in VSMCs *in-vivo*. Understanding how S1PR1 inhibition in arterial SMC mediates atheroprotection mechanistically will uncover novel therapeutic approaches to prevent atherosclerosis.

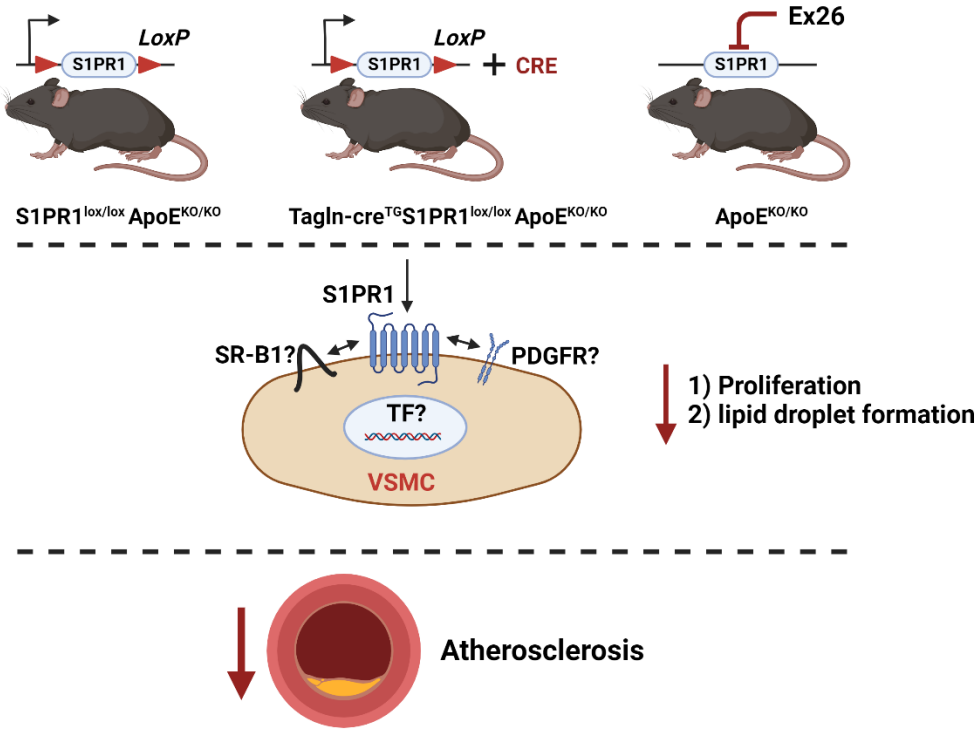

Figure 4.1: Schematic representation of the role of S1PR1 in VSMCs on atherosclerosis

Partial suppression of *S1pr1* caused by hypomorphic *S1pr1*$^{lox/lox}$ allele and inactivation of S1PR1 in VSMCs in apoE-deficient mice reduced cell proliferation and lipid droplet formation. This effect was consistently observed when S1PR1 was inhibited using S1PR1 antagonist Ex26 in cultured VSMCs. While it remains unresolved whether this effect of S1PR1 on proliferation or lipid droplet formation requires the activation of specific transcription factors (TF), such as KLF4 or BCLAF1, or their interaction with other receptors (such as PDGFR or SB-B1), it is evident that inactivating or pharmacologically inhibiting S1PR1 in VSMC renders protection against atherosclerotic plaque development in apoE-deficient mice.

4.5 References

Abel, E Dale, Odile Peroni, Jason K Kim, Young-Bum Kim, Olivier Boss, Ed Hadro, Timo Minnemann, Gerald I Shulman, and Barbara B Kahn. 2001. 'Adipose-selective targeting of the GLUT4 gene impairs insulin action in muscle and liver', *Nature*, 409: 729-33.

Ackert-Bicknell, Cheryl L, and Clifford J Rosen. 2016. 'Passenger gene mutations: unwanted guests in genetically modified mice', *Journal of bone and mineral research: the official journal of the American Society for Bone and Mineral Research*, 31: 270.

Al-Jarallah, Aishah, Xing Chen, Leticia Gonzalez, and Bernardo L Trigatti. 2014. 'High density lipoprotein stimulated migration of macrophages depends on the scavenger receptor class B, type I, PDZK1 and Akt1 and is blocked by sphingosine 1 phosphate receptor antagonists', *PloS one*, 9: e106487.

Al-Jarallah, Aishah, and Bernardo L Trigatti. 2010. 'A role for the scavenger receptor, class B type I in high density lipoprotein dependent activation of cellular signaling pathways', *Biochimica et Biophysica Acta (BBA)-Molecular and Cell Biology of Lipids*, 1801: 1239-48.

Alexander, Matthew R, and Gary K Owens. 2012. 'Epigenetic control of smooth muscle cell differentiation and phenotypic switching in vascular development and disease', *Annual review of physiology*, 74: 13-40.

Assinder, Stephen J, Jo-Ann L Stanton, and Priya D Prasad. 2009. 'Transgelin: an actin-binding protein and tumour suppressor', *The international journal of biochemistry & cell biology*, 41: 482-86.

Baldán, Angel, Liming Pei, Richard Lee, Paul Tarr, Rajendra K Tangirala, Michael M Weinstein, Joy Frank, Andrew C Li, Peter Tontonoz, and Peter A Edwards. 2006. 'Impaired development of atherosclerosis in hyperlipidemic Ldlr−/− and ApoE−/− mice transplanted with Abcg1−/− bone marrow', *Arteriosclerosis, thrombosis, and vascular biology*, 26: 2301-07.

Bennett, M. R., S. Sinha, and G. K. Owens. 2016. 'Vascular Smooth Muscle Cells in Atherosclerosis', *Circ Res*, 118: 692-702.

Braun, Anne, Bernardo L Trigatti, Mark J Post, Kaori Sato, Michael Simons, Jay M Edelberg, Robert D Rosenberg, Mark Schrenzel, and Monty Krieger. 2002. 'Loss of SR-BI expression leads to the early onset of occlusive atherosclerotic coronary artery disease, spontaneous myocardial infarctions, severe cardiac dysfunction, and premature death in apolipoprotein E–deficient mice', *Circulation research*, 90: 270-76.

Cahalan, Stuart M, Pedro J Gonzalez-Cabrera, Nhan Nguyen, Miguel Guerrero, Elizabeth A George Cisar, Nora B Leaf, Steven J Brown, Edward Roberts, and Hugh Rosen. 2013. 'Sphingosine 1-phosphate receptor 1 (S1P1) upregulation and amelioration of experimental autoimmune encephalomyelitis by an S1P1 antagonist', *Molecular Pharmacology*, 83: 316-21.

Chakraborty, Raja, Fatima Zahra Saddouk, Ana Catarina Carrao, Diane S Krause, Daniel M Greif, and Kathleen A Martin. 2019. 'Promoters to study vascular smooth muscle: mistaken identity?', *Arteriosclerosis, thrombosis, and vascular biology*, 39: 603-12.

Chang, Lin, Luis Villacorta, Rongxia Li, Milton Hamblin, Wei Xu, Chunyan Dou, Jifeng Zhang, Jiarui Wu, Rong Zeng, and Y Eugene Chen. 2012. 'Loss of perivascular adipose tissue on peroxisome proliferator–activated receptor-γ deletion in smooth muscle cells impairs intravascular thermoregulation and enhances atherosclerosis', *Circulation*, 126: 1067-78.

Chappell, Joel, Jennifer L Harman, Vagheesh M Narasimhan, Haixiang Yu, Kirsty Foote, Benjamin D Simons, Martin R Bennett, and Helle F Jørgensen. 2016. 'Extensive proliferation of a subset of differentiated, yet plastic, medial vascular smooth muscle cells contributes to neointimal formation in mouse injury and atherosclerosis models', *Circulation research*, 119: 1313-23.

Curtiss, Linda K. 2006. "Is two out of three enough for ABCG1?" In, 2175-77. Am Heart Assoc.

Dora, Natalie J, Aaron JF Crookshanks, Karen KY Leung, T Ian Simpson, John O Mason, David J Price, and John D West. 2016. 'Analysis of compound heterozygotes reveals that the mouse floxed Pax6 tm1Ued allele produces abnormal eye phenotypes', *Transgenic research*, 25: 679-92.

Ehler, Elisabeth, Eduard Babiychuk, and Annette Draeger. 1996. 'Human foetal lung (IMR-90) cells: Myofibroblasts with smooth muscle-like contractile properties', *Cell motility and the cytoskeleton*, 34: 288-98.

Flaherty, Lorraine. 1981. 'Congenic strains', *The mouse in biomedical research*, 1: 215-21.

Fuller, Mark, Omid Dadoo, Viktoria Serkis, Dina Abutouk, Melissa MacDonald, Neel Dhingani, Joseph Macri, Suleiman A Igdoura, and Bernardo L Trigatti. 2014. 'The effects of diet on occlusive coronary artery atherosclerosis and myocardial infarction in scavenger receptor class B, type 1/low-density lipoprotein receptor double knockout mice', *Arteriosclerosis, thrombosis, and vascular biology*, 34: 2394-403.

Galvani, Sylvain, Marie Sanson, Victoria A Blaho, Steven L Swendeman, Hideru Obinata, Heather Conger, Björn Dahlbäck, Mari Kono, Richard L Proia, and Jonathan D Smith. 2015. 'HDL-bound sphingosine 1-phosphate acts as a biased agonist for the endothelial cell receptor S1P1 to limit vascular inflammation', *Science signaling*, 8: ra79-ra79.

Gonzalez, Leticia, Alexander S Qian, Usama Tahir, Pei Yu, and Bernardo L Trigatti. 2017. 'Sphingosine-1-phosphate receptor 1, expressed in myeloid cells, slows diet-induced atherosclerosis and protects against macrophage apoptosis in ldlr KO mice', *International Journal of Molecular Sciences*, 18: 2721.

Hill, Robert A, Lei Tong, Peng Yuan, Sasidhar Murikinati, Shobhana Gupta, and Jaime Grutzendler. 2015. 'Regional blood flow in the normal and ischemic brain is controlled by arteriolar smooth muscle cell contractility and not by capillary pericytes', *Neuron*, 87: 95-110.

Hughes, Jeniter E, Suseela Srinivasan, Kevin R Lynch, Richard L Proia, Pawel Ferdek, and Catherine C Hedrick. 2008. 'Sphingosine-1-phosphate induces an antiinflammatory phenotype in macrophages', *Circulation research*, 102: 950-58.

Jacks, Tyler, T Shane Shih, Earlene M Schmitt, Roderick T Bronson, Andre Bernards, and Robert A Weinberg. 1994. 'Tumour predisposition in mice heterozygous for a targeted mutation in Nf1', *Nature genetics*, 7: 353-61.

Keul, P., A. Polzin, K. Kaiser, M. Graler, L. Dannenberg, G. Daum, G. Heusch, and B. Levkau. 2019. 'Potent anti-inflammatory properties of HDL in vascular smooth muscle cells mediated by HDL-S1P and their impairment in coronary artery disease due to lower HDL-S1P: a new aspect of HDL dysfunction and its therapy', *FASEB J*, 33: 1482-95.

Keul, Petra, Markus Tölle, Susann Lucke, Karin von Wnuck Lipinski, Gerd Heusch, Mirjam Schuchardt, Markus van der Giet, and Bodo Levkau. 2007. 'The sphingosine-1-phosphate analogue FTY720 reduces atherosclerosis in apolipoprotein E–deficient mice', *Arteriosclerosis, thrombosis, and vascular biology*, 27: 607-13.

Kimura, Takao, Hideaki Tomura, Chihiro Mogi, Atsushi Kuwabara, Alatangaole Damirin, Tamotsu Ishizuka, Akihiro Sekiguchi, Mitsuteru Ishiwara, Doon-Soon Im, and Koichi Sato. 2006. 'Role of scavenger receptor class B type I and sphingosine 1-phosphate receptors in high density lipoprotein-induced inhibition of adhesion molecule expression in endothelial cells', *Journal of Biological Chemistry*, 281: 37457-67.

Kimura, Takao, Hideaki Tomura, Koichi Sato, Masaaki Ito, Isao Matsuoka, Doon-Soon Im, Atsushi Kuwabara, Chihiro Mogi, Hiroshi Itoh, and Hitoshi Kurose. 2010. 'Mechanism and role of high density lipoprotein-induced activation of AMP-activated protein kinase in endothelial cells', *Journal of Biological Chemistry*, 285: 4387-97.

Kitano, T., S. Usui, S. I. Takashima, O. Inoue, C. Goten, A. Nomura, K. Yoshioka, M. Okajima, S. Kaneko, Y. Takuwa, and M. Takamura. 2019. 'Sphigosine-1-phosphate receptor 1 promotes neointimal hyperplasia in a mouse model of carotid artery injury', *Biochem Biophys Res Commun*, 511: 179-84.

Kluk, Michael J, Chantal Colmont, Ming-Tao Wu, and Timothy Hla. 2003. 'Platelet-derived growth factor (PDGF)-induced chemotaxis does not require the G protein-coupled receptor S1P1 in murine embryonic fibroblasts and vascular smooth muscle cells', *FEBS letters*, 533: 25-28.

Lee, M. H., K. M. Appleton, H. M. El-Shewy, M. G. Sorci-Thomas, M. J. Thomas, M. F. Lopes-Virella, L. M. Luttrell, S. M. Hammad, and R. L. Klein. 2017. 'S1P in HDL promotes interaction between SR-BI and S1PR1 and activates

S1PR1-mediated biological functions: calcium flux and S1PR1 internalization', *J Lipid Res*, 58: 325-38.

Liao, Mingmei, Junmei Zhou, Fen Wang, Yasmin H Ali, Kelvin L Chan, Fei Zou, Stefan Offermanns, Zhisheng Jiang, and Zhihua Jiang. 2017. 'An X-linked Myh11-CreERT2 mouse line resulting from Y to X chromosome-translocation of the Cre allele', *genesis*, 55: e23054.

Luk, Fu Sang, Roy Y Kim, Kang Li, Daniel Ching, David K Wong, Sunil K Joshi, Isabella Imhof, Norman Honbo, Holly Hoover, and Bo-Qing Zhu. 2016. 'Immunosuppression with FTY720 Reverses Cardiac Dysfunction in Hypomorphic ApoE Mice Deficient in SR-BI Expression that Survive: Myocardial Infarction Caused by Coronary Atherosclerosis', *Journal of cardiovascular pharmacology*, 67: 47.

Lusis, Aldons J, Janet Yu, and Susanna S Wang. 2007. 'The problem of passenger genes in transgenic mice', *Arteriosclerosis, thrombosis, and vascular biology*, 27: 2100-03.

Miano, J. M., E. A. Fisher, and M. W. Majesky. 2021. 'Fate and State of Vascular Smooth Muscle Cells in Atherosclerosis', *Circulation*, 143: 2110-16.

Murgai, Meera, Wei Ju, Matthew Eason, Jessica Kline, Daniel W Beury, Sabina Kaczanowska, Markku M Miettinen, Michael Kruhlak, Haiyan Lei, and Jack F Shern. 2017. 'KLF4-dependent perivascular cell plasticity mediates pre-metastatic niche formation and metastasis', *Nature medicine*, 23: 1176-90.

Nelson, Peter R, Shinji Yamamura, Leila Mureebe, Hiroyuki Itoh, and K Craig Kent. 1998. 'Smooth muscle cell migration and proliferation are mediated by distinct phases of activation of the intracellular messenger mitogen-activated protein kinase', *Journal of vascular surgery*, 27: 117-25.

Nofer, J. R., M. Bot, M. Brodde, P. J. Taylor, P. Salm, V. Brinkmann, T. van Berkel, G. Assmann, and E. A. Biessen. 2007. 'FTY720, a synthetic sphingosine 1 phosphate analogue, inhibits development of atherosclerosis in low-density lipoprotein receptor-deficient mice', *Circulation*, 115: 501-8.

Nofer, Jerzy-Roch, Markus Van Der Giet, Markus Tölle, Iza Wolinska, Karin von Wnuck Lipinski, Hideo A Baba, Uwe J Tietge, Axel Gödecke, Isao Ishii, and Burkhard Kleuser. 2004. 'HDL induces NO-dependent vasorelaxation via the lysophospholipid receptor S1P 3', *The Journal of clinical investigation*, 113: 569-81.

Ohkura, Sei-ichiro, Soichiro Usui, Shin-ichiro Takashima, Noriko Takuwa, Kazuaki Yoshioka, Yasuo Okamoto, Yutaka Inagaki, Naotoshi Sugimoto, Teppei Kitano, and Masayuki Takamura. 2017. 'Augmented sphingosine 1 phosphate receptor-1 signaling in cardiac fibroblasts induces cardiac hypertrophy and fibrosis through angiotensin II and interleukin-6', *PloS one*, 12: e0182329.

Out, Ruud, Menno Hoekstra, Reeni B Hildebrand, Janine K Kruit, Illiana Meurs, Zhaosha Li, Folkert Kuipers, Theo JC Van Berkel, and Miranda Van Eck. 2006. 'Macrophage ABCG1 deletion disrupts lipid homeostasis in alveolar

macrophages and moderately influences atherosclerotic lesion development in LDL receptor-deficient mice', *Arteriosclerosis, thrombosis, and vascular biology*, 26: 2295-300.

Poti, Francesco, Sara Costa, Valeria Bergonzini, Margherita Galletti, Elisa Pignatti, Christian Weber, Manuela Simoni, and Jerzy-Roch Nofer. 2012. 'Effect of sphingosine 1-phosphate (S1P) receptor agonists FTY720 and CYM5442 on atherosclerosis development in LDL receptor deficient (LDL-R−/−) mice', *Vascular pharmacology*, 57: 56-64.

Potì, Francesco, Fabio Gualtieri, Sandro Sacchi, Gabriele Weißen-Plenz, Georg Varga, Martin Brodde, Christian Weber, Manuela Simoni, and Jerzy-Roch Nofer. 2013. 'KRP-203, sphingosine 1-phosphate receptor type 1 agonist, ameliorates atherosclerosis in LDL-R−/− mice', *Arteriosclerosis, thrombosis, and vascular biology*, 33: 1505-12.

Potì, Francesco, Manuela Simoni, and Jerzy-Roch Nofer. 2014. 'Atheroprotective role of high-density lipoprotein (HDL)-associated sphingosine-1-phosphate (S1P)', *Cardiovascular research*, 103: 395-404.

Ranalletta, Mollie, Nan Wang, Seongah Han, Laurent Yvan-Charvet, Carrie Welch, and Alan R Tall. 2006. 'Decreased atherosclerosis in low-density lipoprotein receptor knockout mice transplanted with Abcg1−/− bone marrow', *Arteriosclerosis, thrombosis, and vascular biology*, 26: 2308-15.

Riverso, M, V Montagnani, and B Stecca. 2017. 'KLF4 is regulated by RAS/RAF/MEK/ERK signaling through E2F1 and promotes melanoma cell growth', *Oncogene*, 36: 3322-33.

Rosenfeldt, Hans M, John P Hobson, Michael Maceyka, Ana Olivera, Victor E Nava, Sheldon Milstien, and Sarah Spiegel. 2001. 'EDG-1 links the PDGF receptor to Src and focal adhesion kinase activation leading to lamellipodia formation and cell migration', *The FASEB Journal*, 15: 2649-59.

Rykaczewska, Urszula, Quanyi Zhao, Peter Saliba-Gustafsson, Mariette Lengquist, Malin Kronqvist, Otto Bergman, Zhiqiang Huang, Kent Lund, Katarina Waden, and Zara Pons Vila. 2022. 'Plaque evaluation by ultrasound and transcriptomics reveals BCLAF1 as a regulator of smooth muscle cell lipid transdifferentiation in atherosclerosis', *Arteriosclerosis, thrombosis, and vascular biology*, 42: 659-76.

Shankman, Laura S, Delphine Gomez, Olga A Cherepanova, Morgan Salmon, Gabriel F Alencar, Ryan M Haskins, Pamela Swiatlowska, Alexandra AC Newman, Elizabeth S Greene, and Adam C Straub. 2015. 'KLF4-dependent phenotypic modulation of smooth muscle cells has a key role in atherosclerotic plaque pathogenesis', *Nature medicine*, 21: 628-37.

Sheikh, Abdul Q, Janet K Lighthouse, and Daniel M Greif. 2014. 'Recapitulation of developing artery muscularization in pulmonary hypertension', *Cell reports*, 6: 809-17.

Shen, Zhuxia, Chao Li, Ryan A Frieler, Alena S Gerasimova, Soo Jung Lee, Jing Wu, Michael M Wang, Carey N Lumeng, Frank C Brosius III, and Sheng Zhong Duan. 2012. 'Smooth muscle protein 22 alpha-Cre is expressed in myeloid cells in mice', *Biochemical and Biophysical Research Communications*, 422: 639-42.

Smith, Elenoe C, Alexandra M Teixeira, Rachel C Chen, Lin Wang, Yuan Gao, Katherine L Hahn, and Diane S Krause. 2013. 'Induction of megakaryocyte differentiation drives nuclear accumulation and transcriptional function of MKL1 via actin polymerization and RhoA activation', *Blood, The Journal of the American Society of Hematology*, 121: 1094-101.

Tamama, K., H. Tomura, K. Sato, E. Malchinkhuu, A. Damirin, T. Kimura, A. Kuwabara, M. Murakami, and F. Okajima. 2005. 'High-density lipoprotein inhibits migration of vascular smooth muscle cells through its sphingosine 1-phosphate component', *Atherosclerosis*, 178: 19-23.

Tanimoto, Tatsuo, Andreea O Lungu, and Bradford C Berk. 2004. 'Sphingosine 1-phosphate transactivates the platelet-derived growth factor β receptor and epidermal growth factor receptor in vascular smooth muscle cells', *Circulation research*, 94: 1050-58.

Trigatti, Bernardo, Helen Rayburn, Marisa Viñals, Anne Braun, Helena Miettinen, Marsha Penman, Miki Hertz, Mark Schrenzel, Ludwig Amigo, and Attilio Rigotti. 1999. 'Influence of the high density lipoprotein receptor SR-BI on

reproductive and cardiovascular pathophysiology', *Proceedings of the National Academy of Sciences*, 96: 9322-27.

Waters, C., B. Sambi, K. C. Kong, D. Thompson, S. M. Pitson, S. Pyne, and N. J. Pyne. 2003. 'Sphingosine 1-phosphate and platelet-derived growth factor (PDGF) act via PDGF beta receptor-sphingosine 1-phosphate receptor complexes in airway smooth muscle cells', *J Biol Chem*, 278: 6282-90.

Wendling, Olivia, Jean-Marc Bornert, Pierre Chambon, and Daniel Metzger. 2009. 'Efficient temporally-controlled targeted mutagenesis in smooth muscle cells of the adult mouse', *genesis*, 47: 14-18.

Xiao, Yunbin, Hongyan Peng, Chenliang Hong, Zhi Chen, Xicheng Deng, Aiping Wang, Fang Yang, Li Yang, Chen Chen, and Xuping Qin. 2017. 'PDGF promotes the warburg effect in pulmonary arterial smooth muscle cells via activation of the PI3K/AKT/mTOR/HIF-1α signaling pathway', *Cellular Physiology and Biochemistry*, 42: 1603-13.

Yang, Chen, Xuan Xiao, Liang Huang, Fan Zhou, Lin-hui Chen, Yu-Yan Zhao, Shun-Lin Qu, and Chi Zhang. 2021. 'Role of Kruppel-like factor 4 in atherosclerosis', *Clinica chimica acta*, 512: 135-41.

Zhang, Songwen, Michael H Picard, Eliza Vasile, Yu Zhu, Robert L Raffai, Karl H Weisgraber, and Monty Krieger. 2005. 'Diet-induced occlusive coronary atherosclerosis, myocardial infarction, cardiac dysfunction, and premature death in scavenger receptor class B type I-deficient, hypomorphic apolipoprotein ER61 mice', *Circulation*, 111: 3457-64.

Zheng, Bin, Mei Han, Michel Bernier, Xin-hua Zhang, Fang Meng, Sui-bing Miao, Ming He, Xin-ming Zhao, and Jin-kun Wen. 2009. 'Krüppel-like factor 4 inhibits proliferation by platelet-derived growth factor receptor β-mediated, not by retinoic acid receptor α-mediated, phosphatidylinositol 3-kinase and ERK signaling in vascular smooth muscle cells', *Journal of Biological Chemistry*, 284: 22773-85.

Zisman, Ariel, Odile D Peroni, E Dale Abel, M Dodson Michael, Franck Mauvais-Jarvis, Bradford B Lowell, Jørgen FP Wojtaszewski, Michael F Hirshman, Antti Virkamaki, and Laurie J Goodyear. 2000. 'Targeted disruption of the glucose transporter 4 selectively in muscle causes insulin resistance and glucose intolerance', *Nature medicine*, 6: 924-28.

Major Resources Table

Animals (in vivo studies)

Species	Vendor or Source	Background Strain	Sex	Persistent ID / URL
C57BL/6J	Bred in house from founders from Jackson labs	C57BL/6J	Male and Female	
S1PR1$^{lox/lox}$	Gift from Dr. Richard L. Proia	C57BL/6J	Male and Female	
ApoE$^{KO/KO}$	Bred in house from founders from Jackson labs	C57BL/6J	Male and Female	
S1PR1$^{lox/lox}$ ApoE$^{KO/KO}$	Generated in lab from founders from Dr. Proia's lab and Jackson labs	C57BL/6J	Male and Female	
LysM$^{cre/cre}$ ApoE$^{KO/KO}$	Generated in lab from founders from Jackson Labs	C57BL/6J	Male and Female	
LysM$^{cre/cre}$ S1PR1$^{lox/lox}$ ApoE$^{KO/KO}$	Generated in lab from founders from Dr. Proia's lab and Jackson labs	C57BL/6J	Male and Female	
Tagln-cre^{TG} S1PR1$^{lox/lox}$ ApoE$^{KO/KO}$	Generated in lab from founders from Dr. Proia's lab and Jackson labs	C57BL/6J	Male and Female	

Genotyping Primers

Gene	Primer Name	Primer Design (5'→3')	Product size (bp)
LysM	oIMR3068 oIMR3067 oIMR3066	TTA CAG TCG GCC AGG CTG AC CTT GGG CTG CCA GAA CTC CCC AGA AAT GCC AGA TTA CG	WT: 350 bp MUT: 700 bp
S1PR1	Lox1 Lox3	GAG CGG AGG AAG TTA AAA CCT CCT AAG AGA TTG CAG CAA	WT: 200 bp MUT: 250 bp
Tagln	oIMR1084 oIMR1085 oIMR7338	GCG GTC TGG CAG TAA AAA CTA TC GTG AAA CAG CAT TGC TGT CAC TT	WT: 324 bp MUT: 100 bp

	oIMR7339	CTA GGC CAC AGA ATT GAA AGA TCT GTA GGT GGA AAT TCT AGC ATC ATC C	
ApoE	oIMR0180 oIMR0181 oIMR0182	GCC TAG CCG AGG GAG AGC CG TGT GAC TTG GGA GCT CTG CAG C GCC GCC CCG ACT GCA TCT	WT: 155 bp MUT: 245 bp

RT-PCR primers

Gene	**Primer Design (5'→3')**	**NCBI Ref number**
S1PR1	Fwd-5' -ACT TTG CGA GTG AGC TG-3' Rev-5' -AGT GAG CCT TCA GTT ACA GC-3'	NM_007901.5
S1PR2	Fwd-5' -TTC TGG AGG GTA ACA CAG TGG T-3' Rev-5' -ACA CCC TTT GTA TCA AGT GGC A-3'	NM_010333.4
S1PR3	Fwd-5' -TGG TGT GCG GCT GTC TAG TCA A-3' Rev-5' -CAC AGC AAG CAG ACC TCC AGA-3'	NM_010101.4
CD68	Fwd-5' -ACTTCGGGCCATGTTTCTCT-3' Rev-5' –GCTGGTAGGTTGATTGTCGT-3'	NM 001291058.1
α-SMA	Fwd-5' -CAGGCATGGATGGCATCAATCAC-3' Rev-5' -ACTCTAGCTGTGAAGTCAGTGTCG-3'	NM007392
GAPDH	Fwd-5' -ACCACAGTCCATGCCATCAC -3' Rev-5' -TCCACCACCCTGTTGCTGTA -3'	NM_001289726.1

Antibodies

Target antigen	Vendor or Source	Catalog #	Working concentration	Lot # (preferred but not required)	Persistent ID / URL
FITC CD3	BD Biosciences	555274	5 µg/ml	Various	https://www.bdbiosciences.com/en-ca/products/reagents/flow-cytometry-reagents/research-reagents/single-color-antibodies-ruo/fitc-rat-anti-mouse-cd3-molecular-complex.555274
BV510 CD45	Biolegend	103138	2 µg/ml	Various	https://www.biolegend.com/en-us/products/brilliant-violet-510-anti-mouse-cd45-antibody-7995
PerCP-Cyanine5.5 CD45R (B220)	eBioscience	45-0452-80	2 µg/ml	Various	https://www.thermofisher.com/antibody/product/CD45R-B220-Antibody-clone-RA3-6B2-Monoclonal/45-0452-80
PE CD11b (M1/70.15)	eBioscience	12-0112-82	4 µg/ml	Various	https://www.thermofisher.com/antibody/product/CD11b-Antibody-clone-M1-70-Monoclonal/12-0112-82
PE-Cy7 Ly6C	Biolegend	128018	4 µg/ml	Various	https://www.biolegend.com/en-us/products/pe-cyanine7-anti-mouse-ly-6c-antibody-6063
PE-Dazzle-594 Ly6G	Biolegend	127648	4 µg/ml	Various	https://www.biolegend.com/en-us/search-results/pe-dazzle-594-anti-mouse-ly-6g-antibody-12246

PE-Cy5 CD4	BD Biosciences	553050	4 µg/ml	Various	https://www.bdbiosciences.com/en-ca/products/reagents/flow-cytometry-reagents/research-reagents/single-color-antibodies-ruo/pe-cy-5-rat-anti-mouse-cd4.553050
PE-Cy7 CD8a	BD Biosciences	552877	4 µg/ml	Various	https://www.bdbiosciences.com/en-ca/products/reagents/flow-cytometry-reagents/research-reagents/single-color-antibodies-ruo/pe-cy-7-rat-anti-mouse-cd8a.552877
PE NK1.1	BD Biosciences	553165	4 µg/ml	Various	https://www.bdbiosciences.com/en-ca/products/reagents/flow-cytometry-reagents/research-
Alexa Fluor 594 anti-mouse CD45.2	Biolegend	109850	2.5 µg/ml	Various	https://www.biolegend.com/en-us/products/alexa-fluor-594-anti-mouse-cd45-2-antibody-13446
Anti-alpha smooth muscle actin antibody	Abcam	Ab5694	1:200	various	https://www.abcam.com/en-at/products/primary-antibodies/alpha-smooth-muscle-actin-antibody-ab5694
rat anti-mouse CD107b antibody	BD biosciences	553322	1:50	various	https://www.bdbiosciences.com/en-ca/products/reagents/western-blotting-and-molecular-reagents/purified-rat-anti-mouse-cd107b.553322
Anti-Ki67 antibody	Abcam	Ab15580	1:50	various	https://www.abcam.com/en-at/products/primary-

					antibodies/ki67-antibody-ab15580
Goat anti-rabbit Alexa Fluor 488	Invitrogen	A-11008	1:500	various	https://www.thermofisher.com/antibody/product/Goat-anti-Rabbit-IgG-H-L-Cross-Adsorbed-Secondary-Antibody-Polyclonal/A-11008
Goat anti-rabbit Alexa Fluor 594	Invitrogen	A-11037	1:500	various	https://www.thermofisher.com/antibody/product/Goat-anti-Rabbit-IgG-H-L-Highly-Cross-Adsorbed-Secondary-Antibody-Polyclonal/A-11037
goat anti-rat Alexa Fluor™ 488	Invitrogen	A-11006	1:500	various	https://www.thermofisher.com/antibody/product/Goat-anti-Rat-IgG-H-L-Cross-Adsorbed-Secondary-Antibody-Polyclonal/A-11006

Cultured Cells

Name	Vendor or Source	Sex (F, M, or unknown)	Catalogue Number
HASMC	Thermofisher Scientific	unknown	# C0075C
C57BL6 VSMC	Isolated from the aorta	Female	n/a
S1PR1$^{lox/lox}$ VSMC	Isolated from the aorta	Female	n/a
apoE$^{KO/KO}$ VSMC	Isolated from the aorta	Female	n/a
S1PR1$^{lox/lox}$ apoE$^{KO/KO}$ VSMC	Isolated from the aorta	Female	n/a
Tagln-cre^{TG} S1PR1$^{lox/lox}$ apoE$^{KO/KO}$ VSMC	Isolated from the aorta	Female	n/a

Assays

Assay Name	Vendor	Catalog Number
Plasma total cholesterol	Thermo Fisher Scientific	TR13421
Plasma free cholesterol	Wako Diagnostics	993-02501
Plasma HDL cholesterol	Wako Diagnostics	997-01301
Plasma triglycerides	Wako Chemicals	998-02992
MTT	Cayman Chemicals	10009365-480

Other

Chemicals	Source / Repository	Catalogue Number
FBS	Thermo Fisher Scientific/Gibco	SH30396.03
PBS	Thermo Fisher Scientific/Gibco	10010023
L-Glutamine	BioShop	GLU102
Penicillin/Streptomycin	Thermo Fisher Scientific	15140122
Iscove's Modified Dulbecco's Medium (IMDM)	Thermo Fisher Scientific/Gibco	31980030
HBSS	Thermo Fisher Scientific	14025092
DMEM/Ham’s F12	Wisent Bioproducts	319-075-CL
Thioglycollate	Sigma-Aldrich	T9032
Trypsin	Thermo Fisher Scientific	R001100
BSA	Sigma Aldrich	A3059
Oil Red O	Bio Basic	OD0395
Mayer’s hematoxylin solution	Sigma Aldrich	SLCG9021
1-Step Fix/Lyse Solution (10X)	eBioscience	00-5333-57
123count eBeads	Thermo Fisher Scientific	01-1234-42
Tissue-Tek® OCT compound	Thermo Fisher Scientific	6769006

Goat serum 4′,6-diamidino-2-phenylindole (DAPI)	Cedarlane Invitrogen	CL1200 D-1306
Permafluor mountant	Fisher Scientific	TA030FM
SEW2871	Cayman Chemicals	256414-75-2
Recombinant PDGF-BB Mouse	BioLegend	558804
Collagenase Type II	Worthington Biochem	LS004176
Soybean Trypsin Inhibitor	Worthington Biochem	LS003570
Elastase	Worthington Biochem	LS002279
Cholesterol-cyclodextrin complex	Sigma-Aldrich	C4951
High-Fat-Diet	Dyets Inc	112286
Osmotic mini pumps	Alzet® Osmotic pumps	Model 2006
Ex26	Tocris Bioscience	5833